

# Antimicrobial drug LbL-assembled delivery system for orthopaedic nanocomposite bone cements

A thesis submitted in accordance with the conditions  
governing candidates for the degree of  
Philosophiae Doctor in Cardiff University

by

Yazan Al Thaher

June 2018

Cardiff School of Pharmacy and Pharmaceutical Science  
Cardiff University

## Summary

Total joint replacement (TJR) is commonly used for the treatment of end stage arthritis. The use of Poly-methylmethacrylate (PMMA) bone cement is a gold standard TJR, where it is frequently used for local delivery of antibiotics to provide prophylaxis from prosthetic joint infections (PJI). Currently used antibiotic loaded bone cements have many limitations, including burst release which fall below inhibitory levels leading to the selection of antibiotic resistant strains. This study aims to provide a controlled release for antimicrobial agents from bone cement to provide prophylaxis from postsurgical infections.

For this purpose, gentamicin and chlorhexidine were loaded alone or in combination on silica nanoparticles surface using layer-by-layer coating technique (LbL). A novel LbL construct was built using hydrolysable and non-hydrolysable polymers. The nanoparticles were characterised by transmission electron microscopy, thermogravimetric analysis, zeta measurement, and drug release in different media. Then, antimicrobial agents LbL coated nanoparticles were incorporated into PMMA cement and the nanocomposite is characterized for drug release, antimicrobial, mechanical, rheological properties and cytocompatibility.

The build-up of LbL coating was confirmed by thermogravimetric analysis and zeta measurements. The release of antimicrobial agents was controlled for > 30 days for different drugs used. The nanocomposite drug release profile also continued > 30 days at concentration higher than the commercial formulation containing the same amount of antibiotics, where burst release for few days were observed. Moreover, the nanocomposite showed superior antimicrobial inhibition for bacterial growth, without adversely affecting the mechanical properties. Different nanocomposites showed cytocompatibility when tested against Saos-2 cells.

Techniques from a variety of disciplines were employed in this study and this interdisciplinary approach has allowed many features of PMMA bone cement to be investigated. The developed nanocomposites can have the potential to reduce PJIs, and the newly developed LbL nano-delivery system may have wider application in a variety of biomaterials.

## **Declaration of Authorship**

This work has not been submitted in substance for any other degree or award at this or any other university or place of learning, nor is being submitted concurrently in candidature for any degree or other award.

Signed .....(Yazan Al Thaher)      Date .....

### **STATEMENT 1**

This thesis is being submitted in partial fulfilment of the requirements for the degree of PhD.

Signed .....(Yazan Al Thaher)      Date .....

### **STATEMENT 2**

This thesis is the result of my own independent work/investigation, except where otherwise stated, and the thesis has not been edited by a third party beyond what is permitted by Cardiff University's Policy on the Use of Third Party Editors by Research Degree Students. Other sources are acknowledged by explicit references. The views expressed are my own.

Signed .....(Yazan Al Thaher)      Date .....

### **STATEMENT 3**

I hereby give consent for my thesis, if accepted, to be available online in the University's Open Access repository and for inter-library loans after expiry of a bar on access previously approved by the Academic Standards and Quality Committee.

Signed .....(Yazan Al Thaher)      Date .....

## **Acknowledgements**

I would like to acknowledge and thank the following people for all their help, support and guidance over the course of my postgraduate study. Without their collaboration and contribution this research project would not have been possible.

Firstly, I would like to express a great deal of gratitude to my supervisors: Dr. Polina Prokopovich, Dr. Stefano Perni whose knowledge and experience has provided invaluable guidance, assistance and advice. I would also like to show appreciation to my colleagues at the School of Pharmacy for their assistance. Also, I would like to express my gratitude to the technical staff at the School of Engineering and Chemistry for providing expertise and help with equipment used in this study.

I am thankful to Philadelphia University (Jordan) for supporting this research. Without the funding, and help from them, this project would not be possible.

Finally, I would like to thank my family, friends and colleagues for always supporting and encouraging me throughout the course of my education. I owe my deepest gratitude to my loving parents Mohammed, Basema for raising me with the utmost patience. I would like to thank my wife Marwa and my daughters Zaina and Salma for their patience and support.

## Research outputs

Al Thaher, Yazan, Perni, Stefano and Prokopovich, Polina 2017. Nano-carrier based drug delivery systems for sustained antimicrobial agent release from orthopaedic cementous material. *Advances in Colloid and Interface Science* 249, pp. 234-247. [10.1016/j.cis.2017.04.017](https://doi.org/10.1016/j.cis.2017.04.017).

Alotaibi, Hadil Faris, Al Thaher, Yazan, Perni, Stefano and Prokopovich, Polina 2018. Role of processing parameters on surface and wetting properties controlling the behaviour of layer-by-layer coated nanoparticles. *Current Opinion in Colloid & Interface Science* 10.1016/j.cocis.2018.02.008.

Al Thaher, Yazan, Latanza, Silvia, Perni, Stefano and Prokopovich, Polina 2018. Role of poly-beta-amino-esters hydrolysis and electrostatic attraction in gentamicin release from layer-by-layer coatings. *Journal of Colloid and Interface Science*. 526, pp. 35–42. <https://doi.org/10.1016/j.jcis.2018.04.042>.

## Peer reviewed conference contributions

Al Thaher, Yazan, Perni, Stefano and Prokopovich, Polina. Nanotechnology based antimicrobial drug delivery system for orthopaedic application. Proceedings of the 28th Annual Conference of the European Society for Biomaterials (ESB), 4-8 September 2017, Athens/Greece.

Poster prize: Al Thaher, Yazan, Perni, Stefano and Prokopovich, Polina. Nanotechnology based antimicrobial drug delivery system for orthopaedic application. Proceedings of the 15th Speaking of Science conference (SoS), 3<sup>rd</sup> May 2017, Cardiff/UK.

Al Thaher, Yazan, Perni, Stefano and Prokopovich, Polina. Role of polyelectrolyte hydrolysis and electrostatic attraction in gentamicin release from Layer-by-Layer coated silica nanoparticles Proceedings of the 22nd International Symposium on Surfactants in Solution (SIS), 3-8 June 2018, Oklahoma/USA.

# Contents

Contents	vi
List of figures	xiii
List of Tables	xxi
List of abbreviations	xxiii
1 Introduction	1
1.1 Total joint replacement	1
1.1.1 Revision surgery	2
1.2 Cemented and cementless joint replacements	3
1.2.1 Total knee replacement	5
1.2.2 Total hip replacement	7
1.3 PMMA bone cements	8
1.4 Prosthetic infections	14
1.4.1 Treatment	15
1.4.2 Prophylaxis	17
1.5 Limitations for antibiotic loaded bone cements	20
1.5.1 Antibiotic elution properties from bone cement	20
1.5.2 Development of antimicrobial resistance	20
1.5.3 Antibiotics effect on the mechanical properties of bone cement	21
1.6 Novel bone cement nano-formulations	22
1.6.1 Role of nanotechnology	22
1.6.2 Nanotechnology based antibiotic based antimicrobial bone cements	23
1.6.3 Non-antibiotic based antimicrobial bone cements	27
1.7 Drug delivery systems and nano-formulations for potential use in bone cements	32

1.8	Aim of the project.....	34
2	General methods.....	37
2.1	Nanoparticles preparation and characterisation.....	37
2.1.1	Chemicals .....	37
2.1.2	Nanoparticle preparation.....	37
2.1.3	Nanoparticles surface and material characterisation .....	40
2.1.4	Gentamicin release quantification.....	41
2.1.5	Chlorhexidine release quantification.....	42
2.1.6	Statistical analysis .....	44
2.2	Bone cement preparation and characterization.....	45
2.2.1	Chemicals .....	45
2.2.2	Bone cement preparation.....	45
2.2.3	Rheology testing.....	46
2.2.4	Drug release quantification .....	47
2.2.5	Antimicrobial testing.....	47
2.2.6	Mechanical testing.....	50
2.2.7	Water uptake testing.....	54
2.2.8	Cytotoxicity testing .....	54
2.2.9	Nanoparticles distribution in bone cement:.....	62
2.2.10	Statistical analysis .....	63
3	Gentamicin controlled release from Layer-by-Layer coated silica nanoparticles.....	64
3.1	Introduction .....	64
3.2	Materials and methods.....	66
3.2.1	Chemicals .....	66
3.2.2	Gel permeation chromatography (GPC) .....	66

3.2.3	Nanoparticle preparation.....	67
3.2.4	Nanoparticles surface and material characterisation.....	70
3.2.5	Gentamicin release quantification.....	70
3.2.6	Statistical analysis .....	71
3.3	Results .....	72
3.3.1	B1 hydrolysis kinetics (GPC).....	72
3.3.2	Nanoparticles surface and material characterization.....	72
3.3.3	Gentamicin release quantification.....	79
3.4	Discussion.....	85
3.4.1	Size measurements .....	85
3.4.2	Zeta potential measurements .....	85
3.4.3	Thermogravimetric analysis (TGA).....	87
3.4.4	Gentamicin release quantification.....	87
3.5	Conclusion.....	90
4	Chlorhexidine controlled release from Layer-by-Layer coated silica nanoparticles.....	92
4.1	Introduction .....	92
4.2	Materials and methods.....	94
4.2.1	Chemicals .....	94
4.2.2	Nanoparticle preparation.....	94
4.2.3	Nanoparticle surface and material characterisation .....	95
4.2.4	Chlorhexidine release quantification.....	96
4.2.5	Statistical analysis .....	96
4.3	Results .....	97
4.3.1	Nanoparticle surface and material characterization .....	97
4.3.2	Chlorhexidine release quantification.....	100

4.4	Discussion.....	102
4.4.1	Size measurements .....	102
4.4.2	Zeta potential measurements .....	103
4.4.3	Thermogravimetric analysis .....	104
4.4.4	Chlorhexidine release quantification.....	105
4.5	Conclusion.....	107
5	Gentamicin nanoparticle-containing bone cement.....	108
5.1	Introduction .....	108
5.2	Materials and methods.....	109
5.2.1	Chemicals .....	109
5.2.2	Nanoparticle preparation.....	109
5.2.3	Bone cement preparation.....	110
5.2.4	Gentamicin release quantification.....	110
5.2.5	Rheology testing.....	112
5.2.6	Antimicrobial testing.....	112
5.2.7	Mechanical testing.....	112
5.2.8	Water uptake testing.....	113
5.2.9	Nanoparticles distribution in bone cement.....	113
5.2.10	Cytotoxicity testing .....	113
5.2.11	Statistical analysis .....	114
5.3	Results .....	115
5.3.1	Bone cement settling time .....	115
5.3.2	Gentamicin release profile .....	117
5.3.3	Antimicrobial analysis.....	120
5.3.4	Mechanical properties .....	121
5.3.5	Water uptake testing.....	122

5.3.6	Nanoparticles distribution in bone cement.....	124
5.3.7	Cytotoxicity analysis .....	126
5.4	Discussion.....	133
5.4.1	Surface and material properties of bone cement .....	133
5.4.2	Gentamicin release profile .....	136
5.4.3	Antimicrobial efficacy.....	138
5.4.4	Cytocompatibility.....	141
5.5	Conclusion.....	143
6	Chlorhexidine nanoparticle containing bone cement .....	144
6.1	Introduction .....	144
6.2	Materials and methods.....	145
6.2.1	Chemicals .....	145
6.2.2	Nanoparticle preparation.....	146
6.2.3	Bone cement preparation.....	146
6.2.4	Rheology testing.....	146
6.2.5	Chlorhexidine release quantification.....	146
6.2.6	Antimicrobial testing.....	148
6.2.7	Mechanical testing.....	148
6.2.8	Water uptake testing.....	149
1.1.1	Nanoparticles distribution in bone cement.....	149
6.2.9	Cytotoxicity testing .....	149
6.2.10	Statistical analysis .....	150
6.3	Results .....	150
6.3.1	Chlorhexidine release profile .....	150
6.3.2	Antimicrobial analysis.....	153
6.3.3	Bone cement settling time .....	155

6.3.4	Mechanical properties .....	157
6.3.5	Water uptake testing .....	159
6.3.6	Nanoparticles distribution in bone cement.....	160
6.3.7	Cytotoxicity analysis .....	163
6.4	Discussion.....	174
6.4.1	Chlorhexidine release profile .....	174
6.4.2	Antimicrobial efficacy.....	176
6.4.3	Surface and material properties of bone cement .....	178
6.4.4	Cytocompatibility testing .....	181
6.5	Conclusion.....	184
7	Gentamicin and chlorhexidine nanoparticle containing bone cement .....	185
7.1	Introduction .....	185
7.2	Materials and methods.....	187
7.2.1	Chemicals .....	187
7.2.2	Nanoparticle preparation.....	187
7.2.3	TGA.....	188
7.2.4	Bone cement preparation.....	189
7.2.5	Rheology testing.....	189
7.2.6	Bone cement drug release quantification .....	189
7.2.7	Antimicrobial testing.....	191
7.2.8	Mechanical testing.....	191
7.2.9	Water uptake testing .....	192
7.2.10	Nanoparticles distribution in bone cement.....	192
7.2.11	Cytotoxicity testing .....	192
7.2.12	Statistical analysis .....	193
7.3	Results .....	194

7.3.1	Nanoparticles surface and material characterization.....	194
7.3.2	Bone cement settling time .....	196
7.3.3	Bone cement drug release profile .....	198
7.3.4	Antimicrobial analysis.....	200
7.3.5	Mechanical testing.....	202
7.3.6	Water uptake testing .....	204
7.3.7	Nanoparticles distribution in bone cement.....	205
7.3.8	Cytotoxicity analysis .....	206
7.4	Discussion.....	218
7.4.1	Nanoparticle surface and material characterization .....	218
7.4.2	Drug release profile .....	218
7.4.3	Antimicrobial efficacy.....	221
7.4.4	Surface and material properties of bone cement .....	223
7.4.5	Cytocompatibility.....	226
7.5	Conclusion.....	227
8	Conclusion.....	229
9	Future work .....	232
10	References .....	234

## List of Figures

Figure 1: Total joint replacements undertaken during 2014: (a) Hip and (b) Knee prosthesis, adapted from National Joint Registry (NJR 2015). .....	1
Figure 2: Total hip replacement: (a) cemented implant, (b) cementless implant. ...	4
Figure 3 : Cemented total hip replacement (functions of bone cement). .....	5
Figure 4: Number of TKR procedures performed in the UK between the years 2003-2014, adapted from NJR, 2015. ....	7
Figure 5: The number of THR in UK between the years 2003-2014, adapted from NJR, 2015. ....	8
Figure 6: Free radical polymerization reaction of PMMA. ....	9
Figure 7: LBL procedure. ....	40
Figure 8: Representative calibration curve for gentamicin. ....	42
Figure 9: Representative calibration curve for chlorhexidine. ....	44
Figure 10: Procedure for antimicrobial testing of bone cement. ....	49
Figure 11: Compression test according to ISO5833 2002. ....	50
Figure 12: Idealized curve of load vs. displacement for cement (ISO5833 2002). .....	51
Figure 13: Bending test according to ISO5833 2002. ....	52
Figure 14: Four-point bending test (ISO5833 2002). ....	53
Figure 15: Fracture toughness test according to ISO 13586 2000. ....	54
Figure 16: Calibration curve for nitrite production. ....	60
Figure 17: FPLC calibration curve. ....	67
Figure 18: GPC hydrolysis study for B1. ....	72
Figure 19: Examples of TEM images for: (a) amino functionalised silica nanoparticles, (b) Q10 chitosan layered nanoparticles, (c) Q10 B1 layered nanoparticles. ....	73

Figure 20: Zeta potential for amino functionalised silica nanoparticles (layer 0) and for 40 layers of a repeating unit of (alginate-gentamicin-alginate-chitosan) to build 10 quadruple layers ( $n = 3 \pm \text{SD}$ ).	74
Figure 21: Zeta potential for amino functionalised silica nanoparticles layer with 40 layers of a repeating unit of (alginate-gentamicin-alginate-B1) to build 10 quadruple layers ( $n = 3 \pm \text{SD}$ ).	76
Figure 22: Thermogravimetric curves for amino functionalised silica nanoparticles and the same nanoparticles layered with different number of quadruple layers (Q1, Q3, Q5, Q7 and Q10) using chitosan as a polycation ( $n = 3 \pm \text{SD}$ ).	76
Figure 23: Thermogravimetric curves for amino functionalised silica nanoparticles and the same nanoparticles layered with different number of quadruple layers (Q1, Q3, Q5, Q7 and Q10) using B1 as a polycation ( $n = 3 \pm \text{SD}$ ).	78
Figure 24: Cumulative gentamicin release in PBS (pH 7.3) from Q1, Q3, Q5, Q7 and Q10 layered using chitosan as a polycation ( $n = 3 \pm \text{SD}$ ).	80
Figure 25: Cumulative gentamicin release in acetate buffer (pH 5) from Q1, Q3, Q5, Q7 and Q10 layered with chitosan as a polycation ( $n = 3 \pm \text{SD}$ ).	80
Figure 26: Thermogravimetric analysis for chitosan layered nanoparticles after destroying LbL in pH 2 buffer ( $n = 3 \pm \text{SD}$ ).	81
Figure 27: Gentamicin release in PBS (pH 7.3) from Q1, Q3, Q5, Q7 and Q10 layered using B1 as a polycation ( $n = 3 \pm \text{SD}$ ).	82
Figure 28: Gentamicin release in acetate buffer (pH 5) from Q1, Q3, Q5, Q7 and Q10 layered with B1 as a polycation ( $n = 3 \pm \text{SD}$ ).	83
Figure 29 : Zeta values for pure sodium alginate solutions and B1 (2mg/ml) at different pH values ( $n = 3 \pm \text{SD}$ ).	84
Figure 30: TEM images for: (a) amino functionalised silica nanoparticles (b) Q10 of chlorhexidine loaded silica nanoparticles with B1 as a polycation.	97
Figure 31: Zeta potential for 10 quadruple layers with the repeating unit (alginate-chlorhexidine-alginate-B1) ( $n = 3 \pm \text{SD}$ ).	98

Figure 32: Thermogram for silica nanoparticles layered with different number of quadruple layer containing chlorhexidine (n = 3 ± SD).....	99
Figure 33 : Cumulative chlorhexidine release in PBS (pH 7.3) from Q1, Q3, Q5, Q7 and Q10 layered.....	101
Figure 34 : Cumulative chlorhexidine release in acetate buffer (pH 5) from Q1, Q3, Q5, Q7 and Q10 layered nanoparticles (n = 3 ± SD). ....	101
Figure 35: Storage (G') and loss (G'') modulus for Palacos-R. ....	115
Figure 36: Storage (G') and loss (G'') modulus for Palacos-NP.....	116
Figure 37: Storage (G') and loss (G'') modulus for Cemex-Genta. ....	116
Figure 38: Storage (G') and loss (G'') modulus for Cemex-NPs.....	117
Figure 39 : Cumulative gentamicin release from commercial bone cements (Cemex Genta, Palacos R), and nanocomposite samples (n=3+SD). ....	118
Figure 40: Cumulative percentage release of gentamicin from commercial bone cements (Cemex Genta, Palacos R) and nanocomposite samples (n=3+SD). ...	119
Figure 41: Antimicrobial testing for different types of bone cements (Palacos R, Cemex Genta, Palacos 3% NPs, Cemex 9% NPs) against different bacterial strains (n=3+SD). ....	121
Figure 42: Compressive strength of commercial and nanocomposite bone cements before and after incubation in PBS pH 7.3 at 37 °C for 3 months (n=6+SD).....	122
Figure 43: Water uptake for different types of gentamicin containing bone cements after incubation in PBS buffer, pH 7.3 (n=3+SD). ....	123
Figure 44: Nanoparticle distribution in Palacos bone cement (3% NPs w/w) (bar=20µm).....	124
Figure 45: Nanoparticle distribution in Cemex bone cement (9% NPs w/w) (bar=20µm).....	125
Figure 46: Viability of osteoblasts exposed to different types of bone cements: Palacos R, Palacos NP, Cemex-Genta, Cemex NP, assessed through MTT test as viability ratio (Nanocomposite/commercial cement) (n=6+SD). ....	126

Figure 47: Viability of osteoblasts exposed to different types of bone cements: Palacos R, Palacos NP, Cemex-Genta, Cemex NP, assessed through LDH test: (a) percentage viability, (b) viability ratio (Nanocomposite/commercial cement) (n=6+SD).....	127
Figure 48: Alizarin red assay for osteoblasts after 21 days grown on different types of bone cements: Palacos R, Palacos NP, Cemex-Genta, Cemex NP. ....	128
Figure 49: Live/dead images for Cemex Genta cement with two different scales. (Top: 100 $\mu$ m bar, bottom: 20 $\mu$ m bar). ....	129
Figure 50: Live/dead images for Cemex nanoparticles cement with two different scales. (Top: 100 $\mu$ m bar, bottom: 20 $\mu$ m bar). ....	130
Figure 51: Actin/dapi images for Cemex Genta cement with two different scales. (Top: 100 $\mu$ m bar, bottom: 20 $\mu$ m bar). ....	131
Figure 52: Actin/dapi images for Cemex nanoparticles cement with two different scales. (Top: 100 $\mu$ m bar, bottom: 20 $\mu$ m bar). ....	132
Figure 53: Cumulative chlorhexidine release in PBS (pH 7.3) from Cemex® with different concentrations of chlorhexidine powder (0.5, 1, 2, 3, 4, 5% w/w) (n=3+SD).....	151
Figure 54: Cumulative chlorhexidine release in PBS (pH 7.3) from Palacos-1% chlorhexidine powder, Palacose-3% chlorhexidine NPs, Cemex-3% chlorhexidine powder, Cemex-9% chlorhexidine NPs (n=3+SD). ....	152
Figure 55: Cumulative percentage chlorhexidine release in PBS (pH 7.3) from Palacos-1% chlorhexidine powder, Palacose-3% chlorhexidine NPs, Cemex-3% chlorhexidine powder, Cemex-9% chlorhexidine NPs (n=3+SD). ....	153
Figure 56: Antimicrobial testing for Cemex cement containing different concentrations for chlorhexidine powder (0.5, 1, 2, 3, 4, 5% w/w) (n=3+SD)..	154
Figure 57: Antimicrobial testing for different types of bone cements (from Palacos-1% chlorhexidine powder, Palacose-3% chlorhexidine NPs, Cemex-3% chlorhexidine powder, Cemex-9% chlorhexidine NPs) (n=3+SD). ....	155
Figure 58: Storage ( $G'$ ) and loss ( $G''$ ) modulus for Cemex-chlorhexidine powder. ....	156

Figure 59: Storage ( $G'$ ) and loss ( $G''$ ) modulus for chlorhexidine Cemex-NPs. .....	157
Figure 60: Compressive strength testing for different types of bone cements (from Palacos-1% chlorhexidine powder, Palacose-3% chlorhexidine NPs, Cemex-3% chlorhexidine powder, Cemex-9% chlorhexidine NPs) (n=6+SD).	158
Figure 61: Water uptake for different types of chlorhexidine containing bone cements after incubation in PBS buffer, pH 7.3 (n=3+SD). ....	160
Figure 62: Nanoparticle distribution of Palacos chlorhexidine nanoparticles (3% w/w) (bar=20 $\mu$ m). ....	161
Figure 63: Nanoparticle distribution of Cemex chlorhexidine nanoparticles (9% w/w) (bar=20 $\mu$ m). ....	162
Figure 64: Viability of osteoblasts exposed to different types of bone cements: Cells control, Cemex, Cemex-chlorhexidine powder, Cemex with NPs, assessed through MTT test at Optical density of 570 nm presented as viability ratio (composite/commercial cement) (n=6+SD). ....	164
Figure 65: Viability of osteoblasts exposed to different types of bone cements: Cells control, Cemex, Cemex-chlorhexidine powder, Cemex with NPs, assessed through LDH test: (a) percentage viability, (b) viability ratio (composite/commercial cement) (n=6+SD). ....	165
Figure 66: Nitrite production for osteoblasts exposed to different bone cements: Cells control, Cemex, Cemex-chlorhexidine powder, Cemex with NPs (n=6+SD). ....	166
Figure 67: Alizarin red assay for osteoblasts after 21 days grown on different types of bone cements: Cells control, Cemex, Cemex-chlorhexidine powder, Cemex with NPs (n=6+SD). ....	167
Figure 68: Live/dead images for Cemex cement with two different scales. (Top: 100 $\mu$ m bar, bottom: 20 $\mu$ m bar). ....	168
Figure 69: Live/dead images for Cemex chlorhexidine powder cement with two different scales. (Top: 100 $\mu$ m bar, bottom: 20 $\mu$ m bar). ....	169

Figure 70: Live/dead images for Cemex chlorhexidine nanoparticles cement with two different scales. (Top: 100 $\mu\text{m}$ bar, bottom: 20 $\mu\text{m}$ bar). .....	170
Figure 71: Actin/dapi images for Cemex cement with two different scales. (Top: 100 $\mu\text{m}$ bar, bottom: 20 $\mu\text{m}$ bar). .....	171
Figure 72: Actin/dapi images for Cemex chlorhexidine powder cement with two different scales. (Top: 100 $\mu\text{m}$ bar, bottom: 20 $\mu\text{m}$ bar). .....	172
Figure 73: Actin/dapi images for Cemex chlorhexidine nanoparticles cement with two different scales. (Top: 100 $\mu\text{m}$ bar, bottom: 20 $\mu\text{m}$ bar). .....	173
Figure 74: TGA for Silica nanoparticles, 7:3-Q7: 7 quadruple layers of 7:3 NPs combination, 8:2-Q8: 8 quadruple layers of 8:2 combination, 9:1-Q9: 9 quadruple layers of 9:1 combination, 7:3-Q10: 10 quadruple layers of 7:3 NPs combination, 8:2-Q10: 10 quadruple layers of 8:2 combination, 9:1-Q10: 10 quadruple layers of 9:1 combination, Pure chl <sub>x</sub> -Q10: 10 quadruple layers containing chlorhexidine (n = 3 $\pm$ SD). .....	194
Figure 75: The build-up of organic matter with increasing number of quadruple layers. ....	195
Figure 76: Storage ( $G'$ ) and loss ( $G''$ ) modulus for Cemex alone bone cement. ....	197
Figure 77: Storage ( $G'$ ) and loss ( $G''$ ) modulus for Cemex-9:1 NP.....	197
Figure 78: Gentamicin cumulative release from Cemex bone cement containing different types of NPs (7:3, 8:2 and 9:1) (n = 3 $\pm$ SD). .....	199
Figure 79: Chlorhexidine cumulative release from Cemex bone cement containing different types of NPs (7:3, 8:2 and 9:1) (n = 3 $\pm$ SD). .....	199
Figure 80: Antimicrobial testing of Cemex cement containing different types of NPs (7:3, 8:2 and 9:1) (n = 3 $\pm$ SD). ....	201
Figure 81: Antimicrobial testing against gentamicin resistant clinical strains for Cemex cement containing different types of NPs (7:3, 8:2 and 9:1) (n = 3 $\pm$ SD). ....	201

Figure 82: Compressive strength testing for Cemex alone and with different types of NPs (7:3, 8:2 and 9:1) at zero time and after 3 months of incubation on PBS at 37°C. ((n = 3 ± SD). .....	203
Figure 83: Water uptake study for Cemex and Cemex nanocomposite containing different types of NPs (7:3, 8:2 and 9:1) after incubation in PBS buffer, pH 7.3 (n=3+SD). .....	204
Figure 84: Nanoparticle distribution of Cemex-9:1 nanocomposite (9% w/w) (bar=20µm). .....	205
Figure 85: Viability of osteoblasts exposed to different types of bone cements: Cells control, Cemex, Cemex nanocomposite containing different NPs (7:3, 8:2 and 9:1), assessed through MTT test at Optical density of 570 nm presented as viability ratio (nanocomposite/Cemex) (n=6+SD). .....	206
Figure 86: Viability of osteoblasts exposed to different types of bone cements: Cells control, Cemex, Cemex nanocomposite containing different NPs (7:3, 8:2 and 9:1), assessed through LDH test: (a) percentage viability, (b) viability ratio (nanocomposite/Cemex) (n=6+SD). .....	208
Figure 87: Nitrite production for osteoblasts exposed to different types of bone cements: Cells control, Cemex, Cemex nanocomposite containing different NPs (7:3, 8:2 and 9:1) (n=6+SD). .....	209
Figure 88: Alizarin red assay for osteoblasts after 21 days grown on different types of bone cements: Cells control, Cemex, Cemex nanocomposite containing different NPs (7:3, 8:2 and 9:1) (n=6+SD). .....	210
Figure 89: Live/dead images for Cemex-7:3 nanocomposite with two different scales. (Top: 100 µm bar, bottom: 20 µm bar). .....	212
Figure 90: Live/dead images for Cemex-8:2 nanocomposite with two different scales. (Top: 100 µm bar, bottom: 20 µm bar). .....	213
Figure 91: Live/dead images for Cemex-9:1 nanocomposite with two different scales. (Top: 100 µm bar, bottom: 20 µm bar). .....	214
Figure 92: Actin/dapi images for Cemex-7:3 nanocomposite with two different scales. (Top: 100 µm bar, bottom: 20 µm bar). .....	215

Figure 93: Actin/dapi images for Cemex-8:2 nanocomposite with two different scales. (Top: 100  $\mu\text{m}$  bar, bottom: 20  $\mu\text{m}$  bar).....216

Figure 94: Actin/dapi images for Cemex-9:1 nanocomposite with two different scales. (Top: 100  $\mu\text{m}$  bar, bottom: 20  $\mu\text{m}$  bar).....217

## List of Tables

Table 1: Composition of some commercially available PMMA bone cements (Lewis, 2009). .....	10
Table 2 : Mechanical properties for some bioactive cements, PMMA and human bone (cortical and cancellous bone). .....	13
Table 3: Antibiotic combinations used for the impregnation of PMMA bone cement spacers for hip and knee prosthetic infections. ....	17
Table 4: Some of the commercially available antibiotic loaded bone cement brands .....	19
Table 5: Summary of mechanical properties for different PMMA nanocomposites. ....	26
Table 6: Summary list of nanotechnology based antibiotic loaded PMMA bone cements. ....	27
Table 7: Summary list of nanotechnology non-antibiotic based antimicrobial PMMA bone cements .....	31
Table 8: 10 quadruple layers' abbreviations and constituents used for LbL coating on silica nanoparticles. ....	39
Table 9: 10 quadruple layers' abbreviations and constituents using chitosan as polycation.....	68
Table 10: 10 quadruple layers abbreviations and constituents using B1 as a polycation.....	69
Table 11: Size measurements calculated from TEM images for amino functionalised silica nanoparticles, Q10 layered with chitosan or B1 as a polycation ( $n = 3 \pm SD$ ). ....	74
Table 12: Percentage of organic material in amino functionalised silica nanoparticles and the same nanoparticles layered with different number of quadruple layers (Q1, Q3, Q5, Q7 and Q10) using chitosan as a polycation ( $n = 3 \pm SD$ ). ....	77

Table 13 : Percentage of organic material in amino functionalised silica nanoparticles and the same nanoparticles layered with different number of quadruple layers (Q1, Q3, Q5, Q7 and Q10) using B1 as a polycation (n = 3 ± SD). .....	79
Table 14 : Organic matter in chitosan layered nanoparticles after trying to destroy LbL in pH 2 buffer (n = 3 ± SD). .....	82
Table 15 : 10 quadruple layers containing chlorhexidine as an antimicrobial agent, and B1 as a polycation.....	95
Table 16 : Percentage of organic matter in silica nanoparticles layered with different number of quadruple layers containing chlorhexidine (n = 3 ± SD). ..	100
Table 17 : Composition of gentamicin containing bone cement. ....	111
Table 18: Bending strength and modulus, and fracture toughness for Cemex bone cement. ....	122
Table 19: Some protocols used in literature to test the antimicrobial properties of PMMA bone cements. ....	139
Table 20: Composition of chlorhexidine containing bone cements. ....	148
Table 21: Bending strength and modulus, and fracture toughness for chlorhexidine loaded Cemex nanocomposite as compared to commercial gentamicin loaded Cemex-Genta®. ....	158
Table 22: The antimicrobial agent added in each quadruple layer (alginate-chlorhexidine or gentamicin-alginate-B1) to give three coating combinations 9:1, 8:2 and 7:3 nanoparticles. ....	188
Table 23: Composition of chlorhexidine and gentamicin containing bone cements. ....	190
Table 24: Percentage of organic matter in different layers of chlorhexidine NPs and chlorhexidine gentamicin combination NPs calculated from Figure 74 (n = 3 ± SD). ....	195
Table 25: Bending strength and modulus, and fracture toughness for Cemex and Cemex containing 9:1 NPs. ....	203

## List of Abbreviations

APTS	3-Aminopropyltriethoxysilane
ALBC	Antibiotic loaded bone cements
ANOVA	One-way analysis of variance
BaSO <sub>4</sub>	Barium sulphate
BHI	Brain heart infusion
CFU	Colony forming unit
CNT	Carbon nanotubes
CPC	Calcium phosphate cement
DLS	Dynamic light scattering
DMPT	N, N-Dimethyl para-toluidine
DMSO	Dimethyl sulfoxide
FBS	Fetal bovine serum
FPLC	Fast Protein Liquid Chromatography
GPC	Gel permeation chromatography
HACC	Hydroxypropyl trimethyl ammonium chloride chitosan
HAP	Hydroxyapatite nano-rods
HPLC	High Performance Liquid Chromatography
LbL	Layer-by-layer
LDH	Lactase dehydrogenase
LEFM	Linear elastic fracture mechanics
MIC	Minimum inhibitory concentration
MMA	Methyl methacrylate
MSN	Mesoporous silica nanoparticles
MTT	Methylthiazolyl tetrazolium
NJR	National Joint Registry
NO	Nitric oxide
NP	Nanoparticles
OPA	O-phthaldialdehyde reagent solution
PAA	Poly (allylamine)
PAH	Poly (allylamine hydrochloride)
PBAE	Poly-beta-amino-ester
PBS	Phosphate buffer saline
PEO	Polyethylene oxide
PJI	Prosthetic joint infections
PLGA	Poly (lactic-co-glycolic acid)
PMMA	Poly (methyl methacrylate)
PPO	Polypropylene oxide
PSS	Polystyrene sulfonate
PTFE	Polytetrafluoroethylene

Q	Quadruple layer
QCS	Quaternary ammonium chitosan derivative
RPM	Revolutions per minute
SBF	Simulated body fluids
SD	Standard deviation
SiNH <sub>2</sub>	Amino functionalised silica
TEM	Transmission electron microscopy
TEOS	Tetraethyl orthosilicate
TGA	Thermogravimetric analysis
THR	Total hip replacement
TJR	Total joint replacement
TKR	Total knee replacement
TPGDA	Tripropylene glycol diacrylate
UV	Ultraviolet
ZrO <sub>2</sub>	Zirconium dioxide

# 1 Introduction

## 1.1 Total joint replacement

The replacement of a dysfunctional joint with an orthopaedic implant is reserved as the last choice for the treatment of joint diseases. Arthritic and degenerative diseases is a leading cause of disability worldwide (Kim et al., 2012). The most common form of arthritis is osteoarthritis which affects around 15% of the population (Johnson and Hunter, 2014). In the United States (US), more than 26 million people are suffering from osteoarthritis (Litwic et al., 2013), while that number reaches 8.5 million in the United Kingdom (UK) (Conaghan et al., 2015).

Total joint replacement (TJR) is the treatment of choice for patients with end-stage arthritis when less invasive therapies fail to alleviate the severe pain or dysfunction of the joint (*Figure 1*) (Cram et al., 2012). This procedure showed noticeable progress in patients' quality of life (Singh et al., 2015; Wang et al., 2012). According to the National Joint Registry (NJR, 2015), the predominant indication for TJR was osteoarthritis (more than 90% in hip and knee replacements) between the years 2003 and 2014. Whereas, a small percentage undertook TJR for other reasons, such as avascular necrosis, trauma, infection and inflammatory arthritis.

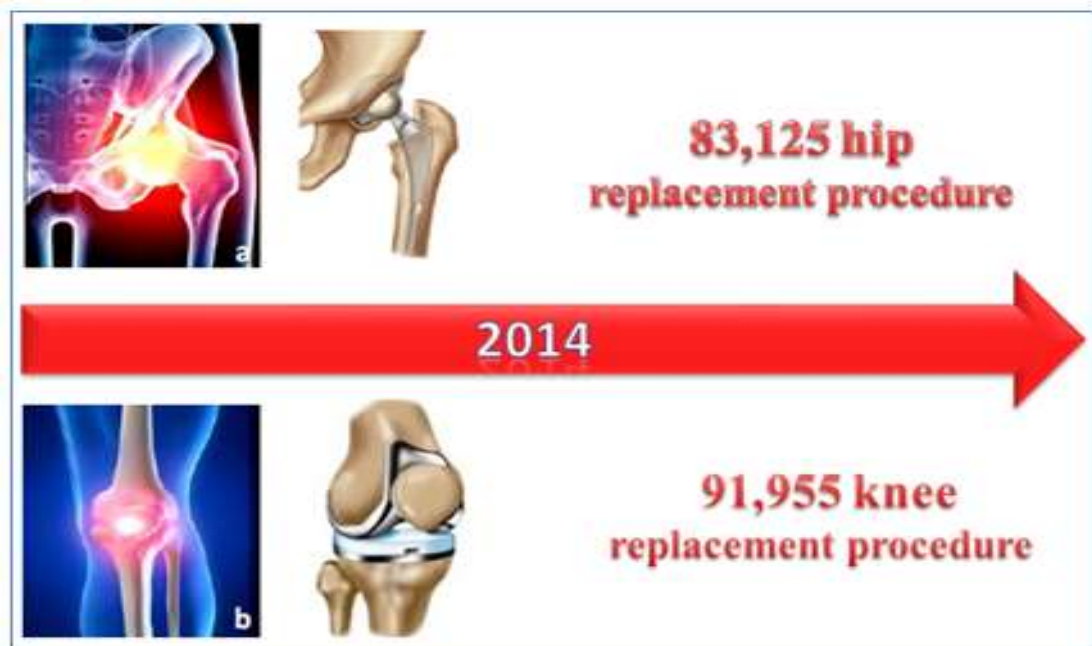


Figure 1: Total joint replacements undertaken during 2014: (a) Hip and (b) Knee prosthesis, adapted from National Joint Registry (NJR 2015).

The popularity of total hip and total knee replacements is increasing worldwide which places a huge burden on health care systems (Bumpass and Nunley, 2012; Kurtz et al., 2005; Skyttä et al., 2011). In the US, over 1 million hip and knee replacement are performed annually (Maradit et al., 2015). This number is expected to increase drastically in the next 20 years because of ageing as well as growing prevalence of risk factors such as obesity (Kurtz et al., 2009; Liddle et al., 2014). In the UK, the same trend is apparent; between the years 2003 and 2014 708,644 and 772,113 primary hip and knee replacements were performed, respectively. In 2014, 83,125 hip and 91,955 knee replacements were performed in the UK (NJR, 2015).

### **1.1.1 Revision surgery**

Despite the ability of TJR to improve the quality of life and retrieve mobility to many patients, the life expectancy for this procedure is around 10-15 years (Labek et al., 2011; Pabinger et al., 2013; Patel et al., 2015), hence there is a need for revision surgeries. Revision surgeries are the joint replacements performed after primary TJR because of implant failure. In the US, revision surgeries account for 18% of hip and 8% of knee total replacements performed each year (Ong et al., 2010). Similarly, revisions in the UK are 11 % (8925) of hip and 6 % (5873) of knee primary procedures performed in 2014 (NJR, 2015). The main reasons for infection are aseptic loosening, pain and infection.

Compared to primary surgery, revision surgery is more complex and takes longer time to perform (Patel et al., 2010). In addition, clinical and functional outcomes are poorer such as pain, joint stiffness and stability, muscle impairment and atrophy, with lower patient satisfaction and quality of life after surgery, because of complexity and nature of revision surgery (Greidanus et al., 2011). As a result, revision is accompanied by higher complication rates, longer patient hospital stays and the use of a more expensive implants (Kallala et al., 2015; Maradit et al., 2013). Accordingly, revision surgery is associated with higher costs when compared to primary replacements, as well as relatively shorter survival (Bhandari et al., 2012). For example, the cost of primary knee replacement is around \$15000, while the cost of revision surgery is higher and can reach \$ 24000 (Maradit et al.,

2013). In the UK, health care costs for revision surgery were estimated to be 80 million in the year 2010 (Vanhegan et al., 2012).

Infection after joint replacements is a severe problem that not only decreases the success rates of surgery, but also can be life threatening to patients. Despite antibiotic prophylaxis and operation under laminar flow, infection rates in the first two years of primary replacement are 1% in knee replacements, 2% in hip replacements and can reach 9% in other types of TJRs. Also, infection rates are significantly higher after revision surgeries (up to 40%) (Cobo and Del, 2011; Zimmerli et al., 2004). These percentages translate into large numbers when we look at the total numbers of TJRs done annually. For example, 2,400 revision procedures were performed in the UK in 2014 due to infection (NJR, 2015) and 22,000 revisions of infected knee and hip replacements were done in the US in 2009 (Kurtz et al., 2012). Prosthetic infections extend hospitalization time, readmissions and length of antimicrobial treatment, hence increasing the economic burden on health care systems; the cost of treatment for an incident of prosthetic infection can reach \$50000 which is more than 3 times the cost of primary surgery and 2 times the cost of revision surgery (Lamagni, 2014).

## **1.2 Cemented and cementless joint replacements**

Nowadays, there are two main types for TJRs, namely, cemented and cementless joint replacements (*Figure 2*). In cemented TJRs, bone cement is widely used for fixation of prosthesis. Poly (methyl methacrylate) (PMMA) based bone cement is the gold standard material used in such procedures. This type of TJR involves complete removal of the impaired joint, after that a cavity is made inside the bone. The surgeon fills the cavity with PMMA bone cement. Then, the metallic implant is placed and positioned in the cavity while the cement sets. Cementless TJRs follow the same procedure except that the implant is inserted in direct contact with a bone without using a cement (NHS choices, 2014).

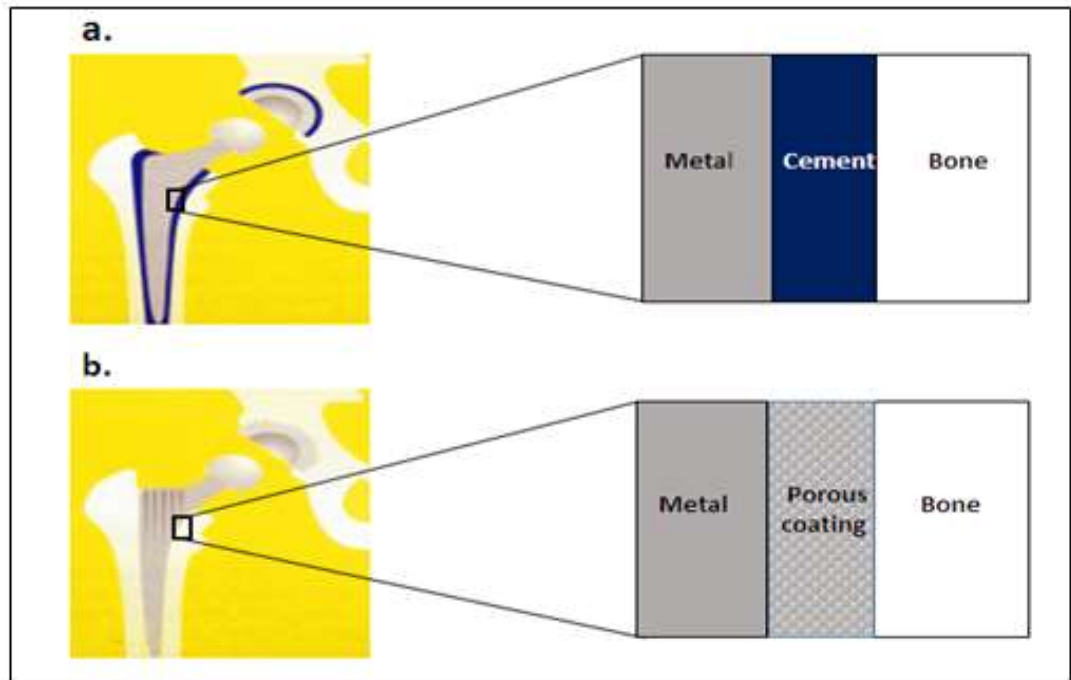


Figure 2: Total hip replacement: (a) cemented implant, (b) cementless implant.

Bone cements are routinely used in TJRs to fasten the orthopaedic implant in place; transfer mechanical stresses and loads between the stiff metallic implant and bone tissue; and, commonly, to provide prophylaxis from post-surgical prosthetic infections by releasing one or more antibiotic such gentamicin or tobramycin (*Figure 3*) (Magnan et al., 2013). In addition, advantages for using bone cement include that the bone cavity does not have to be perfect match with the implant and the use of bone cement reduces the need for blood transfusions, because of reduced blood loss and the cement tamponade effect (Bidolegui et al., 2014; Choy et al., 2014). Furthermore, the most important reason for using PMMA bone cement in TJR is the outstanding long-term survivorship (98% at ten years and 91% at 20 years) (Demey et al., 2011; Kendrick et al., 2015). However, there are always concerns about cemented replacements because of their degradation products and debris, as well as deterioration of bone cement interface and third body wear (Zhang et al., 2015). These concerns led researchers to seek new alternatives for fixation, i.e. cementless fixation.

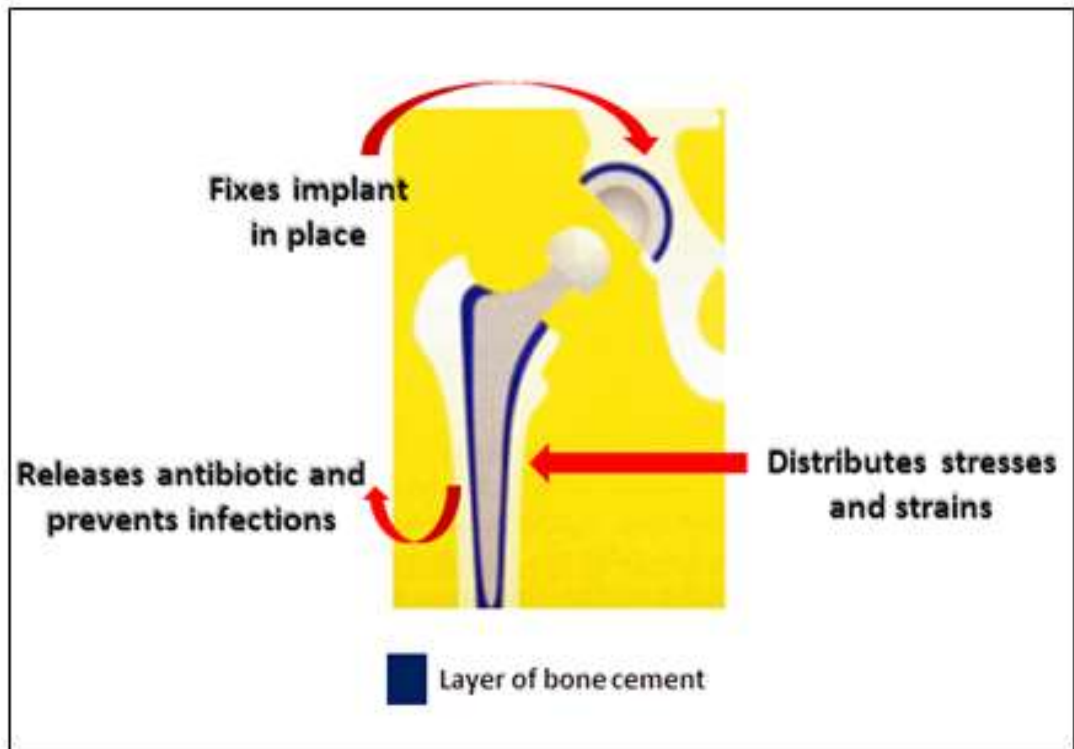


Figure 3 : Cemented total hip replacement (functions of bone cement).

Cementless replacements depend on biological fixation or osteo-integration of the implant to the bone; advocates of this type of fixation believe that bone ingrowth through the micropores of the metallic implant can achieve more durable fixation with bone (Figure 2). The claimed advantages of cementless fixation are: shorter operation time, ease of revision, and improved longevity for active younger patients (Kallala et al., 2013). However, cementless fixation has inconsistent long-term results and is not regularly used in most centres, because it is accompanied with a high rate of revision (NAR, 2010; NJR, 2015; SHA, 2013).

### 1.2.1 Total knee replacement

The use of cemented implant is the 'gold standard' in total knee replacement (TKR) in the last 3 decades and has high success rates of more than 95% at 15 years with long term durability (Demey et al., 2011). Many articles reported outstanding long-term results for cemented TKR. Crowder et al. (2005) analysed 32 patients with cemented implants, he reported survivorship rate of 100% in 15 years and 93.7% in 20 years after TKR procedure. Gill et al. (1997) reported 96.5 % survivorship 18 years after the procedure in patients 55 years old or younger.

Ritter et al. (2007) also reported 97.6% success rate in the same age group when followed for 9.1 years. Vessely et al. (2006) looked at 244 patients with cemented TKR, survivorship was 95.7% in 15 years after the procedure. A study, including 265 patients with posterior stabilized prosthesis, had 94.1% success rate over 16 years (Font-Rodriguez et al., 1997).

Many authors have directly compared cemented fixation with cementless fixation in TKR (Barrack et al., 2004; Rorabeck, 1999). Rand et al. (2003) carried out a survivorship analysis for 11606 patients at 10 years. The success rate was 92% in patients with cemented prostheses, whereas only 61% success rate reported in patients without cement ( $P < 0.0001$ ). Barrack et al. (2004) compared 82 cementless mobile bearing knees with 73 cemented knees, 8% of cementless knees were revised, while no revision found in cemented knees. Rorabeck (1999) looked at 484 patients of hybrid and cemented knee fixation, reporting 9.6% revision rate in hybrid group (uncemented femur and cemented tibia), compared to 1.6% in the cemented group after 3 years. Figure 4 shows the number of TKR in UK between the years 2003-2014 (NJR, 2015).

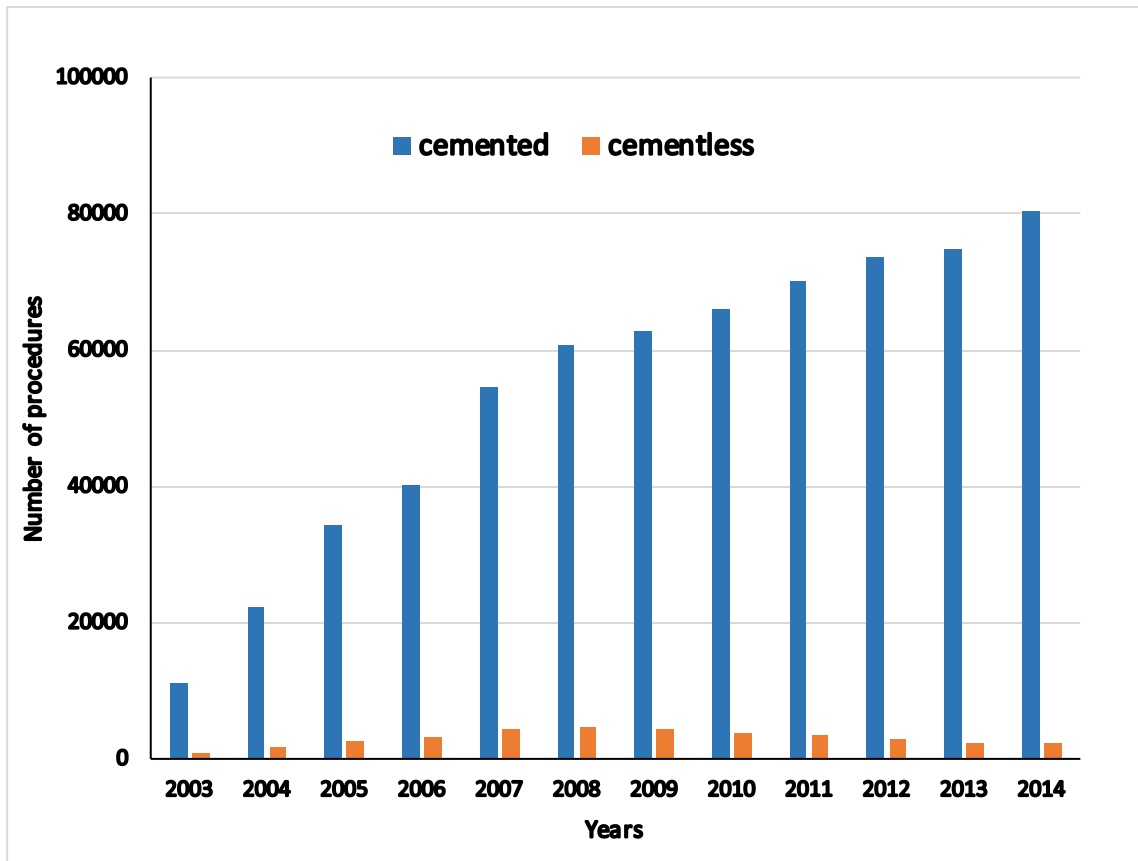


Figure 4: Number of TKR procedures performed in the UK between the years 2003-2014, adapted from NJR, 2015.

### 1.2.2 Total hip replacement

Clinical studies performed on total hip replacement (THR) with cemented implants have convincing long-term results. Berry et al. (2002) reported a survivorship rate of 80% in 25 years after the procedure in 1689 patients with cemented implant. Another study about cemented implant including 226 patients reported similar survival rate of 81% in 25 years (Sochart and Porter, 1997). However, a tendency towards cementless hip replacement has been seen in recent days, because of the significant improvement in survival rate for cementless stems. In patients using cementless BiCONTACT stem, the survival rate is 94.4% in 15 years (Tsukada and Wakui, 2016). Emerson et al. (2002) looked at 181 patients with cemented and cementless hip implant. The survivorship was 84 % in cemented group, while it was 100% in cementless group. Cementless implant is specifically selected for young active patients who have greater physical loads with greater failure rates secondary to loosening, whereas cemented implants are used for older patients

with poor bone quality (Liu et al., 2015; Wyatt et al., 2014). Figure 5 shows the number of THR in the UK between the years 2003-2014 (NJR, 2015).

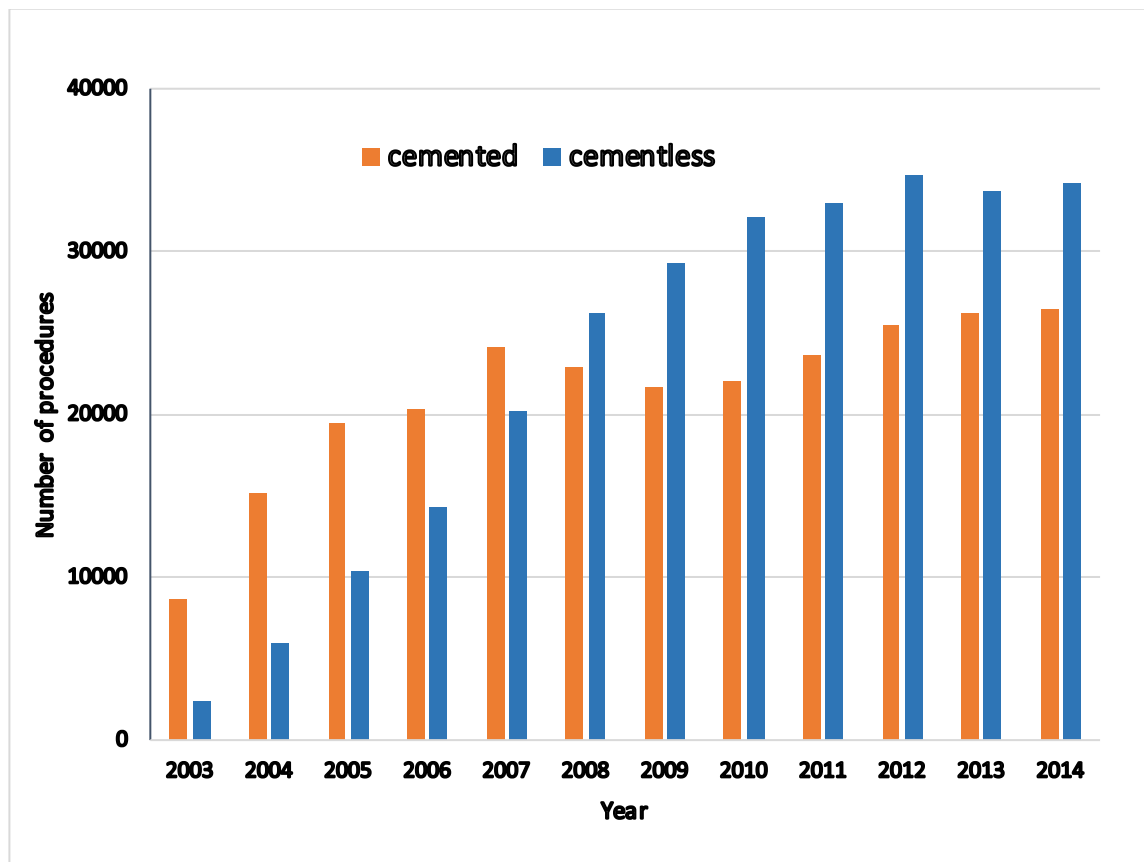


Figure 5: The number of THR in UK between the years 2003-2014, adapted from NJR, 2015.

### 1.3 PMMA bone cements

Poly(methyl methacrylate) polymer (PMMA) is a polymer based on methyl methacrylate (MMA) monomer units. PMMA cement is prepared by mixing two constituents together: PMMA polymer powder and liquid MMA monomer (Figure 7). After mixing the two components, the hardened bone cement is formed by an exothermic free radical polymerization reaction, as the liquid monomer polymerizes around the pre-polymerized powder producing heat (Vaishya *et al.*, 2013). The heat of the setting reaction can reach (66-82.5 °C). The setting time for the cement is relatively short (less than 15 min) and the cement must be inserted into the bone before cement hardening, otherwise the procedure cannot be completed (Boner et al., 2009). Premature polymerization of the liquid component may happen because of exposure to heat and light. Therefore, Hydroquinone is added as a stabilizer to prevent polymerization before mixing of the cement

constituents. Benzoyl peroxide is added to the powder to initiate the free radical polymerization reaction, while N,N-Dimethyl para-toluidine (DMPT) is added as an accelerator to facilitate the polymerization reaction between the polymer and monomer at room temperature (Chaudhry and Dunlop, 2012). Barium sulphate (BaSO<sub>4</sub>) or zirconium dioxide (ZrO<sub>2</sub>) are added as radiopaque agent to allow X-ray imaging because PMMA is not radiopaque (O'Brien et al., 2010).

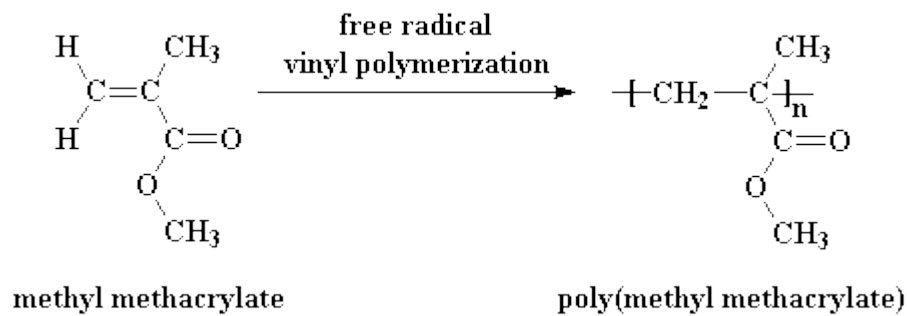


Figure 6: Free radical polymerization reaction of PMMA

At present, many commercial bone cements are marketed by different manufacturers (Table 1: *Composition of some commercially available PMMA bone cements* (Lewis, 2009).). The main differences between different formulations are the molecular weight of PMMA, the ratio between homopolymer and copolymer, the ratio between powder and liquid, the radiopacifier and other additives such as antibiotics. Different copolymer of different acrylic monomers are added to modify the mechanical properties of the cement, such as styrene and Ethyl methacrylate (Nien and Chen, 2006) (Table 1).

Constituent*	Cemex® XL Genta LV	Copal®	Endurance™ Gentamicin	Palacos® R+G	SmartSet® GHV
Powder					
Poly (methyl methacrylate) (PMMA)	82.78	-	65.28	-	-
Methyl methacrylate (MMA)/styrene co-polymer	-	-	18.65	-	-
PMMA/MMA co-polymer	-	82.65	-	82.15	80.46
Benzoyl peroxide (BPO)	3.00	0.75	1.85	0.78	0.96
Barium sulfate	10.00	-	10.00	-	-
Zirconium dioxide	-	10.03	-	15.01	14.37
Gentamicin sulfate	4.22	3.76	4.22	2.06	4.22
Clindamycin hydrochloride	-	2.82	-	-	-
Chlorophyll		0.002	-	0.002	-
Liquid					
MMA	98.20	97.98	98.00	97.98	97.50
N, N dimethyl-p-toluidine (DMPT)	1.80	2.02	≤2.00	2.02	≤2.50
Hydroquinone	75	75	75	75	75
Chlorophyll	-	0.002	-	0.002	-

*\*The amount of each constituent of a cement is in wt. /wt. %, except for hydroquinone, which is ppm*

Table 1: Composition of some commercially available PMMA bone cements (Lewis, 2009).

The main drawback of PMMA bone cement is the absence of bone bonding ability, i.e. bioactivity. This can lead to the formation of fibrous tissue around the implant and a space for the wear particles to accumulate (Freemont, 2012). As a result, bone resorption around the implant causes loosening and failure of the implant after a long period of time, which is the most commonly reported reason for revision in cemented replacements (NJR, 2015). Despite the extensive research done on developing alternatives for PMMA in THR and TKR, PMMA stays to be the biomaterial of choice in TJRs since the 1960s, because of its acceptable long-

term survivorship and long-established clinical history as well as excellent mechanical properties (Vaishya et al., 2013). Extensive research has been directed on developing new bioactive bone cements that integrate with bone, and improving the biocompatibility as well as mechanical properties of PMMA bone cements (Ni et al., 2006; Oonishi, 2012).

One of the examples on bone cements with bioactive properties is calcium phosphate bone cement (CPC), which has been studied since 1980s (Zhang et al., 2014). Their poor mechanical properties such as strength, toughness and brittleness limited their application to low load-bearing arthroplasties e.g. craniofacial and maxillofacial surgeries (*Table 2*). Despite CPCs bioactive properties, their inferior mechanical properties are not sufficient to replace the use of PMMA in high load-bearing arthroplasties such as knee and hip replacements (Ambard and Mueninghoff, 2006; Krüger and Groll, 2012). The mechanism for setting reaction involves a dissolution-precipitation process that occurs at body temperature, without causing tissue necrosis in the surrounding tissue unlike the exothermic setting reaction for PMMA (Yu et al., 2010). Despite the presence of many CPC formulations, the final product only could be either brushite or hydroxyapatite. Brushite is a metastable form that may transform into hydroxyapatite at  $\text{pH} > 4$  *in vivo* (Chen et al., 2013). CPCs are microporous in nature which helps in the penetration of biological fluids, hence they are resorbable and can be replaced by bone (Schwarz et al., 2009). In addition, the micropores enhance the ability of CPCs to load drugs which is an appealing option for any type of biomaterial (Ginebra et al., 2012; Habraken et al., 2007).

Apatite/wollastonite is another bioactive bone cement that has been researched for use in knee and hip replacements. Apatite/wollastonite glass bioactive ceramics have currently many medical applications and used as bone filler or bulk material (Cannillo et al., 2009). Also, they have higher mechanical properties than other bioactive ceramics and cortical bone (*Table 2*). However, they cannot be used in high load arthroplasties such as hip and knee replacements, because their fracture toughness is lesser and elastic modulus is greater than those of cortical bone (Kokubo et al., 2003).

Dental cements have been also researched for orthopaedic application such as glass polyalkenoate and Bioglass (Dickey et al., 2013; Neo et al., 1992). Glass polyalkenoate is a dental cement with good mechanical properties (*Table 2*), but the release of aluminium from the glass phase causes defective bone mineralization and limits their use in the orthopaedic field (Boyd et al., 2008). In order to avoid this problem aluminium was replaced with Zn, as it has a positive effect on osteoblast proliferation and increases bone mass. However, Zn based glass polyalkenoate has substantially inferior mechanical and setting properties compared with aluminium containing counterparts (Dickey et al., 2013). Moreover, resin modified glass polyalkenoate, another biomaterial, was developed in an attempt to improve the poor mechanical properties of conventional glass polyalkenoate. Although it has good mechanical properties, they suffer from volumetric shrinkage after curing which causes mechanical failure at the implant interface (Cook et al., 1999; Nourmohammadi et al., 2008).

		Strength (MPa)		Young's modulus (GPa)	Fracture toughness, $K_{IC}$ (MPam <sup>1/2</sup> )	Reference
		Compressive	Bending			
Bioglass® (45S5)		-	42	35	-	(Kokubo et al., 2003)
glass polyalkenoate		175.21	-	12.82	0.63	(Higgs et al., 2001)
Hydroxyapatite		39-103	-	4.5-9	0.15-0.5	(Zhang et al., 2011)
Apatite/wollastonite		1080	220	118	2.0	(Kokubo et al., 2003)
PMMA		73-117	50-125	2.552	1.03-2.32	(Lee, 2005; Lewis, 1997)
Human bone	Cancellous	2-12	-	0.05-0.5	-	(Kokubo et al., 2003)
	Cortical	100-230	50-150	7-30	2-12	(Kokubo et al., 2003)

Table 2 : Mechanical properties for some bioactive cements, PMMA and human bone (cortical and cancellous bone).

None of the previously mentioned bioactive cements have the required mechanical properties to be used in high load bearing arthroplasties. Despite the lack of bone-bonding properties of PMMA, it is still the only biomaterial to be used in cemented hip and knee arthroplasties. Therefore, PMMA fails to achieve a long-lasting replacement making aseptic loosening the most common cause for revision. Newly developed bone cement should have both bone-bonding properties (bioactivity), as well as mechanical properties that match those of bone and optimally have antimicrobial properties (Kenny and Buggy, 2003).

## 1.4 Prosthetic infections

The success of TJRs in relieving pain and improving the quality of life for patients is increasingly growing. Infection is considered the most serious problem after joint prosthesis implantation, which decreases success rate of the surgery and can be life threatening to patients in some cases (Cobo and Del, 2011). Prosthetic infections are difficult to diagnose and occur at variable times after the primary surgery. Management of prosthetic infections is complex and needs multiple procedures and prolonged antimicrobial therapy with poor functional outcome (Zimmerli et al., 2004). This places considerable burden on medical resources and health care expenditure, because of the high cost of prosthetic joint infection incidence treatment that can reach up to \$50000 (Lamagni, 2014). Efforts have been made to reduce the risk of prosthetic infections such as the use of perioperative antimicrobial prophylaxis and surgical laminar airflow environment, however the incidence of prosthetic infection is still high and can reach up to 2% in total hip and knee replacement, and even higher after revision surgeries (up to 40%) (Cobo and Del, 2011).

Prosthetic infections have 3 classifications based on the onset of infection, namely, (i) early, (ii) delayed, (iii) late infections. For early infections, the signs and symptoms of infections appear in the first 3 months after surgery, and the infection are usually because of bacterial contamination during or after surgery caused by highly virulent microorganisms. Early infections account for up to 45% of prosthetic infections. In delayed infections, the first signs and symptoms appear after 3 months to 2 years after surgery. The cause of delayed infections are low virulent microorganisms inoculated during surgery. In late infections, the onset starts after 2 years from surgery, and caused by seeding via the blood from an infection in other body parts such as skin, respiratory or urinary tract infections (Fsadni and Fsadni, 2013; Trampuz and Widmer, 2006; Zimmerli and Ochsner, 2003).

Biofilm formation is the typical mode of growth for bacteria involved in prosthetic infections, which adds to the difficulty and length of treatment. The microorganisms in biofilms form ordered and complex clusters enclosed by a hydrophilic polymeric matrix (Fsadni and Fsadni, 2013; Zimmerli et al., 2004).

Biofilms shelter microorganisms from antibiotics and host immune defence, as well as increase bacterial resistance and reduce susceptibility to antibiotics by 500-5000 times compared to planktonic, free floating bacteria (Cobo and Del, 2011). In addition, the implant acts as a binding site for bacterial accumulation into biofilms and decreases the minimum dose of bacteria needed to cause infection (Zimmerli et al., 2004).

The most commonly encountered bacteria in prosthetic joint infections are coagulase-negative staphylococci (30-43%) and *Staphylococcus aureus* (12-23%), followed by streptococci (9-10%), Gram-negative bacilli (3-6%), enterococci (3-7%), and anaerobes (2-4%). Polymicrobial infections, which usually occur postoperatively, are seen in (10-12%) and they are difficult to treat. (Fsadni and Fsadni, 2013; Trampuz and Zimmerli, 2005).

#### **1.4.1 Treatment**

The treatment of prosthetic infection aims to relieve patients from pain, restore joint mobility and eradicate infections. Treatment of such infections is typically challenging and complex with combined aggressive surgical interventions and antimicrobial therapy, which make it hard to achieve all the 3 aims together. Management of prosthetic infections should be customised for each patient and usually includes one of 3 main types of surgical interventions (Cobo and Del, 2011; Strange et al., 2016). First, prosthetic retention with debridement of all infected tissue and irrigation, which is a choice for early postoperative or late haematogenous infections with retention of the prosthesis and long-term antibiotic treatment (Brimmo et al., 2016; Buller et al., 2012). Second, prosthetic exchange, the most frequently used, by one stage or two stage revision. In one stage revision, the removal of all foreign material debridement and reimplantation of a new prosthesis are done in the same procedure (Zahar et al., 2015). While in two stage revision, the removal of foreign material and debridement are done, and the reimplantation of a new prosthesis is delayed for a variable period of time (typically after > 6 weeks) (Vielgut et al., 2015). Third, salvage procedure including resection arthroplasty, arthrodesis and amputation which are the last choice when infection management is not achievable by the previously mentioned interventions (Aslam and Darouiche, 2012).

Two stage revision has become the standard procedure in the treatment of deep tissue prosthetic infections (Masters et al., 2013). The two-stage approach gives sufficient time for debridement and removal of the infected tissues, the determination of the infecting microorganism and its sensitivity to antibiotics, modifying the antimicrobial therapy before reimplantation. However, extended hospitalization increases the surgery costs, while delayed mobilization and risk of other surgery is cautiously considered, particularly in elderly people (Ritter and Farris, 2010).

In two stage surgery, the use of antibiotic-impregnated spacers is considered the gold standard for the eradication of infection and avoiding limb shortening (Romanò et al., 2012; Stammers et al., 2015). Spacers are bone cement pieces that is placed in the joint place to prevent muscle contractions and preserve their length. The use of a temporary spacer in two-stage surgery in knee replacement gives the patient the ability to move, also provides good alignment of the knee between the two stages (Cooper and Valle, 2013; Haddad et al., 2000). Success rates with the use of antibiotic impregnated PMMA interim spacer/prosthesis are reported to be higher than 90% (Jaekel et al., 2012). The advantage offered by such spacer is delivering high level of antibiotic locally, while maintaining joint mobility (Anagnostakos et al., 2006). *Table 3* shows common antibiotic combinations used for the impregnation of PMMA bone cement spacers.

<b>Reference</b>	<b>Antibiotic combination used per 40g PMMA</b>
(Bertazzoni et al., 2004)	0.76 g gentamicin $\pm$ 1 g vancomycin
(Anagnostakos et al., 2009; Whittaker et al., 2009)	0.25 g gentamicin $\pm$ 2 g vancomycin
(Masri et al., 1998)	1.2-4.8 g tobramycin $\pm$ 1-2 g vancomycin
(Hsieh et al., 2004)	4 g vancomycin $\pm$ 2 g piperacillin
Koo <i>et al.</i> , 2001	1 g gentamicin $\pm$ 1 g vancomycin +1 g cefotaxime
(Evans, 2004; Ha, 2006; Kurd et al., 2010)	3.6-4.8 g tobramycin $\pm$ 4 g vancomycin
(Park et al., 2010)	4.5 g piperacillin-tazobactam $\pm$ 2 g vancomycin  $\pm$ 1 g erythromycin

Table 3: Antibiotic combinations used for the impregnation of PMMA bone cement spacers for hip and knee prosthetic infections.

#### **1.4.2 Prophylaxis**

Antibiotic loaded bone cements (ALBC)s are routinely used in hip and knee TJRs, not only in the treatment of prosthetic infections, but also to prevent infections after cemented replacements, and their use has become a well-established practise along with peri-operative systemic antibiotics (Engesaeter et al., 2006; Parvizi et al., 2008). More than 90% of surgeons use ALBC in primary TKR in the UK (Malik et al., 2005), Sweden (Robertsson et al., 2001), and Norway (Engesaeter et al., 2006). The use of ALBC in knee replacements reduces the percentage of prosthetic infection compared to bone cements lacking antibiotics (Chiang and Chiu, 2012; Srivastav et al., 2009). Similarly, the use of ALBC in hip replacements improves survivorship by reducing the risk of prosthetic infections after primary replacements (Dunbar, 2009; Espehaug et al., 2002). A meta-analysis evaluating

the efficacy of ALBC in hip replacements reported that the use of ALBC reduces prosthetic infections after primary hip replacements from 2.3% to 1.2%, and 40% after revision (Parvizi et al., 2008).

Local antibiotic release from the bone cement gives higher concentration in the joint compared with systemic antibiotics, which are hindered by limited blood circulation at the site of implantation (Nandi et al., 2009; H. L. Tan et al., 2012). Moreover, local delivery of antibiotics avoids the adverse effects of high antibiotic levels in the blood, such as nephrotoxicity and ototoxicity (Chandrika and Garneau-Tsodikova, 2016). Hence, ALBC provide an alternative strategy for the prosthetic infection prophylaxis.

The antibiotic loaded acrylic bone cements available commercially can be either a premixed powder, where the antibiotic is blended with the cement powder by the manufacturer, or an off-label formulation. In off-label formulations the antibiotic powder is provided separately to be mixed with the cement by the surgeon during surgery (Lewis and Janna, 2006; Meyer et al., 2011). Low concentrations of the antibiotic (0.5-1.0 g per 40 of powder) are used for primary arthroplasty prophylaxis and second stage of a two-stage revision arthroplasty, while high concentrations (2.0-4.0 g per 40 g powder) are used for the treatment of existing active infection (Lewis, 2009).

<b>Brand</b>	<b>Antibiotics</b>	<b>Antibiotic used per 40g PMMA</b>	<b>Manufacturer</b>
Palacos R+G	Gentamicin	1.0 g	Zimmer
Palacos LV+G	Gentamicin	1.0 g	Zimmer
CMW 1	Gentamicin	1.0 g	DePuy
CMW 2	Gentamicin	1.0 g	DePuy
SmartSet GHV	Gentamicin	1.0 g	DePuy
SmartSet GMV	Gentamicin	1.0 g	DePuy
Simplex P	Tobramycin	1.0 g	Stryker
Copal G+V	Gentamicin ±Vancomycin	0.5 g ±2.0 g	Heraeus
Copal G+V	Gentamicin ±Clindamycin	1.0 g ±1.0 g	Heraeus

Table 4: Some of the commercially available antibiotic loaded bone cement brands

The choice of antibiotic for incorporation in the bone cement depends on several factors. Desirable antibiotic characteristics include availability in powder form, broad antibacterial spectrum, thermal stability to withstand the high exothermic temperature of the setting reaction, elution from the bone cement for prolonged period of time, low allergic effects and most importantly low influence on the mechanical properties of the bone cement (Anagnostakos and Kelm, 2009). Among the antibiotics used, which usually meet these criteria, are aminoglycoside (gentamicin and tobramycin) (Scott and Higham, 2003) and glycopeptides (vancomycin) (Jackson et al., 2011). The combination of antibiotics from more than one group gives a wide antimicrobial spectrum (Duey et al., 2012). *Table 4* shows some of the commercially available bone cement brands and the incorporated antibiotics.

## **1.5 Limitations for antibiotic loaded bone cements**

### **1.5.1 Antibiotic elution properties from bone cement**

The elution kinetics of antibiotics from PMMA bone cements are highly variable and depend on many factors. Different brands of bone cements come with different compositions, viscosities and porosities (Gálvez-López et al., 2014; Penner et al., 1999). Hence the difference in their ability to release antibiotics. Porosity is introduced into the cement by the formation of air bubbles during the exothermic setting reaction and depends on the viscosity and manipulation technique (Dunne and Orr, 2001). Porosity increases antibiotic elution from bone cement but at the same time has a negative impact on its mechanical properties (Xu et al., 2001). Among other factors affecting elution kinetics is type of antibiotic used or antibiotic combinations (Buttaro et al., 2005; Duey et al., 2012).

The ideal ALBC should sustain the release of antibiotic at high concentration above inhibitory concentrations for a long period of time to prevent early onset infections and avoid the development of resistant bacterial strains (Anagnostakos and Kelm, 2009). However, the antibiotic release from ALBC, in reality, is characterised by initial uncontrolled burst release for the first few hours after surgery. Subsequently, the antibiotic release drops rapidly below inhibitory levels within few days, and does not provide long term sustained delivery of antibiotics (Dunne et al., 2008; Gasparini et al., 2014; Moojen et al., 2008; Squire et al., 2008). Moreover, more than 90% of the loaded antibiotic may still be entrapped within the hydrophobic PMMA matrix (Dunne et al., 2007; Van et al., 2000). The initial burst release occurs when the ALBC is exposed to fluid surrounding the joint and mainly a surface phenomenon because of the presence of antibiotic agglomerates on the surface of bone cement, while the sustained release over the next few days is a bulk phenomenon and more affected by the porosity of cement (van de Belt et al., 2001).

### **1.5.2 Development of antimicrobial resistance**

Antibiotic burst release from the bone cement is followed by slow release of antibiotic at low concentrations below the minimum inhibitory concentration needed to kill bacteria (Gasparini et al., 2014; Moojen et al., 2008). This slow release increases the chances for selecting resistant microbial strains which raises

concerns about future effectiveness of antibiotics used in ALBCs (Campoccia et al., 2010; Fulkerson et al., 2006). The bacterial strains selected at low antibiotic concentrations are generally highly resistant (Sandegren, 2014). Some experimental studies show the capacity of pathogens to grow on the surface of ALBC and the ability to form biofilms (van de Belt et al., 2001; Zimmerli et al., 2004). Anguita-Alonso *et al.* (2005) investigated the susceptibility of *Staphylococcus* taken from patients with prosthetic infection against gentamicin and tobramycin (aminoglycoside antibiotics). 41% and 66% of bacteria were resistant to gentamicin and tobramycin respectively. Corona et al. (2014) compared antibiotic susceptibility between patients having infection for the first time and patients with previous use of ALBC and found a significantly higher resistance, indicating the risk of selecting aminoglycosides resistant strains after using ALBC.

### **1.5.3 Antibiotics effect on the mechanical properties of bone cement**

Addition of antibiotics to bone cements has a negative impact on their mechanical properties. Small quantities of antibiotics (< 1g per 40 g of bone cement) slightly decrease compressive and bending strength of bone cement but stays in the acceptable range stated by the standard ISO 5833:2002, while high antibiotic quantities cause a significant decrease in the mechanical properties (Krause and Hofmann, 1989; Lewis and Janna, 2006). The acceptable ranges for the mechanical properties of a set bone cement are > 70 MPa compressive strength, > 1800 MPa bending modulus and >50 MPa bending strength (Lee, 2005). High dose ALBCs (>2g per 40g cement) are only used temporarily in spacers for the treatment of prosthetic infection in two stage surgery, because their poor mechanical properties, while low dose ALBCs (< 2g per 40g cement) are used for prophylaxis where mechanical properties are important for implant fixation (Dunne et al., 2008; Paz et al., 2015). Persson et al. (2006) reported a detrimental decrease in the bending (-22%) and fatigue strength (-15%) of bone cement when vancomycin was added at 2.5% w/w. (He et al., 2002) observed that the use of gentamicin at concentrations below 3% had no significant effect on the compressive and elastic modulus of bone cement; however, higher concentrations caused significant decrease in these two parameters.

## **1.6 Novel bone cement nano-formulations**

### **1.6.1 Role of nanotechnology**

Currently used antibiotics have many limitations including microbial resistance, narrow therapeutic index, cytotoxicity and side effects linked to non-selectivity in their mode of action and poor release profiles from carrier systems. Nanotechnology, which refers to the production and application of materials in the size range (1-100nm), has been used in the treatment of many diseases such as cancer (Tiwari, 2012), inflammation (Chaudhary et al., 2014), hypertension (McLendon et al., 2015). The success of nanotechnology in improving drug release in the treatment of many diseases makes it an appealing approach for application in antimicrobial therapy. Nowadays, the development of antimicrobial resistance is rapidly increasing compared to the discovery of new antimicrobial agents. Therefore, the development of nanotechnology drug delivery systems or new antimicrobial nanomaterials can be used to overcome the problems of insufficient delivery of antimicrobial agents and resistance to currently used antimicrobials (Huh and Kwon, 2011).

Novel nanotechnology drug delivery systems offer many advantages to overcome the current challenges with antimicrobial therapy. Nanoparticles have unique physicochemical properties such as large ratio of surface area to mass, small size, and ease of structural or functional modification. The antibiotics can be loaded into nanoparticles by physical encapsulation, adsorption or chemical conjugation where the drug release profiles can be significantly altered compared to free drug counterpart, enhancing poor delivery of drugs and sustaining release (Sharma et al., 2012). In addition, specific microbial resistance mechanisms to antibiotics can be overcome by the use of nano-systems, which act on multiple biological pathways present in most types of bacteria (Kalhapure et al., 2015). Moreover, nano-carriers can be used for the delivery of multiple antibiotics to provide synergistic effect against resistant strains (Zhang et al., 2010). Nanoparticles labelled antibiotics increase binding to bacteria and the concentration at the site of infection. These improvements can be attributed to the enhanced solubility of drugs and controlled release profiles. Also, nano-systems decrease side effects by enhancing cellular internalization and uniform distribution in the target tissue, and improving the pharmacokinetic profiles and patient compliance to antibiotics

(Mansour et al., 2009). Compared to antibiotic synthesis, the preparation of nanoparticles is cost-effective giving stable formulations for long term storage. Although, antibiotics can be degraded easily at harsh conditions, nanoparticles can withstand harsh conditions such as high temperature and sterilization (Huh and Kwon, 2011).

The use of nanotechnology as antimicrobial treatment offers another platform to fill the gap where antibiotic frequently fail. The advantages of non-antibiotic based antimicrobial agents are their diversity of mode of action, broad spectrum of activity against multidrug resistant strains and biofilms (Beyth et al., 2015). This can be done through the delivery of nanoparticles with antimicrobial properties such as silver (Ge et al., 2014), dendrimer (Abid et al., 2017), etc. Alternatively, non-antibiotic biocidal agents can be loaded in nano-carrier systems to enhance its activity and its antimicrobial properties (Chen and Liu, 2015).

### **1.6.2 Nanotechnology based antibiotic based antimicrobial bone cements**

Nanotechnology based antibiotic delivery systems is becoming a new approach for solving the limitation of antimicrobial therapy. Nanoparticles can be used to improve the release kinetics of antibiotics by enhancing delivery and providing controlled release. These improvements are attributed to large area to mass ratio and small size, and different ways available for modification and for antibiotic loading (Sharma et al., 2012). Many nanotechnology based antibiotic carriers have been researched to improve the antibiotic release profile from PMMA bone cement including liposomes (Ayre et al. 2016), mesoporous silica, carbon nano-tubes, hydroxyapatite nano-rods (Shen *et al.* 2016) and clay nanotubes (Wei et al., 2012).

Although liposomes have miscibility problems in non-aqueous environment because of their hydrophilic surface, they were used to improve gentamicin distribution within PMMA bone cement. Liposomes have been largely used as drug carrier in aqueous suspensions, and have miscibility problems when mixed with PMMA leading to phase separation (Miller et al., 2011). Ayre et al. (2016) solved the problem of phase separation by using Pluronic on the surface of liposomes (Ayre et al., 2016).

Pluronic are surfactants made of interconnected chains of polyethylene oxide (PEO) and poly propylene oxide (PPO) subunits. It is hypothesized that the

hydrophilic PEO will attach to the hydrophilic surface of liposomes, while the PPO will attach to the hydrophobic matrix of PMMA. Liposomes were suspended to the liquid MMA part of cement before mixing with PMMA powder. Moreover, pelleted liposomes of 100 nm size were prepared by extrusion and ultra-centrifuged with 3 different Pluronic surfactants (L31, L43, and L61). Gentamicin release from liposomal bone cement was sustained for 30 days with 22% of the loaded antibiotic released compared to 9% from commercial formulation. Gentamicin release was characterized by burst release in the first 72 hrs for commercial bone cement, while liposomal cement showed nearly linear release profile. Despite the slight reduction in compressive strength, the liposomal formulation enhanced the toughness, bending strength and Vickers hardness of cement when compared to Palacos R+G. The addition of liposomes improved the dispersion of gentamicin in bone cement and improved the mechanical properties as well.

In another work, Shen *et al.* (2016) mesoporous silica nanoparticles (MSN) were used to improve the release kinetics of gentamicin from PMMA bone cement (Shen et al., 2016). The presence of 10% MSN enhanced the release for more than 60% of loaded gentamicin over 80 days. Furthermore, the concentration of MSN was found to be crucial to build a nano network to facilitate the diffusion of gentamicin molecules. Hence, MSN concentration below 6 % could not improve gentamicin release. The compressive strength of MSN functionalised bone cements is nearly the same as the commercial bone cement. However, the bending modulus is reduced by 10%. Moreover, the 10% MSN bone cement was cytocompatible with 3T3 mouse fibroblasts, showing 96% cell viability in 3T3 mouse.

Carbon nanotubes (CNT) were also tested for enhancing gentamicin release from PMMA bone cement. Although 5% CNT loaded bone cement lead to 75% release of gentamicin for 60 days, the compressive strength reduced by 90% compared with the commercial bone cement. Furthermore, CNT showed high toxicity to 3T3 mouse fibroblasts with 85% cell viability. Cytotoxicity of CNTs is a concern for its application in biological systems and it has also attracted more attention in recent investigation (Firme and Bandaru, 2010). In the same work, hydroxyapatite nano-rods (HAP) were loaded with gentamicin by wet impregnation and loaded

into PMMA bone cement at 32% concentration. At this concentration, 75% gentamicin was released over 60 days. Despite low cytotoxicity of HAP, as it is one of major compositions of bone structure, the compressive strength is decreased by 50% compared to the commercial bone cement.

In another study, clay nanotubes Halloysite was used to improve gentamicin release from PMMA bone cement (Wei et al., 2012). Halloysite is a naturally occurring nanotube with a length of 500–1000 nm, diameter of 50 nm, and lumen of 15 nm. Therefore, it is highly biocompatible as confirmed by blue cell essays on HeLa and MCF-7 cell lines (Vergaro et al., 2010). PMMA bone cement was loaded with 5-8% Halloysite and with 10-15% gentamicin. The release profile was characterised by burst in the first few days. After that, gentamicin release slowly continued for 250 hours. Furthermore, the addition of 5-7% Halloysite nanotubes improves the tensile strength and adhesive properties, except for flexural strength which is slightly reduced with higher concentration such as is 5% which gives both higher tensile strength and good flexural properties. *Table 5* summarizes the mechanical properties of previously mentioned nanocomposites and *Table 6* is a list of different nanotechnology based antibiotic loaded PMMA bone cements.

	Compressive strength (MPa)	Bending strength (MPa)	Bending Modulus (MPa)	Fracture Toughness (MPam <sup>1/2</sup> )	Vickers Hardness (MPa)
Liposomes (L31)	80.8	79	3200	3.0	26.6
Mesoporous silica	85	-	2100	-	-
Carbon nano-tubes	8.7	-	-	-	-
Hydroxyapatite nano-rods	43.5	-	-	-	-
Clay nano-tubes	-	35	-	-	-

Table 5: Summary of mechanical properties for different PMMA nanocomposites.

Nano-carrier	% of NPs in bone cement	Loading capacity of gentamicin	Duration of release	% of gentamicin released	Tested bacteria	Limitation	Reference
Liposomes		----	30 days	22	S. aureus	--	(Ayre et al. 2016)
Mesoporous silica	10	----	80 days	60	---	--	(Shen et al., 2011)
Carbon nano-tubes	5	----	60 days	75	----	Cytotoxicity, negative impact on mechanical properties	(Shen et al., 2016)
Hydroxyapatite nano-rods	32	----	60 days	75	----	Negative impact on mechanical properties	(Shen et al., 2016)
Clay nano-tubes	5-7	10-15	10 days	60	S. aureus, E. coli	Burst release	(Wei et al. 2012)

Table 6: Summary list of nanotechnology based antibiotic loaded PMMA bone cements.

### 1.6.3 Non-antibiotic based antimicrobial bone cements

Quaternary ammonium compounds attracted research because of their antimicrobial properties and stable structure (Abid et al., 2017). Chitosan quaternary ammonium nanoparticles impregnated bone cement showed antimicrobial activity against viable bacterial at a concentration of 15% w/w (Shi et al., 2006). In another study, hydroxypropyl trimethyl ammonium chloride chitosan loaded (HACC) bone cement inhibited biofilms caused by methicillin-resistant *Staphylococcus* strains showing in vitro release for 120 hours (Tan et al., 2012), with enhanced physical and osteogenic properties (Tan et al., 2012). HACC-loaded bone cement was further evaluated in vivo for the treatment of Methicillin-resistant *Staphylococcus epidermidis* infection of the tibial metaphysis in a rabbit model, and exhibited effectiveness in the inhibition of bone infections (Tan et al., 2014). One quaternary ammonium dendrimer of tripropylene glycol

diacrylate (TPGDA) was mixed with bone cement at a concentration of 10%. At this concentration, TPGDA modified bone cement showed antimicrobial activity for 30 days. In addition, the dendrimer bone cement composite was potent to kill 108 CFU/mL of bacteria on regular intervals of 5 days for a month. However, the addition of dendrimer resulted in a reduction of compressive strength (>15%) compared to the original sample. Furthermore, the MTT (Methylthiazolyl tetrazolium) assay for the dendrimer modified bone cement showed 12.5% reduction in the viable cells compared to the control, and further determination of cytotoxicity is needed (Abid et al., 2017). *Table 7* summarizes some examples of antimicrobial bone cements with potential application in total joint arthroplasties.

Quaternary ammonium chitosan derivative nanoparticles (QCS) achieved a 103-fold reduction in the number of viable bacterial cells upon contact with the surface when added at concentration of 15% to bone cement. Chitosan in the form of nanoparticles is better in preserving the mechanical properties of the bone cement compared to powdered chitosan, i.e. Young modulus and bending modulus is >90% of the original bone cement values. When the Chitosan (powder not Nanoparticles) loading was decreased to 15%, the Young's modulus and bending modulus are about 90% of the corresponding properties of the original bone cement. This can be explained by the homogenous distribution of nanoparticles inside the bone cement matrix, which minimizes the macroscopic cracks in cement mantle. QCS nanoparticles showed higher antimicrobial activity compared to chitosan nanoparticles at the same concentration, where the viable cell number declined by about three orders and two orders of magnitude, respectively. However, The MTT assay showed that there is no significant difference in cytotoxicity between the chitosan NP, QCS NP and the non-toxic control (Shi et al., 2006).

Silver nanoparticles have many applications in medical field as safe and effective antimicrobial agents, such as bandages, catheters and surgical scrubs (Ge et al., 2014). Oei et al. (2012) investigated the antimicrobial properties of a PMMA bone cement impregnated with silver nanoparticles (Oei et al., 2012). Despite in vitro release of silver ions for 28 days and broad spectrum antimicrobial activity, the mechanical properties of bone cement was negatively affected at the concentration used (1% w/w) and showed lower bending modulus. Silver nanoparticles prepared

with different capping agents were studied for bone cement impregnation. Prokopovich et al. (2015) reported a broad spectrum antimicrobial activity of silver nanoparticles capped with oleic acid at low concentrations of 0.05 w/w %, without affecting the mechanical properties and cytotoxicity of the bone cement (Prokopovich et al., 2015). Similar preferable antimicrobial and mechanical properties were identified when silver nanoparticles capped with tiopronin were impregnated in PMMA bone cement at a concentration of 0.1 w/w % (Prokopovich et al., 2013).

In another study, Perni et al. (2015) developed a propyl paraben nanoparticle loaded bone cement at a concentration of 7% w/w (Perni et al., 2015). Nanoparticles at this concentration exhibited wide spectrum antimicrobial killing with no detrimental effect on mechanical properties and cytocompatibility.

Type of Antimicrobial nanoparticles	% of NPs in bone cement	Duration of release	% released	Antimicrobial spectrum	Tested bacteria	Mode of action	Limitations	Reference
Chitosan	15	---	---	Broad spectrum (Gram positive and Gram negative)	S. aureus, S. epidermidis	Interaction with negatively charged cell wall and cell lysis.	---	(Shi et al., 2006)
QCS	15	---	---	Broad spectrum (Gram positive and Gram negative)	S. aureus, S. epidermidis	Interaction with negatively charged cell wall and cell lysis.	---	(Shi et al., 2006)
dendrimer	10	30 days	---	Broad spectrum (Gram positive and Gram negative)	S. aureus, E coli, P. aeruginosa	Interaction with negatively charged cell wall and cell lysis.	Cytocompatibility problems	(Abid et al., 2017)
Silver nanoparticles	1	28 days	---	Broad spectrum (Gram positive and Gram negative)	P. aeruginosa, A. baumannii, S. aureus, P. mirabilis	Ag NPs or Ag ions can interact with DNA replication, respiratory chain and cell division.	Negative effect on mechanical properties	(Oei et al., 2012)
oleic acid capped Silver nanoparticles	0.05	---	---	Broad spectrum (Gram positive and Gram negative)	S.aureus MRSA S. epidermidis A. baumannii	Ag NPs or Ag ions can interact with DNA replication, respiratory chain and cell division.	---	(Prokopovich et al., 2015)
Tiopronin capped Silver nanoparticles	0.1	---	---	Broad spectrum (Gram positive and Gram negative)	MRSA	Ag NPs or Ag ions can interact with DNA replication, respiratory chain and cell division.	---	(Prokopovich et al., 2013)

Propyl paraben	7	5	---	Broad spectrum antibacterial (Gram positive and Gram negative) and antifungal activity	S. aureus MRSA S. epiermidis A. baumannii	Inhibition of the synthesis DNA and RNA or ATPases and phosphotransfer ases	---	(Perni et al., 2015)
----------------	---	---	-----	--	--	---	-----	----------------------

Table 7: Summary list of nanotechnology non-antibiotic based antimicrobial PMMA bone cements

## 1.7 Drug delivery systems and nano-formulations for potential use in bone cements

One of the novel approaches for enhancing the delivery of aminoglycoside antibiotics is “Layer by Layer” assembly (LbL). LbL has numerous applications in drug delivery (Deshmukh et al., 2013). This coating technique is a versatile method and involves the deposition of alternative oppositely charged polyelectrolytes on different substrates, allowing control of the thickness and composition of coating at nanoscale level in a reproducible manner (Ariga et al., 2011; Vergaro et al., 2011). Tamanna et al. (2015) managed to control the release of gentamicin from gentamicin-loaded mesoporous silica nanoparticles coated using LbL technique (Tamanna et al., 2015). The coating polyelectrolytes were polystyrene sulfonate and poly (allylamine hydrochloride). The coated layer controlled drug release for 10 days with no burst release compared to the same gentamicin loaded nanoparticles without coating.

Mu et al. (2016) evaluated the antimicrobial properties of phosphatidylcholine-decorated Au nanoparticles loaded with gentamicin (size 180 nm), which showed broad spectrum activity and inhibition of biofilm formation (Mu et al., 2016). The presence of phosphatidylcholine on the surface facilitated the electrostatic binding of gentamicin. The nanoparticles were more efficient in the inhibition of *Pseudomonas aeruginosa* and *Staphylococcus aureus* biofilm, when compared to gentamicin or phosphatidylcholine Au nanoparticles without gentamicin. Gentamicin release continued for 7 days in buffer media pH 7.4, and the loading efficiency was 38µg/ml (gentamicin/Au). Cytocompatibility studies were done using RAW 264.7 cells and the nanoparticles were nontoxic and can be engulfed by macrophages.

Fan et al. (2016) loaded chlorhexidine on Ca-silicate mesoporous nanoparticles (size 78.6 nm) using mixing-coupling technique (Fan et al., 2016). The nanoparticles were able to release chlorhexidine as well as Ca<sup>2+</sup> and silicate<sup>2-</sup> ions for up to 9 days in simulated body fluids. They showed antimicrobial activity against *Enterococcus faecalis* which is commonly reported to be involved in root canal infection. The nanoparticles did not show any negative effect on cell

proliferation and showed in vivo mineralization effect, which give them the potential to be used in intra-canal defects or bone infections.

Poly (lactic-co-glycolic acid) (PLGA) is hydrophobic biodegradable and biocompatible polymer that is approved for clinical use. Abdelgahany et al. (2012) prepared gentamicin PLGA nanoparticles through emulsion evaporation method, using two approaches: water/oil/water and solid/oil/water (Abdelghany et al., 2012). The size for the nanoparticles were 251 nm and 359 nm, respectively, with loading efficiency reached up to 22.4 µg/ml. Gentamicin release from the nanoparticles continued for up to 16 days at pH 7.4. In addition, the nanoparticles showed antimicrobial activity against *P. aeruginosa* planktonic bacteria and biofilms, as well as in vivo infected mice model.

Kurtjak et al. (2016) loaded gallium nanoparticles (size 22nm) into hydroxyapatite nano-rods bioactive composite through ultrasonic emulsification (Kurtjak et al., 2016). The gallium nanocomposite showed better antimicrobial properties against *Pseudomonas aeruginosa*, when compared to silver nanocomposite, as illustrated by microdilution assay and MIC (minimum inhibitory concentration) determination. Also, gallium nanoparticles had lower toxicity for human lung fibroblast and mouse fibroblasts.

## 1.8 Aim of the project

Given the severe problems associated with prosthetic infections after total joint replacements, it becomes evident the need to develop antimicrobial bone cements with better performance and outcome for total joint replacement to improve patients' quality of life.

In this context, the present PhD project aims to develop a novel nano-composite antimicrobial bone cement containing antibiotic or non-antibiotic antimicrobial agents or a combination of both, for the prevention of prosthetic infections after total joint replacement which is one of the major causes for revision surgery. The antimicrobial agents to be tested are gentamicin and chlorhexidine, either alone or in combination, to evaluate potential synergism or additive antimicrobial effect needed to overcome the problem of antibiotic resistance mentioned earlier. We hypothesize that the release of antimicrobial agents from the bone cement can be sustained at inhibitory concentrations for a long time (3-6 months) using LbL assembly technique combined with nanotechnology. In order to provide prophylaxis from post-surgical orthopaedic infections, both early and late stage infections. To the best of our knowledge, the LbL assembly technique has not been applied before to control the release of antibiotics from bone cement.

To accomplish this aim, the following objectives were defined:

- (i) Novel nanotechnology based antimicrobial drug delivery system development:

In the initial stage, silica nanoparticles were prepared, which are broadly applied as drug delivery carrier because of their biocompatibility, high loading capacity, ease of synthesis and scale up with reasonable cost. Silica nanoparticles were functionalised with amino group to allow further modifications on their surface through the deposition of cationic or anionic polyelectrolytes, and antimicrobial agents, during LbL multilayer coating process.

Gentamicin has been employed as a model antibiotic, which is a widely-used aminoglycoside antibiotic in TJR, because of its' wide spectrum antimicrobial activity and thermal stability during the exothermic setting reaction of PMMA bone cement. Gentamicin was loaded on the silica nanoparticles using layer by

layer assembly (LbL), allowing control of coating thickness and composition at nanoscale level in a reproducible manner. In addition, chlorhexidine has been employed as a model antimicrobial non-antibiotic agent, which is widely used as antiseptic and disinfectants skin infections, cleaning wounds, preventing dental plaque, yeast infections of the mouth, for disinfecting urinary tract catheters and sterilisation of surgical instrument.

Different polyelectrolytes were used to coat the surface of silica nanoparticles during LbL coating process using hydrolysable and non-hydrolysable polymers, controlling the release of gentamicin, chlorhexidine, or a mixture of both from polyelectrolyte multilayers on the surface of silica nanoparticles. In addition, the polyelectrolytes aid in antibiotic loading between different layers by electrostatic attraction between oppositely charged species. Silica nanoparticles with different coatings and loaded antimicrobial agents were characterised by transmission electron microscopy (TEM), thermogravimetric analysis (TGA), zeta potential, Fourier transform infra-red spectroscopy (FTIR), and drug release testing in different release media representing healthy and infected joint.

(ii) PMMA bone cement loaded with the novel antimicrobial nanoparticles:

After full characterisation of the newly developed novel LbL multilayer nano-drug delivery system, the nanoparticles with different types of coatings and antimicrobial agents were loaded into the PMMA bone cement. Then, the newly formed nanocomposites were evaluated for the following properties:

1. Bone cement settling time.

The influence of nanoparticles on bone cement settling time was determined through rheological tests, in particular dynamic oscillation tests.

2. Antimicrobial agent release quantification.

the release of antimicrobial agents from bone cement was evaluated and compared against commercial formulations e.g. Cemex G and Palacos R *in vitro*.

3. Microbial testing.

The antimicrobial properties were determined once the nanoparticles incorporated into bone cement against common bacteria reported to cause post-orthopaedic surgery infections, such as: *Staphylococcus aureus*, *MRSA*, *S. epidermidis* and *Acinetobacter baumannii*. Moreover, they were compared with the antimicrobial properties of commercial formulations for ALBCs, e.g. Cemex G and Palacos R.

4. Mechanical testing.

Mechanical properties of the nanocomposite were determined against commercial formulations for ALBCs, e.g. Cemex G. In order to assess the effect of incorporated nanoparticles on the mechanical properties of the bone cement, such as compression, bending strength and fracture toughness.

5. Water uptake studies.

When immersed in fluids, the increase of bone cement containing nanoparticles because of water uptake was monitored, and compared to commercial formulations to evaluate the influence of nanoparticles incorporation on the physicochemical properties of the bone cement, in particular hydrophilicity.

6. Nanoparticles distribution:

Fluorescence images were taken for the surface and inside of the bone cement to evaluate the homogeneity of distribution of nanoparticles and compare it to antibiotic powder distribution in commercial cements.

7. Cytotoxicity testing.

The cytocompatibility was verified for the PMMA impregnated bone cement against commercial formulations e.g. Cemex G using relevant cell lines e.g. osteoblasts, to make sure that the newly formed nanocomposite is biocompatible with bone tissue, e.g. Methylthiazolyl tetrazolium (MTT) assay, Lactase dehydrogenase release (LDH) assay test, osteoblast calcium production assay (alizarin red), Nitric oxide production and fluorescence imaging.

## **2 General methods**

This chapter refers to some of the common methods that have been used for the preparation of different nanoparticles and bone cements, and testing their properties throughout this thesis. Later chapters will refer to these methods to reduce repetition with highlighting main differences in nanoparticle and nanocomposite formulation. Test methods that are specific to certain chapters will be described in detail in the appropriate chapter.

### **2.1 Nanoparticles preparation and characterisation**

#### **2.1.1 Chemicals**

Triton X-100, tetraethyl orthosilicate (TEOS), 3-aminopropyltriethoxysilane (APTS), sodium alginate (Mw 80.000-120.000 Da), chitosan (Mw 190.000-310.000 Da), gentamicin sulphate, sodium acetate trihydrate, phosphate buffer solution (PBS) tablets, o-phthaldialdehyde reagent solution (OPA) were purchased from Sigma-Aldrich, UK. Cyclohexane, n-hexanol, ammonium hydroxide (35%), ethanol, methanol, glacial acetic acid and iso-propanol were purchased from Fishers scientific, UK. All reagents were stored according to manufacturer's guidelines and used as received. B1: is a patented biocompatible, biodegradable Poly-beta-amino-ester (PBAE) polymer, the precise structure will remain confidential due to the IP associated, was freshly prepared in the lab before use.

Acetic acid-sodium acetate buffer was prepared as follows: to prepare 100 ml acetic acid-sodium acetate buffer (0.1 M, pH 5), 30 ml of sodium acetate trihydrate ( $\text{CH}_3\text{COONa}\cdot 3\text{H}_2\text{O}$ ) (0.1 M) were added to 70 ml of acetic acid ( $\text{CH}_3\text{CO}_2\text{H}$ ) (0.1 M) solutions and stirred. Phosphate buffer saline (PBS) (pH 7.3) was prepared by dissolving 1 tablet of PBS in 100 ml of deionized water.

#### **2.1.2 Nanoparticle preparation**

##### **2.1.2.1 Amino functionalised silica nanoparticle synthesis**

Silica nanoparticles functionalised with amine groups ( $\text{SiO}_2\text{-NH}_2$ ) were prepared in one-pot synthesis by hydrolysis of TEOS in reverse micro-emulsion and subsequent functionalization with amino group (Stöber method) (Stöber et al., 1968). In a typical synthesis, Triton X-100 (17.7 g) was mixed with 16 ml of n-hexanol, 75 ml of cyclohexane, and 4.8 ml of deionised water under vigorous

stirring. Once the solution was transparent, 600  $\mu$ l of ammonium hydroxide (29.6%) was added. The solution was subsequently sealed and stirred for 20 minutes, followed by addition of 1 ml of TEOS and stirring for 24 hours. The silica nanoparticles surface was functionalised with amino groups by adding 50  $\mu$ l of APTS to the micro-emulsion under stirring and incubating further 24 hours. The SiO<sub>2</sub>-NH<sub>2</sub> nanoparticles were recovered by adding ethanol (200 ml) to break the micro emulsion and centrifuging at 14000 rpm for 10 minutes (LE-80K, Ultracentrifuge, Beckman Coulter, UK) at 20 °C (35280 g). The nanoparticles were vigorously washed three times with deionized water. Finally, the washed nanoparticles were left to dry at room temperature in a fume hood for 24 hours.

#### **2.1.2.2 Layer by Layer (LbL) coating technique**

The amino functionalised silica nanoparticles were layered with different numbers of a repeating sequence of polyelectrolytes: sodium alginate as a polyanion, a polycation (chitosan, B1) and drug with antimicrobial activity (gentamicin or chlorhexidine). Different sequences were composed of a repeating unit of four layers making one quadruple layer (Q). Up to ten quadruple layers were coated onto silica nanoparticles (*Table 9*). The following concentrations of the polyelectrolytes and the drugs in acetic acid-sodium acetate buffer (pH 5) were used in LbL: sodium alginate (2 mg/ml), gentamicin (10 mg/ml) and chitosan (2 mg/ml).

Quadruple layer no.	Abbreviation	Layers on the surface of amino functionalised silica nanoparticles (SiNH <sub>2</sub> )
1	Q1	SiNH <sub>2</sub> -alginate- <b>drug</b> -alginate- <b>polycation</b>
2	Q2	SiNH <sub>2</sub> -Q1-alginate- <b>drug</b> -alginate- <b>polycation</b>
3	Q3	SiNH <sub>2</sub> -Q2-alginate- <b>drug</b> -alginate- <b>polycation</b>
4	Q4	SiNH <sub>2</sub> -Q3-alginate- <b>drug</b> -alginate- <b>polycation</b>
5	Q5	SiNH <sub>2</sub> -Q4-alginate- <b>drug</b> -alginate- <b>polycation</b>
6	Q6	SiNH <sub>2</sub> -Q5-alginate- <b>drug</b> -alginate- <b>polycation</b>
7	Q7	SiNH <sub>2</sub> -Q6-alginate- <b>drug</b> -alginate- <b>polycation</b>
8	Q8	SiNH <sub>2</sub> -Q7-alginate- <b>drug</b> -alginate- <b>polycation</b>
9	Q9	SiNH <sub>2</sub> -Q8-alginate- <b>drug</b> -alginate- <b>polycation</b>
10	Q10	SiNH <sub>2</sub> -Q9-alginate- <b>drug</b> -alginate- <b>polycation</b>

*Table 8: 10 quadruple layers' abbreviations and constituents used for LbL coating on silica nanoparticles.*

The procedure for LbL technique was the following: the dried amino functionalised silica nanoparticles were placed in a test tube and dispersed in 20 ml of sodium alginate solution and stirred for 10 minutes. Then, the dispersed nanoparticles were centrifuged to precipitate nanoparticles. After that, the supernatant was removed and replaced with 20 ml of acetic acid-sodium acetate buffer as a washing step after each layer to remove traces of the layered polyelectrolyte. Then, the buffer was centrifuged and the washed nanoparticles were ready for next layer. For the second layer, 10 ml of gentamicin solution was stirred with the nanoparticles for 10 minutes, centrifuged and washed again with buffer. Next, sodium alginate solution was layered again and washed. Finally, 20 ml of the polycation (either chitosan or B1) solution was used to layer the fourth layer and washed, completing the first quadruple layer. This sequence was repeated to build up 10 quadruple layers on the surface of the silica nanoparticles.

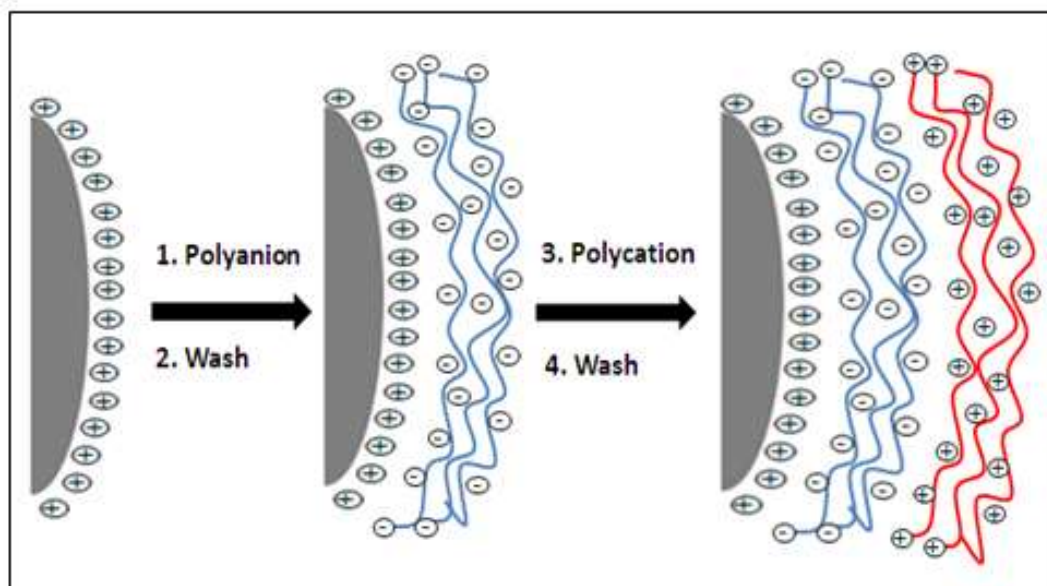


Figure 7: LBL procedure.

### 2.1.3 Nanoparticles surface and material characterisation

#### 2.1.3.1 Nanoparticles size measurements

The size of nanoparticles was characterized using transmission electron microscopy (TEM). A droplet (4  $\mu\text{L}$ ) of nanoparticles suspension was placed on a plain carbon-coated copper TEM grid and left to evaporate in air under ambient laboratory conditions for few hours. Bright field TEM images were taken using a JEOL-1010 microscope at 80 kV equipped with a Gatan digital camera. The magnification of the images was 100,000 X. Then, the images were analysed with the computer software ImageJ® and the diameters of at least 150 particles were measured.

#### 2.1.3.2 Nanoparticles Zeta potential measurements

The electrophoretic mobility for the nanoparticles was measured by dynamic light scattering (DLS), using Malvern Zetasizer, Nano ZS particle characterization system (Malvern Instruments Limited, UK). He-Ne laser (wavelength 633 nm) at an angle of  $17^\circ$  was combined with reference beam to analyse the samples. The measured electrophoretic mobility was converted to zeta potential values ( $\zeta$ ) using Henry equation:

$$UE=2 \varepsilon \zeta f (Ka) / 3\eta$$

Where  $UE$  is the measured electrophoretic mobility,  $(\zeta)$  is the zeta potential,  $(\varepsilon)$  is the dielectric constant,  $(\eta)$  describes the viscosity, and  $f(\kappa a)$  is Henry's function. Smoluchowski's approximation is commonly used to determine zeta potential for electrophoretic measurements in aqueous media using moderate electrolyte concentration, where the value of  $f(\kappa a)$  is equal to 1.5 (Sikora et al., 2015).

For zeta potential measurement, 1 mg of nanoparticles was dispersed in 1 ml of acetic acid-sodium acetate buffer solution using the vortex and the ultrasonic bath (~30min). Then, the suspension was immediately transferred into the capillary cell. Each data value was an average of three measurements.

### **2.1.3.3 Thermogravimetric analysis (TGA)**

Thermogravimetric analysis (TGA) was performed using a Perkin-Elmer TGA 4000 instrument. The samples were heated from 50 to 800 °C with a constant heating rate of 10 °C per minute. Sample weight was recorded and weight loss percentage of each sample was calculated relative to initial weight of sample, prior to heating. The organic and inorganic material percentages were calculated by subtracting the point at initial weight loss (%) up to when the line plateaus.

### **2.1.4 Gentamicin release quantification**

Gentamicin release from the nanoparticles was evaluated by dispersing the drug loaded nanoparticles (10 mg/ml) in 2 buffer media: acetic acid-sodium acetate buffer pH 5 and PBS pH 7.3, where they were kept in eppendorfs. These two pH points were chosen to assess the drug release under healthy joint (pH 7.35-7.45) (Ribeiro et al., 2012), and for infected joint, which are associated with low pH values (pH < 7) or local acidosis (Kinnari et al., 2009).

Then, samples were vigorously stirred in a vortex, and then incubated at 37°C. Samples were taken every 24 hours where 1ml of release medium aliquots were taken after centrifugation, to avoid withdrawing nanoparticles during taking the sample.

The amount of gentamicin released from the nanoparticles in the buffer was quantified through fluorescence spectroscopy instrument using o-phthaldialdehyde reagent (Perni and Prokopovich, 2014), where the reagent reacts

with the amino groups of gentamicin to give a fluorogenic product. 100 µl of buffer containing antibiotic were mixed with 100 µl of iso-propanol and 100 µl of OPA reagent solution. After 30 min at room temperature in the dark, 200 µl of the mixture were transferred in a black 96 wells plate and the fluorescence was determined (excitation wavelength = 340 nm and emission wavelength = 450 nm) with a fluoroscan (FLUOROstar Optina, BMG labtech). Average gentamicin concentrations for each time point was calculated from 3 samples, and cumulative gentamicin release was also calculated for 30 days.

Eight calibration solutions with gentamicin concentrations from 0 µg/ml to 100 µg/ml were prepared for calibration curve, and analysed simultaneously for each 96-well plate run. The standards were prepared by serial dilution of gentamicin stock (100 µg/ml) in the first 3 columns of the 96-well plate, to get three replicates for each point. A linear relationship between concentration and fluorescence was produced (Figure 8).

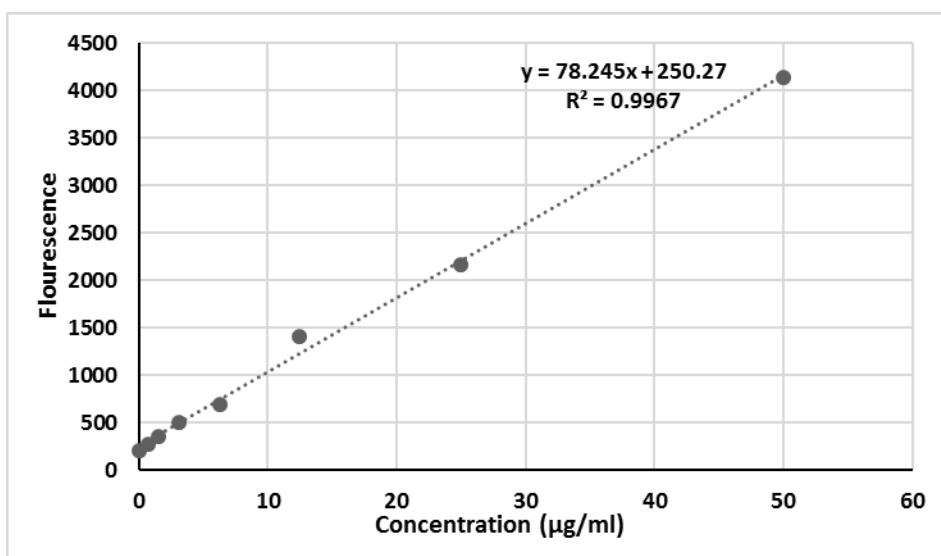


Figure 8: Representative calibration curve for gentamicin.

### 2.1.5 Chlorhexidine release quantification

Chlorhexidine release from the nanoparticles was evaluated by dispersing the drug loaded nanoparticles (10/ml mg) in 2 buffer media: acetic acid-sodium acetate buffer pH 5 and PBS pH 7.3, where they were kept in eppendorfs. These two pH points are chosen to assess the drug release under healthy joint (pH 7.35-7.45)

(Ribeiro et al., 2012), and for infected joint, which are associated with low pH values ( $\text{pH} < 7$ ) or local acidosis (Kinnari et al., 2009).

Then, samples were vigorously stirred in a vortex, and then incubated at  $37^{\circ}\text{C}$ . Samples were taken every 24 hours where 1ml of release medium aliquots were taken after centrifugation, to avoid withdrawing nanoparticles during taking the sample.

The amount of chlorhexidine released from nanoparticles was quantified using reversed-phase High Performance Liquid Chromatography (HPLC) method. The HPLC system from 1100 series Agilent Technologies®. The mobile phase was a mixture of acetate buffer pH 4 (73%), acetonitrile (27%) at a fixed flow rate of 1 ml/min. Injection volume was 20  $\mu\text{l}$  which was detected by UV detector at 239 nm. The analytical column was  $\mu\text{Bondapak C18}$  column Waters® (Ireland, UK), (pore size 125  $\text{Å}$ , 10  $\mu\text{m}$ , 3.9 mm X 150 mm). Standards of known chlorhexidine concentration were analysed to establish a calibration curve for chlorhexidine. The calibration curve was obtained by plotting the concentration ( $\mu\text{g/ml}$ ) of chlorhexidine standard versus peak area under the curve (mAu). The standard concentrations were prepared by serial dilutions of a chlorhexidine stock solution (1 mg/ml) to a range of 0.4-25  $\mu\text{g/ml}$ . Each data point is an average of three replicates.

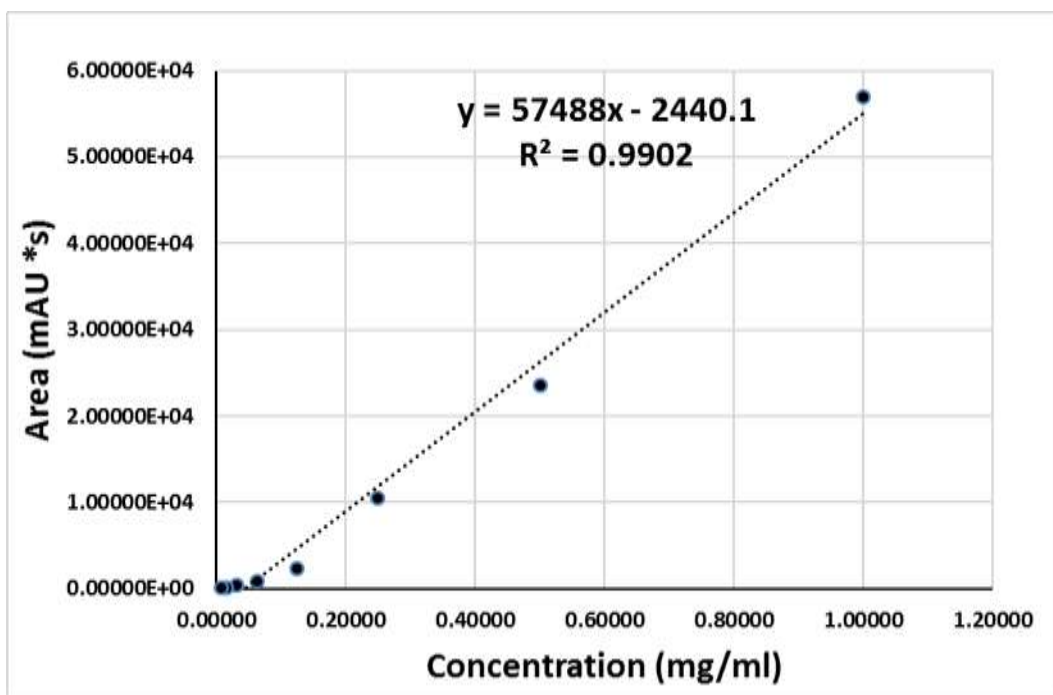


Figure 9: Representative calibration curve for chlorhexidine.

### 2.1.6 Statistical analysis

All data were expressed as means  $\pm$  standard deviation (SD) from at least three values. To assess the statistical significance of results between groups, one-way analysis of variance (ANOVA) was performed. Experimental results were considered statistically significant at 95 % confidence level ( $p < 0.05$ ). All analyses were run using the SPSS® software.

## **2.2 Bone cement preparation and characterization**

### **2.2.1 Chemicals**

Triton X-100, Tetraethyl orthosilicate (TEOS), (3-Aminopropyl) triethoxysilane (APTS), sodium alginate, chitosan, gentamicin sulphate, sodium acetate trihydrate, phosphate buffer solution (PBS) tablets, o-phthaldialdehyde reagent were purchased from Sigma-Aldrich, UK.

Cyclohexane, 1-hexanol, ammonium hydroxide 35%, ethanol, methanol, glacial acetic acid and 1-propanol were purchased from Fishers, UK. All reagents were stored according to manufacturer's guidelines and used as received. Two types of bone cements were used Cemex® (Tecres® SpA, Verona, Italy) and Palacos ® (Heraeus Medical GmbH, Wehrheim, Germany).

B1: is a patented biocompatible, biodegradable cationic polymer, the precise structure will remain confidential due to the IP associated.

### **2.2.2 Bone cement preparation**

PMMA bone cement is formed by a free radical polymerisation reaction between the liquid and powder component upon mixing. Bone cement preparation was carried out according to manufacturer's instructions and the ISO5833:2002 (Implants for surgery-Acrylic resin cements). All the contents of the bone cement were stored at recommended conditions (20-25°C for the powder and 8-15 °C for the liquid in the dark) and conditioned to room temperature (23°C) 2 hours before mixing. The powder component was sifted before weighing and mixed thoroughly, while each liquid component was weighed separately. Finally, both components were hand mixed in a polypropylene bowl with a polypropylene spatula for 1 minute, before being filled into a mould. Polytetrafluoroethylene (PTFE) moulds were used to produce samples with specific dimension for different tests. PTFE withstands the high exothermic temperature of the setting reaction, and allows for easy removal of the samples without adherence or interactions with bone cement. After applying the cement into the mould, the mould was clamped with two steel endplates covered with PTFE film at both ends. After 2 hours, the samples were pushed out of the mould using a steel rod and allowed to cure for 24±2 hours at 23°C. Then, the samples were sanded down to the correct dimensions using 320 grit silicon carbide paper.

### 2.2.3 Rheology testing

The effect of adding the nanoparticles on the cement setting time was evaluated through rheological tests using Anton Paar MRC702 (Anton Paar Ltd., UK), equipped with 6 mm diameter circular flat plates. Dynamic oscillation tests were performed in these measurements, a sinusoidal oscillation strain ( $\sigma$ ), of small amplitude ( $\sigma_0$ ) and frequency ( $\omega$ ), was applied to the sample:

$$\sigma(t) = \sigma_0 \exp(i\omega t)$$

The resulting stress ( $\omega$ ) was compared with the strain giving the complex modulus  $G^*$ .

$$G^* = \frac{\sigma(t)}{\gamma(t)}$$

Because the two sinusoidal waves will have a phase difference,  $\delta$ , the storage ( $G'$ ) and loss modulus ( $G''$ ) can be defined as the component in phase and  $\pi/2$  out of phase with the strain, respectively.

$$G^* = G' + iG''$$

and

$$G' = |G^*| \cos \delta$$

$$G'' = |G^*| \sec \delta$$

Rheological testing was conducted using dynamic time sweep test that takes successive measurements at constant frequency and strain at selected intervals. Test were conducted at room temperature, plate distance 1 mm, a strain of 0.1% and fixed frequency of 1 rad/sec. For all tests, the bone cement solid phase was mixed with the liquid phase quickly with a spatula; the mixture was deposited onto the lower plate and experiments started as fast as possible. To account for the time elapsed during mixing and pouring, a timer was started at the moment of mixing the liquid with powders. Measurement of complex Young modulus and phase angle were taken every 6 seconds for up to 10 minutes. The setting time was

extracted from each curve as the time correspondent to a local maximum of tan delta ( $G''/G'$ ). Each sweep experiment was carried out on three independently prepared cement samples, and results are presented as mean and standard deviation (Perni et al., 2015).

#### **2.2.4 Drug release quantification**

A PTFE mould was used to produce cylindrical samples with 6mm diameter and 10 mm length. Each sample weighed  $0.40 \pm 0.01\text{g}$  and three samples were used for release study for each type of bone cement. The bone cement samples were incubated in 3ml PBS buffer (pH 7) at  $37^\circ\text{C}$ . The release media was replaced each day to attain sink condition, where the concentration of released drug is negligible in comparison to its' saturation solubility. The release samples were stored in the refrigerator ( $2-8^\circ\text{C}$ ) for analysis. The concentration of gentamicin or chlorhexidine was determined in the samples using methods described previously in 2.1.4 and 2.1.5.

#### **2.2.5 Antimicrobial testing**

Cylindrical samples of 12 mm length and 6mm diameter were prepared for as previously described (section 2.2.2) for antimicrobial testing. Brain heart infusion agar (BHI) (Oxoid Ltd., Basingstoke, UK) was prepared by dissolving 47g of brain heart infusion agar powder in one litre of distilled water. The solution was shaken to suspend agar powder evenly, then sterilized in an autoclave at  $121^\circ\text{C}$  for 15 minutes. The solution was allowed to cool to  $45-50^\circ\text{C}$  before being poured into Petri dishes (9 cm diameter). The Petri dishes were cooled to room temperature then stored at  $8-15^\circ\text{C}$  until use. BHI broth was prepared by dissolving 37g of BHI broth powder in one litre of distilled water, then sterilised in an autoclave at  $121^\circ\text{C}$  for 15 minutes. The sterilised broth was allowed to cool to room temperature before being poured into 15 ml sterile tubes and stored at  $8-15^\circ\text{C}$  until use.

Gram-positive bacteria methicillin-resistant *Staphylococcus aureus* (NCTC 12493), *Streptococcus pyogenes* (ATCC 19615), and *Staphylococcus epidermidis* (ATCC 12228) along with Gram-negative bacterium *Acinetobacter baumannii* (NCIMB 9214), *Pseudomonas aeruginosa* (NCIMB 10548),

*Escherichia coli* (NCTC 10418) were used. Also, 12 clinical strains were obtained from Bristol hospital patients with prosthetic joint infections (PJI) in the period 2013-2015 and species were confirmed by polymerase chain reaction. The patients were anonymised by giving a code for each selected strain. These clinical strains are: *E. coli* 59293, *Enterococcus faecalis* 58181, MRSA 23140, MRSA 38924, MRSA 59275, *A. baumannii* 44646, *A. baumannii* 44640, *A. baumannii* 44643, *S. epidermidis* 59272, *S. epidermidis* 53222, *S. epidermidis* 59199. Bacteria frozen stokes were stored at -80°C; strains were streaked on BHI plates weekly and incubated for 18-24 hours at 37°C, then stored at 4°C. The antimicrobial activity of bone cement was tested against different bacterial strains that are most commonly encountered in PJI including: coagulase-negative staphylococci (30-43%) and *Staphylococcus aureus* (12-23%), followed by streptococci (9-10%), Gram-negative bacilli (3-6%), enterococci (3-7%), and anaerobes (2-4%). Polymicrobial infections, which usually occur postoperatively, are seen in PJIs (10-12%) (Fsadni and Fsadni, 2013; Trampuz and Zimmerli, 2005).

The minimum inhibitory concentration (MIC) is defined as the lowest concentration of antimicrobial that inhibits any visual growth of a microorganism after overnight culture. MIC for chlorhexidine and gentamicin was determined against different bacteria tested through standard broth dilution MIC protocol (Wiegand et al., 2008). The bacteria were inoculated in broth and the broth was incubated for 24 hours at 37°C. Then, the broth was diluted 1000 times to get bacterial count in the range of 10<sup>4</sup>-10<sup>5</sup> CFU/ml which is normally used for MIC testing. Each well in a row of 96-well plate was filled with 100 µl of broth bacteria after incubation for 24 hours at 37°C. Then, 100 µl of known drug concentration is added to the first well of each row and carefully mixed. After that, 100 µl were pipetted out of the first well and transferred to the next well on the right and mixed. This procedure was repeated down the row to have gradual serial dilutions of the drug in each well (each well was half the concentration of the well on the left). Then, the plate was incubated for 24 hours at 37°C, and the growth in each well was evaluated visually. MIC was the lowest concentration of the drug showing no growth visually.

Bone cement samples were incubated in 3ml PBS buffer (pH 7) at 37°C. The release samples were stored in the refrigerator (2-8 °C) for microbial testing. Each

bacterial strain was inoculated into BHI broth and incubated for 18-24 hours at 37°C. Then, the inoculated growth was diluted 1000 times, and 20 µl of the diluted broth were added into a sterile 96-well plate. After that, each well was filled with 100 µl of the release media of different types of bone cement, and the plate was incubated for 18-24 hours at 37°C. In the next day, the growth in each well was evaluated visually (Figure 10) (Balouiri et al., 2016). A sufficient growth of the tested bacteria was considered as a positive result, i.e. obvious button or definite turbidity as compared with the positive and negative growth control. Each data point was performed in triplicate for each individual strain, to determine the duration for the release media from the bone cement is still able to inhibit the growth of bacteria.

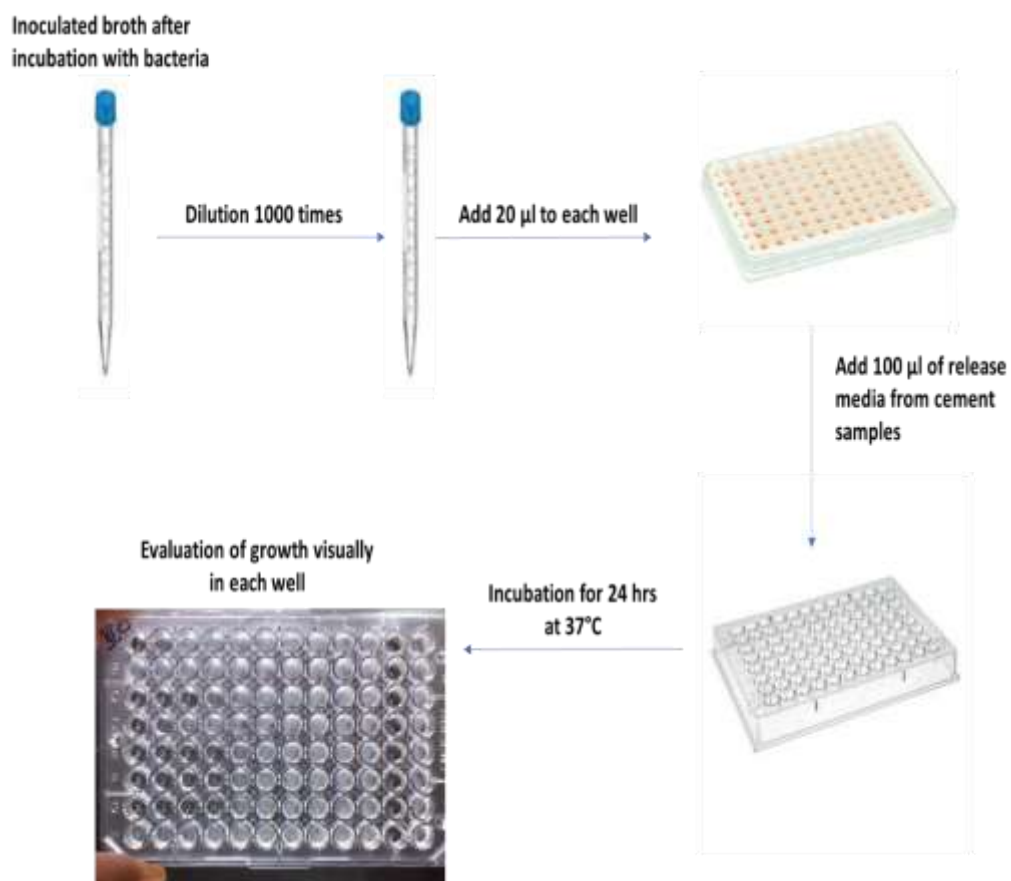


*Figure 10: Procedure for antimicrobial testing of bone cement.*

## 2.2.6 Mechanical testing

### 2.2.6.1 Compressive strength

The compressive strength testing was performed according to the ISO 5833:2002 standard (“ISO 5833:2002,” 2002). Bone cement samples that are  $12\pm 0.01\text{mm}$  in length,  $6\pm 0.01\text{mm}$  in diameter were prepared for this test. The test was performed using a Zwick Roell ProLine table-top Z050/Z100 materials testing machine (Zwick Testing Machines Ltd., Herefordshire, UK), where the sample was loaded incrementally at a constant cross-head speed of  $20\text{ mm/min}$  (Figure 11). Load displacement curves were obtained and loading was stopped at sample failure or when the upper yield point had been passed. The compressive strength ( $\sigma_c$ ) in MPa was calculated by dividing the  $F_{max}$  (Figure 12), the load to cause fracture, by the original cross-sectional area (in  $\text{mm}^2$ ) of the sample as shown in the following equation:

$$\sigma_c = \frac{F_{max}}{\text{cross sectional area}}$$

The  $F_{max}$  is taken from the 2 % offset load or the upper yield point load (whichever occurred first, in N) (Figure 12), an average of five samples were used.

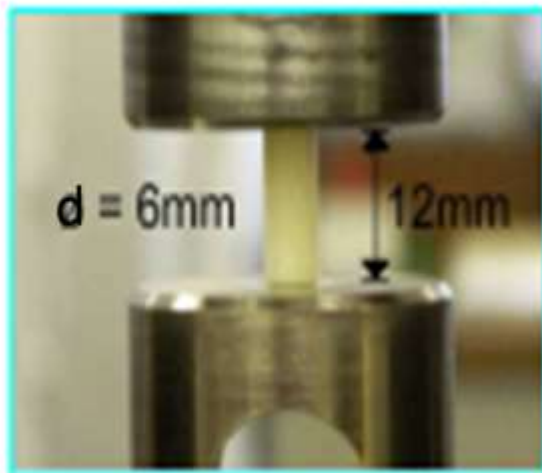


Figure 11: Compression test according to ISO5833 2002.

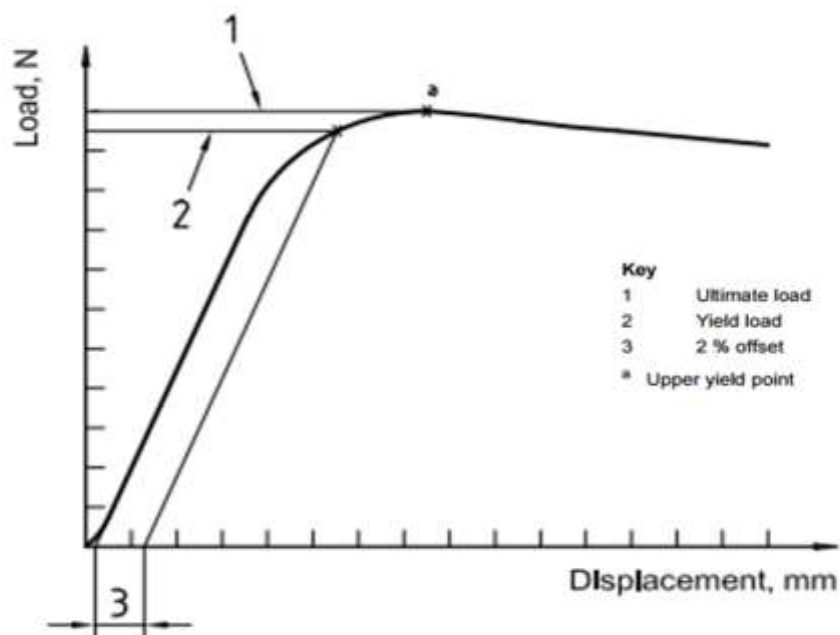


Figure 12: Idealized curve of load vs. displacement for cement (ISO5833 2002).

### 2.2.6.2 Bending strength

The bending strength and modulus determination tests were performed according to the ISO 5833:2002 standard (“ISO 5833:2002,” 2002). The bone cement samples were rectangular with a length of  $75\pm 0.1$  mm, width of  $10\pm 0.1$  mm and thickness of  $3.3\pm 0.1$  mm. The bending test is a four-point test where the distance between the inner loading points is  $20\pm 0.1$  mm, and the outer loading points is  $60\pm 0.1$  mm. The rectangular bending sample was placed at the centre of the

bending rig, and loaded incrementally using a Zwick Roell ProLine table-top Z050/Z100 materials testing machine (Zwick Testing Machines Ltd., Herefordshire, UK) (Figure 13 and Figure 14). During loading, the displacement was recorded as a function of applied force until the failure of sample occurred.

Bending modulus is calculated using equation 1, and equation 2 was used to calculate the bending strength from the average of five samples.

$$E_b = \frac{Fa}{4fbh^3} (3l^2 - 4a^2) \dots\dots\dots \text{equation 1}$$

$$B = \frac{3F_{frac} a}{bh^2} \dots\dots\dots \text{equation 2}$$

Where:

F is the difference between the deflections at 15N and 50N in mm

b is the average width of the specimen in mm

h is the average thickness of the specimen in mm

l is the distance between the outer loading points (60mm)

$\Delta F$  is the load range (50N - 15N)

a is the distance between the inner and outer loading points (20mm)

$F_{fract}$  Force at fracture in N

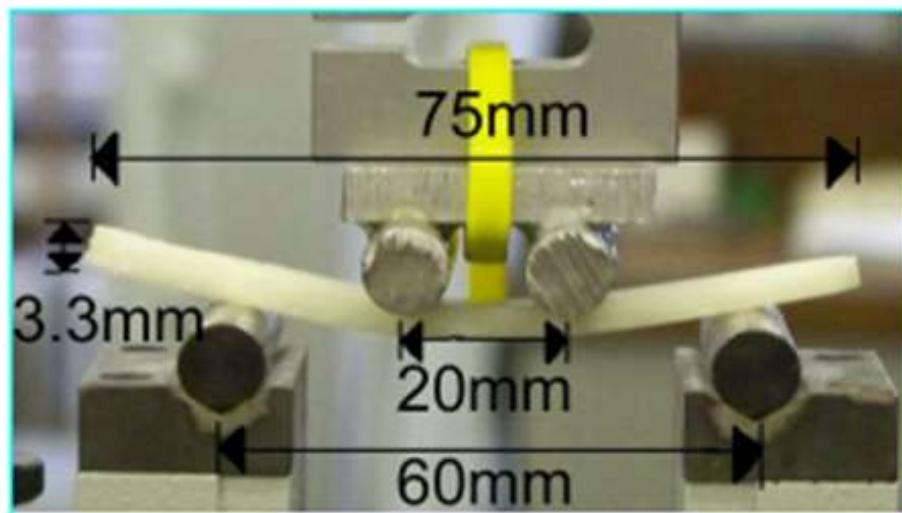
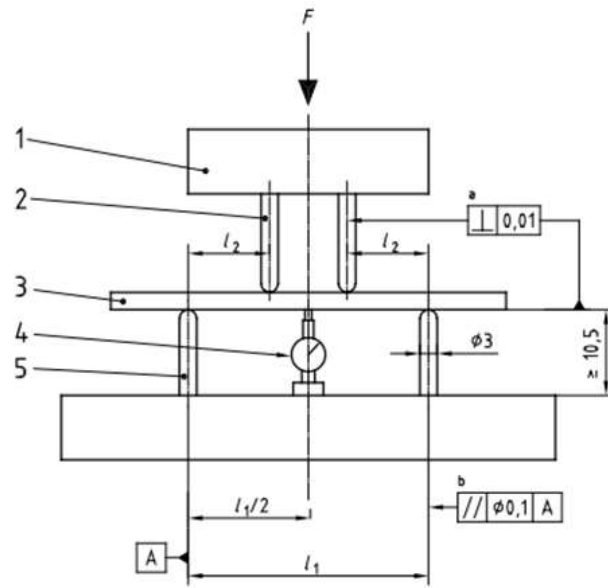


Figure 13: Bending test according to ISO5833 2002.



- Key**
- 1 central loading plunger
  - 2 inner loading points
  - 3 test specimen
  - 4 device for measuring deflection (dial gauge or other device)
  - 5 outer loading points
  - $F$  force
  - $l_1$  distance between outer loading points [(60 ± 1) mm]
  - $l_2$  distance between outer and inner loading points [(20 ± 1) mm]
  - <sup>a</sup> All loading points.
  - <sup>b</sup> Between any two loading points.

Figure 14: Four-point bending test (ISO5833 2002).

### 2.2.6.3 Fracture toughness

The fracture toughness was determined by the ISO13586:2000 Plastics - Determination of fracture toughness ( $G_{IC}$  and  $K_{IC}$ ) – Linear elastic fracture mechanics (LEFM) approach. The bone cement samples were rectangular with a length of  $45 \pm 0.1$  mm, width of  $10 \pm 0.1$  mm and thickness of  $3.3 \pm 0.1$  mm. A sharp chevron notch of 4.4-5.5mm was made at the centre of the sample, using a sharp razor blade. The rectangular bending sample was placed at the centre of the bending rig, and loaded incrementally using a Zwick Roell ProLine table-top Z050/Z100 materials testing machine (Zwick Testing Machines Ltd., Herefordshire, UK) (Figure 15). The fracture toughness is a three-point test, where the distance between the rollers is 40mm. The length of the crack was measured by a Pye Scientific travelling microscope (Pye Scientific, Cambridge, UK), and the width and length of each sample was measured by a Vernier calliper. The results were an average of five samples.

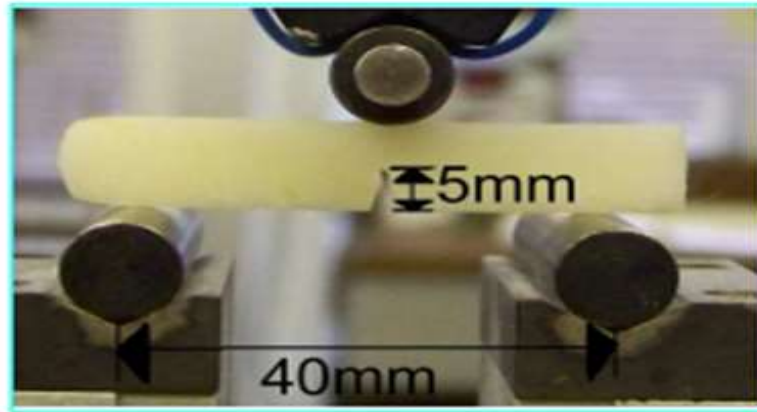


Figure 15: Fracture toughness test according to ISO 13586 2000.

### 2.2.7 Water uptake testing

Bone cement commercial samples and nanocomposites were incubated in 3 ml PBS at 37°C for 3 months; for the first 2 weeks, the samples were weighed daily; after that the samples were weighed every 3 days (Perni et al., 2015). Water uptake studies give an insight about the cement behaviour after being immersed in PBS (pH 7) to simulate the *in-vivo* conditions inside the joint with the synovial fluid.

### 2.2.8 Cytotoxicity testing

The new bone growth of skeletal cells around orthopaedic implants is formed by osteoblasts. These cells are from mesenchymal origin showing the ability to form osteoid components needed for bone matrix deposition (Olivares-Navarrete et al., 2012). Many osteoblast cell models have been developed for research in the field of biomaterials. These include cells isolated from various species, immortalized cells malignant cells and stem cells (Alvarez et al., 2012; Saldaña et al., 2011; Tashiro et al., 2009). Osteosarcoma tumours derived osteoblasts have features similar to osteoblasts, such as expression of specific receptors (e.g. vitamin D3 and calcitonin) (Saldaña et al. 2011), alkaline phosphatase activity and production of proteins specific for bone matrix (Tashiro et al. 2009; Alvarez et al. 2012). However, immortalized cells don't fully resemble osteoblasts because of the origin of osteosarcoma cell and immortalization for cells which led to some phenotypic differences. Immortalized cells are frequently used in biological testing more than primary derived cells because of unlimited number, ease of culturing, higher

phenotypical stability and repeatability of results during testing compared to primary cells (Czekanska et al., 2014).

In this work, Saos-2 human osteosarcoma osteoblast-like cells (ATCC® HTB-85™) were used for cytocompatibility testing which derived from osteosarcoma tumours. Saos-2 cells demonstrated similar alkaline phosphatase activity, mineralization potential and gene regulation to primary human osteoblast cells (Czekanska et al., 2014). In addition, Saos-2 cell line is more suitable for *in vitro* biomaterial biological testing when compared to other cell lines used, such as MG-63, and MC3T3-E1 because they have better similarity in cell proliferation and mineralization to primary human osteoblast cells (Saldaña et al., 2011).

In this work, Saos-2 were cultured in RPMI-1640 medium supplemented with fetal bovine serum (10% v/v) and 1% v/v of a solution of penicillin (5000 U/mL)/streptomycin (5000 mg/mL); cells were incubated at 37°C in humidified atmosphere with 5% CO<sub>2</sub>. Cells were grown till 70% confluence, washed twice with sterile PBS, and detached with trypsin; osteoblast cells were counted (using Trypan Blue to differentiate between viable and nonviable cells). Bone cement samples were prepared for different types of composites (Palacos R, Palacos NP, Cemex Genta, Cemex NP). The bone cement was round disk shaped with a diameter of 10 mm, and 5mm height, where each independent experiment had 6 replicates.

#### **2.2.8.1 MTT 3-(4,5-dimethylthiazol-2-yl)-2,5-diphenyltetrazolium test**

Vybrant® MTT Cell Proliferation Assay Kit (V-13154) (Thermofisher scientific, UK) was used for the determination of the number of viable cells. The MTT assay involves the conversion of the water soluble MTT (3-(4,5-dimethylthiazol-2-yl)-2,5-diphenyltetrazolium bromide) to an insoluble formazan (Liu et al., 1997). The formazan is then solubilized, and its concentration determined by optical density at 560 nm. In a 24-well plate, each bone cement sample was incubated in 1 ml growth media inoculated with approximately 60000 cells/well for 7 days at 37°C in humidified atmosphere with 5% CO<sub>2</sub>. After that, MTT test was done after 1, 2, 4 and 7 days of incubation. On each time point, the medium present in the well was taken off and replaced with 1 ml of fresh medium (phenol red-free). Twenty

microliters of MTT reagent (5 mg/mL in PBS) was added to each well and the plate was incubated for 24 hours at 37°C in humidified atmosphere with 5% CO<sub>2</sub>. After this, 900 µl of the media were removed from each well, and 150 µl of dimethyl sulfoxide (DMSO) was added to each well and the plates were incubated for further 10 min. Two hundred microliters of solution containing the dissolved formazan was put in another 96-well plate and analysed with a spectrophotometer (Tecan® Infinite F50, Austria) at 560 nm.

The media in each well was replaced with fresh media (1 ml of RPMI-1640 medium) warmed up to 37°C in the incubator on day number 4, to supply the cells with nutrients before testing. Replacing media is only needed for the time point day 7, because the previous points (Day 1,2,4) are done before the nutrients in the media are consumed. The viability of cells was plotted as percentage viability, by dividing the optical density of viable cells for the nanocomposite by the optical density of commercial cement as in the following equation:

$$\text{Viability (\%)} = \frac{\text{Optical density of nanocomposite}}{\text{Optical density of commercial cement}} * 100\%$$

#### **2.2.8.2 Lactate dehydrogenase release assay test (LDH)**

The LDH assay is used for measuring the viability of cells along with the MTT test. This assay is based on the reduction of NAD by LDH, where the reduced NAD (NADH) is utilized in the stoichiometric conversion of a tetrazolium dye. The resulting coloured compound is measured spectrophotometrically (Decker and Lohmann-Matthes, 1988). Cell death is determined by the quantification of plasma membrane damage. LDH is a stable enzyme present intracellularly and released into cell culture medium upon damage of the plasma membrane, hence it is used as a marker for cell viability (Legrand et al., 1992). The viability of the osteoblasts was determined using two independent enzyme assays, because LDH is based on the relative concentration of lactate dehydrogenase inside the cells and in the media. Therefore, using a single assay could be inconclusive in case a reduction in metabolic activity which could be indicative of a reduction of viable cells if only MTT was employed (Perni and Prokopovich, 2017). The kit used is “In Vitro Toxicology Assay Kit, LDH based, catalogue number: TOX7” (Sigma-Aldrich,

UK), and viability of cells were assayed according to manufacturer protocols. The kit contains the following components: substrate solution, cofactor solution, dye solution, lysis solution.

In a 24-well plate, each bone cement sample was incubated in 1 ml growth media inoculated with approximately 60000 cells/well for 7 days at 37°C in humidified atmosphere with 5% CO<sub>2</sub>. After that, LDH test were done on days 1, 2, 4 and 7 of incubation. LDH assay was done for the cell culture media before and after adding the cell lysis solution, and cell viability was calculated according to the following equation:

$$\text{Viability (\%)} = \frac{(\text{Total cells} - \text{Dead cells})}{\text{Total cells}} * 100\%$$

*Dead cells: the optical activity (at 490 nm) for the media before adding the lysis solution, which accounts for the dead cells.*

*Total cells: the optical activity (at 490 nm) for the media after adding the lysis solution, which accounts for total number of cells, live and dead cells.*

The assay of dead cells was done by measuring the LDH release into the medium from cells with ruptured cell membrane and lost integrity. 75 µl cell culture media transferred to 96-well plate for each sample. Then, 50 µl was added into each well from the following reagents: substrate solution, cofactor solution, dye solution to determine LDH enzymatic activity. After that, the plate was covered with aluminium foil to protect from light and incubated at room temperature for 30 minutes. Then, the optical density was measured at a wavelength of 490 nm.

The assay for the total cells was done by adding the 75 µl lysis solution to each sample in the 24-well plate containing cells with cement samples, and incubation at 37°C for 30 minutes. The lysis solution ruptures the cell membrane for all cells and causes the release of LDH enzyme to the media. Then, the procedure for testing LDH in the media is repeated as in dead cells. 75 µl cell culture media transferred to 96-well plate for each sample. Then, 50 µl was added into each well from the following reagents: substrate solution, cofactor solution, dye solution to determine LDH enzymatic activity. After that, the plate was covered with

aluminium foil to protect from light and incubated at room temperature for 30 minutes. Then, the optical density was measured at a wavelength of 490 nm.

### **2.2.8.3 Calcium production assay-Alizarin red**

Alizarin Red, an anthraquinone derivative, used to identify calcium in tissue sections and cultured cells in vitro. The reaction is not strictly specific for calcium, since magnesium, manganese, barium, strontium, and iron may interfere, but these elements usually do not occur in sufficient concentration to interfere with the staining. Calcium forms an Alizarin Red S-calcium complex in a chelation process, and the end product is a bright red stain. Alizarin red is a commonly used dye to identify calcium containing osteocyte in differentiated culture of both human and rodent mesenchymal stem cells (Reich et al., 2015).

In a 24-well plate, each bone cement sample was incubated in 1 ml growth media inoculated with approximately 60000 cells/well for 21 days at 37°C in humidified atmosphere with 5% CO<sub>2</sub>. after that, alizarin red test was done after 21 days of incubation. On day 21, the medium present in each well was taken off and replaced with 1 ml of glutaraldehyde 10% (v/v) (Sigma-Aldrich, UK); the plates were incubated for 15 min and washed with deionized water three times. 1 ml of Alizarin Red S 1% (v/v) (Sigma-Aldrich, UK) was added to each well and the plates were incubated for 20 min. After washing with deionized water, 1 ml of acetic acid 10% (v/v) was added to each well and the plates were incubated for 30 min. After this, 200 µl of solution was put in another 96-well plate analysed with a spectrophotometer (Tecan® Infinite F50, Austria) at 450 nm (Tommasi et al., 2016).

### **2.2.8.4 NO**

Nitric oxide (NO) is involved in many physiologic processes (Schmidt and Walter, 1994; Snyder, 1992), such as vasodilation, inflammation thrombosis, immunity and neurotransmission. Nitric oxide is a free radical which has important effects on bone cell function. The endothelial isoform of nitric oxide synthase is widely expressed in bone on a constitutive basis, whereas inducible NO is only expressed

in response to inflammatory stimuli (Danziger et al., 1997). Several methods have been developed for NO quantification in biological systems (Archer, 1993). One of these methods is called Griess deionization reaction quantify nitrite formed from the spontaneous oxidation of NO under physiological conditions (Ignarro et al., 1987; Tracey et al., 1990). Griess reagent kit for nitrite determination (catalogue number: G-7921) (Molecular Probes, Oregon, USA) was used for nitrite quantification from culture media incubated with bone cement sample. Bone cement samples were prepared for different types of composites (commercial and nanocomposites). The samples were round disk shaped with a diameter of 10 mm, and 5mm height, where each time point was a replicate of 6 samples. In a 24-well plate, each bone cement sample was incubated in 1 ml growth media (RPMI 1640 medium containing 10% Fetal bovine serum 'FBS' and 1% penicillin streptomycin) inoculated with approximately 60000 cells/well for 7 days at 37°C in humidified atmosphere with 5% CO<sub>2</sub>. after that, nitrite quantification was done after 1, 2, 4 and 7 days of incubation according to kit manufacturer instructions.

In a 96-well plate, the following were mixed in each well (sample capacity is 300 µL per well): 20 µL of Griess reagent, 150 µL of the nitrite containing sample and 130 µL of deionized water. Then, the 96-well plate was incubated for 30 minutes in the dark at room temperature. A photometric reference sample was prepared by mixing 20 µL of Griess reagent and 280 µL of deionized water. After that, the absorbance of the nitrite containing samples relative to the reference sample was determined in a spectrophotometric microplate reader at wavelength 560 nm. The absorbance of readings was converted to nitrite concentrations using the calibration curve (Figure 16). The calibration points were obtained by preparing nitrite solutions with concentrations between 1-100 µM by diluting the nitrite standard solution (included in the kit) with deionized water.

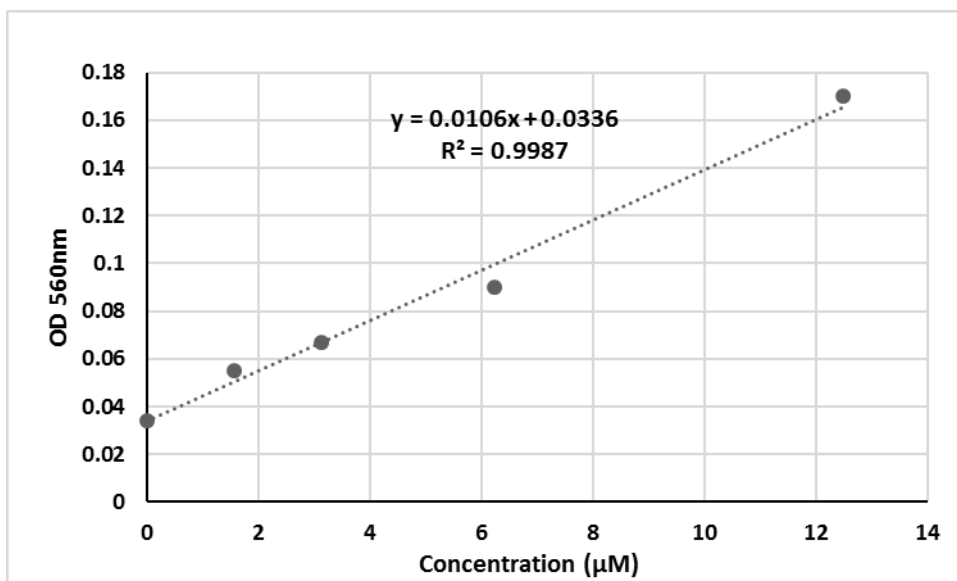


Figure 16: Calibration curve for nitrite production.

### 2.2.8.5 Fluorescence images

#### a. Live/dead

The viability of cells was assessed using simultaneous fluorescence staining of viable and dead cells. Human SAOS-2 cells ( $4 \times 10^4$  cells/well) were seeded directly on glass coverslips in 6-well plates and cultured in RPMI 1640 medium containing 10% FBS and 1% penicillin streptomycin at 37°C in a humidified 5% CO<sub>2</sub>-95% air atmosphere for 24 hours. Fluorescence imaging were performed for cement samples of different types of composites (commercial and nanocomposites). After cell attachment, the medium was replaced with 3 ml of the cement solutes, which was the 24 hours incubation of cements in RPMI 1640 medium containing 10% FBS and 1% penicillin streptomycin. Cells were washed thoroughly three times in PBS 24 hours later. Observation of cell morphology necessitated fluorescent dyes for cell staining. Briefly, for the staining of the viable and dead cell and nuclei, cells were incubated with calcein-AM, propidium iodide (Sigma-Aldrich, St. Louis, MO, USA), and trihydrochloride Hoechst 33342 (Thermo Fisher Scientific, Eugene, OR, USA), respectively. After washing the cells with PBS, 3 ml of staining solution was added to each well (0.1% v/v propidium, 0.2% v/v calcein, 5 µg/ml Hoechst in PBS). Then, the cells were

incubated at 37°C for 30 minutes, and the stain was removed from each and cells were washed with PBS immediately before imaging.

Calcein-AM, acetoxymethyl ester of calcein, is highly lipophilic and cell membrane permeable. Though Calcein-AM itself is not a fluorescent molecule, the calcein generated from Calcein-AM by esterase in a viable cell emits strong green fluorescence (excitation: 490 nm, emission: 515 nm). On the other hand, PI, a nucleus staining dye, cannot pass through a viable cell membrane. It reaches the nucleus by passing through disordered areas of dead cell membrane, and intercalates with the DNA double helix of the cell to emit red fluorescence (excitation: 535 nm, emission: 617 nm) (Lecoeur, 2002). Hoechst 33342 nucleic acid stain is a popular cell-permeant nuclear counterstain that emits blue fluorescence when bound to DNA, and this dye is often used to distinguish condensed nuclei in apoptotic cells. Hoechst 33342 is a cell-permeable DNA stain that is excited by ultraviolet light and emits blue fluorescence at 460-490 nm. Hoechst 33342 binds preferentially to adenine-thymine (A-T) regions of DNA. This stain binds into the minor groove of DNA and exhibits distinct fluorescence emission spectra that are dependent on dye: base pair ratios. (Mocharla et al., 1987). Confocal microscopy (Zeiss, Oberkochen, Germany) was used for visualization of the staining, the magnifying glasses used are 10X and 64X.

#### **b. Actin/dapi**

Actin stains and probes are used in determining the structure and function of the cytoskeleton in living and fixed cells. Human SAOS-2 cells ( $4 \times 10^4$  cells/well) were seeded directly on glass coverslips in 6-well plates and cultured in RPMI 1640 medium containing 10% FBS and 1% penicillin streptomycin at 37°C in a humidified 5% CO<sub>2</sub>-95% air atmosphere for 24 hours. Fluorescence imaging were performed for cement samples of different types of composites (commercial and nanocomposites). After cell attachment, the medium was replaced with 3 ml of the cement solutes, which was the 24 hours incubation of cements in RPMI 1640 medium containing 10% FBS and 1% penicillin streptomycin. Cells were washed thoroughly three times in PBS 24 hours later. Then, for the staining of the F-actin

cytoskeleton and nuclei, cells were fixed with 4% paraformaldehyde in PBS and permeabilized with 0.1% Triton-X-100.

Observation of cell morphology necessitated fluorescent dyes for cell staining. Thus, cells were incubated with tetramethyl rhodamine B isothiocyanate-conjugated phalloidin (Sigma-Aldrich, St. Louis, MO, USA) and trihydrochloride Hoechst 33342 (Thermo Fisher Scientific, Eugene, OR, USA), respectively. 3 ml of staining solution was added to each well (50 µg/ml fluorescent phalloidin conjugate, 5 µg/ml Hoechst in PBS). Then, the cells were incubated at 37°C for 30 minutes, and the stain was removed from each and cells were washed with PBS immediately before imaging.

Phalloidin is a fungal toxin isolated from the poisonous mushroom *Amanita phalloides*. Its toxicity is attributed to the ability to bind F actin in liver and muscle cells (Waggoner et al., 1989). Phalloidin binding to actin filaments to form a complex that is strongly stabilized. Phalloidin has been found to bind only to polymeric and oligomeric forms of actin, and not to monomeric actin. Fluorescent conjugates of phalloidin are used to label actin filaments for histological applications (Small et al., 1988). Confocal microscopy (Zeiss, Oberkochen, Germany) was used for visualization of the staining, the magnifying glasses used are 10X and 64X.

### **2.2.9 Nanoparticles distribution in bone cement:**

The distribution of nanoparticles inside the bone cement was studied by fluorescent images of fluorescent labelled nanoparticles incorporated into the cement. Fluorescent nanoparticles, used for different LbL coatings, were prepared as described in section 2.1.2.1 using deionised water containing 86 mg fluorescein sodium salt (Sigma-Aldrich, St. Louis, MO, USA). Then, the fluorescent nanoparticles were mixed with the bone cement powder and the cement was prepared as described in section 2.2.2. However, a small amount of the cement paste was taken with a spatula before cement hardening, and allowed to set on a glass slide. Confocal microscopy (Zeiss, Oberkochen, Germany) was used for visualization of the fluorescent nanoparticles distribution inside the cement utilizing the glass slides for different types of nanocomposites, the magnifying

glasses used are 10X and 64X. Several images were taken in various locations (at least 10 different locations) to give a reproducible insight about nanoparticles distribution in the cement.

#### **2.2.10 Statistical analysis**

All data were expressed as means  $\pm$  standard deviation (SD) from at least three independent values. To assess the statistical significance of results between groups, one-way analysis of variance (ANOVA) was performed. Experimental results were considered statistically significant at 95 % confidence level ( $p < 0.05$ ). All analyses were run using the SPSS® software.

### **3 Gentamicin controlled release from Layer-by-Layer coated silica nanoparticles.**

#### **3.1 Introduction**

The development of controlled release drug delivery systems is vital for effective therapeutic treatment (Li et al., 2012). High drug loading and prolonged release kinetics are attractive attributes in drug delivery systems for many applications such as biomedical infections (Béraud and Huneault, 2005; Gimeno et al., 2015). Despite the emergence of antibiotic resistant bacteria, the use of antibiotic releasing biomaterials remains the standard and effective approach for the prevention and treatment of biomedical infections (Masters et al., 2013; Schmidmaier et al., 2006; Stammers et al., 2015). Infection and biofilm formation can be prevented through controlled release of antibiotics locally at high concentrations, over prolonged period of time without burst release (Anagnostakos and Kelm, 2009).

One of the novel approaches for enhancing the delivery of a wide range of therapeutic agents is Layer by layer assembly (LbL) (Gentile et al., 2015). This coating technique is based on the deposition of alternative oppositely charged polyelectrolytes on different substrates, allowing control of the thickness and composition of coating at nanoscale level in a reproducible manner (Ariga et al., 2011; Vergaro et al., 2011). Moreover, the coating process is simple, low-cost, scalable, and does not comprise harsh organic conditions, as it involves mild aqueous solutions. Because of its' advantages, LbL has numerous applications in drug delivery (Deshmukh et al., 2013).

Nanoparticles have been extensively explored and successfully applied as drug carriers for antibiotics and others. Among all nano-carriers, silica nanoparticles are commonly preferred as a drug carrier, because of its unique physicochemical properties and biocompatibility and low cost. Silica nanoparticles have as large ratio of surface area to mass, small size, and ease of structural or functional modification because of silanol-containing surface (Feng et al., 2014; Tamanna et al., 2015).

Gentamicin sulphate is a broad spectrum aminoglycoside antibiotic acting against most gram-positive and gram-negative bacterial pathogens that commonly cause device-related infections such as *Staphylococcus aureus*, *S. epidermidis*, *Pseudomonas aeruginosa* and *Escherichia coli* (Donlan, 2001). The bactericidal activity of gentamicin is concentration dependant which inhibit protein synthesis in bacteria (Tam et al., 2006). Gentamicin have been extensively used for to prevent infection in implants coatings (Li et al., 2012), orthopaedic bone cement (Van et al., 2000), and for the treatment of osteomyelitis by incorporation in poly-methacrylic acid beads to provide prophylaxis, where a period of 6 to 8 weeks of release is required (Anagnostakos et al., 2006).

Gentamicin is small molecule with five ionisable amino groups that can attach on negatively charged surfaces after protonation in aqueous media. However, it is difficult to build stable LbL constructs with small molecular weight, because of lack of polymeric nature with multiple ionisable groups for electrostatic interactions (Chuang et al., 2008; Wang et al., 2016). poly- $\beta$ -amino esters (PBAEs), a very well-known class of synthetic polymers obtained from the copolymerization of diacrylate and amines (Lynn and Langer, 2000), have been extensively used in LbL coating for biomedical applications in virtue of their positive charge and possible hydrolysis (Chuang et al. 2008). Wang et al. (Wang et al., 2016) conjugated cationic gentamicin sulphate with polycyclic acid polyanion to enable incorporation in multilayer film as (poly (acrylic acid)-gentamicin/poly(ethylenimine))<sub>n</sub> through LbL method. Chuang et al (Chuang et al., 2008) used a poly ( $\beta$ -amino esters) (Poly with different chain lengths, X = 1, 2, and 6A) with positive charges to construct a multilayer film with [Poly 1/Anion/Gentamicin/Anion]<sub>n</sub> in tetralayers, to enable the incorporation of gentamicin into the LbL construct. The drug release was controlled by the hydrolytic degradation of multilayers without the need for enzymatic or cellular interaction to provide a controlled release of gentamicin for 10 hours after the deposition of 50 tetralayers.

In this chapter, we aim to provide controlled release of gentamicin incorporated directly into multilayer films constructed on the surface of silica nanoparticles using LbL assembly coating method. Multilayer films were constructed using hydrolysable and non-hydrolysable polyelectrolytes to provide controlled release

of gentamicin for more than 4 weeks at high concentrations with high drug loading capacity. This approach represents a convenient and effective strategy to control the release of gentamicin which has many antibacterial applications in infection prevention and treatment.

## **3.2 Materials and methods**

### **3.2.1 Chemicals**

Triton X-100, tetraethyl orthosilicate (TEOS), 3-aminopropyltriethoxysilane (APTS), sodium alginate (Mw 80.000-120.000 Da), chitosan (Mw 190.000-310.000 Da), gentamicin sulphate, sodium acetate trihydrate, phosphate buffer solution (PBS) tablets, o-phthalaldehyde reagent solution (OPA) were purchased from Sigma-Aldrich, UK. Cyclohexane, n-hexanol, ammonium hydroxide (35%), ethanol, methanol, glacial acetic acid and iso-propanol were purchased from Fishers scientific, UK. All reagents were stored according to manufacturer's guidelines and used as received. B1: is a patented biocompatible, biodegradable cationic polymer, the precise structure will remain confidential due to the IP associated, was freshly prepared in the lab before use.

Acetic acid-sodium acetate buffer was prepared as follows: to prepare 100 ml acetic acid-sodium acetate buffer (0.1 M, pH 5), 30 ml of sodium acetate trihydrate ( $\text{CH}_3\text{COONa}\cdot 3\text{H}_2\text{O}$ ) (0.1 M) were added to 70 ml of acetic acid ( $\text{CH}_3\text{CO}_2\text{H}$ ) (0.1 M) solutions and stirred. Phosphate buffer saline (PBS) (pH 7.3) was prepared by dissolving 1 tablet of PBS in 100 ml of deionized water.

### **3.2.2 Gel permeation chromatography (GPC)**

In a 50-ml test tube a solution composed by 100 mg of B1, previously synthesized, and 10 ml of acetate buffer pH5 was incubated at 37°C to start a study of molecular weight degradation. The same procedure was followed for pH 7.4. The determination of the molecular weight was performed by the FPLC (Fast Protein Liquid Chromatography) of Akta Design (Amersham pharmacia biotech-Sweden) supplied with Superdex 75 10/3000 GL column. Firstly, as a starting point (day 0), 0.5 ml of sample for each media was collected and analysed for the determination of the molecular weight. After that, samples were collected every 24 hours and immediately analysed for 30 days. For each sample 2 replicates were taken. A calibration curve was built to correlate the molecular weights and retention

volumes. 7 standards of polymers with known molecular weight purchased from (Fluka Chemie AG and Polymer Laboratories Ltd.,) were used for calibration (Figure 17). For each one 1mg has been diluted with 1 ml of acetate buffer pH 5 and 0.2 ml of this solution was injected into the FPLC using a defined method with a running time of 24 minutes for each run. The column used was Superdex 75 10/3000 GL and the mobile phase was acetate buffer pH 5.

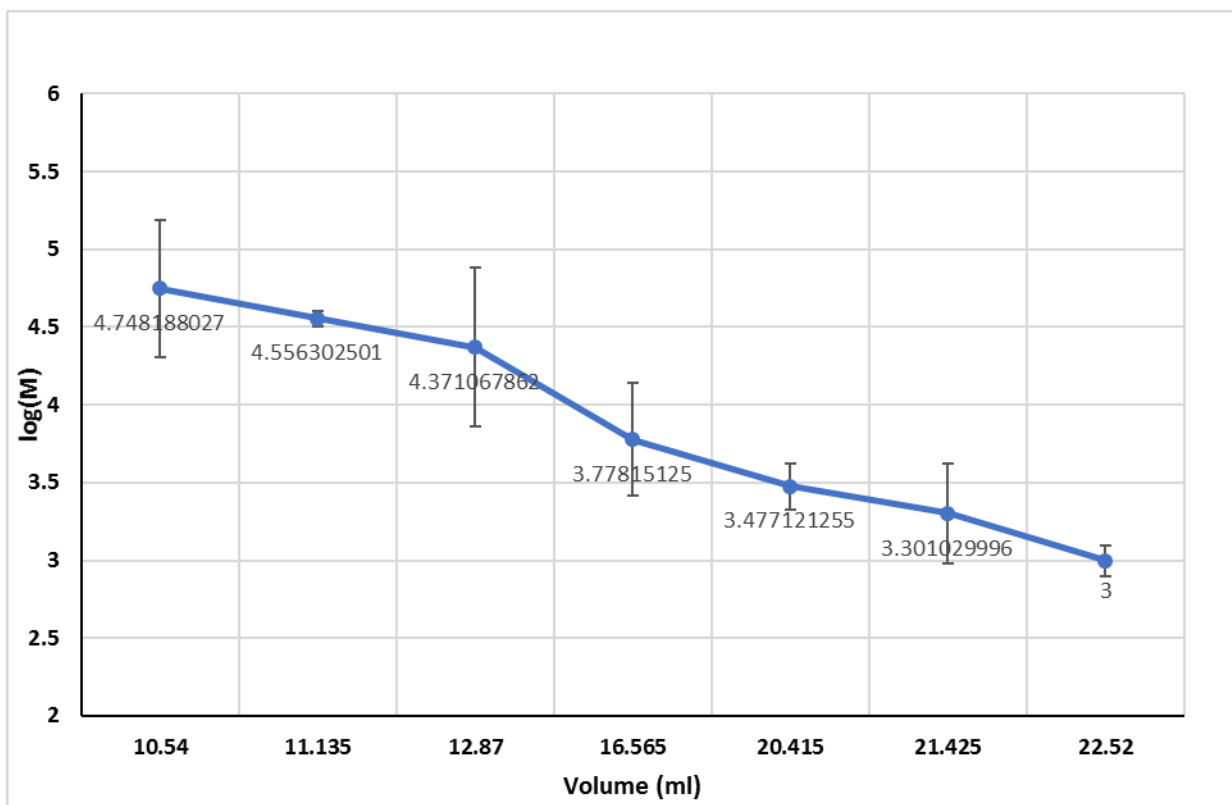


Figure 17: FPLC calibration curve

### 3.2.3 Nanoparticle preparation

#### 3.2.3.1 Amino functionalised silica nanoparticle synthesis

Silica nanoparticles functionalised with amine groups ( $\text{SiO}_2\text{-NH}_2$ ) were prepared in one-pot synthesis by hydrolysis of TEOS in reverse micro-emulsion and subsequent functionalization (Stöber method) (Stöber et al., 1968), as described in section 2.1.2.1.

### 3.2.3.2 Layer by Layer (LbL) coating technique

The silica nanoparticles were layered with different numbers of a repeating sequence of polyelectrolytes (sodium alginate, chitosan, B1) and drug (gentamicin). Two sequences were used, each one was composed of a repeated unit of four layers making one quadruple layer (Q). The first sequence was: sodium alginate, gentamicin, sodium alginate and chitosan, respectively. Up to ten quadruple layers were coated onto silica nanoparticles, named as Q<sub>n</sub> where n represents the number of quadruple layers. (Table 9). The following concentrations of polyelectrolytes and drug in acetic acid-sodium acetate buffer were used in LbL: sodium alginate (2 mg/ml), gentamicin (10 mg/ml) and chitosan (2 mg/ml). (The procedure for LbL coating technique was described in section 2.1.2.2.)

Quadruple layer no.	Abbreviation	Layers on the surface of amino functionalised silica nanoparticles (SiNH <sub>2</sub> )
1	Q1	SiNH <sub>2</sub> -alginate-gentamicin-alginate- <b>chitosan</b>
2	Q2	SiNH <sub>2</sub> -Q1-alginate-gentamicin-alginate- <b>chitosan</b>
3	Q3	SiNH <sub>2</sub> -Q2-alginate-gentamicin-alginate- <b>chitosan</b>
4	Q4	SiNH <sub>2</sub> -Q3-alginate-gentamicin-alginate- <b>chitosan</b>
5	Q5	SiNH <sub>2</sub> -Q4-alginate-gentamicin-alginate- <b>chitosan</b>
6	Q6	SiNH <sub>2</sub> -Q5-alginate-gentamicin-alginate- <b>chitosan</b>
7	Q7	SiNH <sub>2</sub> -Q6-alginate-gentamicin-alginate- <b>chitosan</b>
8	Q8	SiNH <sub>2</sub> -Q7-alginate-gentamicin-alginate- <b>chitosan</b>
9	Q9	SiNH <sub>2</sub> -Q8-alginate-gentamicin-alginate- <b>chitosan</b>
10	Q10	SiNH <sub>2</sub> -Q9-alginate-gentamicin-alginate- <b>chitosan</b>

Table 9: 10 quadruple layers' abbreviations and constituents using chitosan as polycation

For the second sequence, chitosan was replaced with B1 as the polycation using the same solution concentration. As a result, the new sequence for a quadruple layer became: sodium alginate, gentamicin, sodium alginate and B1, respectively. Ten quadruple layers were also layered with the same procedure and concentration used before with chitosan (*Table 10*).

Quadruple layer no.	Abbreviation	Layers on the surface of amino functionalised silica nanoparticles (SiNH <sub>2</sub> )
1	Q1	SiNH <sub>2</sub> -alginate-gentamicin-alginate- <b>B1</b>
2	Q2	SiNH <sub>2</sub> -Q1-alginate-gentamicin-alginate- <b>B1</b>
3	Q3	SiNH <sub>2</sub> -Q2-alginate-gentamicin-alginate- <b>B1</b>
4	Q4	SiNH <sub>2</sub> -Q3-alginate-gentamicin-alginate- <b>B1</b>
5	Q5	SiNH <sub>2</sub> -Q4-alginate-gentamicin-alginate- <b>B1</b>
6	Q6	SiNH <sub>2</sub> -Q5-alginate-gentamicin-alginate- <b>B1</b>
7	Q7	SiNH <sub>2</sub> -Q6-alginate-gentamicin-alginate- <b>B1</b>
8	Q8	SiNH <sub>2</sub> -Q7-alginate-gentamicin-alginate- <b>B1</b>
9	Q9	SiNH <sub>2</sub> -Q8-alginate-gentamicin-alginate- <b>B1</b>
10	Q10	SiNH <sub>2</sub> -Q9-alginate-gentamicin-alginate- <b>B1</b>

Table 10: 10 quadruple layers abbreviations and constituents using B1 as a polycation

### **3.2.4 Nanoparticles surface and material characterisation**

#### **3.2.4.1 Nanoparticles size measurements**

The size of nanoparticles was characterized using transmission electron microscopy (TEM) as described in section 2.1.3.1.

#### **3.2.4.2 Nanoparticles Zeta potential measurements**

The electrophoretic mobility for the nanoparticles was measured by dynamic light scattering (DLS), using Malvern Zetasizer, Nano ZS particle characterization system (Malvern Instruments Limited, UK), as described in section 2.1.3.2.

#### **3.2.4.3 Thermogravimetric analysis (TGA)**

Thermogravimetric analysis (TGA) was performed using a Perkin-Elmer TGA 4000 instrument, as described in section 2.1.3.3.

### **3.2.5 Gentamicin release quantification**

Gentamicin release from the nanoparticles was evaluated by dispersing the drug loaded nanoparticles (10 mg/ml) in 2 buffer media: acetic acid-sodium acetate buffer pH 5, and PBS pH 7.3. These two pH points were chosen to assess the drug release under healthy joint (pH 7.35-7.45) (Ribeiro et al., 2012), and for infected joint, which are associated with low pH values (pH < 7) or local acidosis (Kinnari et al., 2009).

Then, samples were vigorously stirred in a vortex, and then incubated at 37°C. Samples were taken every 24 hours where 1ml of release medium aliquots were taken after Eppendorf centrifugation, to avoid withdrawing nanoparticles during taking the sample.

The amount of gentamicin released from the nanoparticles in the buffer was quantified through fluorescence spectroscopy using o-phthaldialdehyde reagent (Perni and Prokopovich 2014), as described in section 2.1.4.

### **3.2.6 Statistical analysis**

All data were expressed as means  $\pm$  standard deviation (SD) from at least three independent values. To assess the statistical significance of results between groups, one-way analysis of variance (ANOVA) was performed. Experimental results were considered statistically significant at 95 % confidence level ( $p < 0.05$ ). All analyses were run using the SPSS® software.

### 3.3 Results

#### 3.3.1 B1 hydrolysis kinetics (GPC)

The results for B1 hydrolysis study are shown in Figure 18. At pH 7, no hydrolysis was observed for 30 days, because at this neutral condition hydrolysis is difficult as hydrolysis needs an acidic or basic condition to break the ester bonds. B1 maintained the molecular weight for the first 20 days. Then, hydrolysis of B1 was drastic after 20 days at acidic condition.

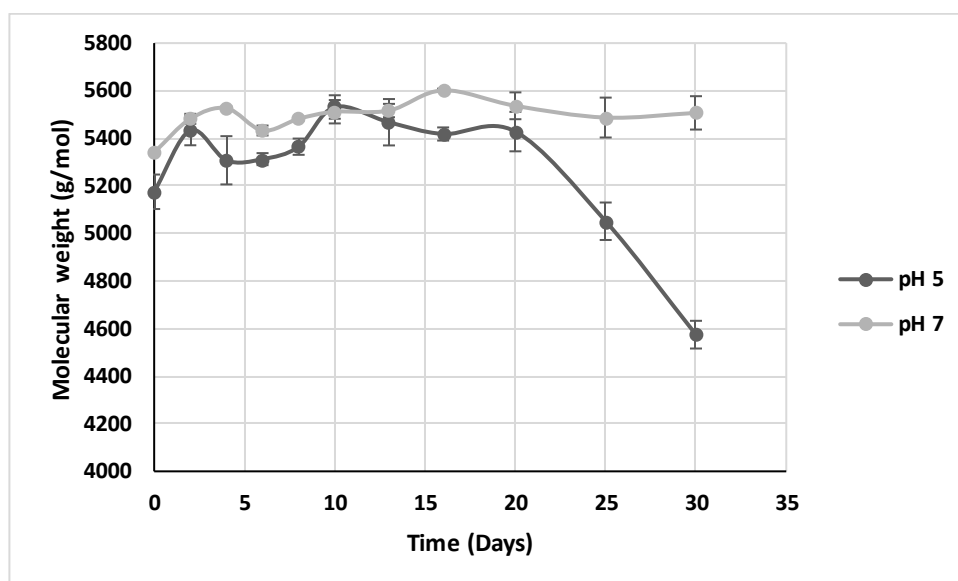


Figure 18: GPC hydrolysis study for B1.

#### 3.3.2 Nanoparticles surface and material characterization

##### 3.3.2.1 Size measurements

TEM images for the amino functionalised silica nanoparticles, Q1 and Q10 are shown in Figure 19 and revealed that the nanoparticles were roundly shaped. Moreover, LbL deposition did not alter either the shape of the nanoparticles but increased their size from around 55 nm to 65 after 10 quadruple layers Table 11.

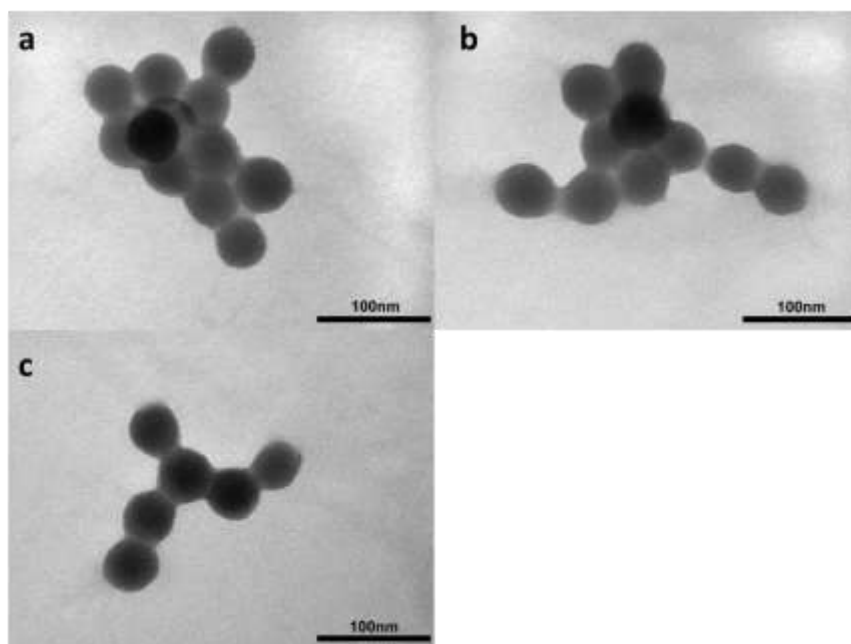


Figure 19: Examples of TEM images for: (a) amino functionalised silica nanoparticles, (b) Q10 chitosan layered nanoparticles, (c) Q10 B1 layered nanoparticles.

Sample	Size (nm)
SiNH <sub>2</sub> nanoparticles	55 ± 8
Q10 (chitosan)	64 ± 8
Q10 (B1)	65 ± 9

Table 11: Size measurements calculated from TEM images for amino functionalised silica nanoparticles, Q10 layered with chitosan or B1 as a polycation ( $n = 3 \pm SD$ ).

### 3.3.2.2 Zeta potential measurements

Zeta potential measurements were done for the amino functionalised silica nanoparticles and after each layering step, as shown (*Figure 20* and *Figure 21*). Zeta potentials were measured for both types of nanoparticles layered with different polycations (chitosan or B1) for ten quadruple layers; the total number of layers needed to build ten quadruple layers is 40 layers. The zeta potential for the amino functionalised silica nanoparticles was  $30.1 \pm 0.95$  mV.

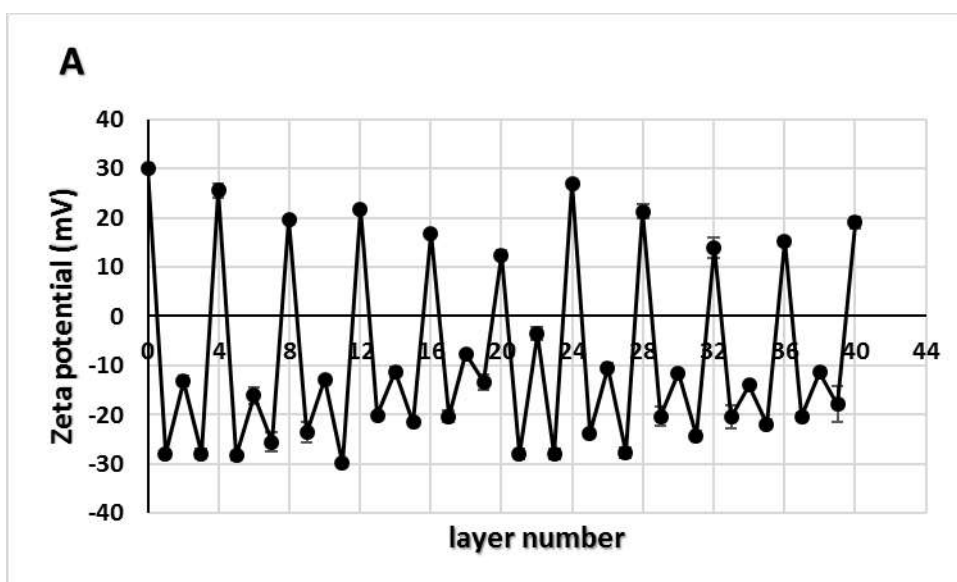


Figure 20: Zeta potential for amino functionalised silica nanoparticles (layer 0) and for 40 layers of a repeating unit of (alginate-gentamicin-alginate-chitosan) to build 10 quadruple layers ( $n = 3 \pm SD$ ).

For chitosan layered nanoparticles (*Figure 20*), the first quadruple layer (layer 1 to 4) showed that layering sodium alginate reversed the zeta potential to a negative value of  $-27.83 \pm 0.95$  mV. Next, the gentamicin layer decreased the negativity of the zeta potential to  $-13.17 \pm 1.12$  mV, but could not reverse it into a positive value because it is a small molecule with small number of ionisable groups compared to polyelectrolytes. Then, the subsequent sodium alginate layer increased the negativity of the zeta potential value  $-27.83 \pm 0.97$  mV back again to nearly the same value seen in the first alginate layer. Then, chitosan layering step reversed the value of zeta potential to a positive value of  $25.47 \pm 1.45$  mV. For quadruple layers 2 to 10 (layer number 5-40), similar trend in the changes of zeta potential value and sign was observed compared to the first quadruple layer. The sodium alginate layer gives a negative zeta potential value, the gentamicin layer decreases the negativity of alginate charge and chitosan layer reverses the negative charge of alginate to a positive zeta potential value.

For B1 layered nanoparticles (*Figure 21*), the first quadruple layer (layer 1 to 4) showed that layering sodium alginate reverses the zeta potential to a negative value of  $-16 \pm 0.31$  mV. Next, the gentamicin layer decreased the negativity of the zeta potential to  $-7.51 \pm 0.44$  mV with similar trend seen previously in chitosan layered nanoparticles. Then, the subsequent sodium alginate layer increased the negativity of the zeta potential value to  $-25.57 \pm 0.23$  mV. Then, B1 layering step reversed the value of zeta potential to a positive value of  $5.35 \pm 0.43$  mV. For quadruple layers 2 to 10 (layer number 5-40), similar trend in the changes of zeta potential was observed compared to the first quadruple layer, except for B1. B1 zeta potential values were close to zero. B1 did not reverse the negativity of sodium alginate, because the zeta potential for a pure solution of B1 is  $+8$  mV compared to  $+25$  mV for chitosan. B1 is a weaker polycation, and sodium alginate projected an overall negative zeta value even on the surface of B1 layered nanoparticles.

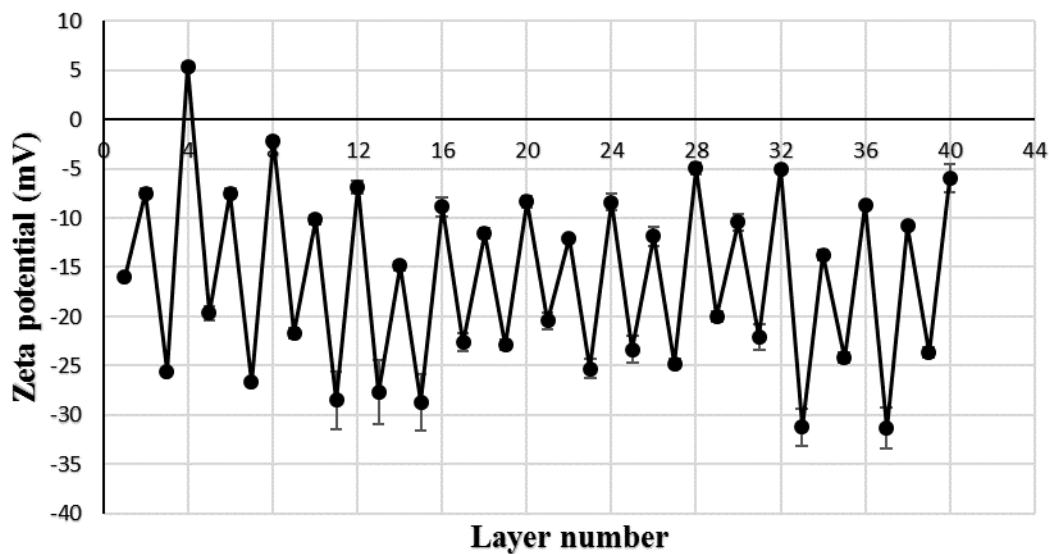


Figure 21: Zeta potential for amino functionalised silica nanoparticles layer with 40 layers of a repeating unit of (alginate-gentamicin-alginate-B1) to build 10 quadruple layers ( $n = 3 \pm SD$ ).

### 3.3.2.3 Thermogravimetric analysis (TGA)

For the purpose of assessing the organic matter content after doing LbL coating, thermogravimetric analysis was performed for amino functionalised silica nanoparticles and the same nanoparticles layered with different number of quadruple layers, using both types of polycations (chitosan or B1) as shown in (figure 22 and figure 23).

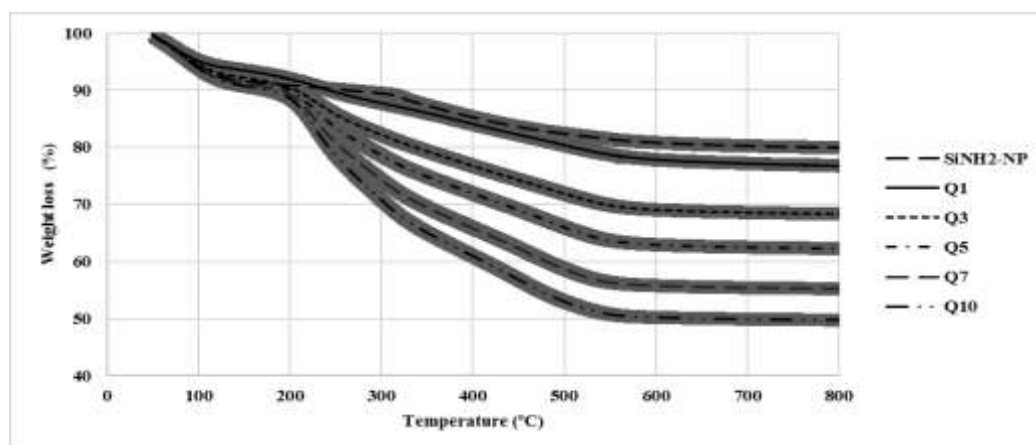


Figure 22: Thermogravimetric curves for amino functionalised silica nanoparticles and the same nanoparticles layered with different number of quadruple layers (Q1, Q3, Q5, Q7 and Q10) using chitosan as a polycation ( $n = 3 \pm SD$ ).

An initial weight loss around (5%) was observed at about 100 °C, which is normally attributed to the evaporation of adsorbed water from the samples (Wang et al., 2014). As a result, the organic content for each sample (Table 12 and Table 13) was calculated based on the weight loss beyond 100 °C, which truly corresponds to the combustion of organic matter (Du et al., 2015).

<b>Samples</b>	<b>Organic content (%)</b>
<b>SiNH<sub>2</sub>-Nanoparticles</b>	14.95 ±1.0
<b>Q1</b>	18.23 ±2.65
<b>Q3</b>	26.68 ±1.98
<b>Q5</b>	32.73 ±1.46
<b>Q7</b>	39.77 ±1.43
<b>Q10</b>	45.24 ±1.11

Table 12: *Percentage of organic material in amino functionalised silica nanoparticles and the same nanoparticles layered with different number of quadruple layers (Q1, Q3, Q5, Q7 and Q10) using chitosan as a polycation (n = 3 ± SD).*

In chitosan layered nanoparticles (Table 12), the organic content for the amino functionalised silica nanoparticles is 14.95 %, due to APTS. The organic content is increased by adding the first quadruple layer as seen for Q1 (18.23%), which makes a 3% increase in the organic content for the first quadruple layer for Q3, the organic matter is increased to reach (26.68%). And the organic content kept increasing, as expected, with addition of more quadruple layers to reach 32.73, 39.77 and 45.24% for Q5, Q7 and Q10, respectively.

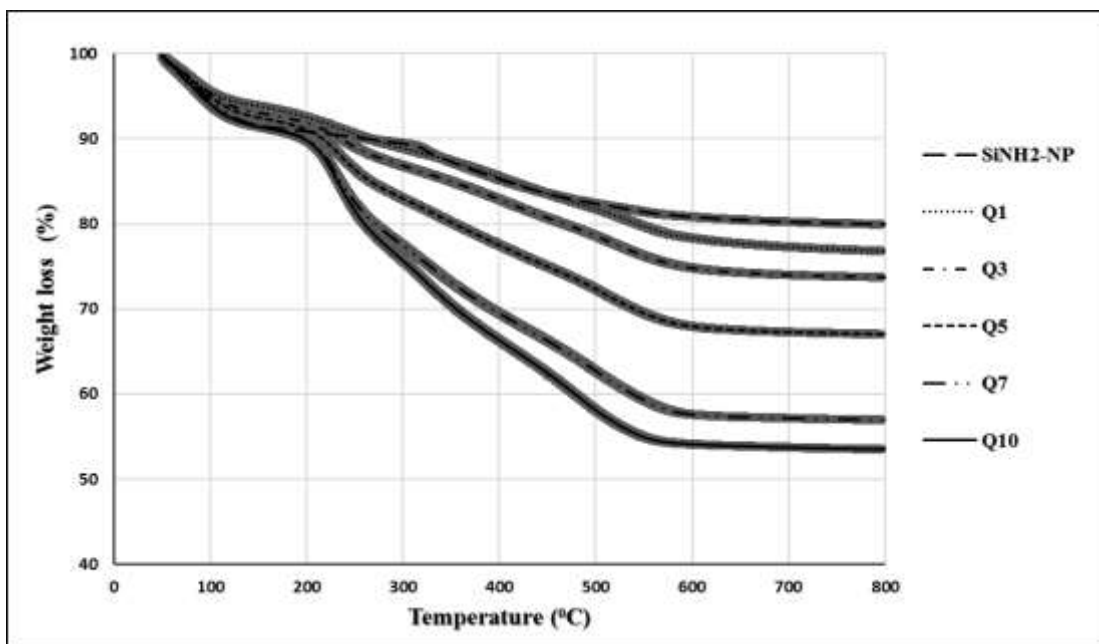


Figure 23: Thermogravimetric curves for amino functionalised silica nanoparticles and the same nanoparticles layered with different number of quadruple layers (Q1, Q3, Q5, Q7 and Q10) using B1 as a polycation ( $n = 3 \pm SD$ ).

In B1 layered nanoparticles (*Table 13*), similarly, the organic content for the amino functionalised silica nanoparticles is 14.95 %. The organic content is increased by adding the first quadruple layer as seen for Q1 (18.07%), which makes a 3% increase in the organic content for the first quadruple layer. In Q3, the organic matter is increased to reach (21.28%). And the organic content kept increasing, as expected, with addition of more quadruple layers to reach 38.07, 38.07 and 41.5% for Q5, Q7 and Q10, respectively.

Samples	Organic content (%)
SiNH <sub>2</sub> -Nanoparticles	14.95 ±1.0
Q1	18.07 ±1.27
Q3	21.28 ±0.93
Q5	27.97 ±1.03
Q7	38.07 ±2.96
Q10	41.5 ±3.66

Table 13 : Percentage of organic material in amino functionalised silica nanoparticles and the same nanoparticles layered with different number of quadruple layers (Q1, Q3, Q5, Q7 and Q10) using B1 as a polycation (n = 3 ± SD).

### 3.3.3 Gentamicin release quantification

The drug release studies for gentamicin loaded silica nanoparticles were carried out in two release media; PBS buffer (pH 7.3), and acetic acid-sodium acetate buffer (pH 5). Gentamicin was quantified by fluorescence detection in each sample. These two pH points were chosen to assess the drug release under healthy joint conditions (pH 7.35-7.45) (Ribeiro et al., 2012), and for infected joint, which are associated with low pH values (pH <7) or local acidosis (Kinnari et al., 2009).

For chitosan layered nanoparticles, most of the drug was released within the first 5 days in the two release media (figure 24 and figure 25). Subsequently, slow gradual release was observed until it reached plateau after 20 days. In PBS buffer (pH 7.3), Q1, Q3, Q5 had nearly the same release profiles (p>0.05), while Q7 and Q10 had significantly higher drug release. In acetic acid-sodium acetate buffer (pH 5), all layers had similar release profile (p>0.05); however, Q7 release profile was marginally higher than other profiles (p<0.05).

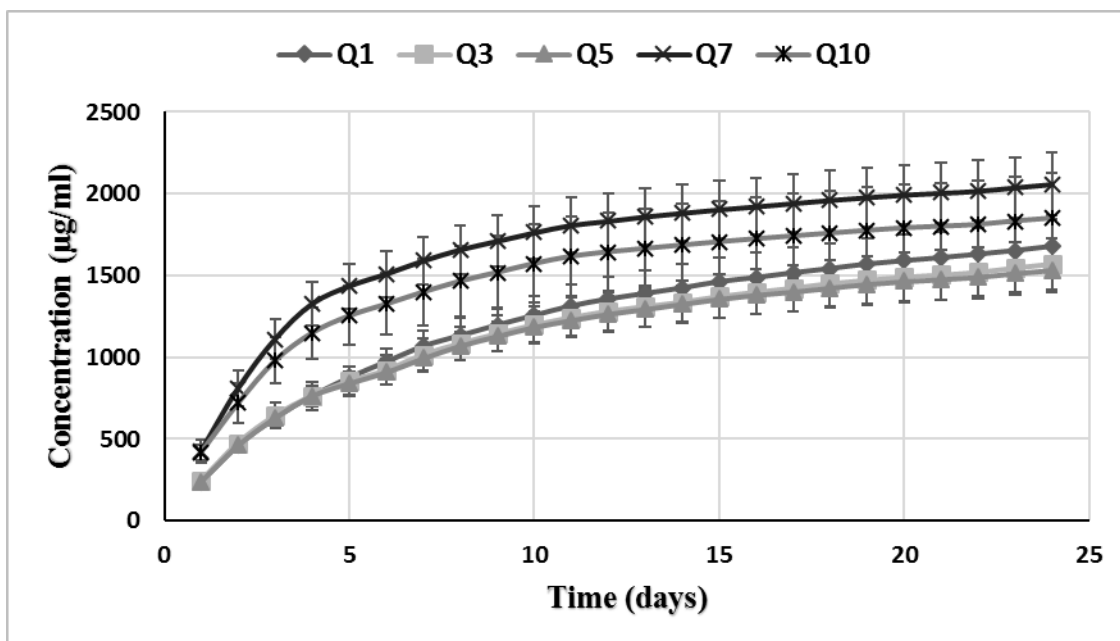


Figure 24: Cumulative gentamicin release in PBS (pH 7.3) from Q1, Q3, Q5, Q7 and Q10 layered using chitosan as a polycation ( $n = 3 \pm SD$ ).

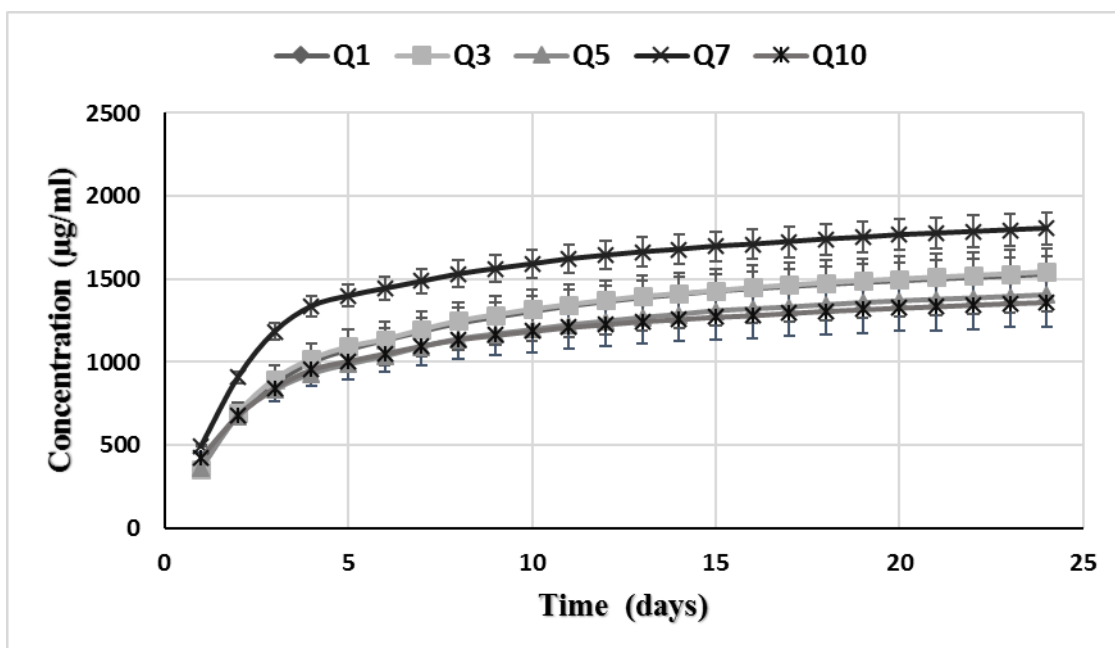


Figure 25: Cumulative gentamicin release in acetate buffer (pH 5) from Q1, Q3, Q5, Q7 and Q10 layered with chitosan as a polycation ( $n = 3 \pm SD$ ).

The similarity in release profiles for different quadruple layers with chitosan suggests that the release occurs from only the last quadruple layer on the surface of nanoparticles. In order to test this hypothesis, different quadruple layers were incubated in hydrochloric acid- potassium chloride buffer (pH 2) at 37 C<sup>0</sup> for 7

days. This condition is considered harsh enough to break all the layers of polyelectrolytes and allow the release of the drug. At pH 2, deionization of carboxylic group of alginate occurs, decreasing the electrostatic interaction with chitosan needed to maintain LbL assembly (Han et al., 2016). After the incubation time, thermogravimetric analysis was carried out (Figure 27), and the % of organic matter were calculated (Table 14). The % of organic matter in nanoparticles after trying to destroy LbL (Table 14) was similar to the organic matter in untreated nanoparticles, ( $p > 0.05$ ) (Table 12). These findings indicate that the layers are hard to hydrolyse and stay intact entrapping gentamicin between them, which explains the similarity in the release profiles for different quadruple layers in different media as gentamicin release occurs most probably only the outer layer of the deposited coating.

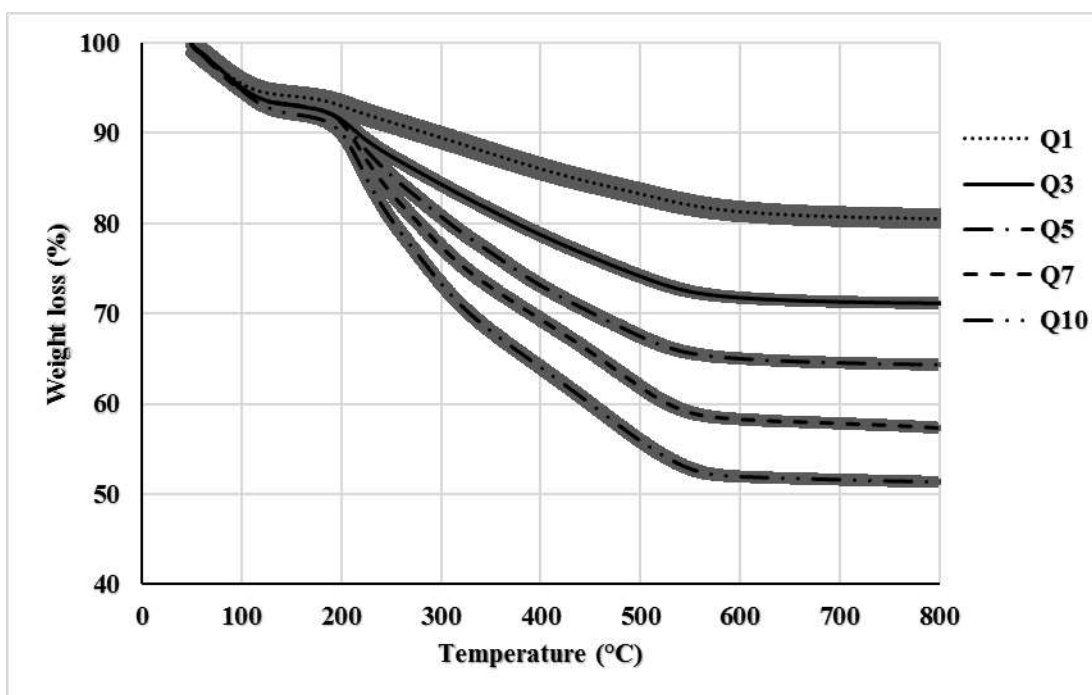


Figure 26: Thermogravimetric analysis for chitosan layered nanoparticles after destroying LbL in pH 2 buffer ( $n = 3 \pm SD$ ).

Samples	Organic content (%)
Q1	14.49 ±2.65
Q3	23.88 ±1.98
Q5	30.67 ±1.46
Q7	37.75 ±1.43
Q10	43.67 ±1.11

Table 14 : Organic matter in chitosan layered nanoparticles after trying to destroy LbL in pH 2 buffer (n = 3 ± SD).

For B1 layered nanoparticles, gentamicin release was continued up to 30 days before reaching plateau (Figure 27 and Figure 28). In pH 7.3 media (Figure 27), Q1 and Q3 had similar release (p>0.05), also Q5 and Q7 had similar release profile and Q10 showed the highest release profile than Q7 (p<0.05). In pH 5 media (Figure 28), Q10 had the highest release profile and Q1 had the lowest. Also, the amount of drug released from Si nanoparticles with the same number of quadruple layers was greater at pH 7.3 than pH 5 (p<0.05).

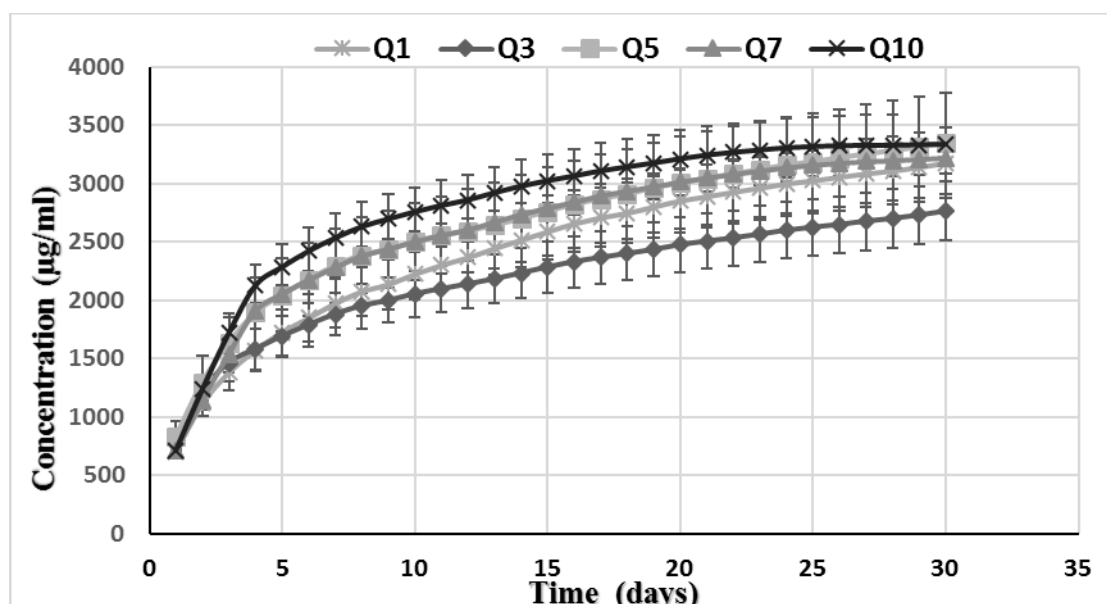


Figure 27: Gentamicin release in PBS (pH 7.3) from Q1, Q3, Q5, Q7 and Q10 layered using B1 as a polycation (n = 3 ± SD).

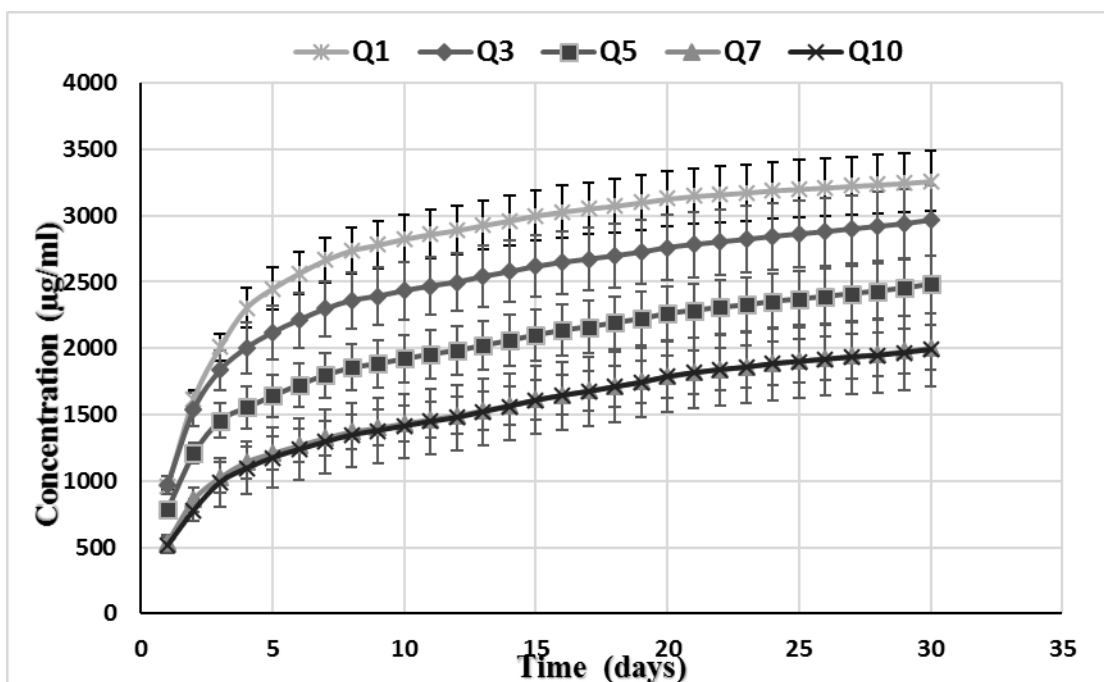


Figure 28: Gentamicin release in acetate buffer (pH 5) from Q1, Q3, Q5, Q7 and Q10 layered with B1 as a polycation ( $n = 3 \pm SD$ ).

The zeta value for alginate and B1 was measured at different pH points (*Figure 29*), to understand the electrostatic interaction between them and explain the release results at different pH media. At pH 7.3, both B1 and alginate were negatively charged, so the electrostatic interaction between them was weak. The amino group of B1 become deprotonated at pH 7.3.

At pH 5, B1 is positively charged and alginate is negatively charged, resulting in strong electrostatic interaction between oppositely charged polyelectrolytes. This strong electrostatic interaction decreased the rate of hydrolysis of B1 and prevented the destruction of LbL construct, and with increasing the number of quadruple layers this phenomenon was more obvious. Consequently, the order of release was reversed and the more quadruple layers on nanoparticles, the lower the release profile. For example, the prevalence of B1 hydrolysis in Q1 give the highest release profile because of low electrostatic interaction involved compared with Q10, which showed the lowest release profile.

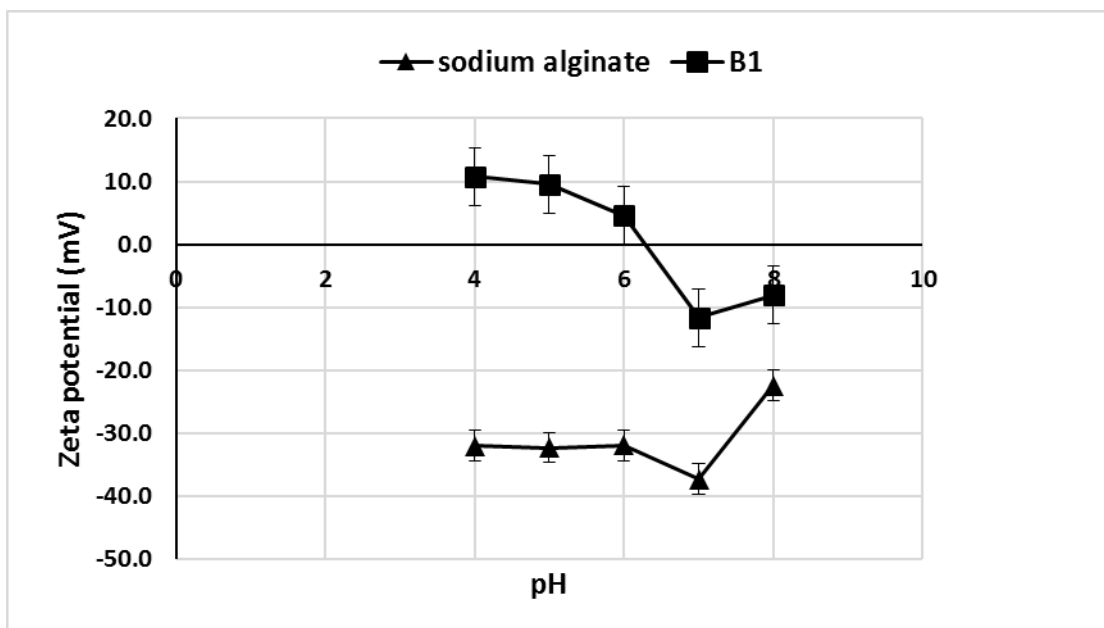


Figure 29 : Zeta values for pure sodium alginate solutions and B1 (2mg/ml) at different pH values ( $n = 3 \pm SD$ ).

## 3.4 Discussion

In this study, a gentamicin nanotechnology based delivery system was developed to provide prophylaxis from post-surgical orthopaedic infections. LbL technique was used for loading gentamicin on amino functionalised silica nanoparticles using two types of quadruple layers: (i) (sodium alginate, gentamicin, sodium alginate and chitosan), (ii) (sodium alginate, gentamicin, sodium alginate and B1). The two quadruple layers differ in the polycation used; either chitosan or B1. Ten quadruple layers were loaded on the surface of the nanoparticles using two types of quadruple layer sequences. The coated nanoparticles were characterized for size, TGA, and zeta potential. In order to evaluate the deposition of polyelectrolyte layers and gentamicin on the surface of the nanoparticles. Finally, *in vitro* release studies were performed to investigate gentamicin release profile from both types of coatings at different joint conditions, healthy joint (pH ~ 7.3) and infected joint associated with local acidosis (pH ~ 5) (Kinnari et al., 2009; Ribeiro et al., 2012).

### 3.4.1 Size measurements

The amino functionalised silica nanoparticles had spherical monodisperse shape, which was confirmed by TEM images of (55 nm). This size is consistent with previously prepared amino functionalised silica nanoparticles in literature (Lu, 2013; Soto-Cantu et al., 2012). After layering different number of electrolytes, there was a small increase in the size of nanoparticles up to (65 nm) as seen in Q10 and calculated from TEM images, which is consistent with polyelectrolyte quadruple layers of about 0.5 nm thickness.

### 3.4.2 Zeta potential measurements

Zeta potential is a straightforward and widely used method for monitoring the multilayer build up, and deposition of polyelectrolyte layers on the surface of nanoparticles during LbL technique (Taladriz-Blanco et al., 2013).

Amino functionalization is a common straightforward method to give the nanoparticles strong charge, because the non-functionalised silica nanoparticles do not have enough charge for the deposition of polyelectrolytes (Soto-Cantu et al., 2012). The zeta value for the amino functionalised silica nanoparticles (*Figure 20*) was consistent with previous studies about amino functionalization of silica

nanoparticles with APTS (Arce et al., 2015) (Niu et al., 2015). The positive charge was due to the protonation of the amino groups at pH 5, which compensates for the negative charge of silanol groups. The zeta potential value after layering sodium alginate was converted into a negative value of nearly  $-30$  mV. Sodium alginate is an anionic polyelectrolyte with carboxylic acid as a functional group. This change of the sign of zeta potential was due to the electrostatic interaction between the carboxylate group of sodium alginate and amino groups on the surface of the nanoparticles. The negative zeta potential value after layering sodium alginate was in accordance with values reported by (Feng et al., 2014).

After layering gentamicin, the value of zeta potential was decreased less negativity value. However, Gentamicin could not reverse it into a positive value since it is a small molecule, with small number of ionisable groups, compared to a polyelectrolyte like sodium alginate. Gentamicin is an aminoglycoside antibiotic with only five amino functional groups. The electrostatic interaction between the amino groups of gentamicin and the carboxylate groups of sodium alginate was the reason for the deposition of gentamicin. After layering sodium alginate over gentamicin, the zeta value was decreased again to almost the same negative value seen in the first alginate layer.

After layering chitosan, the zeta potential was reversed into a positive value of nearly  $+20$  mV. This zeta potential values were similar to those obtained by (Feng et al., 2014). Chitosan is a cationic polyelectrolyte with positively charged amino groups. Chitosan was deposited on the surface of sodium alginate because of the electrostatic interaction between carboxylate groups of sodium alginate and amino groups of chitosan. In B1 layered nanoparticles, layering B1 could not reverse the negativity of zeta value into a positive one, because the zeta value of pure B1 solution is  $+8$  mV compared to  $+25$  mV for chitosan, indicating weaker cationic properties for B1. However, B1 managed to decrease the negativity of coated particles close to zero, but alginate projected an overall negative charge on the surface of coated nanoparticles. Higher concentration of B1 layering solution is possibly needed to reverse the negative zeta value of alginate.

Generally speaking, zeta potential value kept alternating with the same pattern as evident in *Figure 20* and *Figure 21*. This pattern is summarized for one quadruple

layer as follows: (- 30 mV) after layering sodium alginate, less negative value of nearly (-13 mV) after layering gentamicin, more negative value back again to -30 after layering sodium alginate, and finally (+20 mV) after layering chitosan or (-5 mV) in case of B1 in each quadruple layer. Also, the values obtained for nanoparticles coated with alginate or chitosan were close to the zeta values of pure polyelectrolyte solutions, therefore deposition was optimal. This pattern was observed to be nearly the same in the 10 quadruple layers which confirms the deposition of polyelectrolytes and gentamicin during LbL process.

### **3.4.3 Thermogravimetric analysis (TGA)**

TGA is a commonly used type of analysis to assess the presence of organic matter on the surface of nanoparticles, based on the observation of mass loss (Mai et al., 2013). Furthermore, TGA is used to evaluate surface functionalization on the surface of nanoparticles (Zhong et al., 2015). Therefore, during LbL assembly, the deposition of polyelectrolytes on the surface of nanoparticles was evaluated quantitatively using TGA analysis (Wu et al., 2015).

The thermogram for the amino functionalised silica nanoparticles (Figure 22) was similar to the one obtained by (Branda et al., 2010). Moreover, the calculated organic matter percentage for the amino functionalised silica nanoparticles (Table 12) was in agreement with the one reported by (Liu et al., 2015). A consistent increase in the organic content was observed for amino functionalised silica nanoparticles and different quadruple layer with increasing the number of layers on the surface of the amino functionalised silica nanoparticles. This consistent increase in the organic content confirmed the deposition of the layered polyelectrolytes and drug on the surface of the amino functionalised silica nanoparticles.

### **3.4.4 Gentamicin release quantification**

Drug release from a LbL construct occurs as combination of two extreme cases; one is the delamination of the deposited layers and the second the diffusion of the drug through the deposited layers (Smith et al., 2009); each of these two mechanisms have a distinctive release profile. Pure delamination returns a constant release kinetic until all the coating is detached, at this point drug release drops to zero. On the other hand, diffusion returns a Fickian profile (Smith et al., 2009)

with drug release monotonically decreasing from the initial value down to zero. Based on previous studies (Grech et al., 2008; Min et al., 2014; Wong et al., 2010), gentamicin release from LbL coatings is mainly dependent on the number of quadruple layers, the type of polyelectrolytes used, the electrostatic interaction between different polyelectrolytes, and the kinetics of hydrolysis for the polyelectrolytes involved. Moreover, the different kinetics observed at the two pH values impact on both the electrostatic interactions between polyelectrolytes chains (through different level of protonation) and their kinetics of hydrolysis.

In chitosan layered nanoparticles, gentamicin release was not affected by the pH value of the medium (*Figure 24* and *Figure 25*). The electrostatic interaction between chitosan and alginate formed a stable construct at both pH tested; hence the drug could be released only through diffusion; moreover because of the strong interaction between chitosan and alginate gentamicin release could only occur from the superficial layers. The stability of the LbL constructs at pH 2 and the release profiles in both buffers are consistent with such mechanism.

For B1 coated nanoparticles, gentamicin release from different quadruple layers was dependent on pH value because pH affected the ionization of B1, whose charge was positive at pH 5 and close to zero at pH 7 forming a weaker polyelectrolyte interaction with alginate; such higher electrostatic interactions reduce the ability of gentamicin to diffuse through the layer (reduce the diffusion coefficient). B1 showed higher release at pH 7, compared to pH 5, as the weaker the LbL constructs the higher the gentamicin diffusion through the coating. The higher kinetics of release at pH 7 was despite B1 hydrolysis rate was more rapid in acid environment. Therefore, even though the hydrolysis of B1 is considered the key controlling mechanism in drug release from LbL coating, the electrostatic interactions between polyelectrolytes appeared to play the predominant role in the release of the deposited gentamicin. Despite the well-known pH dependent behaviour of PBAEs (Devalapally et al., 2007), role of electrostatic interactions in controlling drug release when PBAE are used in LbL constructs had not been addressed before.

The mechanisms based on electrostatic interactions suggested here would still explain the effect of the intercalating clay (Min et al. 2014) or PAH/PAA (Poly (allylamine hydrochloride)/ Poly (allylamine)) (Wood et al., 2006) layers that were employed to intercalate quadruple layers constructs containing B1 in order to extend the period of effective drug release under the hypothesis that they were being not hydrolysable, would slow down B1 degradation. These intercalating layers exhibit higher charges than B1 at the pH conditions of those experiments hence resulting in a reduced diffusion coefficient for gentamicin.

In chitosan layered nanoparticles, gentamicin release was not affected by the pH value of the medium (*Figure 24* and *Figure 25*). The electrostatic interaction between chitosan and alginate formed a stable construct and prevented the hydrolysis of alginate chitosan layers, and the drug was entrapped between the layers. It is well known that the hydrolysis of chitosan *in vitro*, and other polysaccharides, only occurs via enzymatic hydrolysis, making it possible for the stable construct to release gentamicin *in vivo* (Lim et al., 2008). For PBAE coated nanoparticles, gentamicin release from different quadruple layers was dependent on pH value because pH affected the ionization of PBAE, and PBAE charge became close to zero at pH 7 forming a weak polyelectrolyte interaction with alginate. As a result, PBAE showed higher release at pH 7 compared to pH 5. Also, PBAE hydrolysis rate was more rapid at basic environment, where more degradation of PBAE was in pH 7 compared to pH 5. Moreover, the ability of PBAE to be hydrolysed *in vitro* helped in obtaining higher release profiles compared to chitosan layer nanoparticles.

Wong et al. (2010) achieved controlled gentamicin release for several hours using hydrolytically degradable polyelectrolytes multilayers, with gentamicin sandwiched between different layers of poly ( $\beta$ -amino esters) using LbL technique. In this work, gentamicin release from B1 layered nanoparticles continued for 30 days, which is a considerable improvement from the current PMMA bone cement that release antibiotics for only 6 days (Dunne et al., 2008; Gasparini et al., 2014; Moojen et al., 2008; Squire et al., 2008). The release of gentamicin did not show the initial burst seen in LbL gentamicin quadruple layers

using hydrolysable polyelectrolytes. Furthermore, gentamicin release was sustained for longer period of time with less number of quadruple layers.

Moskowitz et al. (2010) studied the release of gentamicin from a titanium implant coated using LbL technique. The implant was coated with 200 tetralayer of degradable films (tetralayer: poly ( $\beta$ -amino esters), polyacrylic acid, gentamicin, polyacrylic acid). More than 70 % of the drug was released in the first 3 days with continued release for 5 weeks, and the total amount released was 550  $\mu\text{l/ml}$  in at pH 7.4. In another work, Wong et al. (2010) reported gentamicin release from LbL coating composed of 30 units of the same tetralayer of (poly ( $\beta$ -amino esters), polyacrylic acid, gentamicin, polyacrylic acid) for 7 hours in PBS, pH 7.3. Chuang et al. (2008) studied the release of gentamicin from a 100 tetralayers of (poly ( $\beta$ -amino esters), hyaluronic acid, gentamicin, hyaluronic acid) in simulated body fluids, where gentamicin release was controlled for not more than 15 hours. Compared to the previously mentioned work, B1 LbL system showed better outcome in terms of controlling the release kinetics for extended period of time at higher concentrations, using smaller number of quadruple layers.

Gentamicin release with B1 at pH 7 reached high concentration of 3500  $\mu\text{g/ml}$ . This concentration is relatively high compared to minimum inhibitory concentration needed to kill different bacteria involved in orthopedic infections (Drago et al., 2014). This high concentration is promising for further evaluation of release when the nanoparticles are impregnated into the PMMA bone cement. The controlled release manner and long duration of release could provide prophylaxis from early stage infections, but further optimization for gentamicin loading and assessment of release profiles from impregnated bone cements are needed to confirm these assumptions.

### **3.5 Conclusion**

Antimicrobial thin films were constructed through LbL deposition technique using two types of tetralayers. The films were deposited by alternating depositions between alginate and hydrolytically degradable polymers; the antibiotic gentamicin was directly incorporated without the need for pre-modification. LbL was effective in controlling release of antibiotic from silica nanoparticles for at least 4 weeks without initial burst release, giving a promising profile for the

application in infection prevention and treatment, either by using the LbL as a coating for biomedical implants and devices, or by incorporation of the coated nanoparticles into bone cements. Chitosan results in a LbL structure that is too stable to provide release for a long period of time, entrapping gentamicin between the layers. PBAE is more suitable as a polycation to prepare gentamicin releasing silica nanoparticles, and the release profile can be tuned by variations in LbL coating.

For the first time, this work provides evidence that the mechanism of gentamicin release is governed by electrostatic interaction between different polyelectrolytes even when PBAE were employed, confuting the establish assumption that hydrolysis is the key factor when these polymers are used.

Our results also provide guidance in the polyelectrolyte properties required to achieve a desired release profile; i.e. to increase the release kinetic a polyelectrolyte with lower charge is required instead of more easily hydrolysed one; as it would be the case if hydrolysis was the governing mechanism in drug release from LbL coatings.

## **4 Chlorhexidine controlled release from Layer-by-Layer coated silica nanoparticles.**

### **4.1 Introduction**

The use of antibiotics is the traditional approach for the prevention and treatment of PJIs (Parvizi et al., 2008). However, the continuing emergence of resistant microbial strains decreases the effectiveness of antibiotic-based therapies (Allahverdiyev et al., 2011). Hence, it is extremely urgent to develop non-antibiotic therapies for the prevention and treatment of infections in general, especially in PJIs. Anguita-Alonso *et al.* (2005) investigated the susceptibility of *Staphylococcus* taken from patients with prosthetic infection against gentamicin and tobramycin (aminoglycoside antibiotics). 41% and 66% of bacteria were resistant to gentamicin and tobramycin respectively. Corona et al. (2014) compared antibiotic susceptibility between patients having infection for the first time and patients with previous use of ALBC and found a significantly higher resistance, indicating the risk of selecting aminoglycosides resistant strains after using ALBC.

Chlorhexidine is a broad spectrum cationic bactericidal polybiguanide antimicrobial agent (Hidalgo and Dominguez, 2001). It has many applications as a disinfectant and antiseptic for skin infections, cleaning wounds (O'Malley, 2008), sterilization of surgical instruments (Knox et al., 2015), and many dental applications including treatment of dental plaque, gingivitis and endodontic disease (Supranoto et al., 2015). The guanidium groups in its structure is responsible for the antimicrobial activity by binding to bacterial cell membrane causing cell function disruption (Denyer, 1995). Although it has been widely examined in dental cements (Fan et al., 2016), it has not been investigated widely in acrylic bone cements. The use of chlorhexidine in bone cements can enhance its antimicrobial properties because of the superior antimicrobial activity. However, one of the limitations for application of chlorhexidine in bone cement is the decrease in the compressive strength upon powder incorporation (Rodriguez et al., 2015)

Despite chlorhexidine small structure, it can be incorporated in LbL assembly multilayers. Chlorhexidine release from B1 layered nanoparticles continued for 70

days, which is a considerable improvement from the current drug delivery systems that release antimicrobial agents for only few days (Dunne et al., 2008; Gasparini et al., 2014; Moojen et al., 2008; Squire et al., 2008). The release of chlorhexidine did not show the initial burst seen in LbL chlorhexidine quadruple layers using non-hydrolysable polyelectrolytes.

In this chapter, we aim to provide controlled release of chlorhexidine incorporated directly into multilayer films constructed on the surface of silica nanoparticles using LbL assembly coating method. Multilayer films were constructed using the hydrolysable polymer B1, and non-hydrolysable polymer alginate to provide controlled release of chlorhexidine for more than 2 months at high concentrations with high drug loading capacity. This approach represents a convenient and effective strategy to control the release of chlorhexidine which has many antibacterial applications in infection prevention and treatment, particularly the early and delayed stage infections after TJR.

## **4.2 Materials and methods**

### **4.2.1 Chemicals**

Triton X-100, tetraethyl orthosilicate (TEOS), 3-aminopropyltriethoxysilane (APTS), sodium alginate, chlorhexidine diacetate, sodium acetate trihydrate, phosphate buffer solution (PBS) tablets, were purchased from Sigma-Aldrich, UK. Cyclohexane, n-hexanol, ammonium hydroxide (35%), ethanol, methanol, glacial acetic acid and acetonitrile were purchased from Fishers scientific, UK. All reagents were stored according to manufacturer's guidelines and used as received. B1: is a patented biocompatible, biodegradable cationic polymer, the precise structure will remain confidential due to the IP associated, freshly prepared in the lab before use.

Acetic acid-sodium acetate buffer as follows: to prepare 100 ml acetic acid-sodium acetate buffer (0.1 M, pH 5), 30 ml of sodium acetate trihydrate ( $\text{CH}_3\text{COONa}\cdot 3\text{H}_2\text{O}$ ) (0.1 M) were added to 70 ml of acetic acid ( $\text{CH}_3\text{CO}_2\text{H}$ ) (0.1 M) solutions and stirred. Acetate buffer (0.1 M, pH 4) was prepared by mixing 18 ml of sodium acetate trihydrate with 82 ml of acetic acid. Phosphate buffer saline (PBS) (pH 7.3) was prepared by dissolving 1 tablet of PBS in 100 ml of deionized water.

### **4.2.2 Nanoparticle preparation**

#### **4.2.2.1 Amino functionalised silica nanoparticle synthesis**

Silica nanoparticles functionalised with amine groups ( $\text{SiO}_2\text{-NH}_2$ ) were prepared in one-pot synthesis by hydrolysis of TEOS in reverse micro-emulsion and subsequent functionalization (Stöber method) (Stöber et al., 1968), as described in section 2.1.2.1.

#### **4.2.2.2 Layer by Layer (LbL) coating technique**

The silica nanoparticles were layered with different numbers of the repeating sequence of polyelectrolytes (sodium alginate/chlorhexidine/sodium alginate/B1). Up to ten quadruple layers were coated onto silica nanoparticles (*Table 15*). The following concentrations of polyelectrolytes and drug in acetic acid-sodium acetate buffer were used in LbL: sodium alginate (2 mg/ml), Chlorhexidine (10

mg/ml) and B1 (2 mg/ml). (The procedure for LbL coating technique was described in section 2.1.2.2)

Quadruple layer no.	Abbreviation	Layers on the surface of amino functionalised silica nanoparticles (SiNH <sub>2</sub> )
1	Q1	SiNH <sub>2</sub> -alginate-chlorhexidine-alginate- <b>B1</b>
2	Q2	SiNH <sub>2</sub> -Q1-alginate- chlorhexidine -alginate- <b>B1</b>
3	Q3	SiNH <sub>2</sub> -Q2-alginate- chlorhexidine -alginate- <b>B1</b>
4	Q4	SiNH <sub>2</sub> -Q3-alginate- chlorhexidine -alginate- <b>B1</b>
5	Q5	SiNH <sub>2</sub> -Q4-alginate- chlorhexidine -alginate- <b>B1</b>
6	Q6	SiNH <sub>2</sub> -Q5-alginate- chlorhexidine -alginate- <b>B1</b>
7	Q7	SiNH <sub>2</sub> -Q6-alginate- chlorhexidine -alginate- <b>B1</b>
8	Q8	SiNH <sub>2</sub> -Q7-alginate- chlorhexidine -alginate- <b>B1</b>
9	Q9	SiNH <sub>2</sub> -Q8-alginate- chlorhexidine -alginate- <b>B1</b>
10	Q10	SiNH <sub>2</sub> -Q9-alginate- chlorhexidine -alginate- <b>B1</b>

Table 15 : 10 quadruple layers containing chlorhexidine as an antimicrobial agent, and B1 as a polycation

### 4.2.3 Nanoparticle surface and material characterisation

#### 4.2.3.1 Nanoparticle size measurements

The size of nanoparticles was characterized using transmission electron microscopy (TEM), as described in section 2.1.3.1.

#### 4.2.3.2 Nanoparticle zeta potential measurements

The electrophoretic mobility for the nanoparticles was measured by dynamic light scattering (DLS), using Malvern Zetasizer, Nano ZS particle characterization system (Malvern Instruments Limited, UK), as described in section 2.1.3.2.

#### **4.2.3.3 Thermogravimetric analysis**

Thermogravimetric analysis (TGA) was performed using a Perkin-Elmer TGA 4000 instrument, as described in section 2.1.3.3.

#### **4.2.4 Chlorhexidine release quantification**

Chlorhexidine release from the nanoparticles was evaluated by dispersing the drug loaded nanoparticles (10 mg) in 1ml in 2 buffer media: acetic acid-sodium acetate buffer pH 5 and PBS pH 7.3, and kept in eppendorfs. These two pH points are chosen to assess the drug release under healthy joint (pH 7.35-7.45) (Ribeiro et al., 2012), and for infected joint, which are associated with low pH values (pH < 7) or local acidosis (Kinnari et al., 2009).

Then, samples were vigorously stirred in a vortex, and then incubated at 37°C. Samples were taken every 24 hours where 1ml of release medium aliquots were taken after centrifugation, to avoid withdrawing nanoparticles during taking the sample.

The amount of chlorhexidine released from nanoparticles was quantified using reversed-phase High Performance Liquid Chromatography (HPLC) method, as described in section 2.1.5.

#### **4.2.5 Statistical analysis**

All data were expressed as means  $\pm$  standard deviation (SD) from at least three values. To assess the statistical significance of results between groups, one-way analysis of variance (ANOVA) was performed. Experimental results were considered statistically significant at 95 % confidence level ( $p < 0.05$ ). All analyses were run using the SPSS® software.

## 4.3 Results

### 4.3.1 Nanoparticle surface and material characterization

#### 4.3.1.1 Size measurements

TEM images of the amino functionalised silica nanoparticles and Q10 are shown in (Figure 30). The size measurement calculated from TEM images are  $55.1 \pm 8.3$  and  $66.2 \pm 6.2$  for the silica NPs and Q10, respectively.

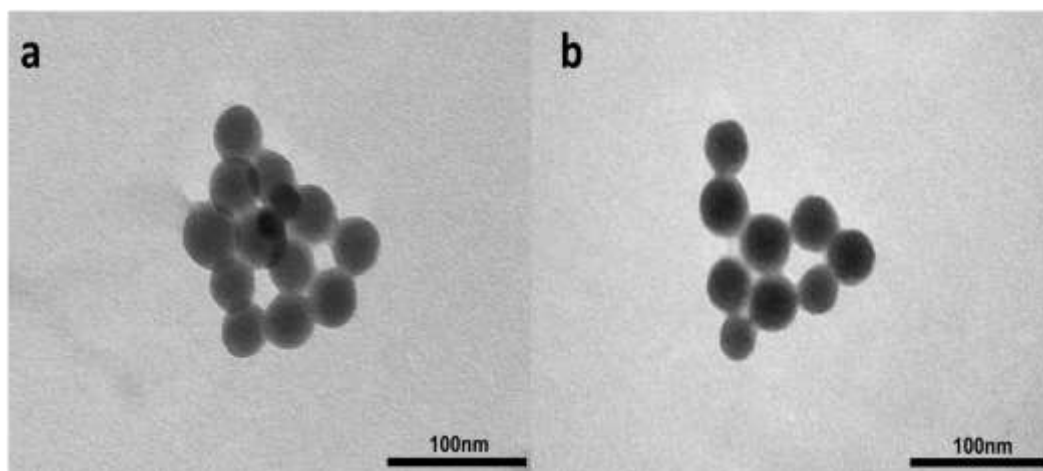


Figure 30:TEM images for: (a) amino functionalised silica nanoparticles (b) Q10 of chlorhexidine loaded silica nanoparticles with B1 as a polycation.

#### 4.3.1.2 Zeta potential measurements

Zeta potential were done for the amino functionalised silica nanoparticles and after each layering step, as shown in Figure 31. Zeta potentials were measured for ten quadruple layers; the total number of layers needed to build ten quadruple layers is 40 layers. The zeta potential for the amino functionalised silica nanoparticles was  $30.1 \pm 0.95$  mV because of the ionized amino groups on the surface.

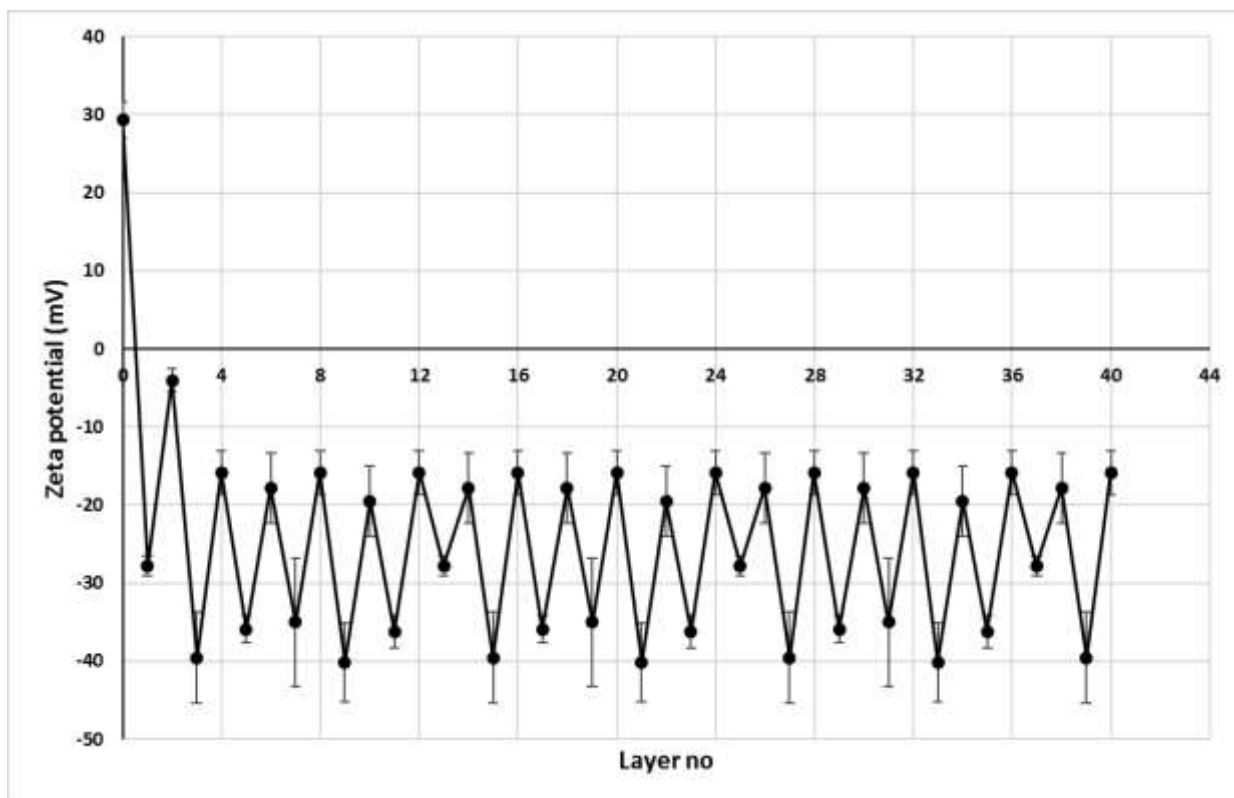


Figure 31: Zeta potential for 10 quadruple layers with the repeating unit (alginate-chlorhexidine-alginate-B1) ( $n = 3 \pm SD$ ).

The first quadruple layer (layer 1 to 4) showed that layering sodium alginate reverses the zeta potential to a negative value of  $-27.8 \pm 1.2$  mV. Next, chlorhexidine layer decreased the negativity of zeta potential to  $-4.0 \pm 1.5$  mV with similar trend seen previously in gentamicin containing nanoparticles. Then, the subsequent sodium alginate layer increased the negativity of the zeta potential value to  $-39.6 \pm 3.5$  mV. Then, B1 layering step reversed the value of zeta potential to a negative value of  $-15.8 \pm 2.8$  mV. For quadruple layers 2 to 10 (layer number 5-40), a similar trend in the changes of zeta potential was observed compared to the first quadruple layer. B1 zeta potential values were negative among different types of layers. B1 did not reverse the negativity of sodium alginate, because the zeta potential for a pure solution of B1 is  $+8$  mV compared to  $-30$  mV for alginate. B1 is a weaker polycation, and sodium alginate projected an overall negative zeta value even on the surface of B1 layered nanoparticles, the same observation was seen in gentamicin containing nanoparticles.

### 4.3.1.3 Thermogravimetric analysis

Thermogravimetric analysis was performed for amino functionalised silica nanoparticles and the same nanoparticles layered with different number of quadruple layers, using B1 as a polycation and chlorhexidine as an antimicrobial as shown in (Figure 32). In order to assess the organic matter content after and the build-up of multilayers after LbL coating process.

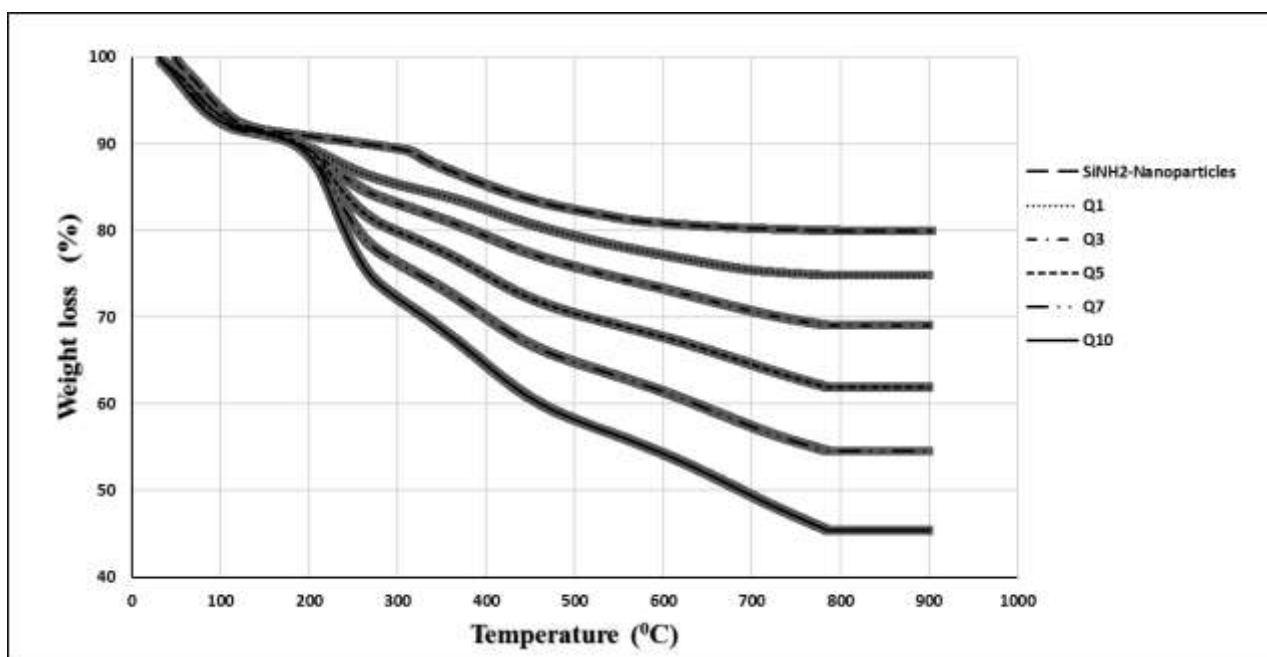


Figure 32: Thermogram for silica nanoparticles layered with different number of quadruple layer containing chlorhexidine ( $n = 3 \pm SD$ ).

An initial weight loss around (5%) was observed at about 100 °C, which is normally attributed to the evaporation of adsorbed water from the samples (Wang et al., 2014). As a result, the organic content for each sample (Table 16) was calculated based on the weight loss beyond 100 °C, which corresponds to the combustion of organic matter (Du *et al.*, 2015).

Samples	Organic content (%)
SiNH <sub>2</sub> -Nanoparticles	14.95 ± 1.00
Q1	20.18 ± 1.51
Q3	25.95 ± 0.36
Q5	33.08 ± 2.14
Q7	40.45 ± 1.45
Q10	49.59 ± 2.25

Table 16 : Percentage of organic matter in silica nanoparticles layered with different number of quadruple layers containing chlorhexidine (n = 3 ± SD).

In B1 layered nanoparticles (*Table 16*), the organic content for the amino functionalised silica nanoparticles is 14.95 %. The organic content is increased by adding the first quadruple layer as seen for Q1 (20.18 %), which makes a 5% increase in the organic content for the first quadruple layer. For Q3, the organic matter was increased to reach (25.95 %). And the organic content kept increasing with addition of more quadruple layers to reach 33.08, 40.45 and 49.59 % for Q5, Q7 and Q10, respectively, as observed previously with gentamicin containing nanoparticles.

#### 4.3.2 Chlorhexidine release quantification

The drug release studies for chlorhexidine loaded silica nanoparticles were carried out in two release media; PBS buffer (pH 7.3), and acetic acid-sodium acetate buffer (pH 5). Chlorhexidine was quantified by HPLC using UV detection in each sample. These two pH points are chosen to assess the drug release under healthy joint conditions (pH 7.35-7.45) (Ribeiro et al., 2012), and for infected joint, which are associated with low pH values (pH < 7) or local acidosis (Kinnari et al., 2009).

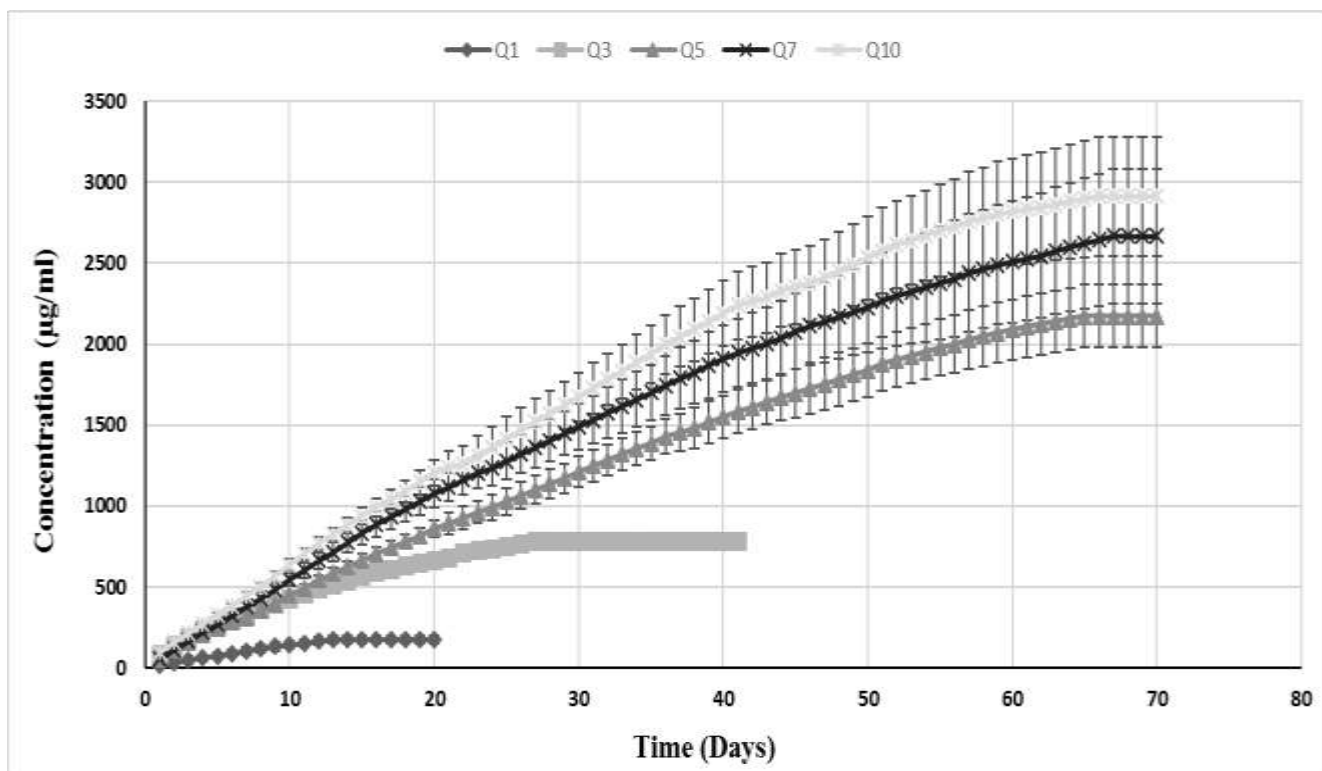


Figure 33 : Cumulative chlorhexidine release in PBS (pH 7.3) from Q1, Q3, Q5, Q7 and Q10 layered nanoparticles ( $n = 3 \pm SD$ ).

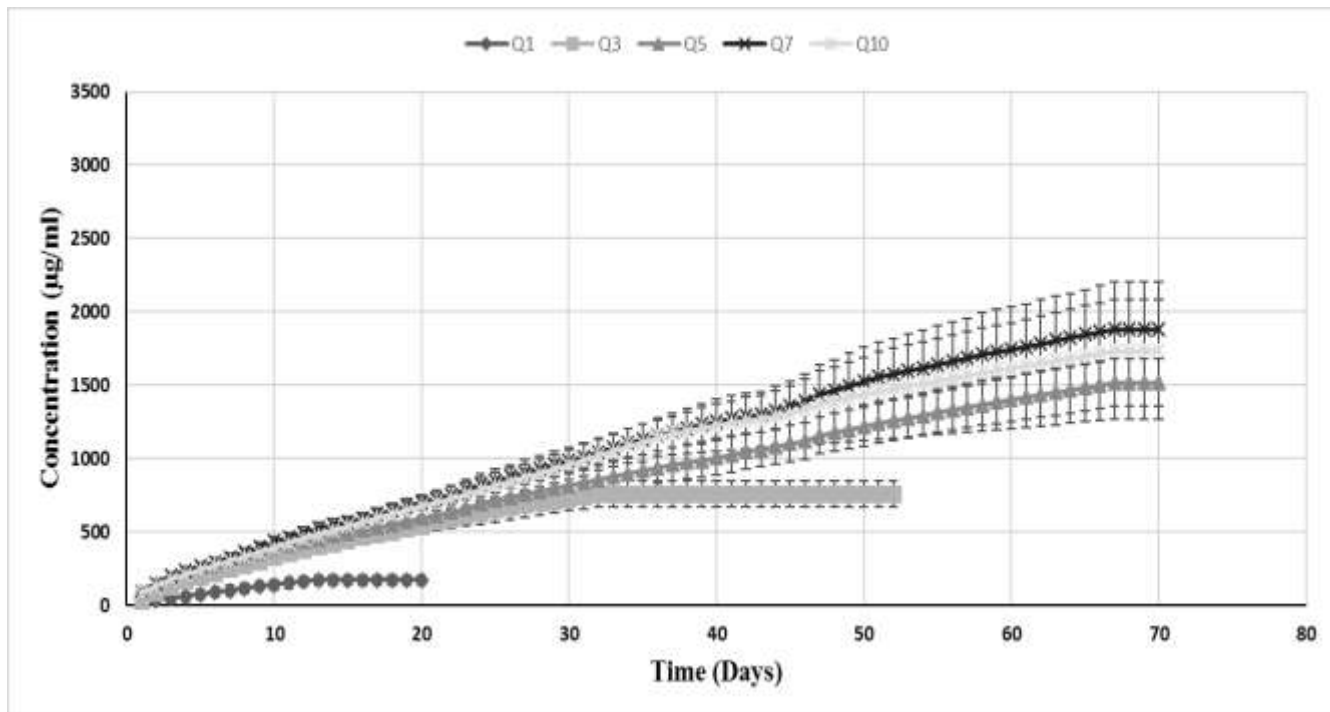


Figure 34 : Cumulative chlorhexidine release in acetate buffer (pH 5) from Q1, Q3, Q5, Q7 and Q10 layered nanoparticles ( $n = 3 \pm SD$ ).

Chlorhexidine release continued up to 70 days before reaching plateau (Figure 33 and Figure 34). In pH 7.3 media (Figure 33), the release profile increased with increasing the number of quadruple layers, with Q10 having the highest release profile. However, there was not a significant difference between Q7 and Q10 release profiles, ( $p>0.05$ ). In pH 5 media (Figure 34), drug release also continued up to 70 days, but with lower release profile concentrations compared to amount of drug released at pH 7.3. the same trend in the increase in the release profiles with increasing the number of quadruple layers was also observed. However, the difference was less evident between Q5, Q7 and Q10, showing release more or less in the same range ( $p>0.05$ ).

## **4.4 Discussion**

In this chapter, a chlorhexidine nanotechnology based delivery system was developed to provide prophylaxis and treatment from post-surgical orthopaedic infections. LbL technique was used for loading chlorhexidine on amino functionalised silica nanoparticles using the quadruple layers (sodium alginate/chlorhexidine/sodium alginate/B1) to build ten quadruple layers on the surface of the nanoparticles. The coated nanoparticles were characterized for size, TGA, and zeta potential. In order to evaluate the deposition of polyelectrolyte layers and chlorhexidine on the surface of the nanoparticles. Finally, *in vitro* release studies were performed to investigate chlorhexidine release profile from both types of coatings at different joint conditions, healthy joint (pH ~ 7.3) and infected joint associated with local acidosis (pH ~ 5) (Kinnari et al., 2009; Ribeiro et al., 2012).

### **4.4.1 Size measurements**

The size of the amino functionalised silica nanoparticles and Q10 for chlorhexidine nanoparticles loaded with chlorhexidine were analysed by TEM. The amino functionalised silica nanoparticles had a size of  $55.1\pm 8.3$  nm. After layering 10 quadruple layers the size increased to  $66.2\pm 6.2$  nm, which is similar to the size of gentamicin loaded silica nanoparticles.

#### 4.4.2 Zeta potential measurements

Zeta potential is a straightforward and widely used method for monitoring the multilayer build up, and deposition of polyelectrolyte layers on the surface of nanoparticles during LbL technique (Taladriz-Blanco et al., 2013). Amino functionalization is a common method to give the nanoparticles a positive charge, because the non-functionalised silica nanoparticles do not have enough charge for the deposition of polyelectrolytes (Soto-Cantu et al., 2012). The zeta value for the amino functionalised silica nanoparticles (*Figure 31*) was consistent with previous studies about amino functionalization of silica nanoparticles with APTS (Arce et al., 2015; Niu et al., 2015). The positive charge was due to the protonation of the amino groups at pH 5, which compensates for the negative charge of silanol groups. The zeta potential value after layering sodium alginate was converted into a negative value of nearly  $-30$  mV. Sodium alginate is an anionic polyelectrolyte with carboxylic acid as a functional group. This change of the sign of zeta potential was due to the electrostatic interaction between the carboxylate group of sodium alginate and amino groups on the surface of the nanoparticles. The negative zeta potential value after layering sodium alginate was in accordance with values reported by (Feng et al., 2014).

After layering chlorhexidine, the value of zeta potential was decreased less negativity value. However, chlorhexidine could not reverse it into a positive value because it is a small molecule (molecular weight: 505.5 g/mole), with small number of ionisable groups, compared to a polyelectrolyte like sodium alginate (Molecular weight  $>10000$  g/mole). Chlorhexidine is a bisbiguanide antiseptic with only ten amino functional groups. The electrostatic interaction between the amino groups of chlorhexidine and the carboxylate groups of sodium alginate was the reason for the deposition of chlorhexidine. After layering sodium alginate over chlorhexidine, the zeta value was decreased again to almost the same negative value seen in the first alginate layer. In B1 layered nanoparticles, layering B1 could not reverse the negativity of zeta value into a positive one, because the zeta value of pure B1 solution is  $+8$  mV compared to  $-30$  mV for alginate which have stronger ionic character. However, B1 managed to decrease the negativity of coated particles close to zero, but alginate projected an overall negative charge on the

surface of coated nanoparticles. Doubling the concentration of B1 could not reverse the negative zeta value of alginate.

Generally speaking, zeta potential value kept alternating with the same pattern as evident in *Figure 31*. This pattern is summarized for one quadruple layer as follows: (-40 mV) after layering sodium alginate, less negative value of nearly (-20 mV) after layering chlorhexidine, more negative value back again to -40 after layering sodium alginate, and finally (-15 mV) in case of B1 in each quadruple layer. Also, the values obtained for nanoparticles coated with alginate was close to the zeta values of pure polyelectrolyte solutions, therefore deposition was optimal. This pattern was observed to be nearly the same in the 10 quadruple layers which confirms the deposition of polyelectrolytes and chlorhexidine during LbL process.

#### **4.4.3 Thermogravimetric analysis**

TGA is a commonly used type of analysis to assess the presence of organic matter on the surface of nanoparticles, based on the observation of mass loss (Mai et al., 2013). Furthermore, TGA is used to evaluate surface functionalization on the surface of nanoparticles (Zhong et al., 2015). Therefore, during LbL assembly, the deposition of polyelectrolytes on the surface of nanoparticles was evaluated quantitatively using TGA analysis (Wu et al., 2015).

The thermogram for the amino functionalised silica nanoparticles (*Figure 32*) was similar to the one obtained by (Branda et al., 2010). Moreover, the calculated organic matter percentage for the amino functionalised silica nanoparticles (*Table 16*) was in agreement with the one reported by (Liu et al., 2015). A consistent increase in the organic content was observed for amino functionalised silica nanoparticles and different quadruple layer with increasing the number of layers on the surface of the amino functionalised silica nanoparticles. This consistent increase in the organic content confirmed the deposition of the layered polyelectrolytes and drug on the surface of the amino functionalised silica nanoparticles. Compared to Q10 from gentamicin loaded nanoparticles (organic content  $41.5\% \pm 3.6$ ), Q10 for the chlorhexidine loaded nanoparticles had higher organic matter of  $49.5\% \pm 2.2$  which is expected because chlorhexidine has higher molecular weight than gentamicin (gentamicin molecular weight 477.5 g/mole).

#### 4.4.4 Chlorhexidine release quantification

Drug release from LbL coatings is mainly dependent on the number of quadruple layers, the type of polyelectrolytes used, the electrostatic interaction between different polyelectrolytes, and the kinetics of hydrolysis for the polyelectrolytes involved (Grech et al., 2008; Min et al., 2014; Wong et al., 2010). Moreover, different pH value for the release media would also affect the behaviour of different polyelectrolytes including their hydrolysis, and further modify drug release.

Chlorhexidine release from different quadruple layers was dependent on pH value because pH affected the ionization of B1, and B1 charge became close to zero at pH 7 forming a weak polyelectrolyte interaction with alginate. As a result, chlorhexidine showed higher release at pH 7 compared to pH 5, a similar trend was observed with gentamicin release (chapter 2). Also, B1 hydrolysis rate was more rapid at basic environment, where more degradation of B1 was in pH 7 compared to pH 5. (Luo et al., 2016) prepared chlorhexidine polymorphs spheres as a template for LbL coating to enhance solubility and control the release of the drug. The size of the spheres was 5.6-20  $\mu\text{m}$  spheres with 90% chlorhexidine content. The LbL coat consisted of 3.5 bilayers of poly(allylamine hydrochloride) (PAH) and polystyrenesulfonate (PSS). The release of chlorhexidine was evaluated in PBS buffer media, where the uncoated spheres showed a burst release in the first 2 hours for all chlorhexidine. While, the coated spheres showed burst release, followed by 7 hours of controlled release with 15% left inside the coated spheres. (Fan et al., 2016) reported a mixing coupling method for incorporating chlorhexidine into calcium silicate nanoparticles, with approximate size of 80 nm at 1:1 ratio by mass. Chlorhexidine release was studied in Simulated body fluids (SBF), where the drug showed burst release of 100  $\mu\text{g/ml}$  after 24 hours of release, followed by a decreased concentration of < 30  $\mu\text{g/ml}$  after 3 days.

In this work, chlorhexidine release from B1 layered nanoparticles continued for 70 days, which is a considerable improvement from the current drug delivery systems that release antimicrobial agents for only few days (Dunne et al., 2008; Gasparini et al., 2014; Moojen et al., 2008; Squire et al., 2008). The release of chlorhexidine did not show the initial burst seen in LbL chlorhexidine quadruple layers using

non-hydrolysable polyelectrolytes. Furthermore, chlorhexidine release was sustained for longer period of time with less number of quadruple layers.

Chlorhexidine release with B1 at pH 7.3 reached high concentration of 3000 µg/ml. This concentration is relatively high compared to minimum inhibitory concentration needed to kill different bacteria involved in orthopedic infections (7.8 µg/ml for *P. aeruginosa* and *A. baumannii*). This high concentration is promising for further evaluation of release when the nanoparticles are impregnated into the PMMA bone cement, especially with a non-antibiotic based antimicrobial agent. The controlled release manner and long duration of release could provide prophylaxis and treatment from early and late stage infections, but further optimization for chlorhexidine loading and assessment of release profiles from impregnated bone cements are needed to confirm these assumptions.

Chlorhexidine use is considered safe in cosmetic products at concentrations up to 0.14% calculated as free base (Andersen, 1999). The use of 2% chlorhexidine gluconate is considered safe for vaginal operative preparation, and not associated with increased vaginal irritation in a gynaecologic surgery (Al-Niimi et al., 2016). However, chlorhexidine application on bone tissue need further investigation to assess cytocompatibility.

## **4.5 Conclusion**

Antimicrobial thin films were constructed through LbL deposition technique, using the sequence (alginate/chlorhexidine/alginate/B1). Chlorhexidine was directly deposited without the need for pre-modification between the layers of alginate, despite it is not a polymeric polyelectrolyte. The LbL construct was effective in controlling the release of chlorhexidine from silica NPs for >2 months without initial burst release, which is considered a promising profile for many applications in prevention and treatment of infections. This construct can be used either as a coating for biomedical devices, or the coated NPs can be incorporated in bone cements. The developed LbL construct showed reproducibility in the case of gentamicin and chlorhexidine, in terms of characterization and release performance, which can have potential application for many other therapeutic molecules with similar physicochemical properties.

## **5 Gentamicin nanoparticle-containing bone cement**

### **5.1 Introduction**

PMMA bone cements use is considered a gold standard in hip and knee replacements. The use of ALBCs is considered a standard practice in the prevention and treatment of PJIs after TJRs, where the loaded cement delivers powdered antibiotics locally (Anagnostakos, 2017; Letchmanan et al., 2017). The most common antibiotics employed in bone cements are aminoglycosides, in particular gentamicin sulphate which is currently employed in several commercial bone cement formulations (Jackson et al., 2011). Gentamicin sulphate is thermostable and can withstand the exothermic polymerization reaction of PMMA bone cement. It is also available in powder form that makes it ideal for mixing with the cement powder as a premixed or off-label formulation (Bertazzoni Minelli et al., 2015).

Although antibiotics are widely incorporated in PMMA bone cements, there are many concerns about the release kinetics of added antibiotics (Liu et al., 2015). In reality, the antibiotic release from the bone cement is a burst for the first few hours after surgery, followed by slow release below inhibitory levels within few days (Swearingen et al., 2016). This release profile does not provide long term prophylaxis from early and delayed stage infections (early infection starts during first 24hrs-1 week, and late infections after 1 month according to orthopaedic surgeons). In addition, less than 10 % of added antibiotics is released, and the majority may be still entrapped within the hydrophobic PMMA matrix (Wendling et al., 2016; Wu et al., 2016).

To overcome these problems, we propose using gentamicin loaded LbL loaded silica nanoparticles (NPs) developed in chapter 3, which contains the patented hydrolysable polymer B1 as a polycation to improve the release kinetics of gentamicin from bone cement. The gentamicin loaded NPs were incorporated in PMMA bone cement commercial formulations Cemex Genta and Palacos R+G, and compared with the same cements loaded with gentamicin powder. The commercial and nanocomposite bone cements were characterised for release, antimicrobial activity, mechanical properties, cytocompatibility and water uptake.

The aim of this work is to achieve a prolonged gentamicin release for several weeks (4-6 weeks) to provide prophylaxis from postsurgical PJI.

## **5.2 Materials and methods**

### **5.2.1 Chemicals**

Triton X-100, Tetraethyl orthosilicate (TEOS), (3-Aminopropyl) triethoxysilane (APTS), sodium alginate, chitosan, gentamicin sulphate, sodium acetate trihydrate, phosphate buffer solution (PBS) tablets, o-phthaldialdehyde reagent were purchased from Sigma-Aldrich, UK.

Cyclohexane, 1-hexanol, ammonium hydroxide 35%, ethanol, methanol, glacial acetic acid and 1-propanol were purchased from Fishers, UK. All reagents were stored according to manufacturer's guidelines and used as received. Two types of bone cements were used Cemex®-Genta (Tecres® S.p.A., Italy) and Palacos R+G® (Heraeus Medical GmbH, Germany).

B1: is a patented biocompatible, biodegradable cationic polymer, the precise structure will remain confidential due to the IP associated.

### **5.2.2 Nanoparticle preparation**

#### **5.2.2.1 Amino functionalised silica nanoparticles synthesis**

Silica nanoparticles functionalised with amine groups ( $\text{SiO}_2\text{-NH}_2$ ) were prepared in one-pot synthesis by hydrolysis of TEOS in reverse micro-emulsion and subsequent functionalization with amino group (Stöber et al. 1968), as described in section 2.1.2.1.

#### **5.2.2.2 Layer by Layer (LbL) coating technique**

The amino functionalised silica nanoparticles were layered with ten quadruple layers of a repeating sequence of (sodium alginate/gentamicin/sodium alginate/B1), described in section 3.2.3.2. The following concentrations of the polyelectrolytes and the drug in acetic acid-sodium acetate buffer (pH 5) were used in LbL: sodium alginate (2 mg/ml), gentamicin (10 mg/ml) and B1 (2 mg/ml). The nanoparticles were coated using the same procedure described in section 2.1.2.2.

### **5.2.3 Bone cement preparation**

Bone cement preparation was carried out according to manufacturer's instructions and the ISO5833:2002 (Implants for surgery-Acrylic resin cements) and as described in section 2.2.2.

### **5.2.4 Gentamicin release quantification**

Commercially available antibiotic loaded bone cements (Palacos R+G, Cemex G) were prepared as described in section 2.2.2. In addition, gentamicin nanoparticle containing bone cement were prepared by the same procedure for commercial cement, except replacing gentamicin powder with gentamicin LbL coated nanoparticles, Table 17 shows the composition of all cements tested. Calculations for the nanoparticle containing bone cements were based on the loading efficiency (30% w/w), to have equal amounts of gentamicin between commercial and nanocomposite bone cements.

	Palacos R+G	Palacos NPs	Cemex Genta	Cemex NPs
<b>Liquid component / g</b>	18.80	18.80	13.30	13.30
Methyl Methacrylate / % w/w	97.87	97.87	98.20	98.20
N-N Dimethyl-p-Toluidine / % w/w	2.13	2.13	1.80	1.80
Hydroquinone / ppm	60.00	60.00	75.00	75.00
<b>Powder Component / g</b>	40.80	40.80	40.00	40.00
Polymethyl Methacrylate / % w/w	83.27	83.27	82.78	82.78
Barium Sulphate / % w/w	-	-	10.00	10.00
Benzoyl Peroxide / % w/w	0.50	0.50	3.00	3.00
Zirconia / % w/w	15.00	15.00	-	-
Gentamicin sulphate / % w/w	1.23	-	3	-
Gentamicin NPs % w/w	-	3	-	9
<b>Powder: Liquid ratio</b>	2.17	2.17	3.01	3.01

*Table 17 : Composition of gentamicin containing bone cement.*

A PTFE mould was used to produce cylindrical samples with 6mm diameter and 10 mm length. Each sample weighed  $0.40\pm 0.01$ g and three samples were used for release study from each type of bone cement. The bone cement samples were incubated in 3ml PBS buffer (pH 7) at 37°C. The release media was replaced each day in order to attain sink condition, where the concentration of released gentamicin is negligible in comparison to its saturation solubility. The release samples were stored in the refrigerator (2-8 °C) for analysis. The concentration of gentamicin was determined in the samples using o-phthalaldehyde method as described previously in section 2.1.4.

### **5.2.5 Rheology testing**

The effect of adding the nanoparticles on the cement settling time was evaluated through rheological tests as described in section 2.2.3.

### **5.2.6 Antimicrobial testing**

Antimicrobial testing was done for the gentamicin powder and NPs containing bone cements listed in *Table 17* (Palacos-1% gentamicin powder, Palacose-3% gentamicin NPs, Cemex-3% gentamicin powder, Cemex-9% gentamicin NPs), using the same protocol described in section 2.2.5. The minimum inhibitory concentration (MIC) for gentamicin was determined against different bacteria tested through standard MIC protocol as described in section 2.2.5. The bacteria tested are methicillin-resistant *Staphylococcus aureus* (NCTC 12493), *Streptococcus pyogenes* (ATCC 19615), *Staphylococcus epidermidis* (ATCC 12228), *Acinetobacter baumannii* (NCIMB 9214), *Pseudomonas aeruginosa* (NCIMB 10548), *Escherichia coli* (NCTC 10418).

### **5.2.7 Mechanical testing**

Mechanical testing was performed as described in section 2.2.6 for different bone cements (Palacos-1% gentamicin powder, Palacose-3% gentamicin NPs, Cemex-3% gentamicin powder, Cemex-9% gentamicin NPs). Compressive strength testing was performed at 0 and 3 months' time. Also, bending and fracture toughness testing were performed at zero time.

### **5.2.8 Water uptake testing**

Bone cement commercial samples and nanocomposites (Palacos-1% gentamicin powder, Palacos-3% gentamicin NPs, Cemex-3% gentamicin powder, Cemex-9% gentamicin NPs ) were incubated in 3 ml PBS at 37°C for 3 months; for the first 2 weeks, the samples were weighed daily; after that the samples were weighed every 3 days (Perni et al., 2015), as described in section 2.2.7. Water uptake was calculated by dividing the increase in sample weight at different time points by the initial sample weight at time zero, and plotted as a percentage. Water uptake studies give an insight about the cement behaviour after being wetted in solution to simulate the *in-vivo* conditions inside the joint with the synovial fluid.

### **5.2.9 Nanoparticles distribution in bone cement**

The distribution of nanoparticles in Palacose-3% gentamicin NPs and Cemex-9% gentamicin NPs was studied by fluorescence imaging using fluorescent nanoparticles as described in section 2.2.9.

### **5.2.10 Cytotoxicity testing**

#### **5.2.10.1 MTT**

MTT test was done for Palacos-1% gentamicin powder, Palacose-3% gentamicin NPs, Cemex-3% gentamicin powder, Cemex-9% gentamicin NPs for days 1,2,4 and 7 using the same protocol described in section 2.2.8.1 .

#### **5.2.10.2 LDH**

LDH assay test was done for Palacos-1% gentamicin powder, Palacose-3% gentamicin NPs, Cemex-3% gentamicin powder, Cemex-9% gentamicin NPs for days 1,2,4 and 7 using the same protocol described in section 2.2.8.2 .

### **5.2.10.3 Calcium production assay-Alizarin red**

Alizarin red test was done for Palacos-1% gentamicin powder, Palacose-3% gentamicin NPs, Cemex-3% gentamicin powder, Cemex-9% gentamicin NPs for days 1,2,4 and 7 using the same protocol described in section 2.2.8.3.

### **5.2.10.4 Fluorescence imaging**

Fluorescence imaging (live/dead and actin/dapi) was done for Cemex-3% gentamicin powder, Cemex-9% gentamicin NPs using the same protocol in section 2.2.8.5.

### **5.2.11 Statistical analysis**

All data were expressed as means  $\pm$  standard deviation (SD) from at least three independent values. To assess the statistical significance of results between groups, one-way analysis of variance (ANOVA) was performed. Experimental results were considered statistically significant at 95 % confidence level ( $p < 0.05$ ). All analyses were run using the SPSS ® software.

## 5.3 Results

### 5.3.1 Bone cement settling time

The possible effects of the gentamicin loaded nanoparticles on the kinetics of different bone cements settling time was investigated through the evaluation of the rheological properties of bone cement dough after mixing (Figure 35, Figure 36, Figure 37 and Figure 38). For different bone cements, the storage modulus ( $G'$ ) was greater than the loss modulus ( $G''$ ); the pattern followed a monotonic increase at an initial fast rate that slowed down reaching a plateau. The storage modulus measures the stored energy, representing the elastic portion, and the loss modulus measures the energy dissipated as heat, representing the viscous portion. In Palacos cement, the presence of nanoparticles required similar settling time of 6 minutes (defined as the time needed for the dough to reach constant rheological properties) compared to gentamicin powder mixed Palacos-R (5 minutes). The addition of nanoparticles in Cemex did not change the settling time of the cement (around 6 minutes).

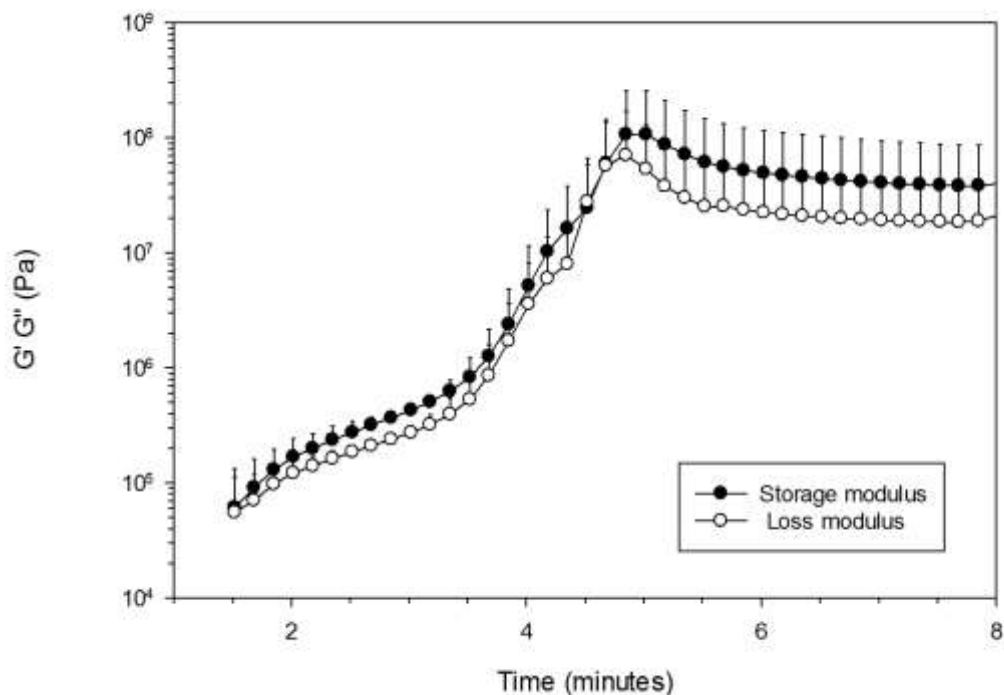


Figure 35: Storage ( $G'$ ) and loss ( $G''$ ) modulus for Palacos-R.

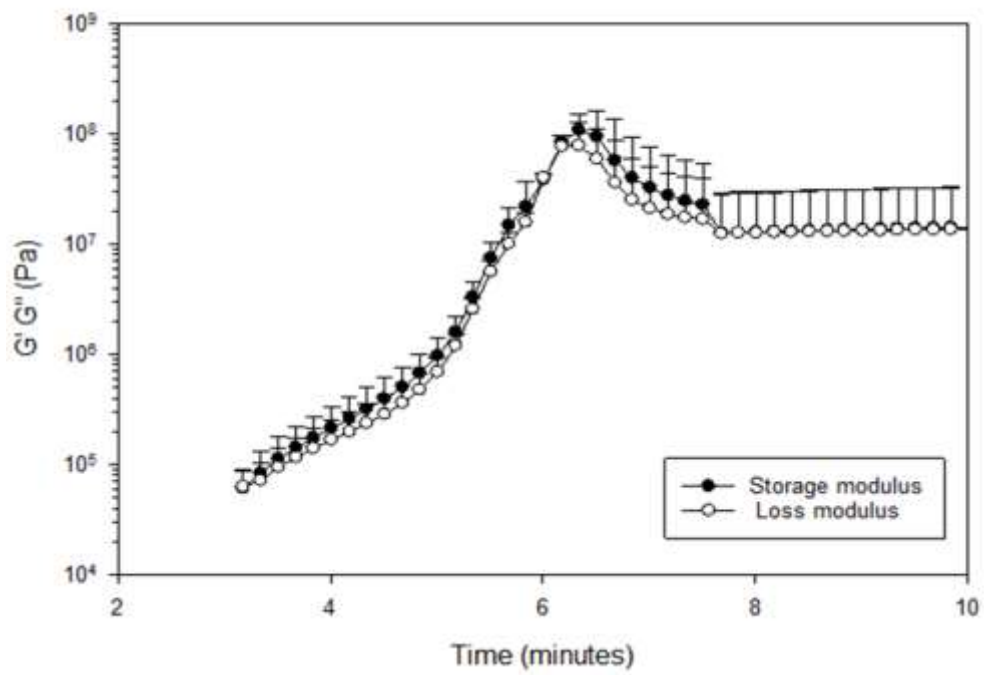


Figure 36: Storage ( $G'$ ) and loss ( $G''$ ) modulus for Palacos-NP.

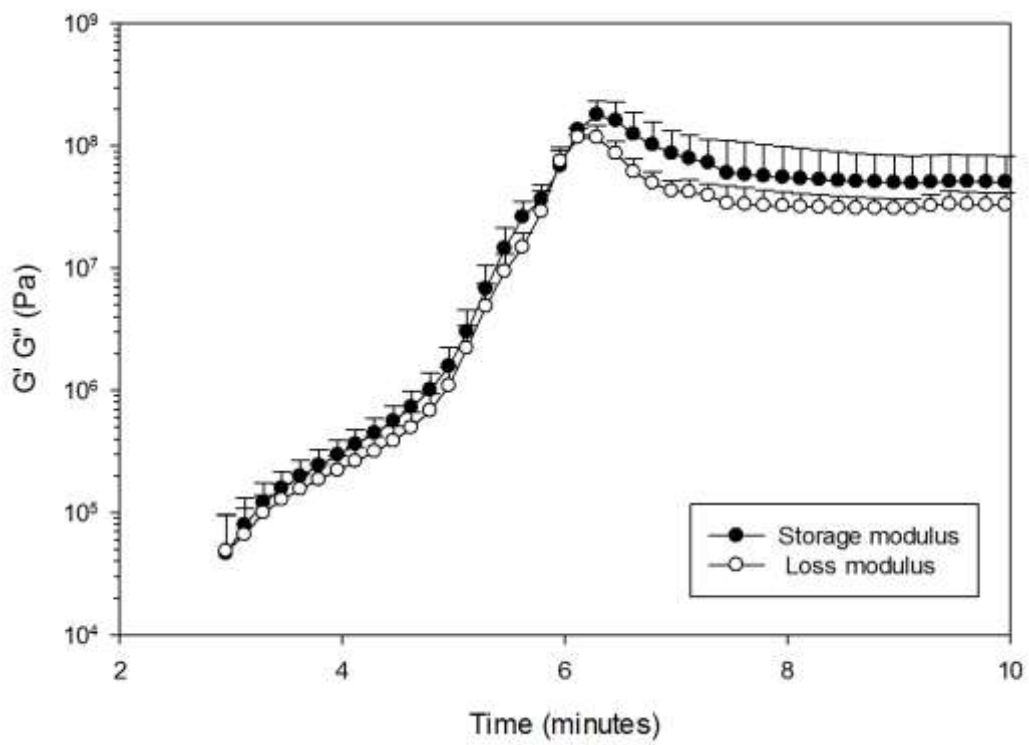


Figure 37: Storage ( $G'$ ) and loss ( $G''$ ) modulus for Cemex-Genta.

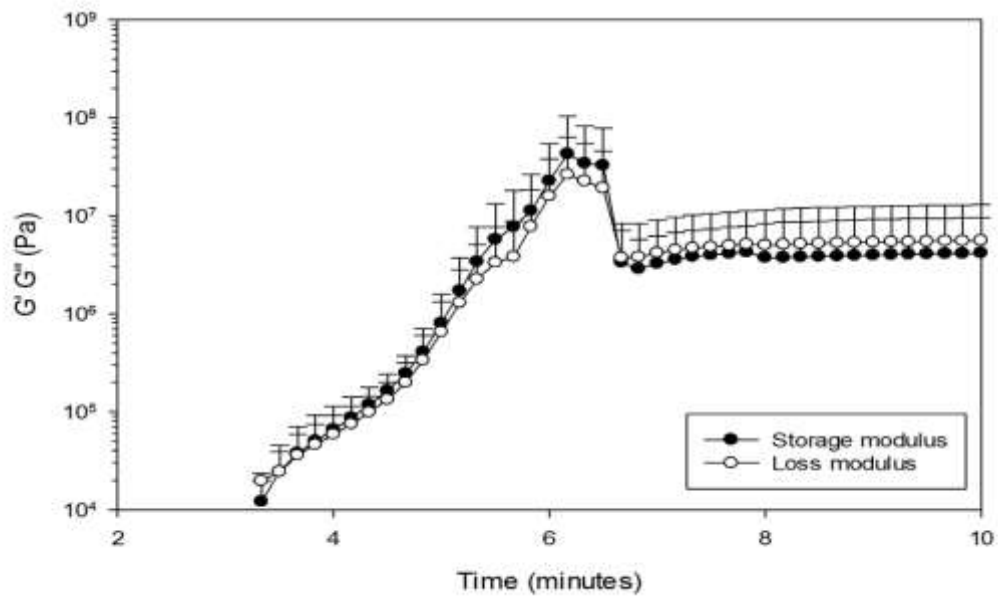


Figure 38: Storage ( $G'$ ) and loss ( $G''$ ) modulus for Cemex-NPs.

### 5.3.2 Gentamicin release profile

Gentamicin release from bone cement was studied in PBS buffer (pH 7.3), which is the pH value in healthy joints (Ribeiro et al., 2012). Gentamicin was quantified by fluorescence detection in each sample, each data point is an average of three independent samples measurements. Figure 39 shows the cumulative release of gentamicin from Cemex Genta (3% of gentamicin powder), Palacos R (1% of gentamicin powder), and the nanocomposite for Cemex Genta (9% of gentamicin nanoparticles), and the nanocomposite for Palacos R (3% of gentamicin nanoparticles) for 30 days.

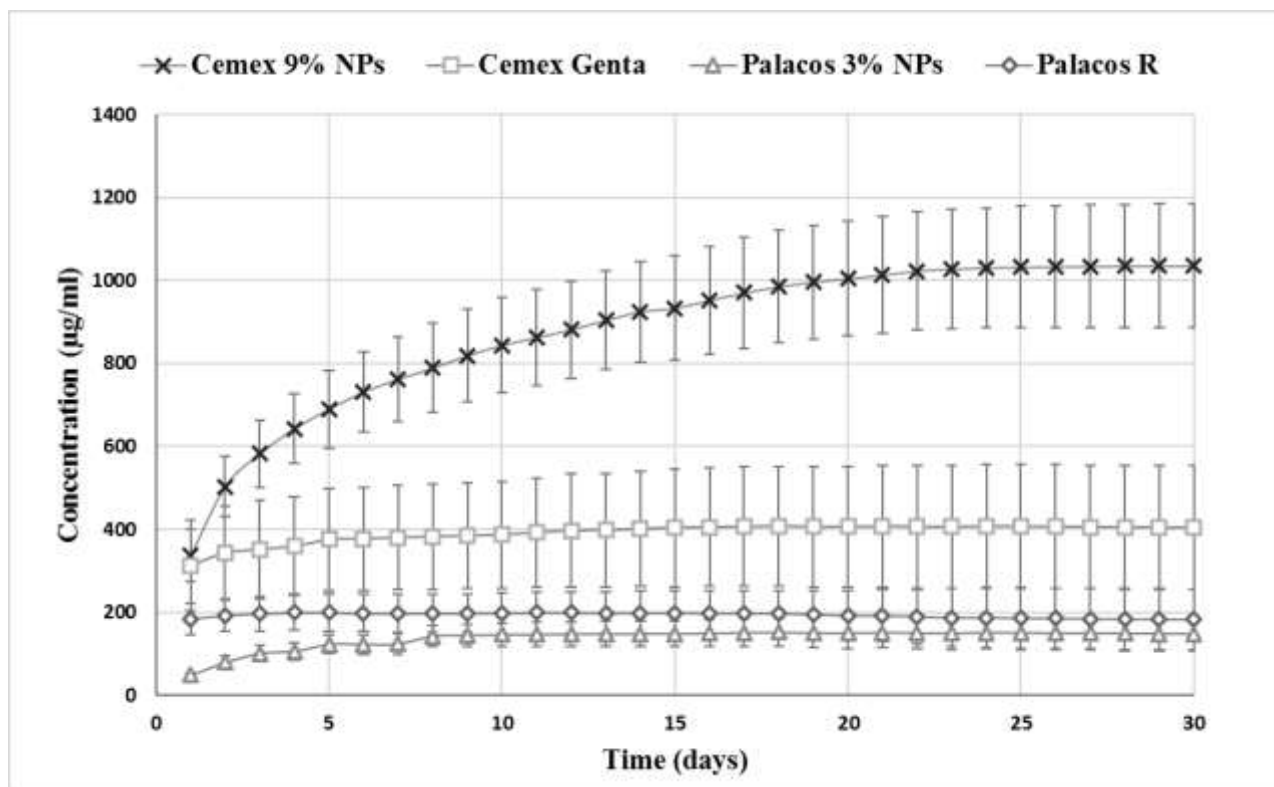


Figure 39 : Cumulative gentamicin release from commercial bone cements (Cemex Genta, Palacos R), and nanocomposite samples (n=3+SD).

All bone cements, except Cemex Gentamicin NP, stopped releasing gentamicin after 15 days. Cemex Genta NP continued releasing gentamicin up to 30 days, at a concentration of higher than 1000 µg/ml, while Cemex Genta achieved a concentration of 400 µg/ml. The release was burst for the first 7 days for all the cements, except for Cemex Genta NP the release was little burst only in the first 3 days after that the release was nearly first order which controlled until 30 days. Cemex NP released significantly higher amount of gentamicin compared to Cemex Genta ( $p < 0.05$ ), (more than 2.5 times amount of gentamicin). Also, Cemex Genta release was characterised by burst in the first 7 days, with no more than 400 µg/ml.

Palacos R and Palacos R nanocomposite achieved similar gentamicin release concentration of 200 µg/ml ( $p > 0.05$ ). The release in Palacos R was burst in the first 2 days and after that gentamicin release reached plateau. However, in the first 7 days, gentamicin was released gradually in Palacos NP which was lower than the initial burst release in Palacos R, and gentamicin release was controlled for up to 10 days before reaching plateau. In general, when assessing the release in the first 15 days, the standard deviations experienced for all nanocomposite bone

cements were smaller than those experienced by the commercial cements with powder gentamicin.

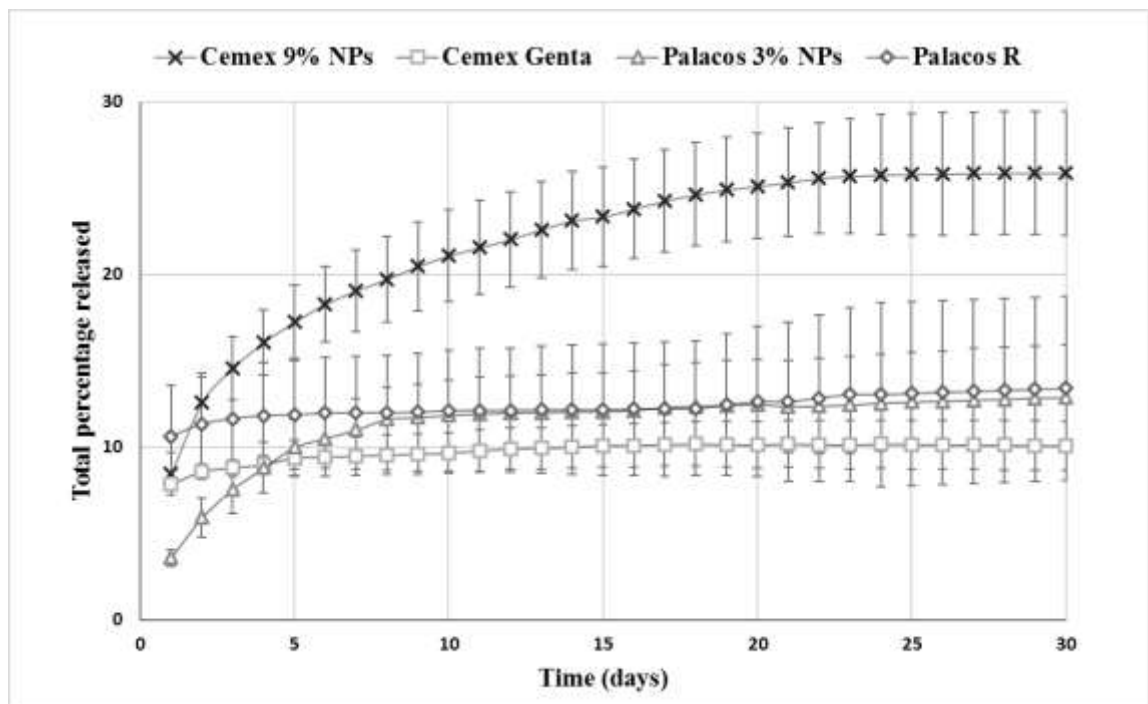


Figure 40: Cumulative percentage release of gentamicin from commercial bone cements (Cemex Genta, Palacos R) and nanocomposite samples ( $n=3+SD$ ).

In terms of total percentage release (Figure 40), Cemex Genta with nanoparticles performed significantly better than the other types of bone cements. At 5 days, a similar percentage release was seen by Palacos R and Palacos nanocomposite, however after this time point the Palacos nanocomposite achieved a higher percentage. After 7 days, Palacos R and Palacos nanocomposite achieved 12% total gentamicin release, while Cemex Genta released roughly 10%. In the case of Palacos nanocomposite, the gentamicin release was controlled over the first 8 days, compared to the burst seen in bone cements containing gentamicin powder. In Cemex nanocomposite, the percentage of gentamicin released was 26% which is 2.5 times higher from the gentamicin powder Cemex Genta. The release was controlled over the first 20 days before reaching plateau after 30 days, with minimal burst effect.

### 5.3.3 Antimicrobial analysis

Antimicrobial testing against selected bacterial strains, that is commonly encountered in PJIs, was performed for Cemex Genta, Palacos R, Cemex NPs and Palacos NP, (Figure 41). The minimum inhibitory concentration (MIC) for gentamicin was determined against different bacteria tested, and was found to be the following: *S. aureus* 15.6 µg/ml, *S. epidermis* 0.98 µg/ml, *MRSA* 15.6 µg/ml, *S. pyogenes* 7.8 µg/ml, *E. coli* 7.8 µg/ml, *P. aeruginosa* 7.8 µg/ml. The nanoparticle containing bone cements showed longer duration of bacterial growth inhibition compared to the gentamicin powder bone cements. Cemex NPs inhibited the growth of all bacteria for more than 23 days, except for *Pneumonia* and *E. coli* but longer than other bone cement types (p-value < 0.03). However, Cemex Genta inhibited bacterial growth for nearly 15 days, with less inhibition duration for *S. pneumonia* and *E. coli* (p-value > 0.7 when compared to Palacos R and Palacos NP). Palacos NPs showed different antimicrobial activity depending on bacteria tested, with short duration of inhibition (less than 8 days) against *S. aureus* ATCC9144, *MRSA*, *A. baumannii*, *E. coli* 59284, *S. pneumonia*, (p-value > 0.5) and longer duration of inhibition (more than 13 days) against *S. pyogenes* ATCC12344, *E. coli* NCTC10418 and *S. aureus* NCIMB9518 (p-value > 0.5). Palacos R showed the weakest antimicrobial activity with duration of inhibition less than 8 days for all types of bacteria, except for *S. aureus* NCIMB9518, and *S. pyogenes* ATCC12344 (p-value > 0.5).

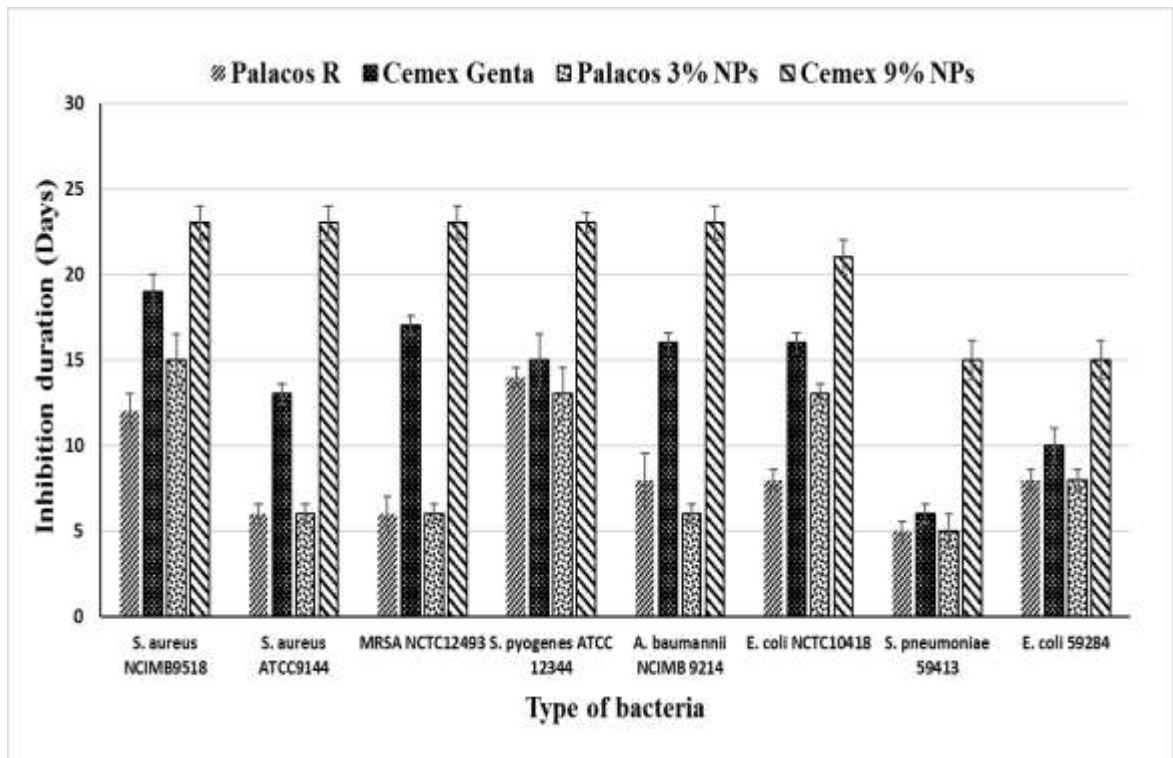


Figure 41: Antimicrobial testing for different types of bone cements (Palacos R, Cemex Genta, Palacos 3% NPs, Cemex 9% NPs) against different bacterial strains ( $n=3+SD$ ).

### 5.3.4 Mechanical properties

The compressive strength of different types of bone cements was tested after 24 hours in air, and after 3 months of incubation in release media PBS, pH 7.4 at 37 °C (Figure 42) according to ISO standard 5833:2002. At 24 hours and after 3 months, all nanoparticle containing bone cements had similar compressive strength to the commercial ones ( $p>0.05$ ). For Palacos G+R and Palacos NPs, there was no significant difference in the compressive strength ( $p\text{-value} > 0.05$ ) at zero time and after 3 months. For Cemex Genta and Cemex NP, there was no significant difference in the compressive strength ( $p\text{-value} > 0.05$ ) at zero time and after 3 months. In addition, incubation for 3 months did not adversely affect the compressive strength of the bone cement ( $p\text{-values} > 0.10$ ). Bending strength and fracture toughness were only tested for Cemex G and Cemex NPs (Table 18), because Palacos cement was not able to sustain the release of gentamicin for a long time (Figure 39). Cemex NPs showed similar bending strength and fracture toughness to Cemex G ( $p\text{-value} > 0.6$ ). The acceptable ranges for the mechanical properties of a set bone cement are  $> 70$  MPa compressive strength,  $> 1800$  MPa bending modulus and  $> 50$  MPa bending strength (Lee, 2005).

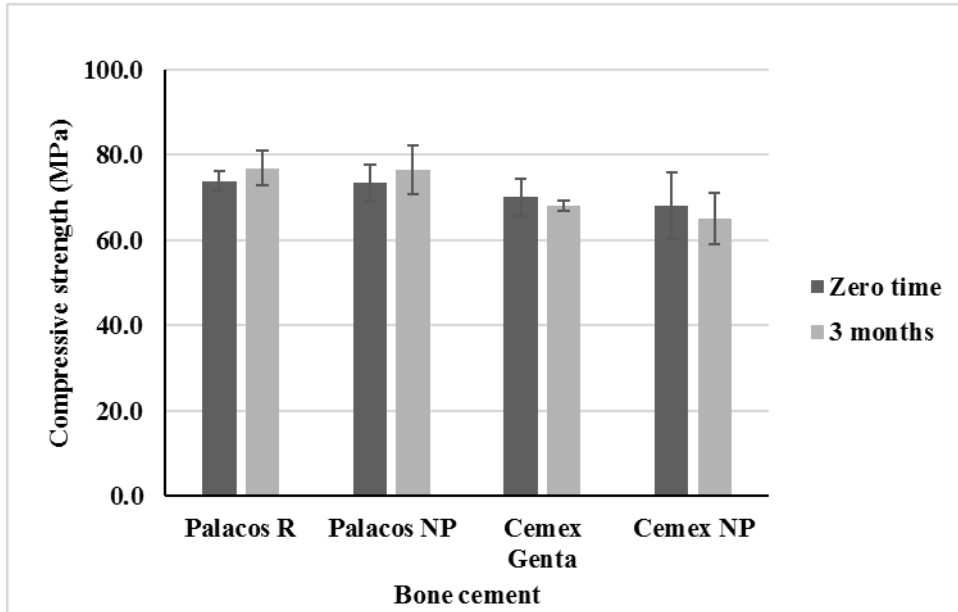


Figure 42: Compressive strength of commercial and nanocomposite bone cements before and after incubation in PBS pH 7.3 at 37 °C for 3 months ( $n=6+SD$ ).

	Bending strength (MPa)	Bending modulus (MPa)	Fracture toughness (MPam <sup>1/2</sup> )
Cemex-Genta	54.3 ± 2.0	2901 ± 62	2.4 ± 0.5
Cemex-NP	51.2 ± 4.1	2964 ± 101	2.2 ± 0.3

Table 18: Bending strength and modulus, and fracture toughness for Cemex bone cement.

### 5.3.5 Water uptake testing

The weight of the different types of bone cement was recorded after incubation in PBS buffer media pH 7.3, to study the water uptake behaviour for up to 30 days (Figure 43). The nanocomposite water uptake behaviour was similar to that of the commercial cements ( $p>0.05$ ). The bone cement samples increased in weight during the first 4-5 days because of water uptake, and after that, the amount of water in the samples remained stable.

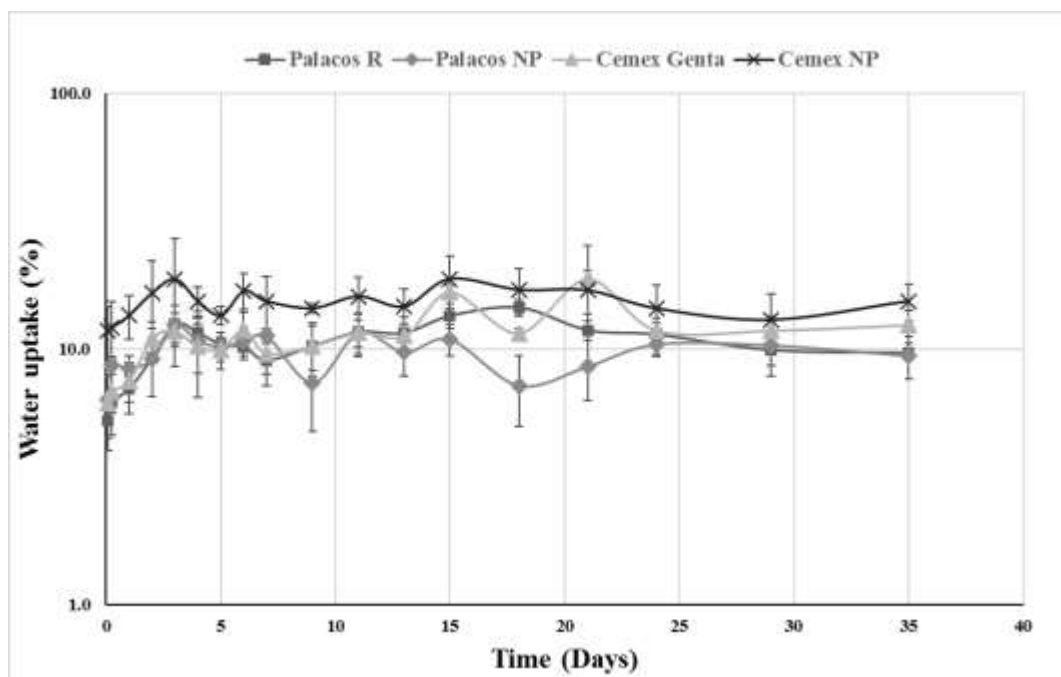
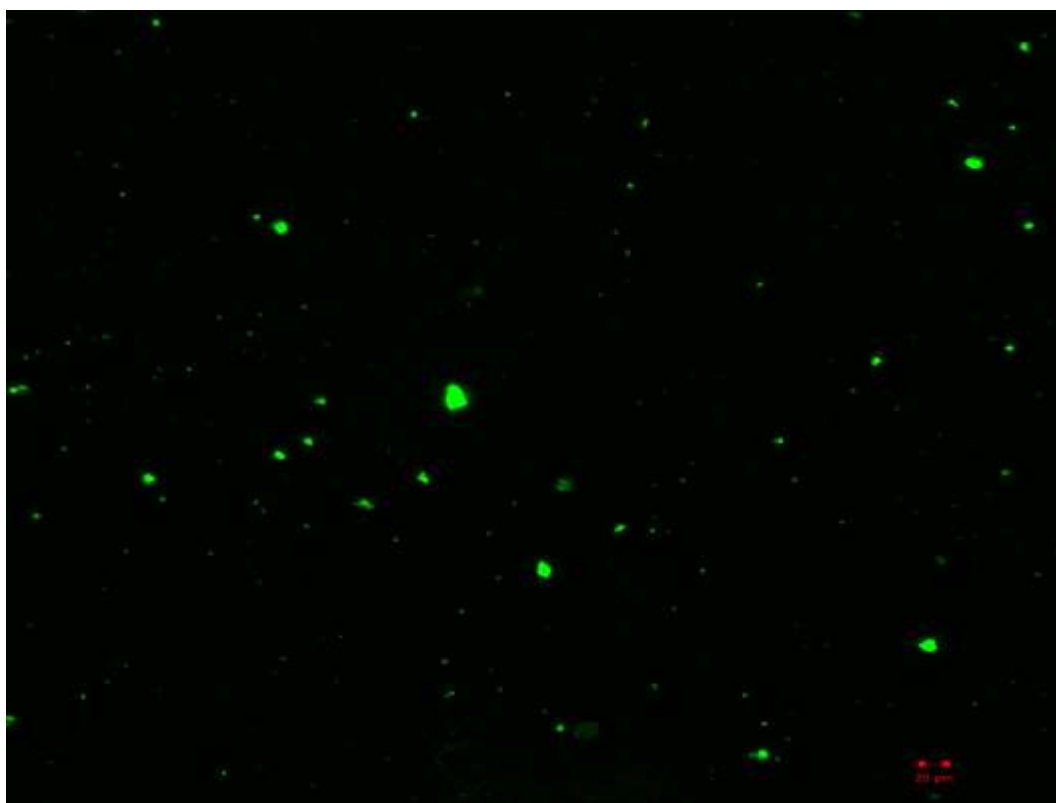


Figure 43: Water uptake for different types of gentamicin containing bone cements after incubation in PBS buffer, pH 7.3 (n=3+SD).

### 5.3.6 Nanoparticles distribution in bone cement

The distribution of nanoparticles inside the bone cement was studied by fluorescence imaging of fluorescence-labelled nanoparticles incorporated into the cement. Figure 44 shows nanoparticle distribution in Palacos bone cement (3% NPs w/w). Figure 45 nanoparticle distribution in Cemex bone cement (9% NPs w/w). In both types of cement, nanoparticles were homogeneously distributed throughout the cement matrix, with minimal agglomeration at higher concentration of nanoparticles in cement, as seen in Cemex 9% NPs w/w. The nanoparticles agglomeration and size was higher in Cemex nanocomposite compared to Palacos, because it has higher concentration of nanoparticle 9% NPs w/w.



*Figure 44: Nanoparticle distribution in Palacos bone cement (3% NPs w/w) (bar=20 $\mu$ m).*

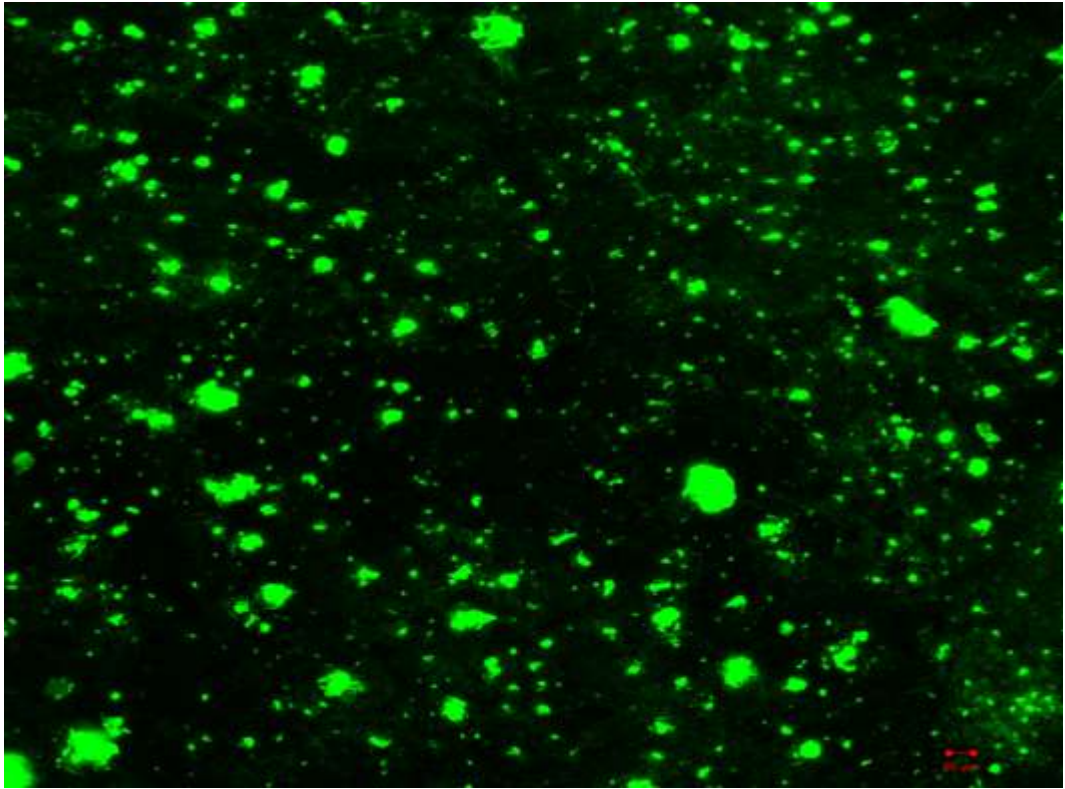


*Figure 45: Nanoparticle distribution in Cemex bone cement (9% NPs w/w) (bar=20 $\mu$ m).*

### 5.3.7 Cytotoxicity analysis

#### 5.3.7.1 MTT assay

Relative to osteoblasts exposed to Palacos R commercial formulation, one day exposure to Palacos NP resulted in 10% insignificant reduction in osteoblast proliferation, and 6 % reduction after 7 days ( $p$ -value > 0.94). At 2 and 4 days, osteoblast proliferation had returned to normal levels. While relative to osteoblasts exposed to Cemex Genta, 1-7 days exposure to Cemex NP resulted in similar osteoblast proliferation with maximum insignificant reduction of 10% at days 4 ( $p$ -value >0.464) (Figure 46).

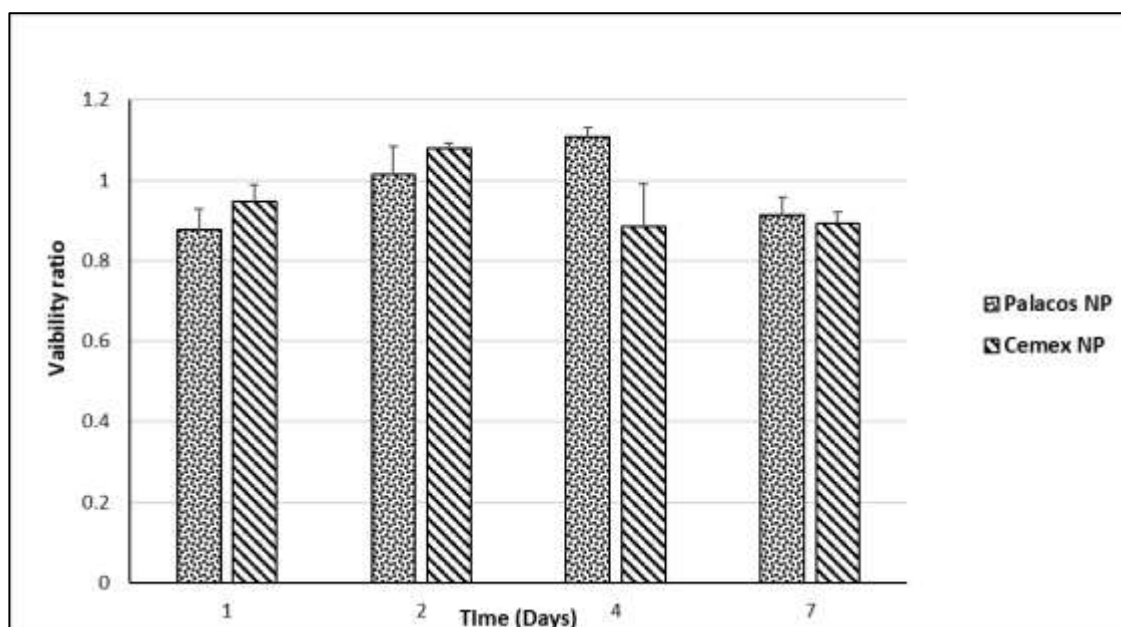


Figure 46: Viability of osteoblasts exposed to different types of bone cements: Palacos R, Palacos NP, Cemex-Genta, Cemex NP, assessed through MTT test as viability ratio (Nanocomposite/commercial cement) ( $n=6+SD$ ).

#### 5.3.7.2 LDH assay

The viability of cells exposed to Palacos NP was similar to the commercial cement Palacos R at day 1, 2, and 4 ( $p$ -value > 0.495). However, the viability of cells was reduced to 15% at day 7 ( $P<0.05$ ). For Cemex NP, the viability of cells was similar

to Cemex Genta with maximum reduction of 10% at day 4 (p-value 0.595) (Figure 47).

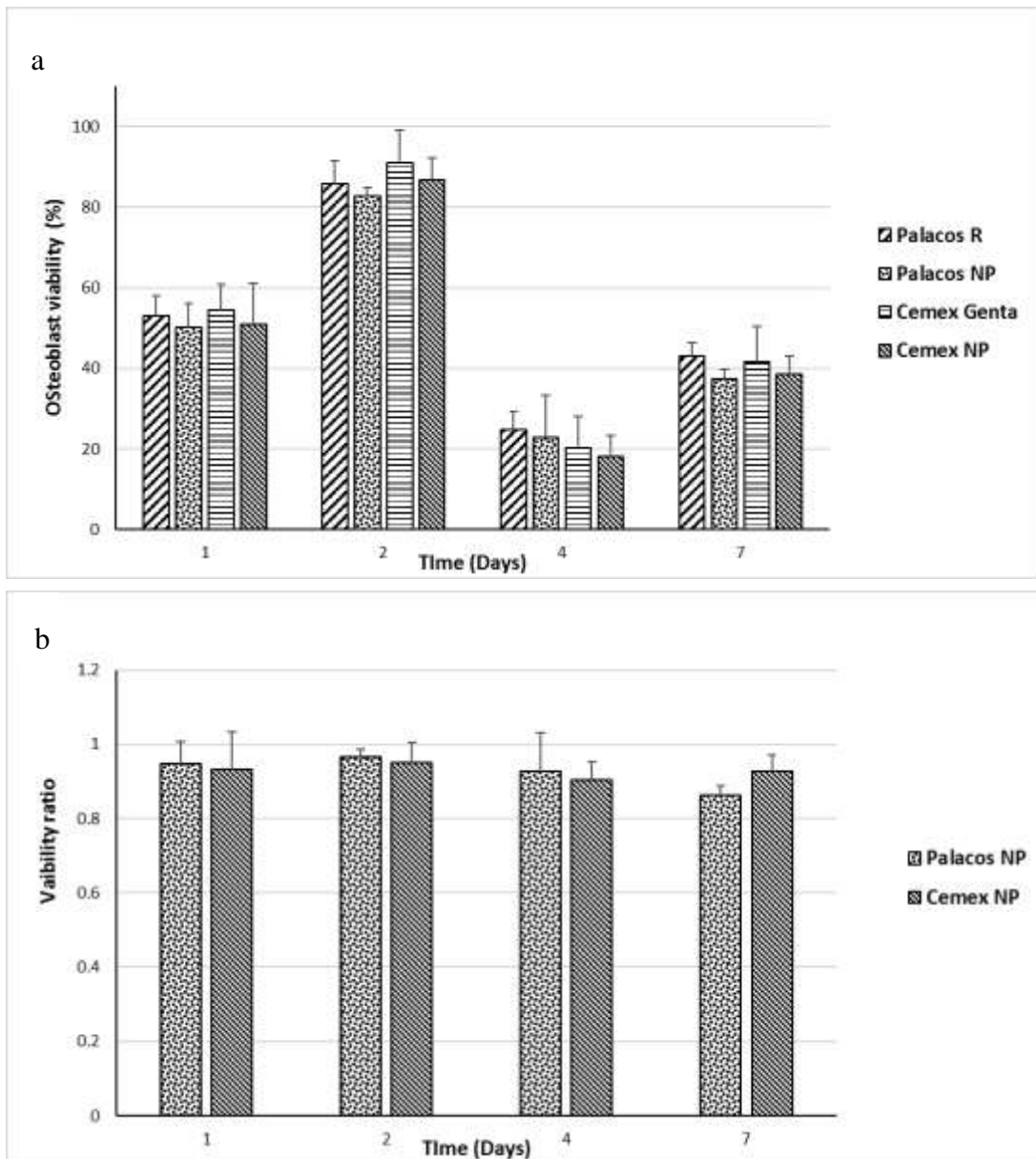


Figure 47: Viability of osteoblasts exposed to different types of bone cements: Palacos R, Palacos NP, Cemex-Genta, Cemex NP, assessed through LDH test: (a) percentage viability, (b) viability ratio (Nanocomposite/commercial cement) ( $n=6+SD$ ).

### 5.3.7.3 Alizarin red

The alizarin red staining is shown in Figure 48, which shows no significant reduction in calcium production for osteoblasts exposed to nanocomposites (Palacos NP and Cemex NP) when compared to commercial cements (p-value >0.05) (Palacos R and Cemex Genta).

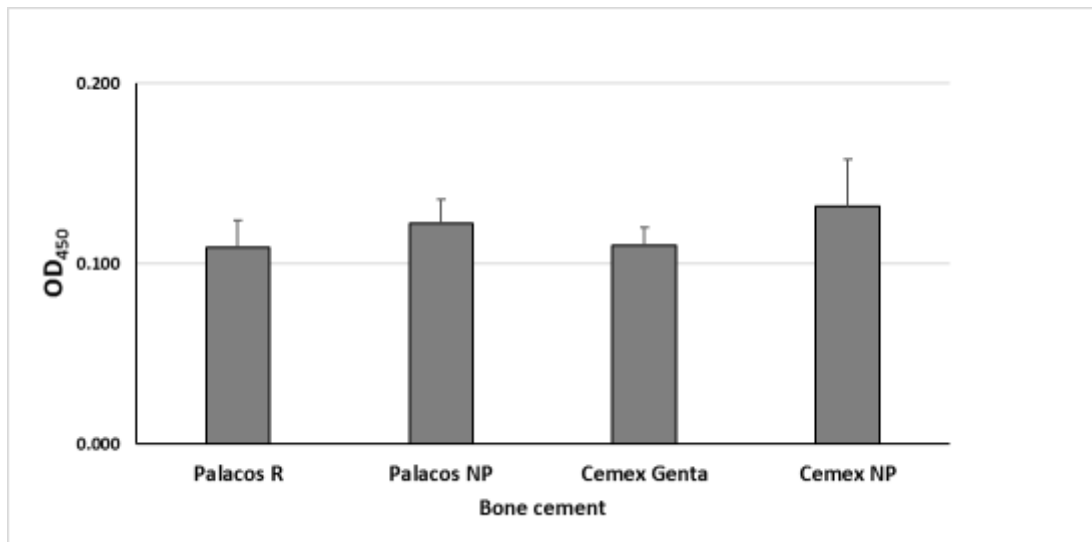
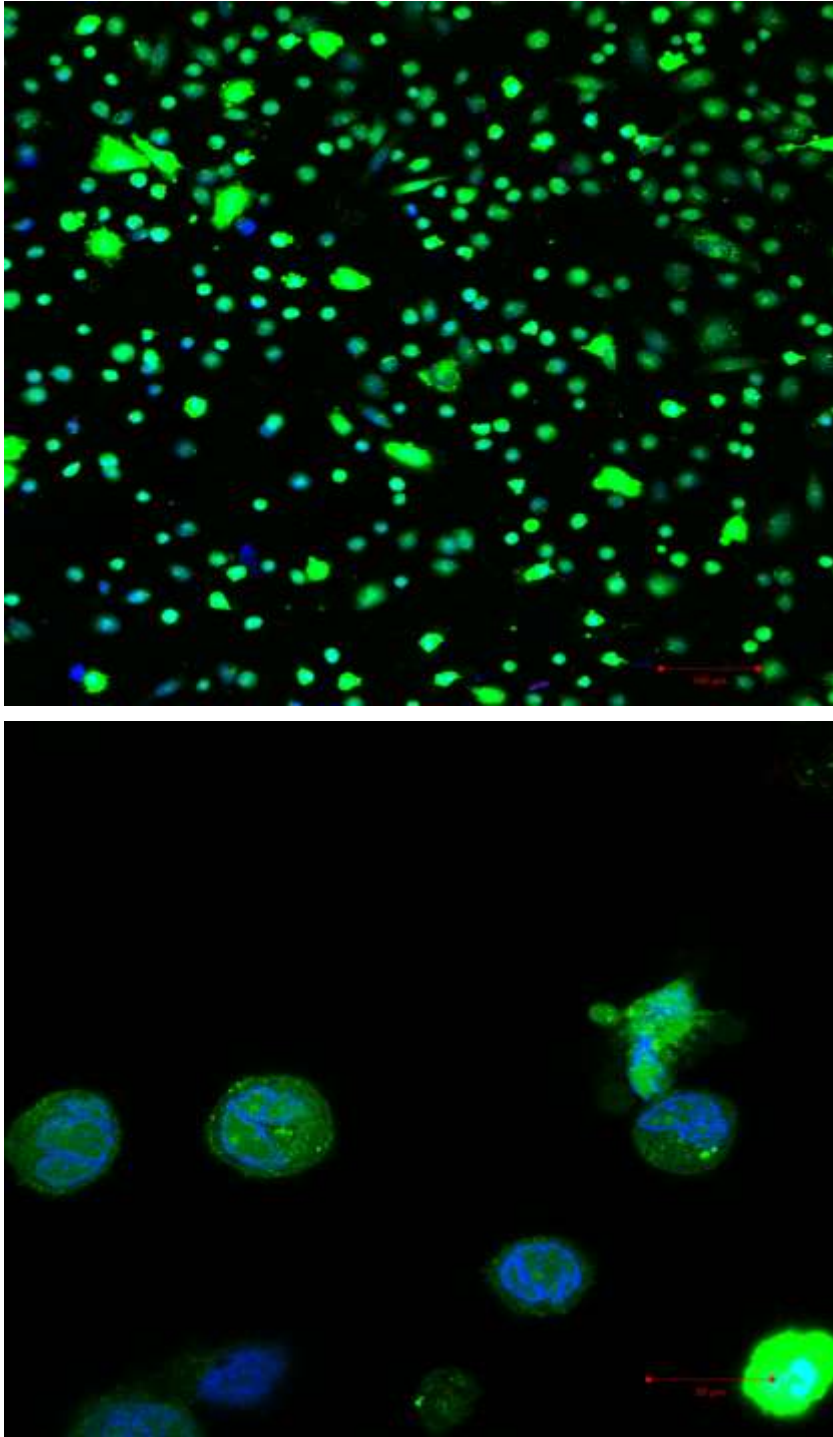


Figure 48: Alizarin red assay for osteoblasts after 21 days grown on different types of bone cements: Palacos R, Palacos NP, Cemex-Genta, Cemex NP.

### 5.3.7.4 Fluorescence images

Live and dead fluorescent images for Cemex Genta (Figure 49) and Cemex nanocomposite (figure 50) show the live cells (green color), dead cells (red color) and cell nuclei (blue color). In addition, actin/dapi fluorescent for Cemex Genta (Figure 51) and Cemex nanocomposite (Figure 52) show actin filaments (red color) and cell nuclei (blue color). Cemex Genta showed similar cell viability (number of cells), actin filament spreading and development for the cells cytoskeleton compared to Cemex NPs.



*Figure 49: Live/dead images for Cemex Genta cement with two different scales. (Top: 100 µm bar, bottom: 20 µm bar).*

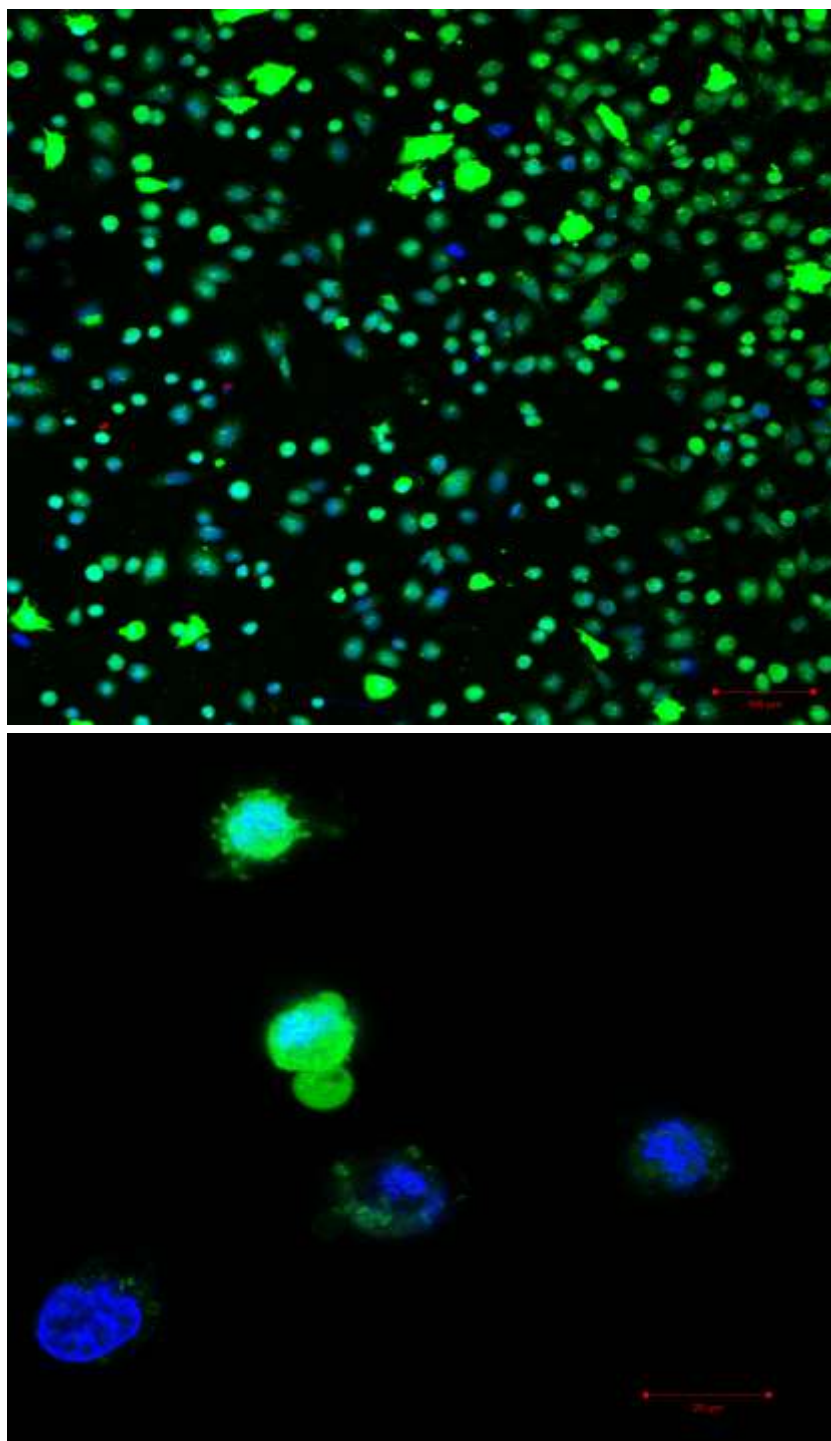


*Figure 50: Live/dead images for Cemex nanoparticles cement with two different scales. (Top: 100  $\mu\text{m}$  bar, bottom: 20  $\mu\text{m}$  bar).*

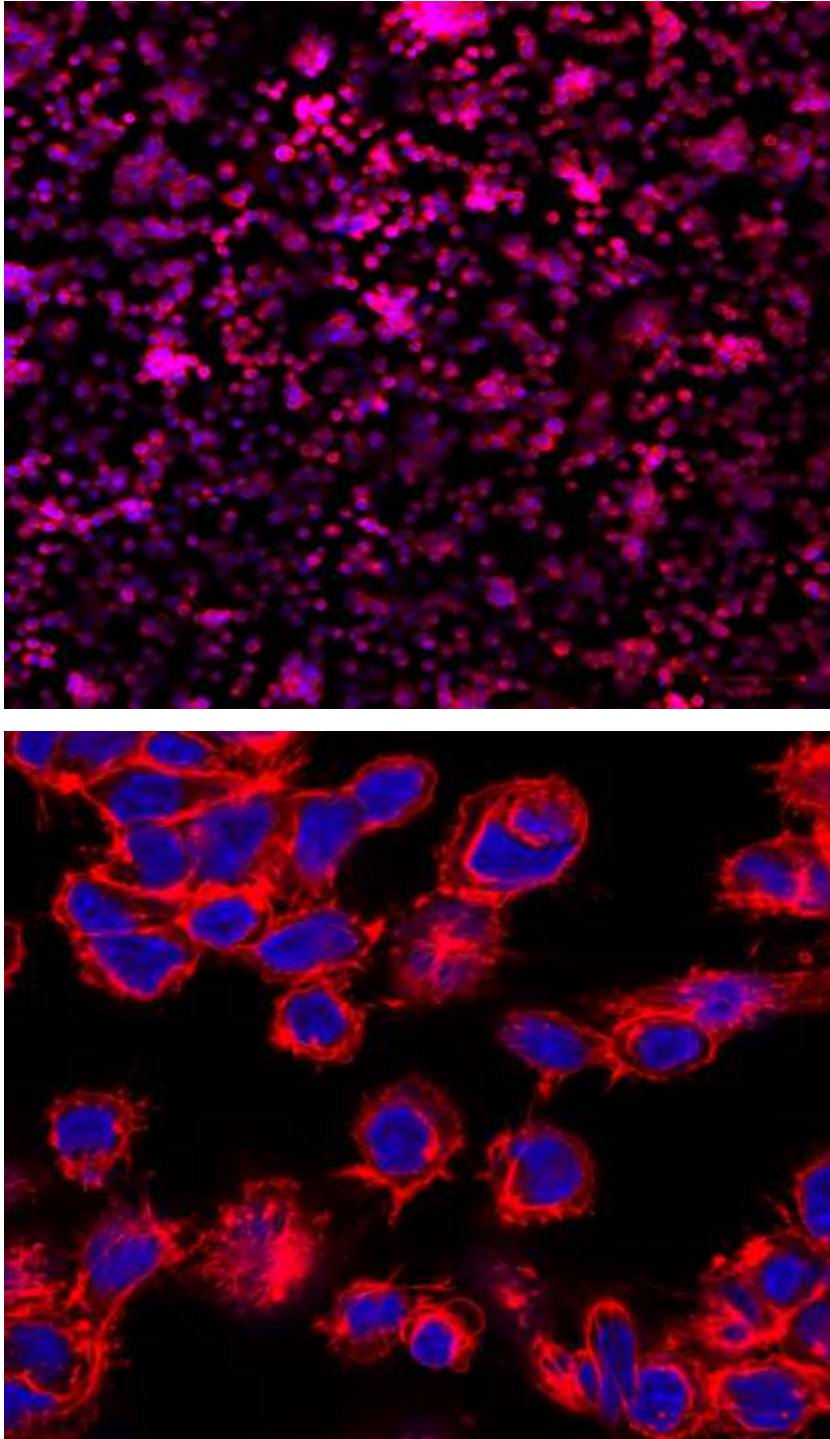


*Figure 51: Actin/dapi images for Cemex Genta cement with two different scales. (Top: 100  $\mu\text{m}$  bar, bottom: 20  $\mu\text{m}$  bar).*

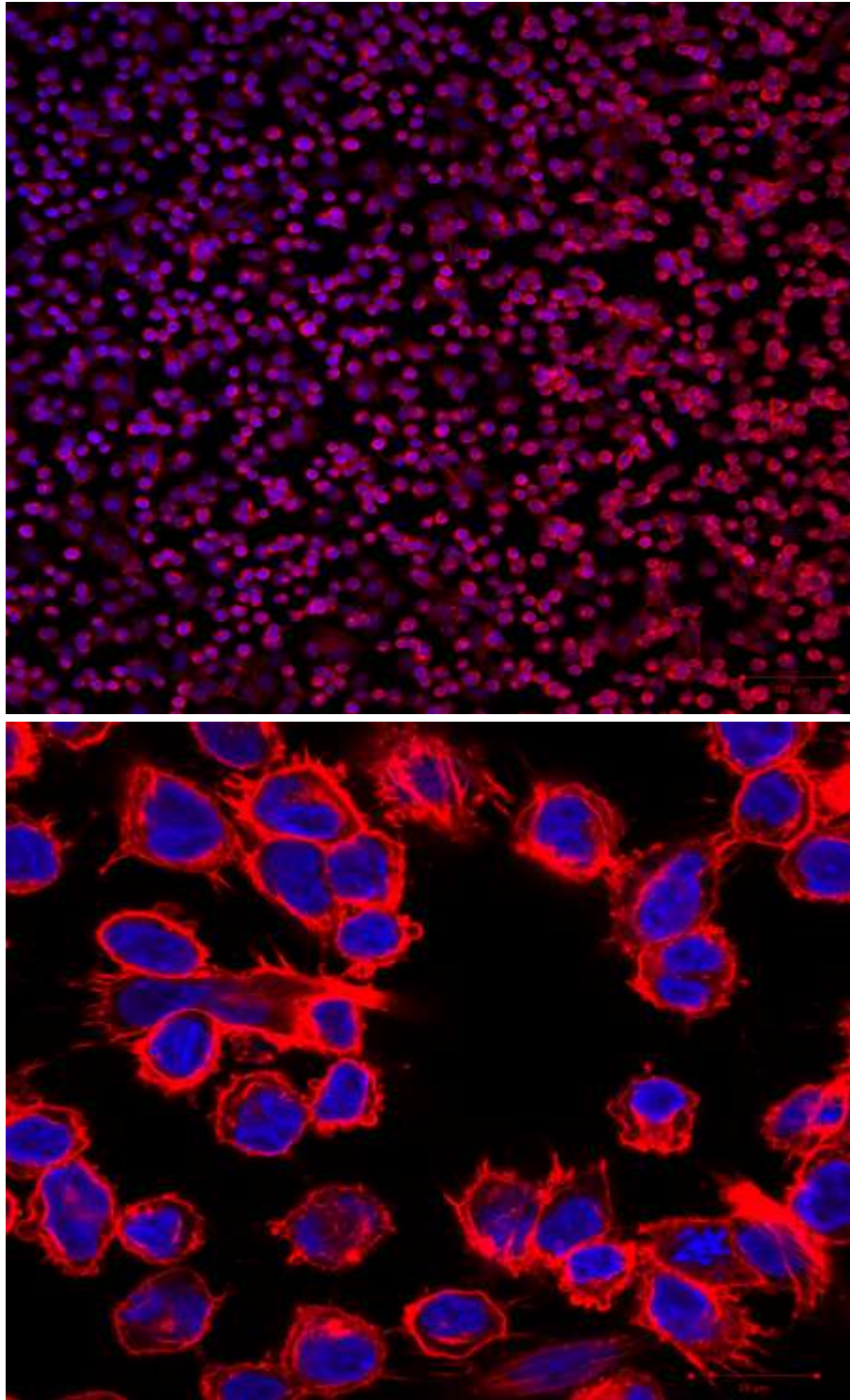


*Figure 52: Actin/dapi images for Cemex nanoparticles cement with two different scales. (Top: 100  $\mu\text{m}$  bar, bottom: 20  $\mu\text{m}$  bar).*

## **5.4 Discussion**

### **5.4.1 Surface and material properties of bone cement**

#### **5.4.1.1 Bone cement settling time**

The settling time is a critical parameter for bone cement use during application and after patient recovery, because it determines the time needed to develop the final mechanical properties of the cement. Therefore, the introduction of nanoparticles into the cement formulation must not have great change to the settling time for the commonly used commercial cements. In this work, the settling time of Cemex-NP bone cement did not alter the settling time for the gentamicin powder containing cement, which was proved by rheological testing. The profiles detected for  $G'$  and  $G''$  were comparable to those presented by others for PMMA bone cements (Farrar and Rose, 2001; Perni et al., 2015).

The time of cement application and prosthesis insertion by the surgeon depends mainly on the rheological properties of the cement and its setting behaviour. In general, implant insertion should be delayed until the cement has developed a sufficient degree of viscosity to resist excessive displacement by the implant, the acceptable setting of PMMA cement is usually between 8-10 minutes (Perni et al., 2015; Vaishya et al., 2013). However, implant insertion should not be delayed such that there is a risk that the procedure cannot be completed due to cement hardening (Vaishya et al., 2013).

#### **5.4.1.2 Mechanical properties**

The addition of antibiotics to bone cement decreases the mechanical properties (Duey et al., 2012; Khaled et al., 2011). As a result, only a small amount of antibiotics is added (< 1g per 40 g of bone cement) to keep the compressive and bending strength within the acceptable ranges needed for the cement mechanical performance. He et al. (2002) observed that the use of gentamicin at concentrations below 3% had no significant effect on the compressive and elastic modulus of bone cement; however, higher concentrations caused significant decrease in these two parameters (He et al. 2002). The acceptable ranges for the mechanical properties of a set bone cement are > 70 MPa compressive strength, > 1800 MPa bending modulus and >50 MPa bending strength (Lee, 2005). The compressive strength and bending strength for different types of bone cements was determined

according to the ISO standard 5833:2002. The fracture toughness was determined by the ISO13586:2000.

The compressive strength is an important parameter in evaluating the mechanical performance of bone cement, because the cemented prosthetic joint is loaded most of the time by compression (Lee, 2005). Shen *et al.* (2016) tested the mechanical strength for a bone cement loaded with 10%, 5%, 32% of mesoporous silica, carbon nano-tubes and hydroxyapatite nano-rods, respectively. The compressive strength for the mesoporous silica (85 MPa) was not adversely affected by the added nanoparticles. While, the carbon nano-tubes (8.7 MPa) and hydroxyapatite nano-rods (43.5 MPa) decreased the compressive strength drastically which stopped further investigations.

(Ayre et al. 2015) tested the compressive strength for a liposomal bone cement formulation, where the gentamicin loaded liposomes were added to the liquid part of the bone cement. The compressive strength of the cement dropped from 104 MPa (without liposomes) to 77 MPa after adding the liposomes. The drop in the compressive strength might be attributed to the presence of water, which affects the free radical polymerisation reaction of methyl methacrylate (Schoonover, Brauer, and Sweeney, 1952). In our work, the added silica NPs did not adversely affect the compressive strength of the bone cement (Figure 42), which is in accordance to with compressive strength of mesoporous silica NPs (Shen *et al.* 2016). The incubation of different types of bone cements in PBS pH 7.3 did not have a significant effect on the compressive strength.

The bending strength and modulus for Cemex-Genta and Cemex-NPs comply with the requirements for set and cured cement in the ISO 5833:2002 Implants for surgery – Acrylic resin cements (bending strength > 50 MPa and bending modulus > 1800 MPa). (Ayre et al. 2015) reported a bending strength of > 60 MPa for, and fracture toughness of 2.5 MPam<sup>1/2</sup> for Palacos bone cement. In this work, the bending strength of Cemex and Cemex nanocomposite was >50MPs, around 3000 bending moduli, and the fracture toughness is 2.2 MPam<sup>1/2</sup>, which is in agreement with literature for different types of bone cements. Letchmanan et al. (2017), reported a bending modulus of > 3000 MPa for mesoporous silica incorporated Simplex-P® bone cement (Stryker Co, UK).

The main function of the cement is to act as an interfacial phase between the high modulus metallic implant and the bone, and to transfer and distribute body weight loads as well as cyclic loads due to movements from prosthesis to bone (Münker et al., 2018). The joint is mainly mechanically stressed by compression, however, other forms of stresses (bending, fracture) are also important to provide adequate fracture resistance and prevent the loosening of the implant. Since the forces transmitted through the hip and knee joint are high about 3 times body weight when walking, rising to 8 times body weight when stumbling. As a result, the bone cement is subjected to high stresses and has to function in a relatively aggressive environment, showing adequate mechanical properties (Lee, 2005).

#### **5.4.1.3 Water uptake studies**

Although the current commercially available bone cements must have enough mechanical properties and pass standards in dry conditions, these properties can change overtime *in vivo*. Aging of the bone cement in simulated physiologic conditions causes a decrease in the mechanical properties of the bone cement, because of the plasticising effect of water uptake by decreasing the attraction between polymer chains and increasing flexibility (Arnold and Venditti, 2001). In addition, the presence of other factors such as high temperatures and stresses also affect the mechanical properties over a long period. (Bettencourt et al., 2004) investigated the hydrolysis of PMMA ester groups in biological fluids, which can be due to the change in the composition of the cement and surface wettability. Water uptake not only affects the mechanical properties of the bone cement, but it was also found to affect the surface properties and structure of the cement leading to a decrease in its molecular weight over long periods of time (Hughes et al., 2003). Thus, an initial determination of the water uptake behaviour is necessary to estimate the change in the physicochemical properties of the bone cement.

In this work, the presence of NPs did not affect the water uptake behaviour of the commercial bone cements (Figure 43). The weight of cement samples stopped increasing after 4-5 days, which also explain the similarity in the compressive strength tested after 3 months. These findings suggest that the presence of NPs,

instead of gentamicin powder, did not change the diffusion of water nor the compressive strength compared to the commercial product, however long-term exposure of the cement to physiological fluids play an important role in changing its overall performance.

#### **5.4.2 Gentamicin release profile**

The use of ALBCs has become a well-established standard to reduce infections after TJR, where large amounts of antibiotics are employed to achieve therapeutic levels of release (up to 1g per 40g of cement) (Engesaeter et al., 2006; Parvizi et al., 2008). However, there are several limitations associated with the release profile of antibiotics from ALBCs. Initially, the antibiotic is released at large amounts in uncontrolled manner, which is described as burst release for the first few hours after surgery. This burst release is followed by a rapid drop in the release profile below inhibitory levels within few days, which increases the selection of resistant antimicrobial strains (Dunne et al., 2008; Gasparini et al., 2014). In addition, more than 90% of the loaded antibiotic stays within the bone cement matrix as agglomerates, affecting the mechanical properties and performance of the cement (Dunne et al., 2007; Van et al., 2000).

Silica nanoparticles have been widely used as drug delivery carrier because of their biocompatibility, high loading capacity, low cost and ease of synthesis. Shen *et al.* (2016) used MSN to improve gentamicin release from PMMA bone cement. Gentamicin was loaded into MSN by wet impregnation, and the bone cement was loaded by 10% of nanoparticles. The release of gentamicin from the loaded cement continued for up to 80 days, where 60% of gentamicin was released. Shen *et al.* (2016) proved that the presence of MSN at concentration above 6 % is crucial for the build of nano-network to facilitate the diffusion of gentamicin molecules. However, nothing was mentioned about the concentration of released gentamicin or the loading efficiency of MSN.

Many nanotechnology-based gentamicin loaded carriers have been studied to improve the release profile of gentamicin from ALBCs. Ayre et al. (2015) loaded gentamicin into liposomes of 100 nm size. Gentamicin release from loaded cement continued for up to 30 days with 22% of the loaded antibiotic released compared to 9% from commercial formulation. Shen *et al.* (2016) incorporated gentamicin

loaded carbon nanotubes and hydroxyapatite into bone cement at concentration of 5% and 32%, respectively. The release of gentamicin was continued for more than 60 days with more than 75% of gentamicin released, however, the compressive strength for the bone cement was drastically decreased limiting further investigation.

This release from our LbL system showed little burst release compared to commercial formulation, and continued up to 30 days. The loading efficiency of gentamicin in the NPs was nearly 30% (w/w), which is lower than Shen et al (2016) because mesoporous silica NPs have higher size (100–300 nm) with pore sizes in the range 5–30 nm allowing higher gentamicin loading inside the pores, compared to our silica nanoparticles where the antibiotic is loading on top by LbL coating technique. The concentrations of NPs used in the bone cement were 9% and 3% in Cemex NP and Palacos NP respectively, to have equivalent amount of gentamicin to the commercial cements. The release of gentamicin was sustained gradually for more than 4 weeks without the need for adding high concentrations of NPs as in the case with Cemex NP. The gentamicin loaded nanocomposite enhanced the total amount of gentamicin released from the bone cement (26% of loaded gentamicin) by 2-3 folds compared to the commercial formulation. The enhancement of release kinetics is attributed to the homogenous distribution of NPs in the bone cement matrix (Figure 44 and Figure 45), that may lead to the formation of nano-network channels to facilitate the diffusion of gentamicin, or simply because of the increased surface area available for gentamicin release from nanoparticles (Shen *et al.* 2016).

(Anagnostakos et al., 2009) studied the maximum peak gentamicin concentration in daily drainage fluids after hip replacement with beads and spacers (*In vivo*), where it reached 1160 µg/mL and 21 µg/mL, respectively after day 1. (Hsieh et al., 2009) studied gentamicin concentration in the joint fluids after revision hip replacement, where he reported a peak of gentamicin of (43.6 µg/mL) on the first day and then gradually decline below (10 µg/mL) in the first week. The reported concentrations of antibiotics released is lower than the our Cemex nanocomposite which released gentamicin at a concentration 400 µg/mL at day 1. It was shown that the bactericidal activity of aminoglycosides is concentration dependent and that high peak to MIC ratios could reduce the emergence of resistant mutants,

however, higher concentrations are associated with more systemic effects in case of systemic administration, or more cytotoxicity in local release (Lefort et al., 2000). Also, gentamicin can be tolerated for up to 800 µg/ml of gentamicin before causing toxicity to cells (Rathbone et al., 2011).

The intraarticular antibiotic concentrations were measured in the first few days after inserting vancomycin-tobramycin-loaded spacers. Highest concentrations measured at day 1 were 19 µg/ml for vancomycin and 107 µg/ml for tobramycin. The concentrations determined from the wound drainage fluids were 10-30 times higher than MICs of infecting organisms (Masri et al., 1998). In another work, the concentration of vancomycin was 57 µg/mL on day 1 from vancomycin-impregnated spacers in the treatment of orthopaedic implant related *S. epidermidis* infections, also determined from the drainage fluids (Isiklar et al., 1999). (Anagnostakos et al., 2009) studied the release of gentamicin and vancomycin from beads and spacers in the drainage fluid using a two-stage protocol in the treatment of infected hip arthroplasties. Peak mean concentrations from PMMA beads and spacers were reached for gentamicin (115.70 µg/ml and 21.15 µg/ml, respectively) and vancomycin (80.40 µg/ml and 37.0 µg/ml, respectively) on day 1. The last measured concentrations for the beads group was 3.70 µg/ml for gentamicin and 23.00 µg/ml for vancomycin after 13 days, and 1.85 µg/ml for gentamicin and 6.60 µg/ml for vancomycin after 7 days in the spacer group.

#### **5.4.3 Antimicrobial efficacy**

Antimicrobial testing was done against common bacteria involved in PJIs, both in early and delayed infections (early infection starts during first 24hrs-1 week, and late infections after 1 month according to orthopaedic surgeons). The protocol used for antimicrobial testing (described in section 2.2.5) allows the comparison in antimicrobial activity between different bone cement formulations *in vitro* by directly incubating the release media from bone cement with tested bacteria. This gives a straightforward comparison between different types of bone cement and simulates the real scenario in the cemented prosthetic joint.

Different protocols are used to evaluate the antimicrobial properties of bone cements in literature (Table 19). Perni et al. (2015) measured the optical density

at 600 nm for an incubated broth with propyl paraben NPs loaded bone cement, after certain dilutions to record bacterial growth curves. Then, the antimicrobial activity for different bone cement formulations can be compared by estimating the duration of the lag phase and the maximum growth rate. Abid et al. (2017) tested the antimicrobial properties of dendrimer loaded bone cement by counting the number of viable bacterial cells after contact with different cement samples every 5 days. In another work, (Ayre et al. 2015) used agar diffusion test to evaluate the antimicrobial properties of liposomal cement formulation. The zones of inhibition were measured around bone cement sample disks and compared to gentamicin disc as a control.

Antimicrobial used	Antimicrobial test protocol	Bacteria tested	Reference
a. Propyl paraben NPs. b. Oleic capped Silver NPs.	Bacterial growth curves.	<i>S. aureus</i> , <i>S. epidermis</i> , <i>A. baumannii</i> , <i>MRSA</i>	(Perni et al. 2015) (Prokopovich et al., 2015)
a. dendrimer b. chitosan c. QCS	Colony count method.	<i>S. aureus</i> , <i>S. epidermidis</i> , <i>E. coli</i> , <i>P. aeruginosa</i>	(Abid et al., 2017) (Shi et al., 2006)
Gentamicin loaded liposomes	Agar diffusion test	<i>S. aureus</i>	(Ayre et al. 2015)

Table 19: Some protocols used in literature to test the antimicrobial properties of PMMA bone cements.

In our work, the antimicrobial activity of different cement formulations was linked to the gentamicin release profile, hence, once the release stopped the growth of bacteria was observed. However, *S. pneumonia* and *E. coli* showed less

vulnerability to released gentamicin, as in the case of Cemex NPs, which might be linked to their high MIC. The antimicrobial activity of Cemex NPs continued for up to 23 days, which is promising for providing prophylaxis from PJIs. For other types of bone cement, the antimicrobial activity of cements continued even after gentamicin release reached a plateau, may be because still there was a small amount of gentamicin leaching out of the cement which is enough for inhibiting the growth of bacteria for an extra few days. The short inhibition duration for the commercial bone cements is in accordance with the reported drop in the concentration of gentamicin below inhibitory levels in the first few days (Anagnostakos et al., 2009; Hsieh et al., 2009).

The aim of incorporating antimicrobials in the PMMA cements used to secure the implant is to prevent the development of infection after primary arthroplasty or aseptic revision or to have local antimicrobial therapy for the treatment of established infection in arthroplasty exchanges for PJI (Anagnostakos, 2017). In some countries, >90% of cemented primary replacement surgeries are performed by using ALBC (Parvizi et al., 2008), despite a lack of high-level evidence to support the effectiveness of this approach. A meta-analysis of six nonrandomized studies found a 50 % reduction in deep infection in > 20,000 primary or aseptic hip revision surgeries. A randomized study using systemic antimicrobial prophylaxis found a decrease in deep infection in diabetics undergoing primary knee arthroplasty (Chiu et al., 2001). ALBC is used for prosthesis reimplantation in the majority of patients undergoing one-stage or two-stage arthroplasty exchanges (Martínez- Moreno Javier et al., 2017). However, new approaches needed to improve the antimicrobial properties of ALBCs, to extend the antimicrobial activity for longer duration. Also, the emergence of resistant antimicrobial strains decreases the effectiveness of antibiotics loaded into PMMA cement (Anguita-Alonso et al., 2005; Helbig et al., 2018). Nanotechnology based antibiotic delivery systems is becoming a new approach for solving the limitation of antimicrobial therapy. Nanoparticles can be used to improve the release kinetics of antibiotics by enhancing delivery and providing controlled release. These improvements are attributed to large area to mass ratio and small size, and different ways available for modification and for antibiotic loading (Sharma et al., 2012; Wei et al., 2012). Also, nanotechnology can serve as a platform for

developing new antimicrobial delivery systems that can help tackling the problem of antibiotic resistant bacterial strains (Abid et al., 2017).

#### **5.4.4 Cytocompatibility**

The present study shows that the gentamicin loaded nanocomposite (Palacos R and Cemex Genta) elicit a small reduction (less than 15%) (p-value 0.94 and 0.46) in osteoblast proliferation, possibly, cells did not have enough nutrients because the media was changed after experiments at day 4. However, this effect was transient, with osteoblasts proliferation returning to normal after 7 days of exposure to cements (Figure 46 and Figure 47). In addition, there was no effect on osteoblast calcium production as shown from the alizarin red staining (Figure 48). At the released gentamicin concentrations, cumulative gentamicin released from Palacos NP was <200 µg/ml in the first 7 days, and <800 µg/ml for Cemex NP (Figure 39), the fluorescence cell images of Cemex Genta showed similar cell viability (number of cells) compared to Cemex NPs. Also, actin filament spreading and development for the cells cytoskeleton was seen in nanocomposite images, which is in agreement with the images obtained by exposing osteoblasts to Silica gentamicin nanoparticles (He et al., 2018).

In a study using human fetal osteoblast cells, soluble gentamicin in concentrations up to 750 µg/ml was not toxic for tested osteoblasts (Belcarz et al., 2009). Moreover, the number of growing cells was not affected by gentamicin concentration up to 1000 µg/ml, but the cellular structure of the cells has slightly changed (Belcarz et al., 2009). In another work, the use of amikacin and tobramycin, which are also aminoglycoside antibiotics as gentamicin, did not result in a significant change in cell number up to 5000 µg/ml, however, 800 µg/ml of gentamicin was toxic to cells, where toxicity was evaluated using alkaline phosphatase assay and DNA assay (Rathbone et al., 2011). In a study evaluating the effect of gentamicin on primary human osteoblast cells in as a model for wound irrigation in spinal surgery. Gentamicin at concentration of 1700 µg/ml induced a reduction of 15-20 % in osteoblast proliferation in the first 48 hours by reducing DNA production and alkaline phosphatase activity, which returned to control values after 72 hours. Also, it did not have any significant effect on osteoblast mineralization and bone

nodule formation (Philp et al. 2017). Critically, the metabolic activity of osteoblasts was significantly decreased by gentamicin at any concentration compared to control, as indicated by the alkaline phosphatase activity which is an early expressed marker for osteogenic differentiation (Ince et al., 2007). However, the expression of mRNA and alkaline phosphatase genes was unaffected even at the highest concentration of 800 µg/ml, which could be explained by the bactericidal activity of gentamicin. It has the ability to bind prokaryotic ribosomes which cause inhibition of protein synthesis and in consequence bacterial death (Ince et al., 2007).

Silica nanoparticles are broadly applied as drug delivery carrier because of their biocompatibility, high loading capacity and surface area, ease of synthesis and scale up with reasonable cost. Silica nanoparticles have a reactive surface with Si-OH groups, which are present also in conventional bioactive glasses, have bioactive properties because they can react with biological fluids to produce nanometre-sized apatite (Izquierdo-Barba et al., 2008; Vallet-Regí and Balas, 2008). The surface of silica particles can serve as nucleation sites causing rapid release of soluble silicon in the form of silicic acid, after ion exchange with H<sup>+</sup> and H<sub>3</sub>O<sup>+</sup> under physiological conditions. This ion exchange changes the pH and influence cell metabolism, function and aids the initial adherence by adsorbing serum glycoproteins, e.g. fibronectin (Izquierdo-Barba et al., 2008; Ravichandran et al., 2013). This makes silica-based materials are promising candidates for biomaterial application as bioceramics or drug delivery carriers because of their bioactive properties.

The main advantage of the use of ALBCs is delivering antibiotic directly into the effect infected joint, allowing achievement of high concentration at the site of action, and minimal or no systemic toxicity which includes ototoxicity, nephrotoxicity and encephalopathy (Martínez- Moreno Javier et al., 2017). The food and drug administration authorized ALBCs for second stage reimplantation after infected arthroplasties. However, the use of these ALBCs for prophylaxis in prosthesis surgery is off-label use (Walker et al., 2017). Aminoglycoside antibiotics (e.g. gentamicin and tobramycin) are commonly used in ALBCs because they satisfy the properties required for antibiotics to be incorporated into bone cements, such as thermo-stability at high temperature, availability in powder

form etc. In addition, their evidence of effectiveness and safety after frequent use in TJR.

Parvizi et al. (2008) conducted a meta-analysis (a statistical approach to combine the results from multiple studies in an effort to increase power over individual studies) that evaluated the efficacy of gentamicin-loaded cement in primary revision arthroplasty. A total of 21 444 knees arthroplasties impregnated with gentamicin or not were evaluated. Only one of the six studies evaluated by the authors reached statistical significance regarding prophylaxis of infection. Also, it was concluded that the ALBC reduced the deep infection rate by approximately 50% (from 2.3% to 1.3% when ALBC was used) with statistical significance in favour of antibiotic loading into bone cement. Based on previously mentioned clinical data, our nanocomposite provides a prolonged released for antibiotics which has a promising application in the clinical field for prophylaxis and treatment of PJIs.

## **5.5 Conclusion**

The LbL coated silica nanoparticles have been successfully incorporated into bone cement commercial formulations Cemex and Palacos, without adversely affecting the mechanical performance. The novel LbL coated silica NPs provided a more controlled, gradual and prolonged release of gentamicin sulphate compared to commercial formulations. The NP containing bone cement showed superior antimicrobial activity against different bacterial stains. The nanocomposites showed cytocompatibility and were nontoxic to osteoblast without adversely affecting calcium production. In conclusion, the application of LbL nano-delivery systems may play a vital role in improving the release of antibiotics and other therapeutic agents from the bone cement, which is needed to reduce infection rates after TJRs.

## 6 Chlorhexidine nanoparticle containing bone cement

### 6.1 Introduction

The continuing emergence of resistant microbial strains limits the success of conventional antibiotic-based therapies in the prevention and treatment of PJIs (Parvizi et al., 2008). Anguita-Alonso *et al.* (2005) It was reported that 41% and 66% of *Staphylococci* isolates, taken from patients with prosthetic joint infections, were resistant to gentamicin and tobramycin respectively, resistance is also reported with *Staphylococcus aureus* (Anguita-Alonso et al., 2005; Helbig et al., 2018). Also, the resistance is significantly higher in patients with previous use of ALBC, which indicates the selection of aminoglycoside resistant strains after using ALBC (Corona et al., 2014; Staats et al., 2017). Consequently, the development of non-antibiotic based therapies is becoming extremely urgent for the treatment and prevention of infections in general, and particularly in PJIs.

Chlorhexidine use in bone cements can enhance its antimicrobial properties because of the superior antimicrobial activity (Bellis et al., 2016; O'Malley, 2008). However, one of the limitations for application of chlorhexidine in bone cement is the decrease in the compressive strength upon powder incorporation (Rodriguez et al., 2015). Although it has been widely examined in dental cements (Fan et al., 2016; Seneviratne et al., 2014; Takahashi et al., 2006), it has not been investigated widely in acrylic bone cements. It has many applications as a disinfectant and antiseptic for skin infections, cleaning wounds (O'Malley, 2008; Peel et al., 2014), sterilization of surgical instruments (Knox et al., 2015; Magalini et al., 2013), and many dental applications including treatment of dental plaque, gingivitis and endodontic disease (Lucchese et al., 2012; Supranoto et al., 2015).

Despite chlorhexidine small structure, it can be incorporated in LbL assembly multilayers as shown in chapter 4. Chlorhexidine release from B1 layered nanoparticles continued for 70 days, which is a considerable improvement from the current drug delivery systems that release antimicrobial agents for only few days (Dunne et al., 2008; Gasparini et al., 2014; Moojen et al., 2008; Squire et al., 2008). The release of chlorhexidine did not show the initial burst as seen in LbL chlorhexidine quadruple layers made of non-hydrolysable (alginate) and hydrolysable (B1) polyelectrolytes.

In this chapter, chlorhexidine loaded in LbL structure silica nanoparticles (NPs) developed in chapter 4, were incorporated in PMMA bone cements to create a novel nanocomposite antimicrobial bone cements. The chlorhexidine loaded NPs and chlorhexidine powders were encapsulated into the PMMA bone cement (Cemex and Palacos) and characterised for drug release, antimicrobial activity, cytocompatibility, water uptake and mechanical properties. The aim of this work is to achieve a prolonged chlorhexidine release for several weeks (4-6 weeks) to provide prophylaxis and treatment from postsurgical PJIs, and to study the feasibility of chlorhexidine as an alternative to aminoglycoside antibiotics (e.g. gentamicin). The chlorhexidine powder and chlorhexidine nanocomposite bone cements were characterised for drug release (chlorhexidine), antimicrobial activity, material and mechanical properties and cytocompatibility.

## **6.2 Materials and methods**

### **6.2.1 Chemicals**

Triton X-100, Tetraethyl orthosilicate (TEOS), (3-Aminopropyl) triethoxysilane (APTS), sodium alginate, chitosan, chlorhexidine diacetate, sodium acetate trihydrate, phosphate buffer solution (PBS) tablets, o-phthaldialdehyde reagent were purchased from Sigma-Aldrich, UK.

Cyclohexane, 1-hexanol, ammonium hydroxide 35%, acetonitrile, ethanol, methanol, glacial acetic acid and 1-propanol were purchased from Fishers, UK. All reagents were stored according to manufacturer's guidelines and used as received. The bone cement was used is Cemex® (Tecres® S.p.A., Italy).

B1: is a patented biocompatible, biodegradable cationic polymer, the precise structure will remain confidential due to the IP associated.

## **6.2.2 Nanoparticle preparation**

### **6.2.2.1 Amino functionalised silica nanoparticles synthesis**

Silica nanoparticles functionalised with amine groups ( $\text{SiO}_2\text{-NH}_2$ ) were prepared in one-pot synthesis by hydrolysis of TEOS in reverse micro-emulsion and subsequent functionalization with amino group (Stöber et al. 1968), as described in section 2.1.2.1

### **6.2.2.2 Layer by Layer (LbL) coating technique**

The amino functionalised silica nanoparticles were layered with ten quadruple layers of a repeating sequence of (sodium alginate/chlorhexidine/sodium alginate/B1). The following concentrations of polyelectrolytes and drug in acetic acid-sodium acetate buffer were used in LbL: sodium alginate (2 mg/ml), chlorhexidine (10 mg/ml) and B1 (2 mg/ml). The nanoparticles were coated by the same described in section 2.1.2.2.

## **6.2.3 Bone cement preparation**

Bone cement preparation was carried out according to manufacturer's instructions and the ISO5833:2002 (Implants for surgery-Acrylic resin cements) and as described in section 2.2.2.

## **6.2.4 Rheology testing**

The storage ( $G'$ ) modulus and ( $G''$ ) loss modulus were recorded to study the effect of adding the nanoparticles on the cement settling time, as described in section 2.2.3.

## **6.2.5 Chlorhexidine release quantification**

Commercially available bone cement (Cemex® and Palacos®) were prepared as described in section 2.2.2. Chlorhexidine powder was added to each bone cement at different concentrations to study the release profile and antimicrobial properties for the bone cement with different concentrations of chlorhexidine. For optimizing the concentration of chlorhexidine powder, different concentrations were added to Cemex® bone cement (0.5-5% w/w). Chlorhexidine LbL coated nanoparticles were added to the bone cement at 9% which is equivalent to 3% pure chlorhexidine powder, Table 20 shows the composition of all cements tested. Calculations for

the nanoparticle containing bone cements were based on the loading efficiency (30% w/w) prepared in chapter 4, to have equal amounts of chlorhexidine between powder and nanoparticle containing bone cements.

	Palacos- chlorhexidine powder	Palacos NPs	Cemex – chlorhexidine powder	Cemex - NPs
<b>Liquid component / g</b>	18.80	18.80	13.30	13.30
Methyl Methacrylate / % w/w	97.87	97.87	98.20	98.20
N-N Dimethyl- p-Toluidine / % w/w	2.13	2.13	1.80	1.80
Hydroquinone / ppm	60.00	60.00	75.00	75.00
<b>Powder Component / g</b>	40.80	40.80	40.00	40.00
Polymethyl Methacrylate / % w/w	83.27	83.27	82.78	82.78
Barium Sulphate / % w/w	-	-	10.00	10.00
Benzoyl Peroxide / % w/w	0.50	0.50	3.00	3.00
Zirconia / % w/w	15.00	15.00	-	-
Chlorhexidine diacetate / % w/w	1.23	-	0.5, 1, 2, 3, 4, 5	-

Chlorhexidine NPs/ % w/w	-	3	-	9
<b>Powder:</b>	2.17	2.17	3.01	3.01
<b>Liquid ratio</b>				

Table 20: Composition of chlorhexidine containing bone cements.

A PTFE mould was used to produce cylindrical samples with 6mm diameter and 10 mm length. Each sample weighed  $0.40 \pm 0.01$ g and three samples were used for release study from each type of bone cement. The bone cement samples were incubated in 3ml PBS buffer (pH 7) at 37°C. The release media was replaced each day in order attain sink condition, where the concentration of released chlorhexidine is negligible in comparison to its' saturation solubility. The release samples were stored in the refrigerator (2-8 °C) for analysis. The concentration of chlorhexidine was determined in the samples using the HPLC method described previously in section 2.1.5.

### 6.2.6 Antimicrobial testing

Antimicrobial testing was done for the chlorhexidine powder and NPs containing bone cement listed in Table 20 (Palacos-1% chlorhexidine powder, Palacos- 3% NPs, Cemex- 3% chlorhexidine powder, Cemex-9% NPs) using the same protocol described in section 5.2.6 and 2.2.5. The minimum inhibitory concentration (MIC) for chlorhexidine was determined against different bacteria tested through standard MIC protocol as described in section 5.2.6 and 2.2.5. The bacteria tested are methicillin-resistant *Staphylococcus aureus* (NCTC 12493), *Streptococcus pyogenes* (ATCC 19615), *Staphylococcus epidermidis* (ATCC 12228), *Acinetobacter baumannii* (NCIMB 9214), *Pseudomonas aeruginosa* (NCIMB 10548), *Escherichia coli* (NCTC 10418).

### 6.2.7 Mechanical testing

Mechanical testing was performed as described in section 5.2.7 and 2.2.6. for different bone cements (Palacos-1% chlorhexidine powder, Palacos- 3% NPs, Cemex- 3% chlorhexidine powder, Cemex-9% NPs). Compressive strength testing was performed at 0 and 3 months' time. Also, bending and fracture toughness

testing were performed. Also, bending and fracture toughness testing were performed at zero time.

### **6.2.8 Water uptake testing**

Different bone cement samples (Palacos-1% chlorhexidine powder, Palacos- 3% NPs, Cemex- 3% chlorhexidine powder, Cemex-9% NPs) were incubated in 3 ml PBS at 37°C for 3 months; for the first 2 weeks, the samples were weighed daily; after that the samples were weighed every 3 days (Perni et al., 2015), as described in section 5.2.8 and 2.2.7. Water uptake was calculated by dividing the increase in sample weight at different time points by the initial sample weight at time zero, and plotted as a percentage. Water uptake studies give an insight about the cement behaviour after being wetted in solution to simulate the *in-vivo* conditions inside the joint with the synovial fluid.

#### **1.1.1 Nanoparticles distribution in bone cement**

The distribution of nanoparticles in Palacose-3% chlorhexidine NPs and Cemex-9% chlorhexidine NPs was studied by fluorescence imaging using fluorescent labelled LbL nanoparticles as described in section 2.2.9.

### **6.2.9 Cytotoxicity testing**

#### **6.2.9.1 MTT**

MTT test was done for Cemex, Cemex- 3% chlorhexidine powder, Cemex- 9% chlorhexidine NP for time points of 1,2,4 and 7 days with the protocol described in section 2.2.8.1.

#### **6.2.9.2 LDH**

LDH assay test was performed for Cemex, Cemex- 3% chlorhexidine powder, Cemex- 9% chlorhexidine NP for days 1,2,4 and 7 using the protocol described in section 2.2.8.2.

### **6.2.9.3 Calcium production assay-Alizarin red**

Alizarin red test was done for Cemex, Cemex- 3% chlorhexidine powder, Cemex- 9% chlorhexidine NP after 21 days using the same protocol described in section 2.2.8.3.

### **6.2.9.4 NO**

The concentration of NO released by cells into the media was determined for Cemex, Cemex- 3% chlorhexidine powder, Cemex- 9% chlorhexidine NP for days 1,2,4 and 7 using the protocol detailed in section 2.2.8.4.

### **6.2.9.5 Fluorescence images**

Fluorescence imaging were performed for Cemex® bone cement of different types of composites (Cemex, Cemex- 3% chlorhexidine powder, Cemex- 9% chlorhexidine NP) using the protocol described in section 2.2.8.5.

### **6.2.10 Statistical analysis**

All data were expressed as means  $\pm$  standard deviation (SD) from at least three independent values. To assess the statistical significance of results between groups, one-way analysis of variance (ANOVA) was performed. Experimental results were considered statistically significant at 95 % confidence level ( $p < 0.05$ ). All analyses were run using the SPSS ® software.

## **6.3 Results**

### **6.3.1 Chlorhexidine release profile**

Chlorhexidine release from bone cement was studied in PBS buffer (pH 7.3), which is the pH value in healthy joints (Ribeiro et al., 2012). Chlorhexidine was quantified by HPLC with UV-detection at 239 nm in each sample, each data point is an average of three independent sample measurements. Figure 53 shows the cumulative release of chlorhexidine from Cemex® bone cement with different concentrations of chlorhexidine powder (0.5, 1, 2, 3, 4, 5% w/w) for 30 days. Different concentrations of chlorhexidine powder were studied to determine the suitable concentration of chlorhexidine to be added.

All bone cements stopped releasing chlorhexidine after 22 days. The total cumulative concentration released from 0.5% cement was 450  $\mu\text{g/ml}$ , and for the (1 and 2 and 3 %) cements was around 600  $\mu\text{g/ml}$ . While, the 4% and 5 % cements released around 750  $\mu\text{g/ml}$ . The increase in the cumulative chlorhexidine release was not proportional to the increase in the concentration of chlorhexidine powder added. Moreover, the release profiles for 3 % were similar to the 5% cement with P-value  $>0.05$ . Therefore, the 3% chlorhexidine powder concentration was chosen for further optimization, which is the normal concentration usually used for the incorporation of antibiotics in commercial bone cements without compromising the mechanical properties of the cement (Lewis, 2009).

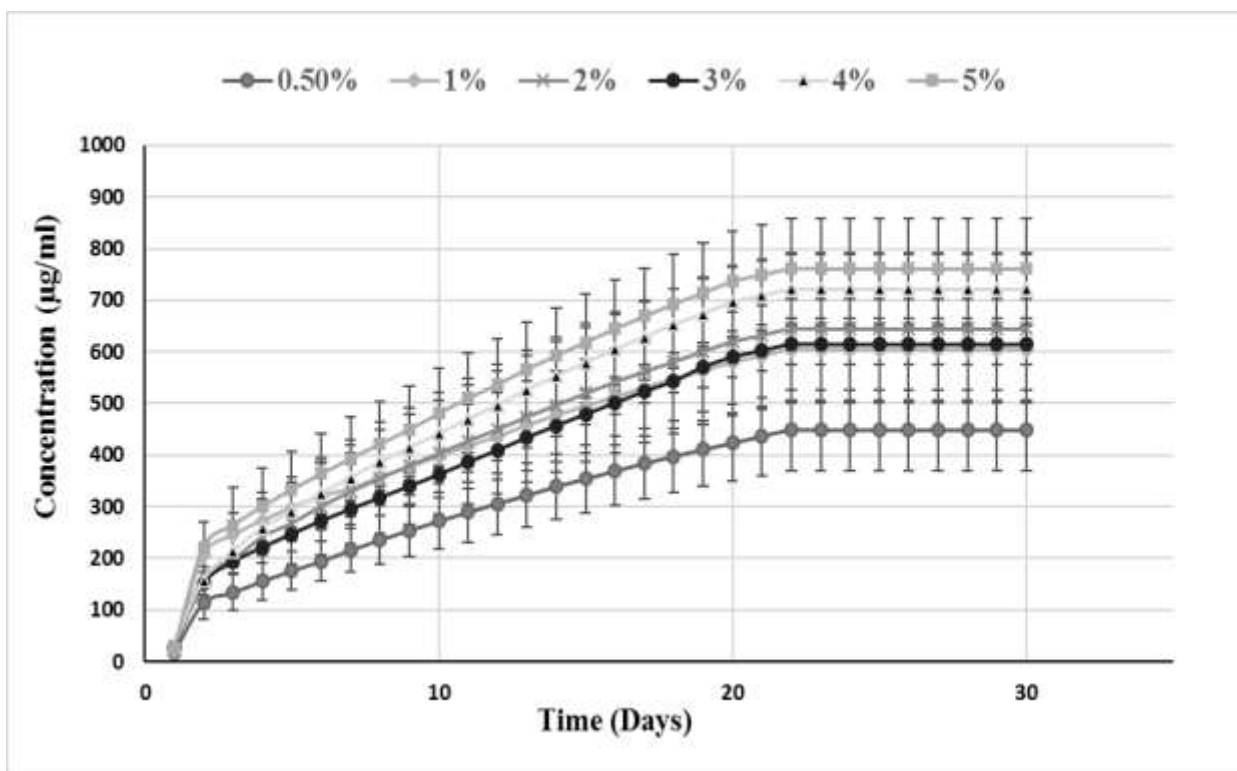


Figure 53: Cumulative chlorhexidine release in PBS (pH 7.3) from Cemex® with different concentrations of chlorhexidine powder (0.5, 1, 2, 3, 4, 5% w/w) ( $n=3+SD$ ).

Based on previous release study (Figure 53), the release of chlorhexidine was studied in Cemex® and Palacos® at 3 and 1 % concentration for chlorhexidine powder, and 9 and 3% concentration for the nanocomposite to have an equivalent amount of chlorhexidine, Figure 54. Palacos® cement stopped releasing chlorhexidine after 5 days for both powder and nanoparticle incorporated cement.

Also, the maximum cumulative concentration reached was  $< 200 \mu\text{g/ml}$ . However, there was a significant difference between the release profile of the chlorhexidine powder containing Cemex® and its nanoparticle counterpart, with  $p\text{-value} < 0.05$ . The chlorhexidine nanocomposite achieved a cumulative concentration of  $1300 \mu\text{g/ml}$  compared to  $600 \mu\text{g/ml}$  in the chlorhexidine powder containing cement. In addition, the release profile continued for up to 30 days in the nanocomposite, which is longer compared to the chlorhexidine powder containing cement (22 days).

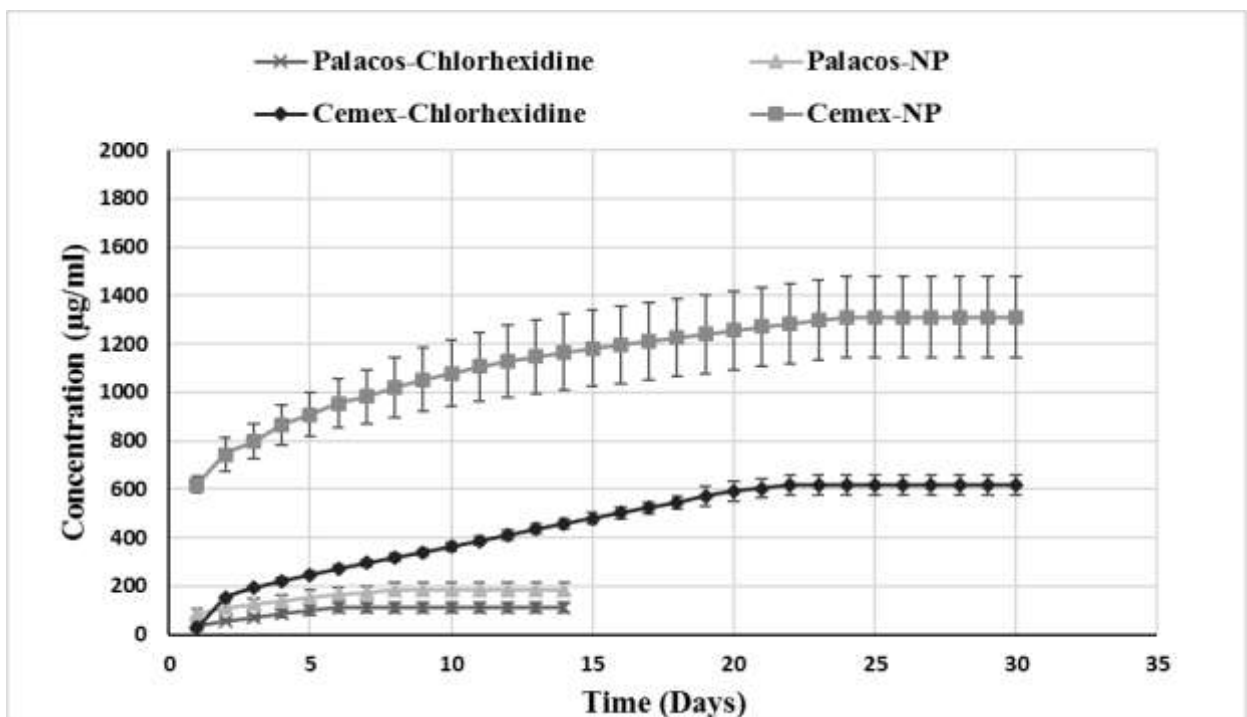


Figure 54: Cumulative chlorhexidine release in PBS (pH 7.3) from Palacos-1% chlorhexidine powder, Palacos-3% chlorhexidine NPs, Cemex-3% chlorhexidine powder, Cemex-9% chlorhexidine NPs ( $n=3+SD$ ).

In terms of total percentage release (Figure 55), Cemex with nanoparticles performed significantly better than the other types of bone cements. After day 7, Palacos chlorhexidine powder and Palacos nanocomposite stopped releasing chlorhexidine, however, Palacos nanocomposite achieved a higher percentage of 15 % compared to 8 % in the earlier cement ( $p\text{-value} < 0.05$ ). In Cemex nanocomposite, the percentage of chlorhexidine released was 33% which is two times higher than the chlorhexidine powder containing Cemex (16 % released) The release was controlled over the first 20 days before reaching plateau after 30 days, with minimal burst effect.

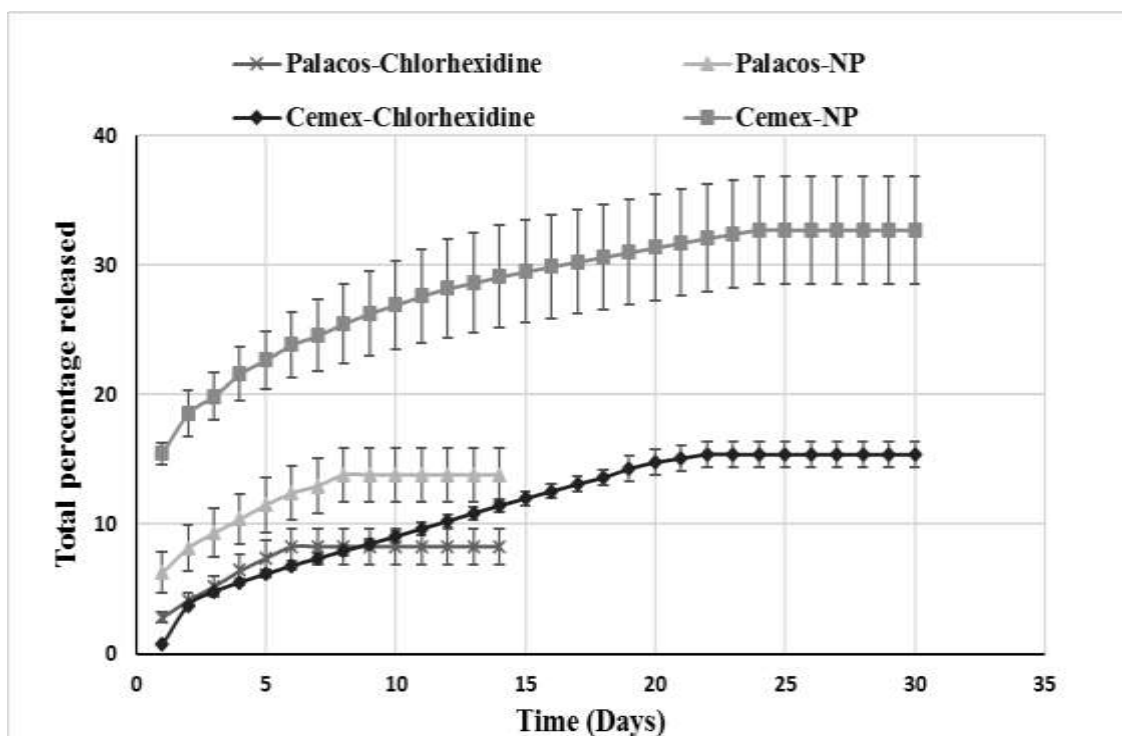


Figure 55: Cumulative **percentage** chlorhexidine release in PBS (pH 7.3) from Palacos-1% chlorhexidine powder, Palacose-3% chlorhexidine NPs, Cemex-3% chlorhexidine powder, Cemex-9% chlorhexidine NPs (n=3+SD).

### 6.3.2 Antimicrobial analysis

Antimicrobial testing against different types of bacteria that are encountered in PJI was performed for Cemex with different concentrations of chlorhexidine (0.5-5% w/w) (Figure 56). The MIC for chlorhexidine was determined against different bacteria tested through standard MIC protocol (Wiegand et al., 2008), and was found to be the following: *S. epidermis* 0.031 µg/ml, *MRSA* 0.98 µg/ml, *S. pyogenes* 1.95 µg/ml, *E. coli* 0.031 µg/ml, *P. aeruginosa* 7.8 µg/ml, *A. baumannii* 7.8 µg/ml. There was no significant difference in the antimicrobial activity for the different bone cements (0.5-5% w/w) against *Acinetobacter baumannii* and *Pseudomonas aeruginosa* (p-value >0.9), which had less than 4 days duration of inhibition. The antimicrobial activity of the 3 and 4 and 5% concentration was around 20 days against *MRSA* and *Escherichia coli* (p-value >0.40). However, the antimicrobial activity against *Streptococcus pyogenes* and *Staphylococcus epidermidis* continued for around to 25 days for the 3 and 4 and

5% cements (p-value >0.5). As a result, the concentration 3% chlorhexidine powder was chosen for further optimization, because it seemed that higher concentrations of chlorhexidine (4 and 5 %) didn't have a significant increase in the antimicrobial activity. The lowest the amount of antimicrobial added to the cement is the better, with the same antimicrobial activity, since higher amounts may compromise the mechanical properties of the cement without improving the antimicrobial properties.

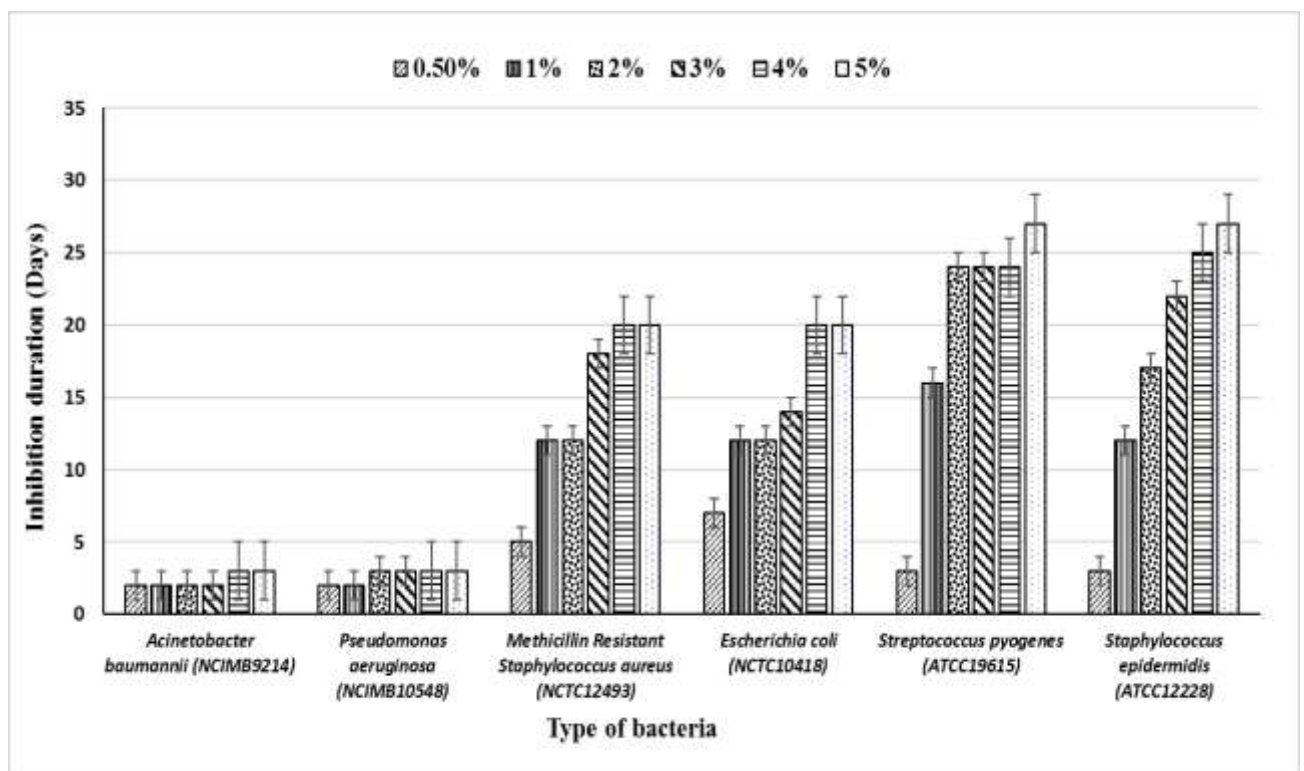


Figure 56: Antimicrobial testing for Cemex cement containing different concentrations for chlorhexidine powder (0.5, 1, 2, 3, 4, 5% w/w) (n=3+SD).

After optimizing the concentration of chlorhexidine, antimicrobial testing against different types of bacteria was performed for Palacos-1% chlorhexidine powder, Palacose-3% chlorhexidine NPs, Cemex-3% chlorhexidine powder, Cemex-9% chlorhexidine NPs) (Figure 57). Cemex containing chlorhexidine nanoparticles bone cement showed longer duration of bacterial growth inhibition compared to other types of bone cement against *Acinetobacter baumannii* and *Pseudomonas aeruginosa* for up to 8 days (p-value<0.05). Palacos chlorhexidine powder and nanoparticles showed same antimicrobial activity against all tested bacteria.

However, Cemex bone cement had superior antimicrobial activity to Palacos because it has higher amount of loaded chlorhexidine. Cemex loaded powder or nanoparticles inhibited the growth for up to 24 days for *Streptococcus pyogenes* and *Staphylococcus epidermidis*. Also, there was no significant difference in the antimicrobial activity of Cemex powder or nanoparticle containing bone cement against *MRSA*, *Streptococcus pyogenes* and *Staphylococcus epidermidis* (p-value >0.70).

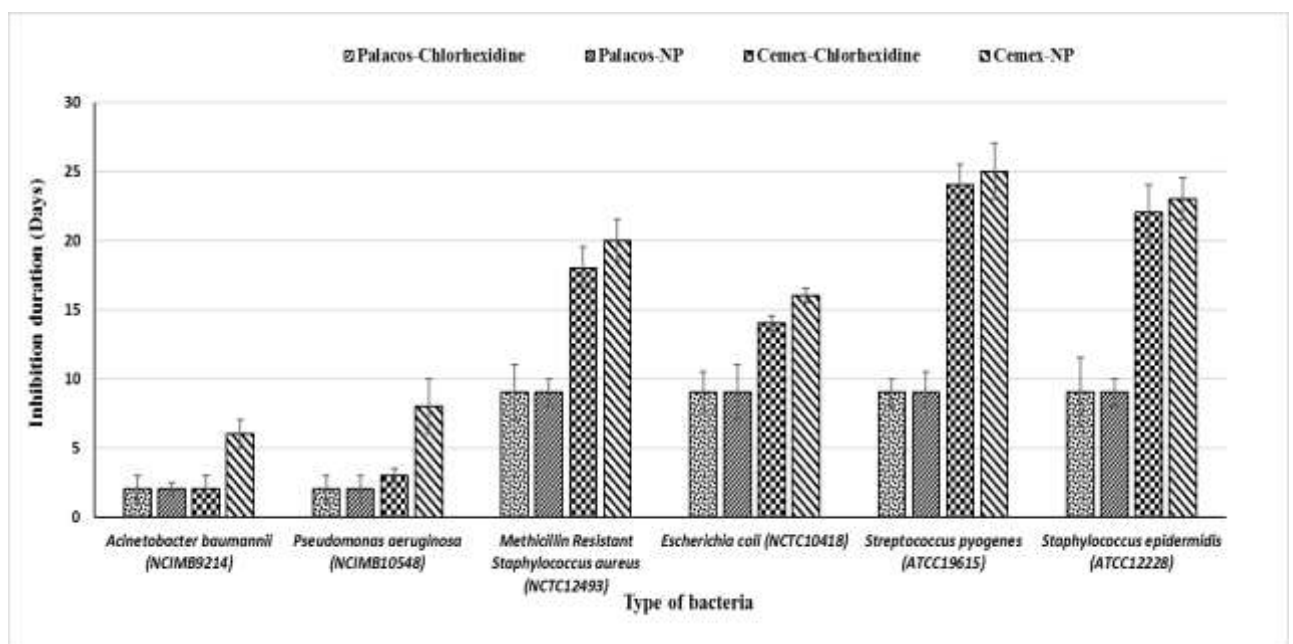


Figure 57: Antimicrobial testing for different types of bone cements (from Palacos-1% chlorhexidine powder, Palacose-3% chlorhexidine NPs, Cemex-3% chlorhexidine powder, Cemex-9% chlorhexidine NPs) (n=3+SD).

### 6.3.3 Bone cement settling time

The possible effects of the chlorhexidine nanoparticles on the kinetics of different bone cements settling time was investigated through the evaluation of the rheological properties of bone cement dough after mixing (Figure 58 and Figure 59). For all types of bone cements, storage modulus ( $G'$ ) was nearly the same as loss modulus ( $G''$ ); the pattern followed an increase at an initial fast rate that slowed down reaching a plateau. The storage modulus measures the stored energy,

representing the elastic portion, and the loss modulus measures the energy dissipated as heat, representing the viscous portion. Viscoelastic parameters, such as storage modulus, loss modulus have been obtained and show the change from primarily viscous to elastic behaviour as the cements set. In Cemex, the presence of nanoparticles required nearly the same settling time of 7 minutes (defined as the time needed for the dough to reach constant rheological properties) compared to chlorhexidine powder mixed cement. Palacos cement was not evaluated because it could not sustain the drug release for a long time with less antimicrobial performance unlike Cemex, which showed better performance.

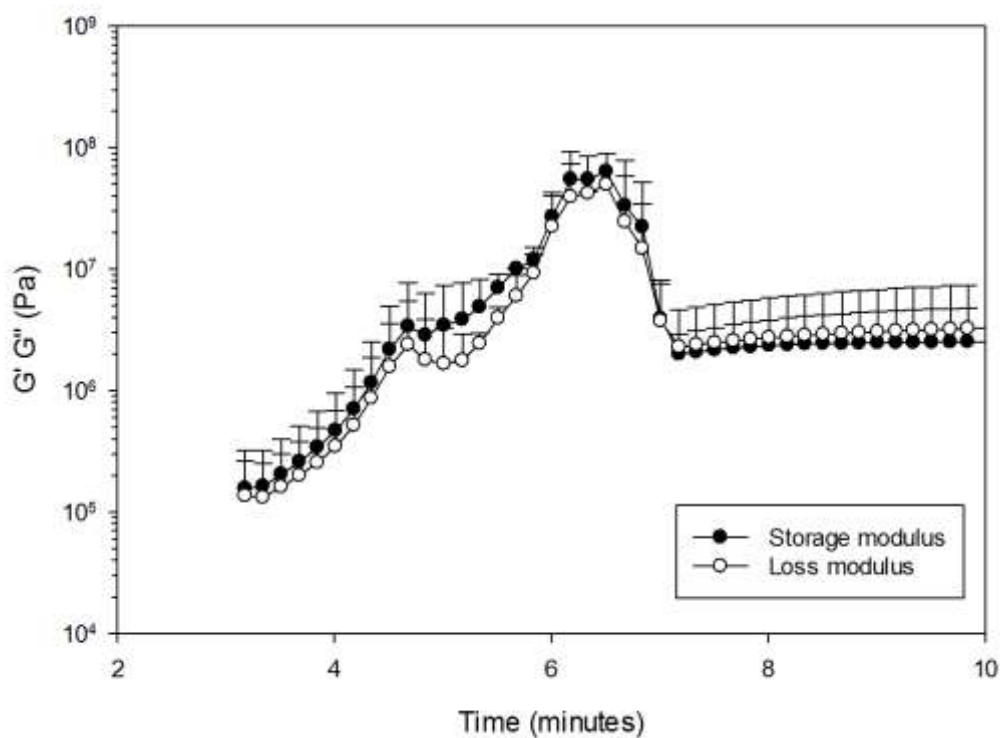


Figure 58: Storage ( $G'$ ) and loss ( $G''$ ) modulus for Cemex-chlorhexidine powder.

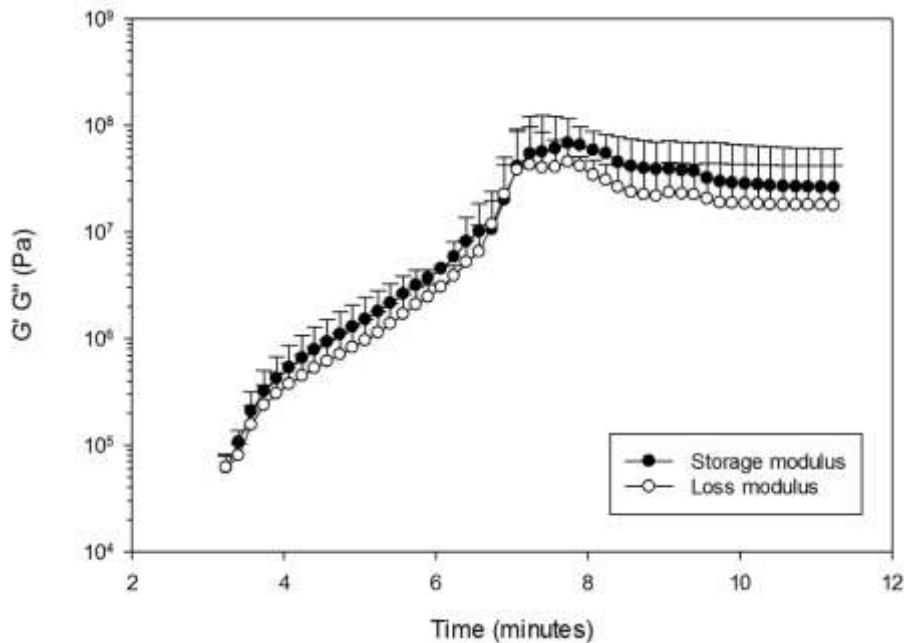


Figure 59: Storage ( $G'$ ) and loss ( $G''$ ) modulus for chlorhexidine Cemex-NPs.

### 6.3.4 Mechanical properties

The compressive strength of different types of bone cements (Cemex and Palacos with chlorhexidine powder or loaded NPs) was tested after 24 hours in air, and after 3 months of incubation in release media PBS, pH 7.4 at 37 °C (Figure 60) according to ISO standard 5833:2002. At 24 hours and after 3 months, all types of bone cement had similar compressive strength ( $p > 0.05$ ). For Palacos with chlorhexidine powder and Palacos NPs, there was no significant difference in the compressive strength ( $p\text{-value} > 0.762$ ) at zero time and after 3 months. For Cemex powder and Cemex chlorhexidine NPs, there was a significant difference in the compressive strength ( $p\text{-value} = 0.001$ ) after 3 months, with the nanoparticles showing higher compressive strength compared to the powder mixed cement. In addition, incubation for 3 months did not adversely affect the compressive strength of the bone cement. The bending and fracture toughness tests were performed for chlorhexidine loaded Cemex nanocomposite, and compared with commercial gentamicin loaded Cemex-Genta® (Table 21). Palacos cement was not evaluated because it could not sustain the drug release for a long time unlike Cemex, which showed better performance. The bending strength for the nanoparticle loaded chlorhexidine cement was similar to commercial cement Cemex-Genta, and meets

the ISO requirements (> 50 MPa). In addition, the fracture toughness for the two cements were similar (p-value > 0.20).

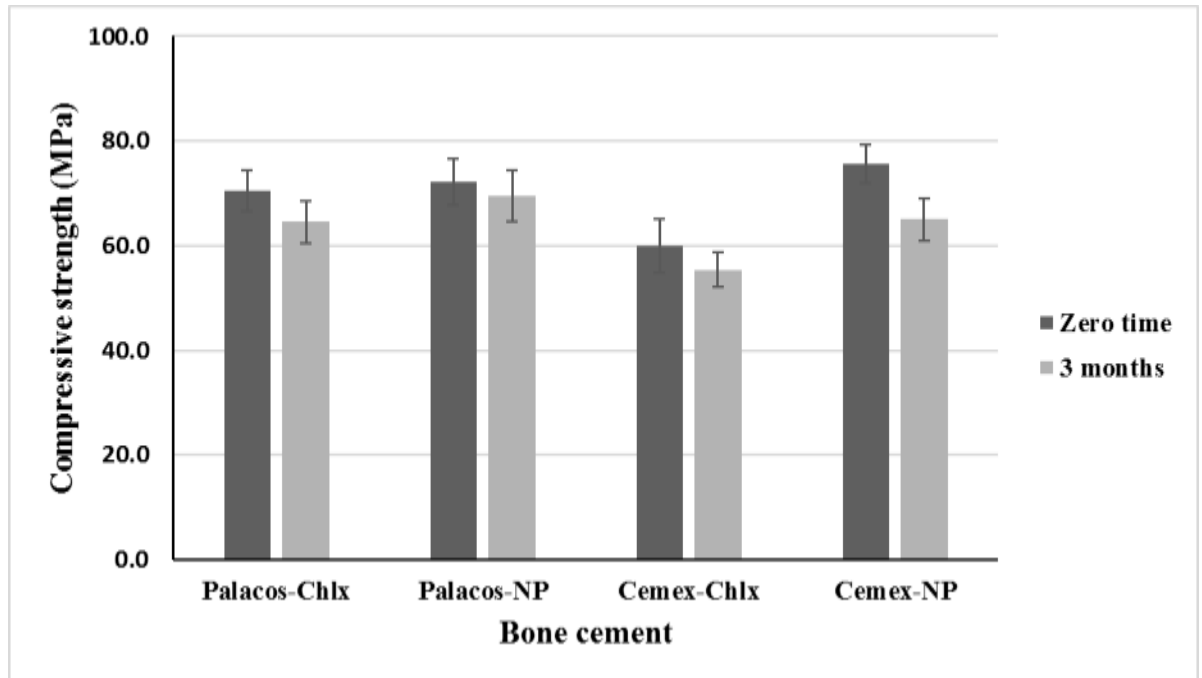


Figure 60: Compressive strength testing for different types of bone cements (from Palacos-1% chlorhexidine powder, Palacose-3% chlorhexidine NPs, Cemex-3% chlorhexidine powder, Cemex-9% chlorhexidine NPs) (n=6+SD).

	Bending strength (MPa)	Bending modulus (MPa)	Fracture toughness (MPam <sup>1/2</sup> )
Cemex-Genta	54.3 ± 2.0	2901 ± 62	2.4 ± 0.5
Cemex-chlorhexidine NPs	51.4 ± 3.6	2744 ± 97	2.1 ± 0.2

Table 21: Bending strength and modulus, and fracture toughness for chlorhexidine loaded Cemex nanocomposite as compared to commercial gentamicin loaded Cemex-Genta®.

### 6.3.5 Water uptake testing

The weight of the different types of bone cement was recorded after incubation in PBS buffer media pH 7.3, to study the water uptake behaviour for up to 22 days (Figure 61

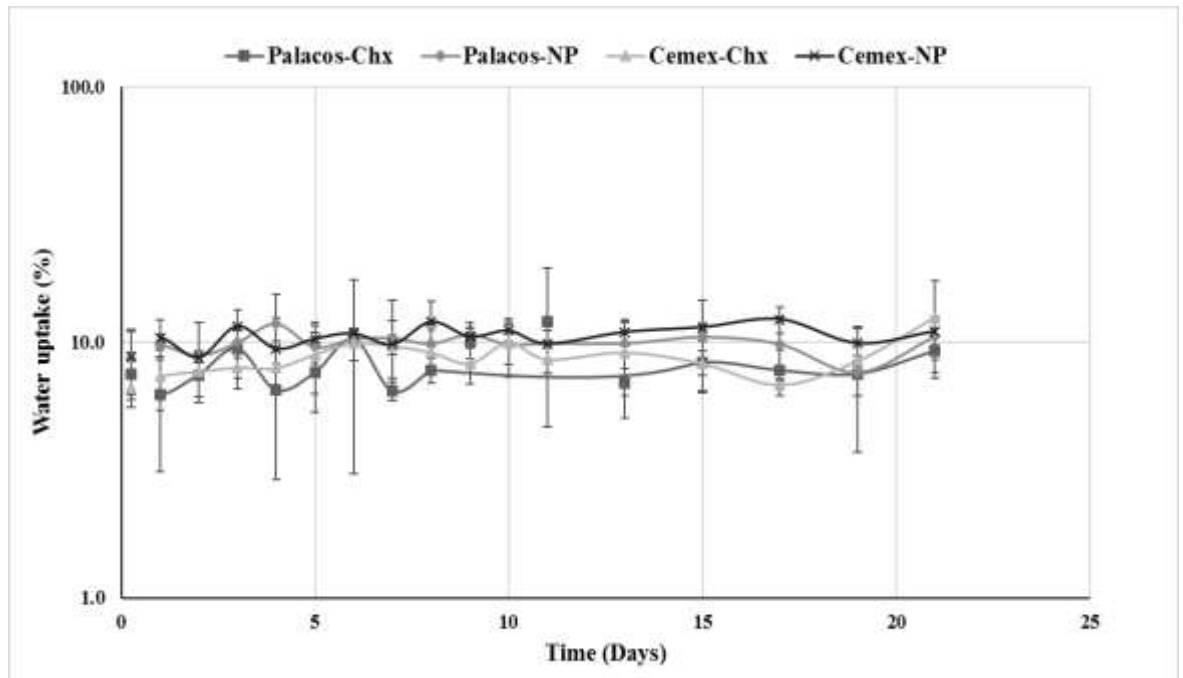


Figure 61). The nanocomposite water uptake behaviour was similar to that of the powder containing cements ( $p>0.05$ ). The bone cement samples increased in weight during the first 4-5 days because of water uptake, and after that, the amount of water in the samples remained stable.

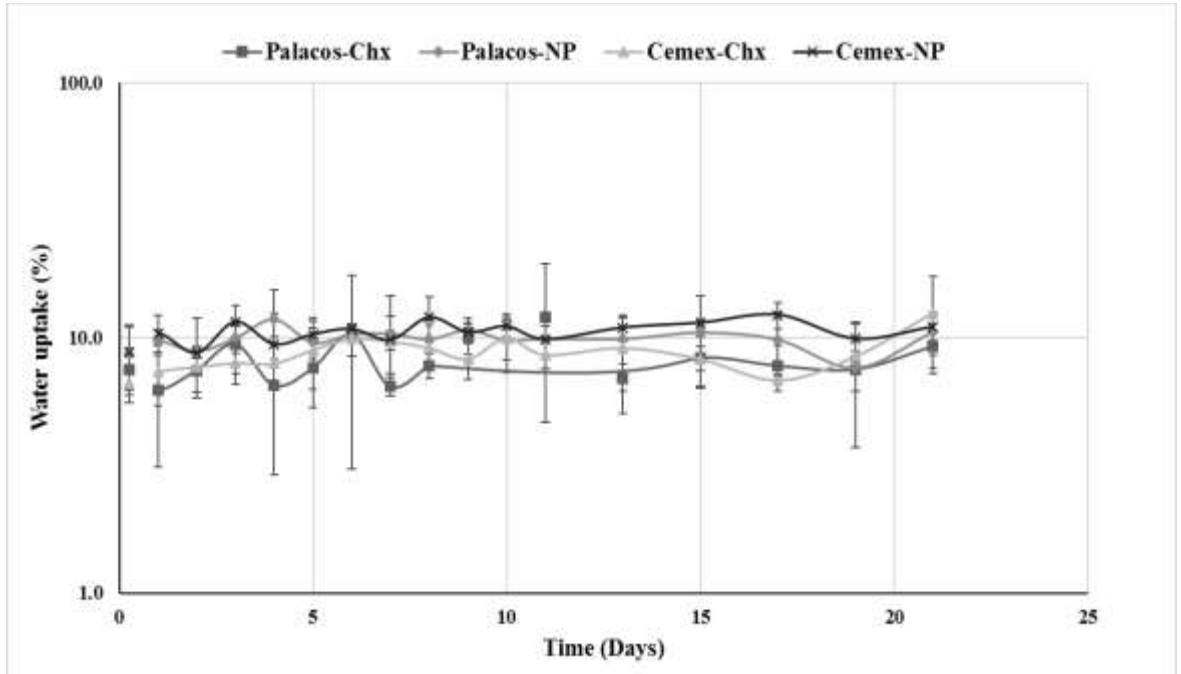
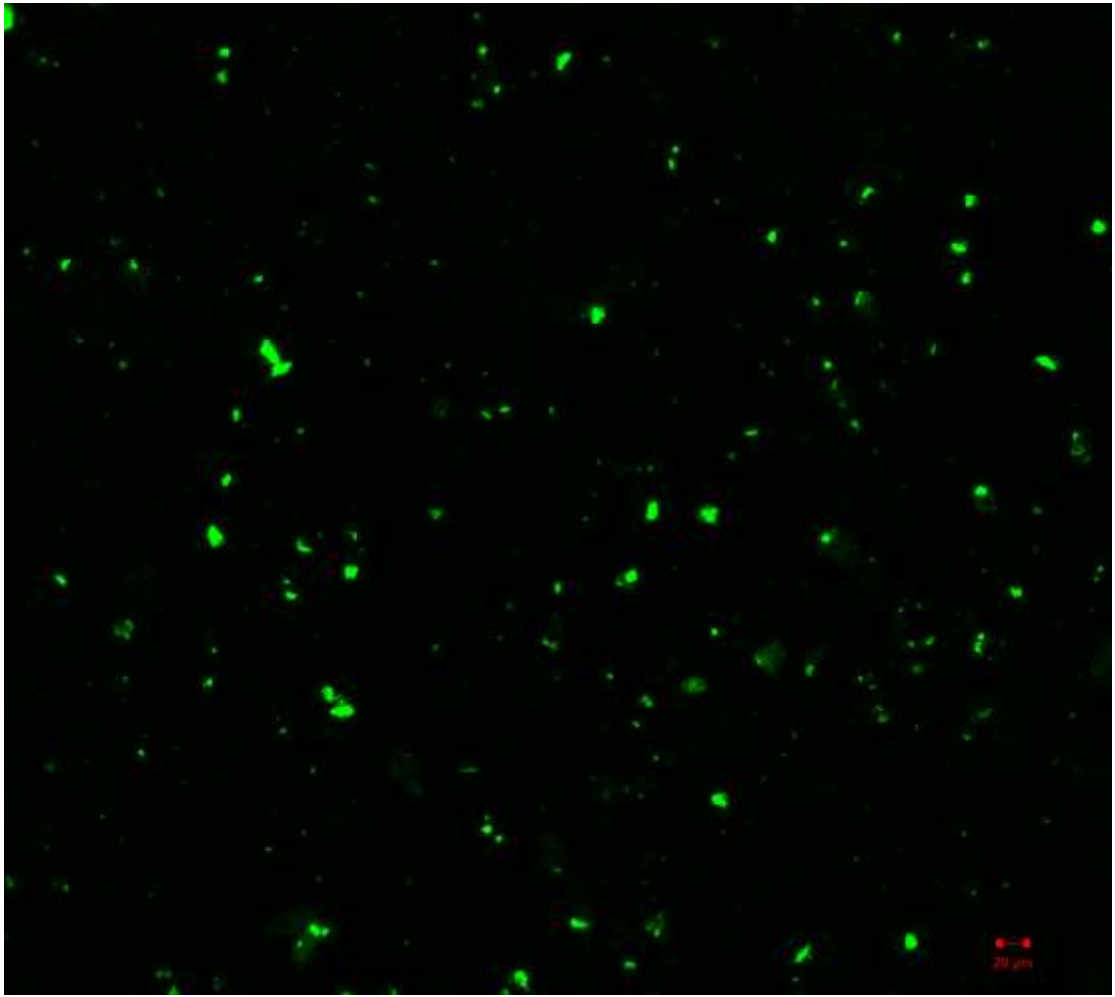


Figure 61: Water uptake for different types of chlorhexidine containing bone cements after incubation in PBS buffer, pH 7.3 (n=3+SD).

### 6.3.6 Nanoparticles distribution in bone cement

The distribution of nanoparticles inside the bone cement was studied by fluorescence imaging of fluorescence-labelled nanoparticles incorporated into the cement. Figure 62 shows nanoparticle distribution in Palacos bone cement (3% NPs w/w). Figure 63 nanoparticle distribution in Cemex bone cement (9% NPs w/w). In both types of cement, nanoparticles were homogeneously distributed throughout the cement matrix, with minimal agglomeration at higher concentration of nanoparticles in cement, as seen in Cemex 9% NPs w/w.



*Figure 62: Nanoparticle distribution of Palacos chlorhexidine nanoparticles (3% w/w) (bar=20 $\mu$ m).*

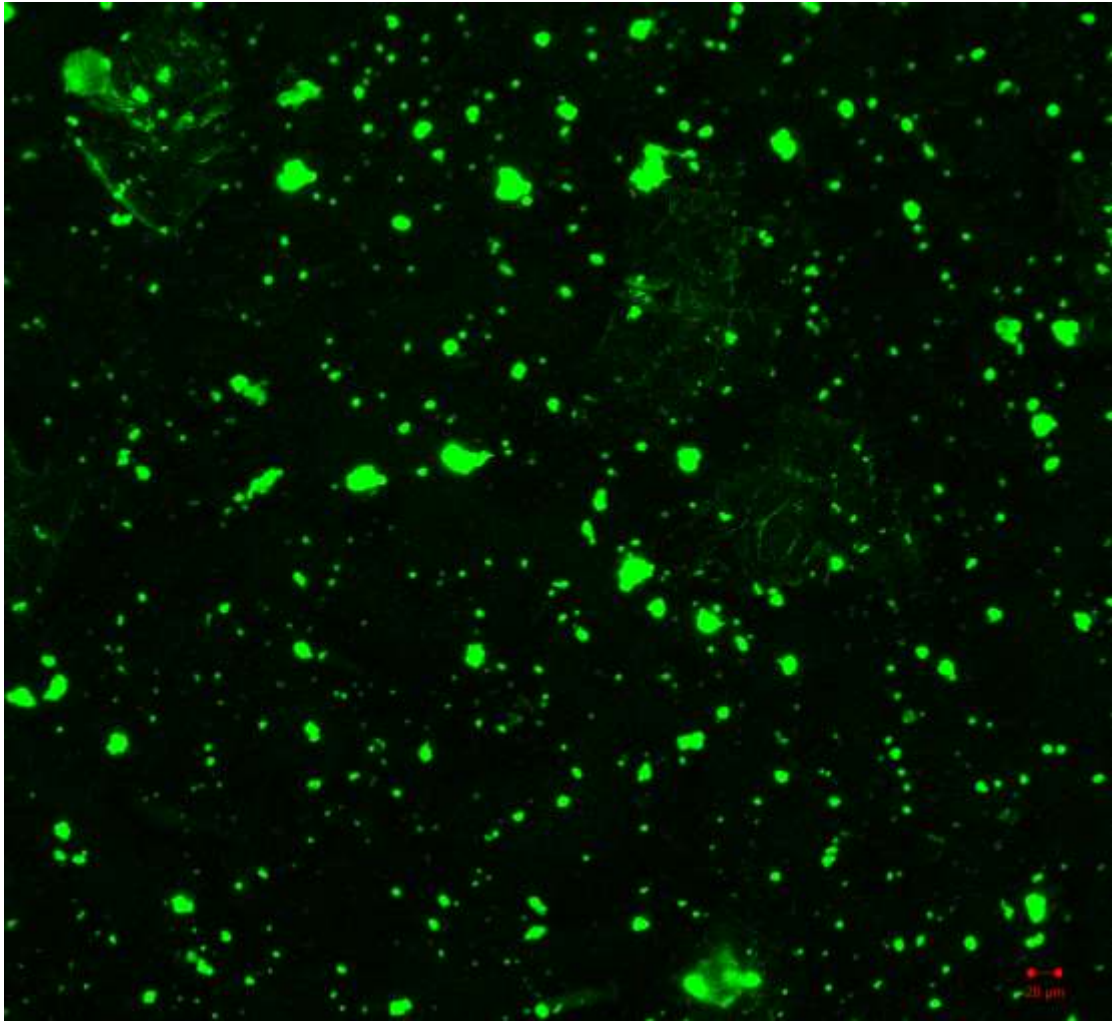


*Figure 63: Nanoparticle distribution of Cemex chlorhexidine nanoparticles (9% w/w) (bar=20 $\mu$ m).*

## **6.3.7 Cytotoxicity analysis**

### **6.3.7.1 MTT**

Relative to osteoblasts exposed to Cemex® commercial formulation (no added antibiotic), Cemex-chlorhexidine and Cemex NPs showed similar cell viability at day 1 (p-value 0.142 and 0.302) (figure 64). However, it was significantly different from cells control with p-value <0.004. At day 2, the viability of cells increased and Cemex-chlorhexidine and Cemex NPs cements showed similar viability (p-value 0.662) which was higher than Cemex® by up to 30% as seen in Cemex NPs (p-value <0.001). At day 4, the viability of osteoblasts dropped to 80% for Cemex-chlorhexidine cement. While, viability dropped to 75% in cells exposed to Cemex-NPs, and was significantly different from cells control (p-value <0.005). This drop could be because cells did not have enough nutrients because the media was changed after experiments at day 4. At day 7, Cemex-chlorhexidine and Cemex NPs showed increased viability which was similar to Cemex® (p-value>0.2).

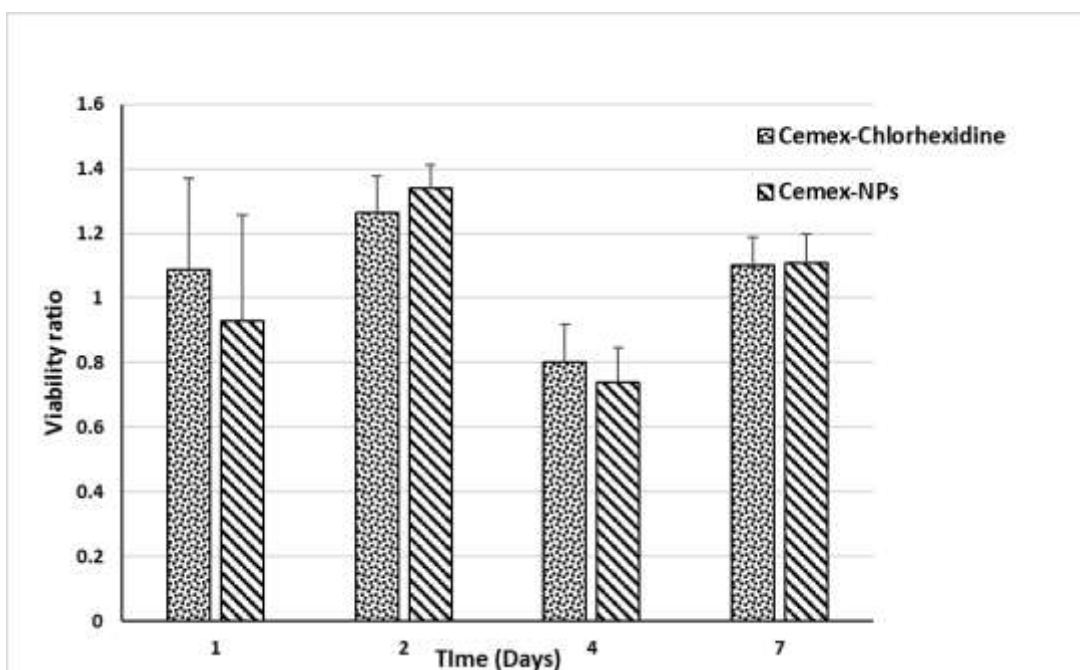


Figure 64: Viability of osteoblasts exposed to different types of bone cements: Cells control, Cemex, Cemex-chlorhexidine powder, Cemex with NPs, assessed through MTT test at Optical density of 570 nm presented as viability ratio (composite/commercial cement) ( $n=6+SD$ ).

### 6.3.7.2 LDH

Relative to the viability of osteoblasts exposed to Cemex® (commercial cement), the viability of Cemex-chlorhexidine was significantly lower with 30% reduction at day 1 ( $p$ -value = 0.033). Cemex-NPs showed similar viability to Cemex® of 85% as seen in Figure 65 ( $p$ -value = 0.538). At day 2, Cemex NPs showed viability similar to Cemex® of 90% ( $p$ -value = 0.657), while Cemex-chlorhexidine showed significantly different viability of 70% ( $p$ -value = 0.023). However, all bone cements showed significantly different osteoblast viability compared to cells control. At day 4, Cemex-chlorhexidine and Cemex-NPs showed similar viability to Cemex® ( $p$ -value >0.141). However, at day 7 the viability of osteoblasts dropped below 60% for both Cemex-chlorhexidine and Cemex-NPs.

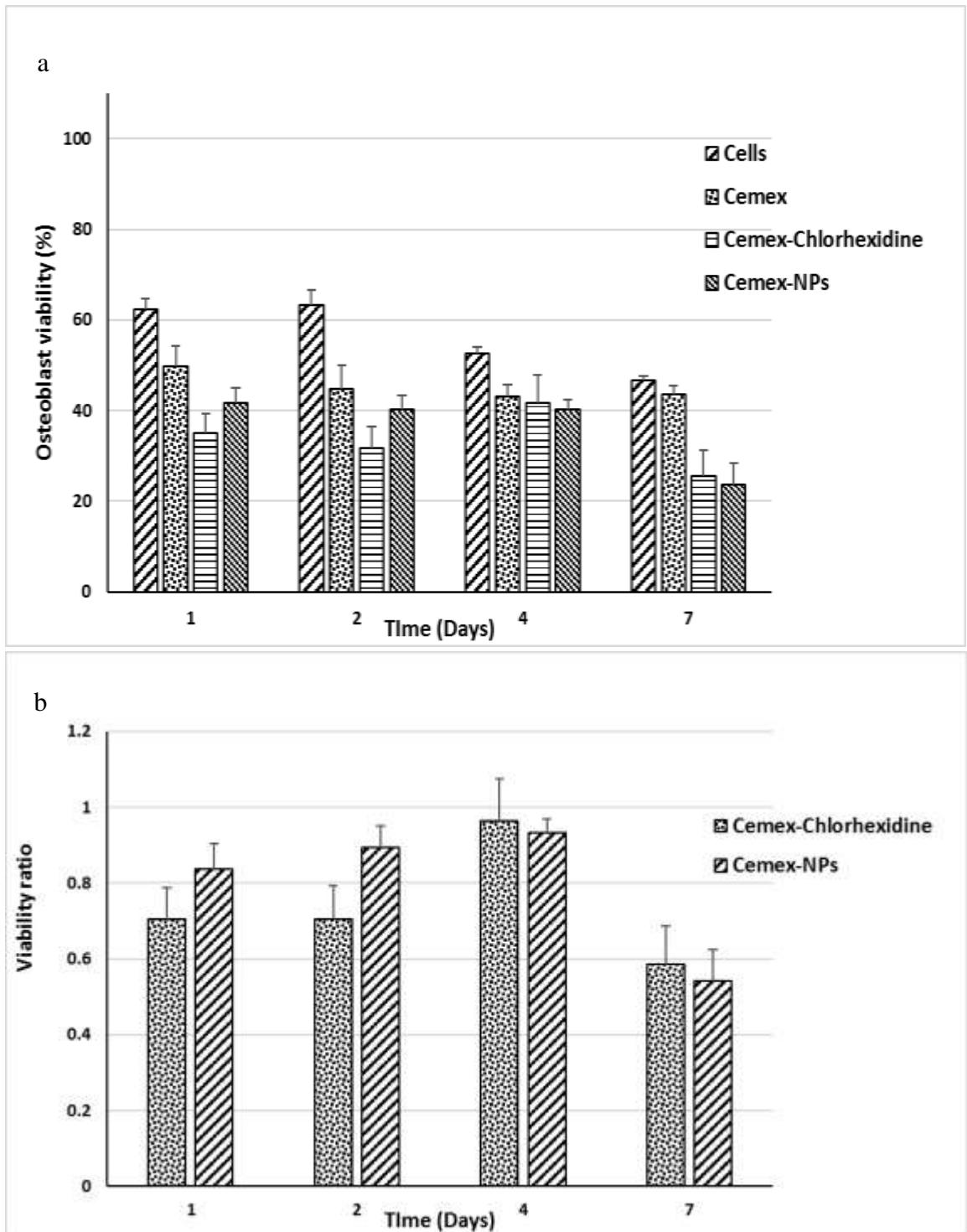


Figure 65: Viability of osteoblasts exposed to different types of bone cements: Cells control, Cemex, Cemex-chlorhexidine powder, Cemex with NPs, assessed through LDH test: (a) percentage viability, (b) viability ratio (composite/commercial cement) ( $n=6+SD$ ).

### 6.3.7.3 NO production

Nitric oxide (NO) is a free radical involved in the regulation of many physiological processes, such as vascular relaxation, neurotransmission, platelet aggregation and in immune regulation (van'T Hof and Ralston, 2001). Nitric oxide is a free radical which has important effects on bone cell function. The endothelial isoform of nitric oxide synthase is widely expressed in bone on a constitutive basis, whereas inducible NO is only expressed in response to inflammatory stimuli (Danziger et al., 1997). In general, Cemex-chlorhexidine and Cemex-NPs showed significantly higher nitrite production at different days tested, when compared to Cemex® or cells control (Figure 66) (p-value <0.05).

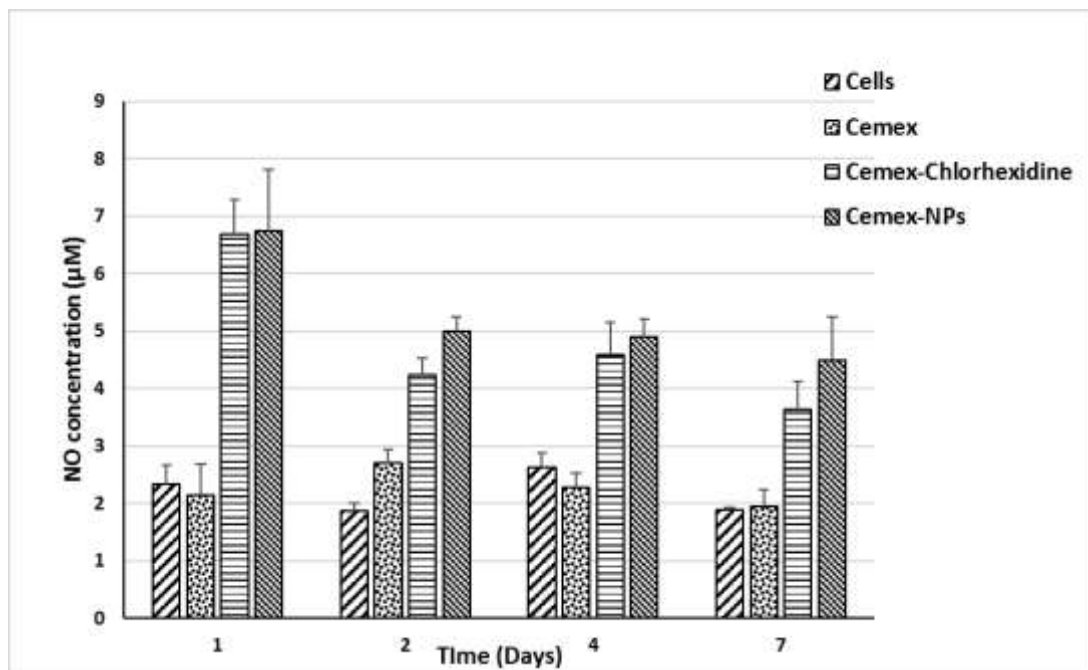


Figure 66: Nitrite production for osteoblasts exposed to different bone cements: Cells control, Cemex, Cemex-chlorhexidine powder, Cemex with NPs (n=6+SD).

#### 6.3.7.4 Alizarin red

The calcium production data are shown in figure 67, where Cemex-chlorhexidine and Cemex-NPs had similar results compared to Cemex® (p-value <0.05).

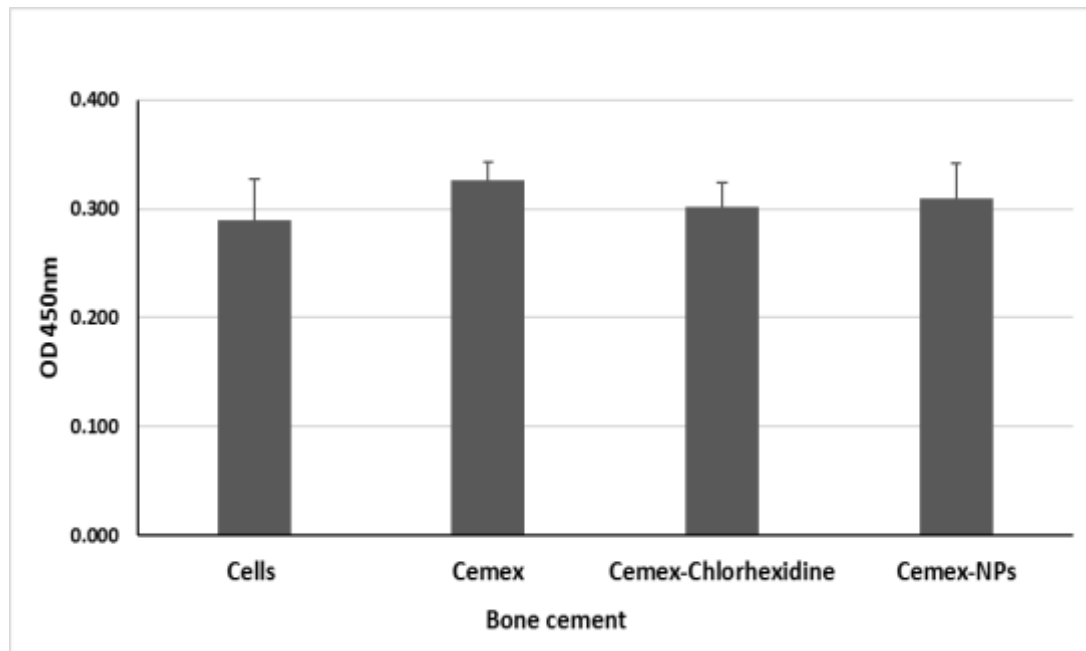
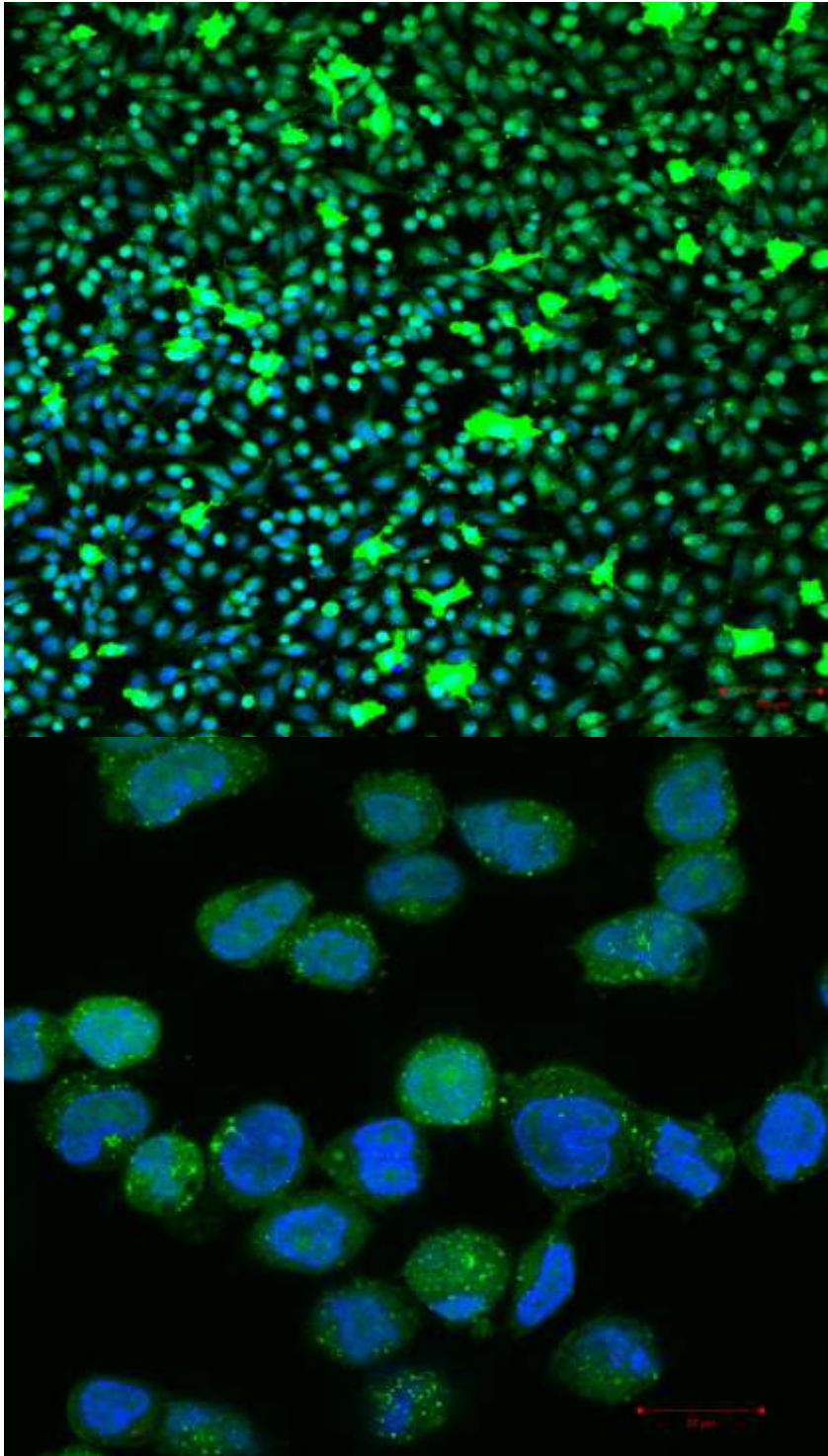


Figure 67: Alizarin red assay for osteoblasts after 21 days grown on different types of bone cements: Cells control, Cemex, Cemex-chlorhexidine powder, Cemex with NPs ( $n=6+SD$ ).

#### 6.3.7.5 Fluorescence images

Live and dead fluorescent images for Cemex (Figure 68), Cemex chlorhexidine powder (Figure 69) and Cemex chlorhexidine nanoparticles (Figure 70) show the live cells (green colour), dead cells (red colour) and cell nuclei (blue colour). In addition, actin/dapi fluorescent images for Cemex (Figure 71), Cemex chlorhexidine powder (Figure 72) and Cemex chlorhexidine nanoparticles (Figure 73) show actin filaments (red colour) and cell nuclei (blue colour). Different types of bone cements showed more or less similar viability in terms of number of cells, and similar actin filament spreading and development for the cells cytoskeleton.



*Figure 68: Live/dead images for Cemex cement with two different scales. (Top: 100  $\mu\text{m}$  bar, bottom: 20  $\mu\text{m}$  bar).*

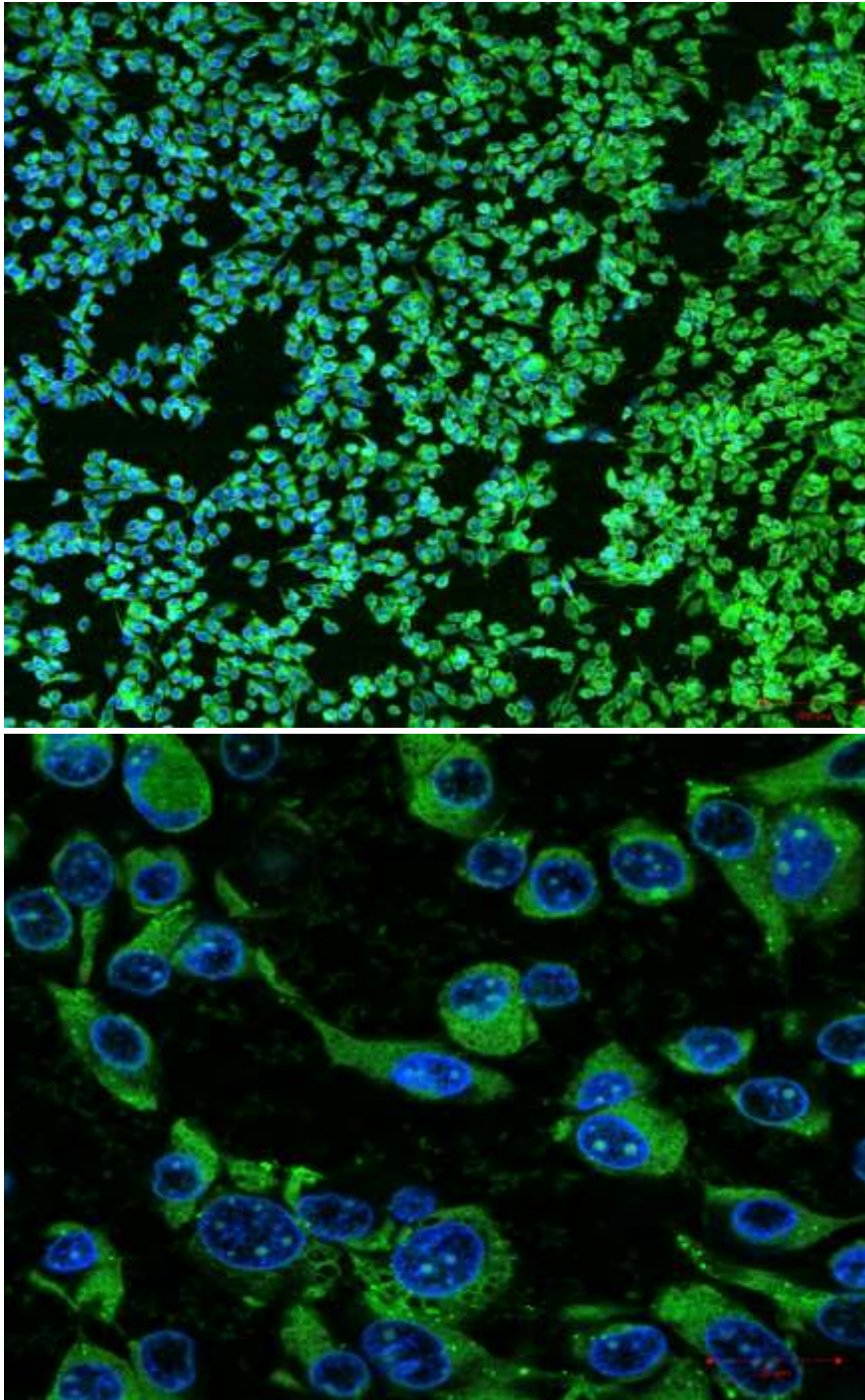


*Figure 69: Live/dead images for Cemex chlorhexidine powder cement with two different scales. (Top: 100  $\mu\text{m}$  bar, bottom: 20  $\mu\text{m}$  bar).*

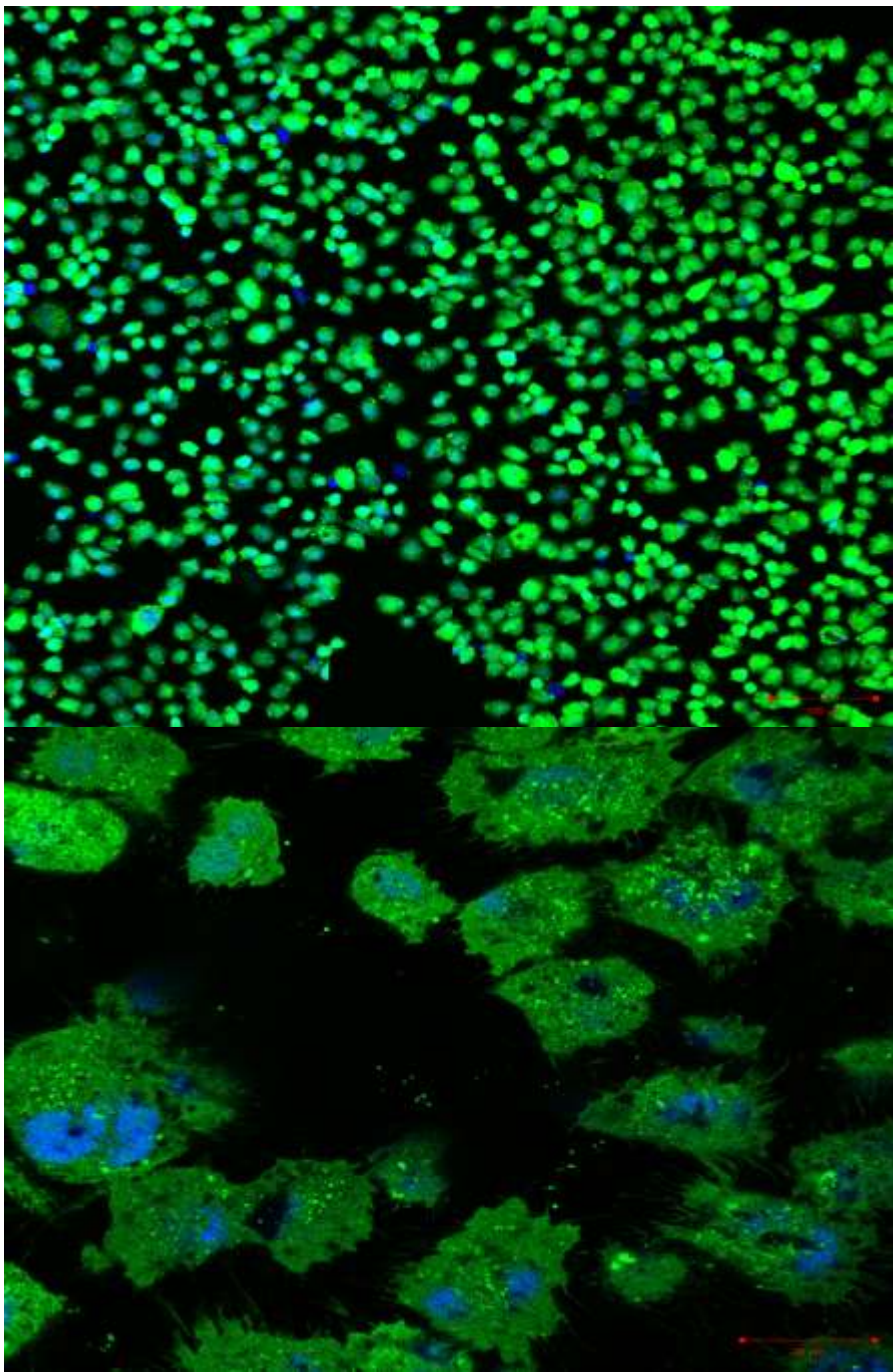


*Figure 70: Live/dead images for Cemex chlorhexidine nanoparticles cement with two different scales. (Top: 100  $\mu\text{m}$  bar, bottom: 20  $\mu\text{m}$  bar).*

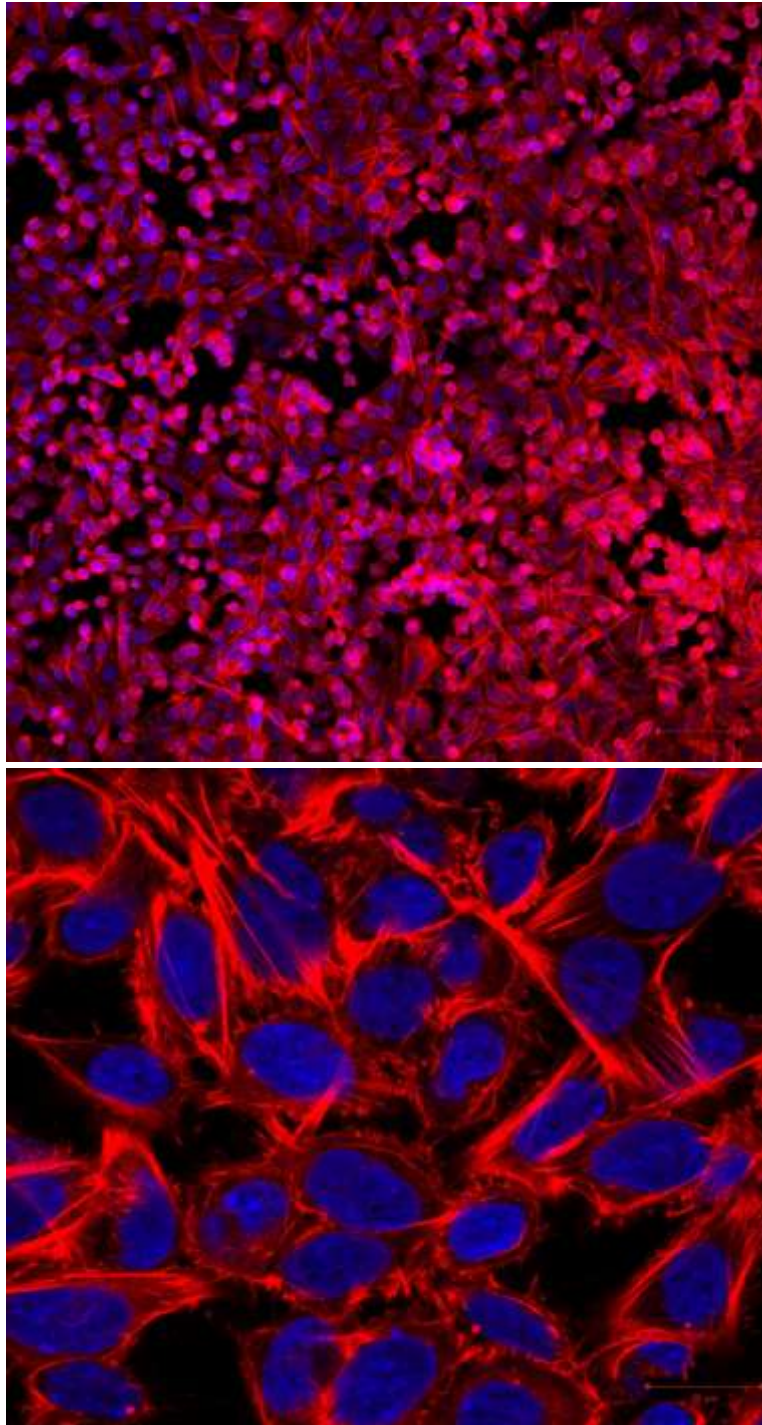


*Figure 71: Actin/dapi images for Cemex cement with two different scales. (Top: 100  $\mu\text{m}$  bar, bottom: 20  $\mu\text{m}$  bar).*

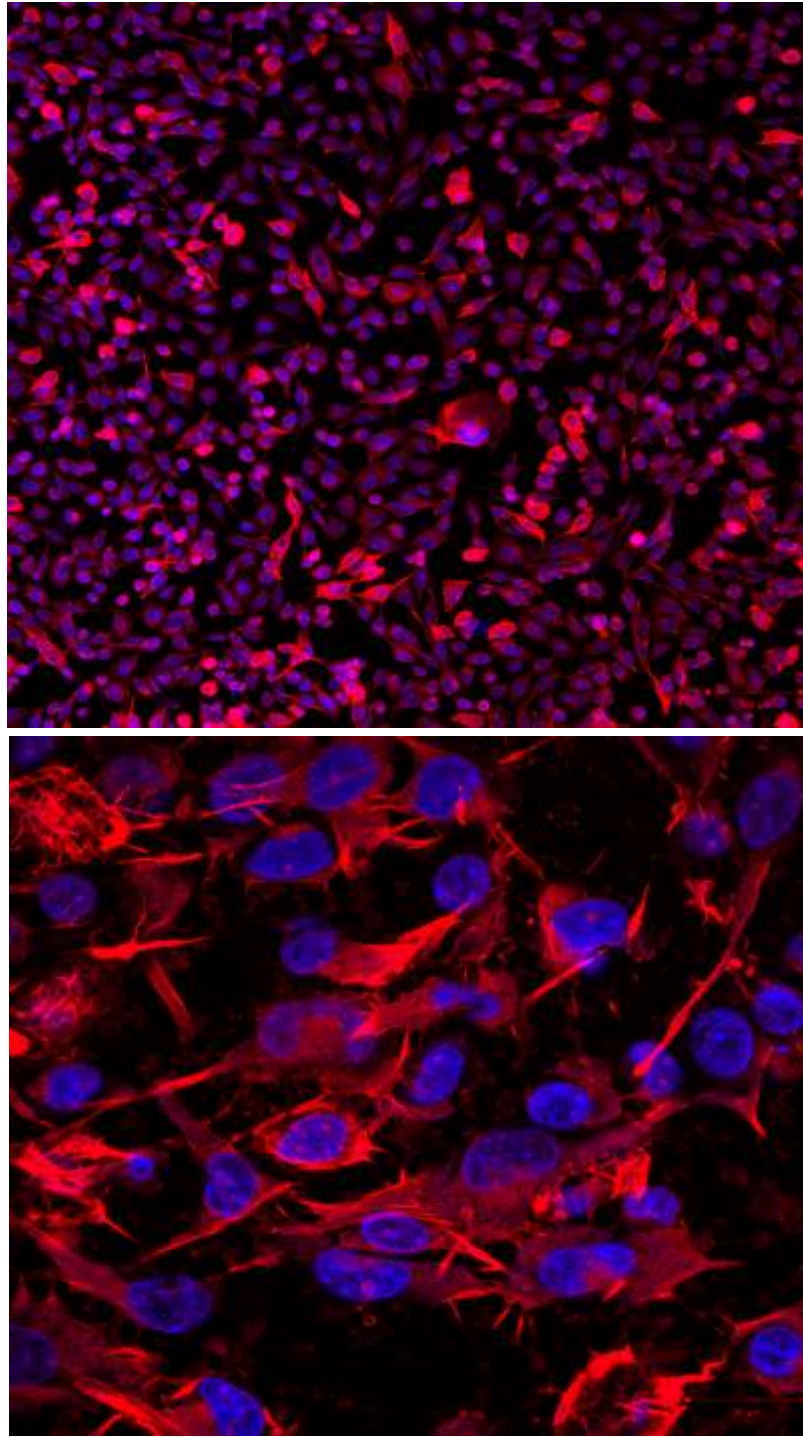


*Figure 72: Actin/dapi images for Cemex chlorhexidine powder cement with two different scales. (Top: 100  $\mu\text{m}$  bar, bottom: 20  $\mu\text{m}$  bar).*

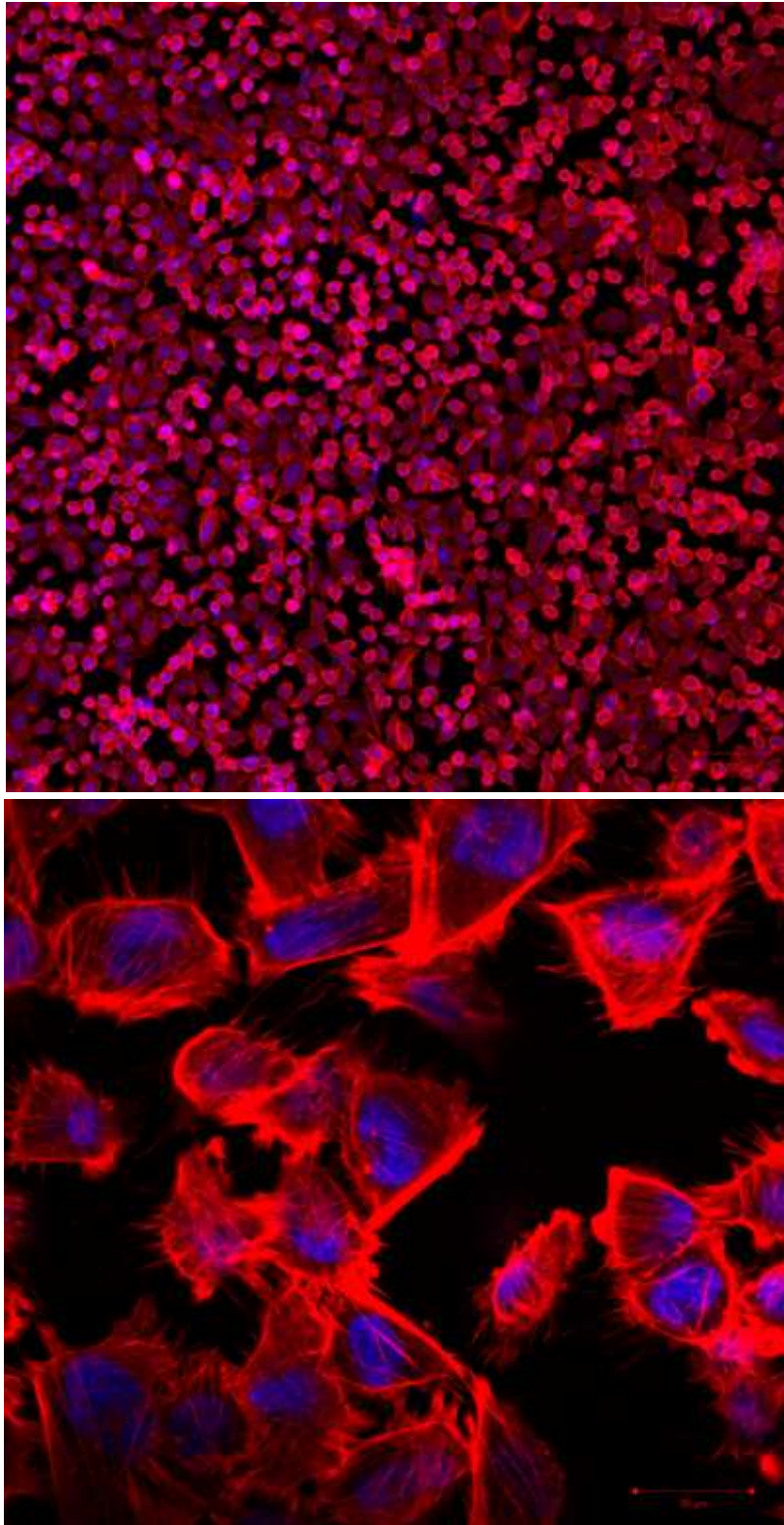


*Figure 73: Actin/dapi images for Cemex chlorhexidine nanoparticles cement with two different scales. (Top: 100  $\mu$ m bar, bottom: 20  $\mu$ m bar).*

## 6.4 Discussion

### 6.4.1 Chlorhexidine release profile

The continuing emergence of resistant microbial strains limits the success of conventional antibiotic-based therapies in the prevention and treatment of PJIs (Corona et al., 2014; Staats et al., 2017). Even though adding large amounts of antibiotics become a well-established method in the prevention and treatment of PJIs. There are many limitations related to the release profile from bone cement including burst release for the first few hours followed by slow release below inhibitory levels in the following days for less than 10% of the incorporated antibiotics (Dunne et al., 2008; Gasparini et al., 2014). Chlorhexidine is a broad spectrum cationic bactericidal polybiguanide antimicrobial agent (Hidalgo and Dominguez, 2001), which can offer an alternative to enhance the antimicrobial properties of bone cement.

The release from our LbL system showed less burst release compared to commercial formulation, and continued up to 30 days. The loading efficiency of chlorhexidine in the NPs was nearly 30% (w/w). The concentrations of NPs used in the bone cement were 9% in Cemex NP. The release of chlorhexidine was sustained gradually for more than 4 weeks, as in the case with Cemex NP. The chlorhexidine loaded nanocomposite enhanced the total amount of chlorhexidine released from the bone cement (up to 35% of loaded chlorhexidine) by up to 2-3 folds compared to the chlorhexidine powder cement. The enhancement of release kinetics, as being observed also in the case of gentamicin loaded nanocomposite in chapter 5, could be attributed to the homogenous distribution of NPs in the bone cement matrix (*Figure 63*), and the formation of nano-network channels to facilitate the diffusion of chlorhexidine (Shen *et al.* (2016), or simply because of the increased surface area available for drug release from nanoparticles. These findings confirm the reproducibility of the developed LbL coated nanoparticles when comparing the release profiles for chlorhexidine and gentamicin from the tested cements.

(Young et al., 2008) evaluated chlorhexidine release from brushite calcium phosphate bone cement added at different concentrations (3, 6, 9, 12 % w/w). The cumulative percentage release was independent of chlorhexidine concentration

with 60 % of the drug released after 24 hours, and 95% after 2 weeks. The rate of release in water followed Fick's law of diffusion and was proportional to the square root of time with 1 mm thick specimens. (Zhao et al., 2011) investigated chlorhexidine release from bone adhesives consisting of fluid photo-polymerizable (lactide-co-propylene glycol-co-lactide) dimethacrylate. Chlorhexidine was added at 10 % w/w of total mixture the release was fast in the first 10 days and then declined with time releasing up to 80 % of total chlorhexidine loaded.

(Riool et al., 2017) developed an antimicrobial coating for orthopaedic implants containing chlorhexidine as the antimicrobial agent. The coating was epoxy-based spin-coated on titanium implant, and loaded with either 5% or 10 % w/w chlorhexidine. The coatings showed potent bactericidal activity *in vitro* against *S. aureus*, with over 80 % of the release ( $19 \mu\text{g}/\text{cm}^2$  for 5% concentration and  $41 \mu\text{g}/\text{cm}^2$  for the 10 %) occurring within the first 24 h. The amount of chlorhexidine released was proportional to the amount of chlorhexidine in the formulation, however the release was burst and stopped after 4 days. (Yan et al., 2017) studied the release of chlorhexidine from glass ionomer cement used aesthetic dentistry to prevent secondary caries. Chlorhexidine was encapsulated in mesoporous silica nanoparticles by wet impregnation with encapsulation efficiency of 44.62% w/w. The loaded nanoparticle incorporated in the dental cement at three concentrations (1%, 5%, and 10% (w/w)). Chlorhexidine release continued for up to 30 days for all concentrations, but the amount released was not proportional to the increase in concentration. This suggests that the released chlorhexidine comes from the nanoparticles on the surface and the deeply embedded ones remained entrapped inside the cement.

Chlorhexidine has many dental applications including treatment of dental plaque, gingivitis and endodontic disease (Karpiński and Szkaradkiewicz, 2015; Supranoto et al., 2015). Chlorhexidine is used for primary and secondary prevention of gingivitis, periodontitis and tooth decay (James et al., 2017). Also, chlorhexidine use decreases plaque, gingivitis bleeding and inflammation (Prasad et al., 2016). Chlorhexidine is available as mouthwash at different concentrations ranging from 0.02% to 0.3%. The type of action is dose dependent, bacteriostatic at low concentrations (0.02%-0.06%) and bactericidal at higher concentrations (0.12%-0.2%). However, chlorhexidine also available in other pharmaceutical

forms as gel, aerosol and spray to be applied directly at the area to be treated (Prasad et al., 2016; Varoni et al., 2012). 30% chlorhexidine remains on the oral mucosa after a single use of chlorhexidine mouthwash and negligible amount is swallowed. The absorption of chlorhexidine is limited through the skin and gastrointestinal tract because of its cationic properties, and chlorhexidine is excreted mainly through faecal matter (Varoni et al., 2012).

Chlorhexidine has many applications as a disinfectant and antiseptic for skin infections, cleaning wounds, sterilization of surgical instruments (O'Malley, 2008). (Knox et al., 2015). Chlorhexidine has many applications in TJR, its use for per-operative skin cleansing is proven to be beneficial in decreasing the incidence of PJIs (Chlebicki et al., 2013). Also, chlorhexidine is widely used in surgical site preparation and hand antisepsis for surgeon (Sistla et al., 2010; Widmer, 2013). Chlorhexidine is used in intra-articular irrigation of infected joints (Smith et al., 2015). The concentration needed for irrigation is required to be above 2% to provide persistent decrease in biofilm. Lower concentration can decrease biofilm formation but rebound growth of biofilm occurs, but higher concentration is associated with higher cytotoxicity to fibroblasts (van Meurs et al., 2014).

#### **6.4.2 Antimicrobial efficacy**

Antimicrobial testing was done against common bacteria involved in PJIs, both in early and delayed infections (early infection starts during first 24hrs-1 week, and late infections after 1 month according to orthopaedic surgeons). (Wendling et al. 2016; Wu et al. 2016). The protocol used for antimicrobial testing (described in section 2.2.5) allows the comparison in antimicrobial activity between different bone cement formulation *in vitro* by directly incubating the release media from bone cement with tested bacteria. This gives a straightforward comparison between different types of bone cement and simulates the real scenario in the cemented prosthetic joint. Maintaining the antimicrobial properties of the bone cement in the first few weeks after surgery is important to provide prophylaxis from PJIs (Aslam and Darouiche, 2012).

Different protocols are used to evaluate the antimicrobial properties of cements in literature (*Table 19*). Rodriguez et al. (2015) evaluated the antimicrobial properties

for chlorhexidine incorporated in PMMA bone cement along with brushite calcium phosphate bone fillers, to improve the bioactivity and antimicrobial properties of acrylic bone cements. Cement samples with chlorhexidine added at 8% w/v had larger zones of inhibition than control samples when tested against *Enterococcus faecalis*. Also, bacterial proliferation assays did not show proliferation, as depicted by the flat-lined growth curve plot for 18 hr after incubation. Zhao et al. (2011) tested the antimicrobial activity of chlorhexidine released from bone adhesives consisting of fluid photo-polymerizable (lactide-co-propylene glycol-co-lactide) dimethacrylate loaded at 10 % w/w. The agar diffusion assay against bacterial strains of *S. aureus* and *MRSA* showed larger zones of inhibition compared to control samples. Also, chlorhexidine released from the polymer and composites in the first 24 hours could effectively inhibit the growth of tested stains. (Yan et al., 2017) used an MTT assay method to evaluate the inhibition of bacterial growth (*S. mutans* UA159) on the surface of a glass ionomer cement, which was loaded with chlorhexidine encapsulated mesoporous silica nanoparticles at different concentrations (1%, 5%, and 10% (w/w)). The mean reduction of relative biofilm viability for three tested concentrations were 97.81% and 98.56% on day-1 and day-30 compared to the control cement without chlorhexidine.

In this work, the antimicrobial activity of different cement formulations was linked to the chlorhexidine release profile, hence, once the release stopped the growth of bacteria was observed. Also, the same observation applied to inhibition of bacterial growth in the gentamicin loaded bone cements in chapter 5. However, *Acinetobacter baumannii* and *Pseudomonas aeruginosa* showed less vulnerability to released gentamicin, as in the case of Cemex NPs, which is linked to their high MIC. The antimicrobial activity of Cemex NPs continued for up to 27 days, which is a promising for providing prophylaxis from PJIs. For other types of bone cement, the antimicrobial activity of cements continued even after chlorhexidine release reached a plateau, may be because still there was a small amount of chlorhexidine leaching out of the cement which is enough for inhibiting the growth of bacteria for an extra few days. The short inhibition duration for chlorhexidine powder containing bone cements, is in accordance with the reported drop in the concentration of antibiotics below inhibitory levels in the first few days in

commercial antibiotic loaded cements (Anagnostakos et al., 2009; Hsieh et al., 2009).

### **6.4.3 Surface and material properties of bone cement**

#### **6.4.3.1 Settling time for bone cement**

The settling time is important for bone cement use during application and after patient recovery, because it determines the time needed to develop the final mechanical properties of the cement. Therefore, the introduction of nanoparticles into the cement formulation must not have great change to the settling time for the commonly used commercial cements. In this work, the settling time of Cemex-NP bone cement did not alter the settling time for the gentamicin powder containing cement, which was proved by rheological testing. The profiles detected for  $G'$  and  $G''$  were comparable to those presented by others for PMMA bone cements (Farrar and Rose, 2001; Pemi et al., 2015).

The rheological behaviour of acrylic bone cements is very important for their mixing/handling and viscoelastic properties during the curing phase. Their behaviour has a significant influence on the cement porosity, degree of bone penetration and strength of the prosthesis/cement interface (Rodrigues et al., 2009). In the case of bone cement, the cement rheologic behaviour changes from being mainly liquid-like immediately after mixing, to being predominantly solid-like properties after setting. Therefore, it is useful to characterise curing of bone cement as viscoelastic materials, where the application of oscillatory shear plays an important role, where  $G'$  (storage modulus) corresponds to the elastic behaviour of the material and  $G''$  (loss modulus) corresponds to the viscous behaviour (Khaled et al., 2011). The initial increase in viscosity is due to the swelling and dissolution of PMMA in liquid monomer, while the final rapid increase in viscosity is due to polymer formation (Farrar and Rose, 2001). The dough time and setting time are described in ISO standard for characterising the handling properties of bone cement. Dough time is defined as the time after mixing of the components at which a freshly exposed cement surface fails to adhere to a powder-free latex glove. The setting time is defined as the time when the temperature of the cement reaches halfway between ambient and the peak exothermic temperature (‘‘ISO

5833:2002," 2002). However, using the viscoelastic parameters such as  $G'$  and  $G''$  provide a better description for the behaviour of the cement and a better measure of handling and setting characteristics (Farrar and Rose, 2001).

#### **6.4.3.2 Mechanical testing**

Incorporating antibiotics in the bone cement compromises the mechanical properties, hence only less than 3% of antibiotics are usually added (Engesaeter et al., 2006; Parvizi et al., 2008). The amount of chlorhexidine added was optimised after finding that increasing the concentration beyond 3% w/w does not have a significant increase in the release profile, or improved the antimicrobial performance. The compressive strength, bending strength, bending modulus and fracture toughness were tested according the relevant standards. The acceptable ranges for the mechanical properties of a set bone cement are  $> 70$  MPa compressive strength,  $> 1800$  MPa bending modulus and  $>50$  MPa bending strength (Lee, 2005). The compressive strength for different types of bone cements was determined according to the ISO standard 5833:2002.

Its commonly reported in literature that the incorporation of chlorhexidine in cements decreases the compressive strength (Holt et al., 2007; Rodriguez et al., 2015). Holt et al. (2007) studied the effect of adding chlorhexidine at 2% w/w concentration on the compressive strength of mineral trioxide aggregate cement used as root-end filling material. The cement samples were testing by an Instron testing machine for compression to fracture after 72 hours curing time. The values recorded showed that samples with chlorhexidine had always significantly lower compressive strength and higher variability (3.25 MPa compared to 38.46 MPa for control). (Takahashi et al., 2006) evaluated the effect of adding chlorhexidine in glass ionomer dental cement used for restorative treatment after the removal of carious lesions. A significant decrease in the compressive strength were observed with increasing the concentration of chlorhexidine above 2% w/w, this decrease is also accompanied by an increase in cement setting time.

(Rodriguez et al., 2015) measured the compressive strength for chlorhexidine loaded acrylic bone cement. The addition of reagent grade chlorhexidine significantly lowered the compressive strength with increasing concentration 2, 4, and 8 % in comparison with the control cement by more than 50%. However, the

addition of chlorhexidine diacetate compressive strength was similar to the control and maintained the mechanical properties compared to control.

In this work, the addition of chlorhexidine powder decreased the compressive strength of the Cemex cement but not Palacos, because the concentration in the former is 3% compared to 1% in the later. The noticeable decrease in the bone cement in Cemex is consistent with literature reporting increasing levels of chlorhexidine in dental and bone cements (Holt et al., 2007; Rodriguez et al., 2015). However, the addition of nanoparticle loaded chlorhexidine did not decrease the compressive strength of the cement when compared to the powder mixed cement and the commercial gentamicin loaded cement (Cemex-Genta) in chapter 5. The same trend was also observed when comparing the compressive strength between gentamicin and chlorhexidine loaded nanoparticles on Cemex. The addition of chlorhexidine in the powder form is detrimental to the mechanical properties of the cement, while the nanoparticles loaded chlorhexidine preserves the cement mechanical properties. The morphology of fractured surfaces of ALBCs revealed cluster of antibiotic powder agglomerations, which may act as crack propagation points that weakens the cement mantle and decrease the mechanical properties (Dunne et al., 2008). Also, chlorhexidine is known to interfere with the free radical polymerization reaction of PMMA due to chlorhexidine free radical quenching effect (Rodriguez et al., 2015), the presence of nanoparticle seems to provide better mixing and less agglomeration inside the cement mantle, which can preserve the mechanical properties of the cement, as seen in nanoparticle distribution fluorescence images *Figure 63*. The bending strength and modulus for Cemex-Genta and Cemex-NPs comply with the requirements for set and cured cement in the ISO 5833:2002 Implants for surgery – Acrylic resin cements (bending strength > 50 MPa and bending modulus > 1800 MPa).

#### **6.4.3.3 Water uptake**

Aging of the bone cement in simulated physiologic conditions causes a decrease in the mechanical properties of the bone cement, because of the plasticising effect of water uptake by decreasing the attraction between polymer chains and

increasing flexibility (Arnold and Venditti, 2001). Although the current commercially available bone cements must have enough mechanical properties and pass standards in dry conditions, these properties can change overtime *in vivo*. In addition, the presence of other factors such as high temperatures and stresses also affect the mechanical properties over a long period. (Bettencourt et al., 2004) investigated the hydrolysis of PMMA ester groups in biological fluids, which can be due to the change in the composition of the cement and surface wettability. Water uptake not only affects the mechanical properties of the bone cement, but it was also found to affect the surface properties and structure of the cement leading to a decrease in its molecular weight over long periods of time (Hughes et al., 2003). Thus, an initial determination of the water uptake behaviour is necessary to estimate the change in the physicochemical properties of the bone cement.

In this work, the presence of NPs did not affect the water uptake behaviour of the commercial bone cements. The weight of cement samples stopped increasing after 4-5 days, which also explain the similarity in the compressive strength tested after 3 months. These findings suggest that the presence of NPs, instead of chlorhexidine powder, did not change the diffusion of water nor the compressive strength compared to the commercial product, however long-term exposure of the cement to physiological fluids play an important role in changing its overall performance.

#### **6.4.4 Cytocompatibility testing**

Chlorhexidine is rapid acting and widely used antiseptic that is well tolerated and available in different formulations and concentrations (Milestone et al., 2008; Oosterwaal et al., 1989), as a skin and mucus membrane antiseptic exhibiting activity against a broad spectrum of organisms (Mangram et al., 1999). Chlorhexidine gluconate is used in formulations such as wipes, cloths, scrubs and solutions in concentrations that range between (0.5%-4%), as single agent or in combination with alcohol (Conroy et al., 1999; Edmiston et al., 2008). It is bacteriostatic at low concentrations (0.0002% to 0.5%) and is bactericidal at much higher concentrations (>0.5%) (Milestone et al., 2008; Oosterwaal et al., 1989). Chlorhexidine has many applications in TJR as pre-operative skin cleansing,

surgical site preparation, surgent team hand antisepsis and intra-articular irrigation of infected joints (Azzam et al., 2010; Garibaldi, 1988; Widmer, 2013).

The rapid antimicrobial activity of chlorhexidine persists for up 48 hours of contact with skin (Hibbard, 2005), which make it an ideal antiseptic for pre-operative skin preparation (Garibaldi, 1988). Chlorhexidine shower before surgery are performed to decrease the skin microbial load before replacement. Also, cloths impregnated with chlorhexidine are available commercially for patients to use before TJR, and advocated because of ease of use and better patient compliance and achieving higher concentrations of chlorhexidine on skin (Edmiston et al., 2008). In addition, chlorhexidine is commonly used to remove transient pathogenic skin flora present at the time of incision (Mangram et al., 1999).

In this work, the use of chlorhexidine in bone cement showed less cell viability to control, which is consistent with previous work on osteoblast cells (Faria et al., 2009; Giannelli et al., 2008; Mariotti and Rumpf, 1999). However, the cell viability is generally higher (>60%, Figure 64 and Figure 65) than what have been previously reported. Regardless of chlorhexidine cytotoxicity and safety issues, it is still commonly used in peri-implant infections dental application and TJRs with many applications before operation as antiseptic shower, cloth and even during surgery as irrigation solution at bactericidal concentration. Despite the fact that the lack of evidence about the safety of antimicrobial agents used in irrigation solutions including chlorhexidine, they are routinely used in the irrigation of infected joints due their perceived benefits (Tejwani and Immerman, 2008).

Antiseptic irrigation is an important step in revision surgery involving debridement of infected joints (Odum et al., 2011). Chlorhexidine antiseptic solution is among many other solutions used that are commonly used for irrigation such as normal saline, castile soap, bacitracin solution, betadine and hypochlorite (Conroy et al., 1999; Owens et al., 2009). Most surgeons use a combination of irrigation solutions for the management of PJIs (Azzam et al., 2010). The optimal concentration of chlorhexidine gluconate is 2 % in irrigation solutions, to provide sufficient decrease in biofilm formation on orthopaedic implants (Smith et al., 2015). Lower concentrations can decrease biofilm growth but can cause rebound growth of biofilm and likely to cause regrowth in *in vivo* models. However, further research

is necessary to establish the safety and effectiveness of chlorhexidine containing irrigation solutions.

Chlorhexidine solution is shown to be cytotoxic to human osteoblasts, fibroblasts and lymphocytes in dose and time dependent manner (Faria et al., 2009; Giannelli et al., 2008; Mariotti and Rumpf, 1999). Chlorhexidine can be cytotoxic to human fibroblasts at low concentrations as 0.02% (van Meurs et al., 2014). Extensive chondrolysis was reported in accidental irrigation of 1% chlorhexidine solution during knee arthroscopy in a case series of five patients (Douw et al., 1998). In an *in vitro* study, low concentrations of chlorhexidine didn't affect cellular proliferation significantly, however, reduced collagen and non-collagen protein production of human gingival fibroblasts (Mariotti and Rumpf, 1999). In another study, chlorhexidine at a concentration of 0.2 % was cytotoxic to Saos-2 cell and human gingival fibroblasts (John et al., 2014). In a study on primary human osteoblast cells, chlorhexidine gluconate chip (2.5 mg) (releasing at concentration of 0.5 %) caused a 51% cell viability compared to control (Almazin et al., 2009). Also, chlorhexidine showed cytotoxic effect on human osteoblastic cell line U2OS cells, where the inhibition concentration of chlorhexidine was approximately 0.005%. The effect of chlorhexidine inhibition of cell proliferation is considered dose dependant, i.e. depends on the exposure dose, frequency and duration. Concentrations higher than 5% was found to inhibit cell proliferation, 0.01% almost completely inhibit DNA synthesis. Chlorhexidine inhibited collagen synthesis of at concentrations >3%, and at 2% decreased about 50% collagen synthesis (Lee et al., 2010). In this work, the concentrations of chlorhexidine released in day 1 is 200-600 µg/ml (0.2-0.6 w/v %) for different nanocomposites.

## 6.5 Conclusion

The chlorhexidine loaded LbL coated silica nanoparticles have been successfully incorporated into bone cement commercial formulation Cemex®, without adversely affecting the mechanical performance. The novel LbL coated silica NPs provided a controlled, gradual and prolonged release of chlorhexidine for up to 30 days. The NP containing bone cement showed superior antimicrobial activity against different bacterial stains. Cytocompatibility testing showed an expected decrease in cell viability for the nanocomposite with osteoblasts. In conclusion, the application of LbL nano-delivery systems may play a vital role in improving the release of antibiotics and other therapeutic agents from the bone cement, which is needed to reduce infection rates after TJRs. Also, it offers an alternative approach for loading non-antibiotic based antimicrobial into bone cement without compromising other properties needed for performance.

## **7 Gentamicin and chlorhexidine nanoparticle containing bone cement**

### **7.1 Introduction**

The emergence of resistant bacterial pathogenic strains has become a significant global health threat (Medernach and Logan, 2018). Rising antibiotic resistance is threatening the vast medical advancements over the decades made by using antibiotics to treat infections. The lack of innovative approaches for the treatment of antibiotic drug resistant bacteria is severely affecting many fields in medicine, including surgery, cancer chemotherapy, sepsis etc (Meer et al., 2016). Also, adding to this problem complexity is the lack of investment in antibiotic drug discovery by pharmaceutical companies because of low return rate compared to chronic diseases drug targets. The development of new classes for this problem is slow, as few classes have been added introduced over the last two decades. Furthermore, significant resistance can develop in a period of months to years after the introduction of new antibiotic for clinical use (Walsh, 2000). For example, after the introduction of daptomycin for clinical use in 2003, resistance in patients was observed with *Enterococcus faecium* and MRSA infections within less than year. Consequently, finding alternative approaches to controlling bacterial infections is solely needed (Dolgin, 2010).

One of the approaches for the treatment of antibiotic resistant strains is the use drug combinations to effectively eradicate the multi drug resistant phenotypes (Markley et al., 2015). This approach includes antibiotic-antibiotic combinations to either directly target resistant mechanisms or to provide more than mode of action by targeting different sites in bacterial cell (Tamma et al., 2012). Combination antibiotic therapy provide many advantages as compared to monotherapy such as a broader antibacterial spectrum, synergistic effects and minimizes the risk for emerging resistance during therapy (Markley et al., 2015). Also, combinations are increasingly used to improve the efficacy of available drugs against multidrug resistant strains (Dolgin, 2010). However, the use of combination antimicrobial therapy is associated with increased risk of side effects i.e. ototoxicity and nephrotoxicity, especially when taken systemically (Prayle et al., 2010). Therefore, it is been recommended to use a the most selective single

agent as soon as the antibiotic susceptibility profile of the causative agent is known, or using a local delivery whenever possible to reduce drugs concentration in the systemic circulation and their consequent side effects (Jackson et al., 2011).

Many causative organisms in prosthetic infections have been reported to be resistant to certain antibiotics, e.g. nearly 50% of *Staphylococci* involved PJIs are now resistant to gentamicin (Staats et al., 2017). *Staphylococcus aureus* have been implicated in up to 55% of PJIs, but other stains can also be found e.g. *Propionibacterium* species. Polymicrobial infections have been increasingly detected with complex microbiological treatment and poor clinical outcome (Helbig et al., 2018). Therefore, this emerging resistance increased interest in using PMMA bone cements with combination antimicrobial agents, such as gentamicin, vancomycin and cefuroxime.

In this chapter, chlorhexidine and gentamicin LbL loaded silica nanoparticles (NPs) were developed, and were incorporated in PMMA bone cements to create a novel nanocomposite combination antimicrobial bone cement. The chlorhexidine and gentamicin loaded NPs were encapsulated into the PMMA bone cement (Cemex®) and characterised for drug release, its antimicrobial activity, cytocompatibility, water uptake and mechanical properties. The aim of this work is to achieve a prolonged chlorhexidine release for several weeks (4-6 weeks) with an initial burst of gentamicin loaded on top of nanoparticles, to provide prophylaxis and treatment from postsurgical PJIs.

## **7.2 Materials and methods**

### **7.2.1 Chemicals**

Triton X-100, Tetraethyl orthosilicate (TEOS), (3-Aminopropyl) triethoxysilane (APTS), sodium alginate, chitosan, chlorhexidine diacetate, sodium acetate trihydrate, phosphate buffer solution (PBS) tablets, o-phthaldialdehyde reagent were purchased from Sigma-Aldrich, UK.

Cyclohexane, 1-hexanol, ammonium hydroxide 35%, acetonitrile, ethanol, methanol, glacial acetic acid and 1-propanol were purchased from Fishers, UK. All reagents were stored according to manufacturer's guidelines and used as received. The bone cement was used is Cemex® (Tecres® S.p.A., Italy).

B1: is a patented biocompatible, biodegradable cationic polymer, the precise structure will remain confidential due to the IP associated.

### **7.2.2 Nanoparticle preparation**

#### **7.2.2.1 Amino functionalised silica nanoparticles synthesis**

Silica nanoparticles functionalised with amine groups ( $\text{SiO}_2\text{-NH}_2$ ) were prepared in one-pot synthesis by hydrolysis of TEOS in reverse micro-emulsion and subsequent functionalization with amino group (Stöber et al. 1968), as described in section 2.1.2.1.

#### **7.2.2.2 Layer by Layer (LbL) coating technique**

The silica nanoparticles were layered with ten quadruple layers of a repeating sequence of (sodium alginate/chlorhexidine or gentamicin/sodium alginate/ B1). The following concentrations of polyelectrolytes and drug in acetic acid-sodium acetate buffer were used in LbL: sodium alginate (2 mg/ml), chlorhexidine or gentamicin (10 mg/ml) and B1 (2 mg/ml). The nanoparticles were coated by the same procedure described in section 2.1.2.2. The following chlorhexidine and gentamicin layer combination were built (Table 22):

- **9:1** nanoparticles, which is 9 quadruple layers containing chlorhexidine and the 10<sup>th</sup> outermost layer containing gentamicin.

- **8:2**, which is 8 quadruple layers containing chlorhexidine and 9<sup>th</sup> and 10<sup>th</sup> top layers containing gentamicin.
- **7:3** nanoparticles, which is 7 quadruple layers containing chlorhexidine and 8<sup>th</sup>, 9<sup>th</sup> and 10<sup>th</sup> outermost layers containing gentamicin.

Quadruple layer no.	Antimicrobial agent added in each quadruple layer on the surface of amino functionalised silica nanoparticles (SiNH <sub>2</sub> )		
	<b>7:3</b>	<b>8:2</b>	<b>9:1</b>
1	chlorhexidine	chlorhexidine	chlorhexidine
2	chlorhexidine	chlorhexidine	chlorhexidine
3	chlorhexidine	chlorhexidine	chlorhexidine
4	chlorhexidine	chlorhexidine	chlorhexidine
5	chlorhexidine	chlorhexidine	chlorhexidine
6	chlorhexidine	chlorhexidine	chlorhexidine
7	chlorhexidine	chlorhexidine	chlorhexidine
8	<b>gentamicin</b>	chlorhexidine	chlorhexidine
9	<b>gentamicin</b>	<b>gentamicin</b>	chlorhexidine
10	<b>gentamicin</b>	<b>gentamicin</b>	<b>gentamicin</b>

*Table 22: The antimicrobial agent added in each quadruple layer (alginate-chlorhexidine or gentamicin-alginate-B1) to give three coating combinations 9:1, 8:2 and 7:3 nanoparticles.*

### 7.2.3 TGA

Thermogravimetric analysis was performed for different types of nanoparticles as described in section 2.1.3.3 to study the build-up of LbL coatings and percentage of organic matter on the surface of the nanoparticles.

#### **7.2.4 Bone cement preparation**

Bone cement preparation was carried out according to manufacturer's instructions and the ISO5833:2002 (Implants for surgery-Acrylic resin cements) and as described in section 2.2.2.

#### **7.2.5 Rheology testing**

The storage ( $G'$ ) modulus and ( $G''$ ) loss modulus were recorded to study the effect of adding the nanoparticles on the cement settling time, as described in section 2.2.3.

#### **7.2.6 Bone cement drug release quantification**

The different types of nanoparticles (7:3, 8:2 and 9:1) were added to Cemex® bone cement at the same concentration (9 %) which is equivalent to 3 % of chlorhexidine powder, Table 23 shows the compositions of all cements tested. Calculations for the nanoparticle containing bone cements were based on the loading efficiency (30% w/w) prepared in chapter 4, to have equal amounts of antimicrobial agents (chlorhexidine and gentamicin) between powder and nanoparticle containing bone cement.

	Cemex – 7:3 NPs	Cemex -8:2 NPs	Cemex-9:1 NPs
<b>Liquid component / g</b>	13.30	13.30	13.30
Methyl Methacrylate / % w/w	98.20	98.20	98.20
N-N Dimethyl-p-Toluidine / % w/w	1.80	1.80	1.80
Hydroquinone / ppm	75.00	75.00	75.00
<b>Powder Component / g</b>	40.00	40.00	40.00
Polymethyl Methacrylate / % w/w	82.78	82.78	82.78
Barium Sulphate / % w/w	10.00	10.00	10.00
Benzoyl Peroxide / % w/w	3.00	3.00	3.00
Zirconia / % w/w	-	-	-
combination NPs	9	9	9
<b>Powder: Liquid ratio</b>	3.01	3.01	3.01

*Table 23: Composition of chlorhexidine and gentamicin containing bone cements.*

A PTFE mould was used to produce cylindrical samples with 6mm diameter and 10 mm length. Each sample weighed  $0.40 \pm 0.01$ g and three samples were used for release study from each type of bone cement. The bone cement samples were

incubated in 3 ml PBS buffer (pH 7) at 37°C. The release media was replaced each day in order to attain sink condition, where the concentration of released chlorhexidine and gentamicin is negligible in comparison to its' saturation solubility. The release samples were stored in the refrigerator (2-8 °C) for analysis. The concentrations of chlorhexidine and gentamicin were determined in the samples as described previously in sections 2.1.4 and 2.1.5.

### **7.2.7 Antimicrobial testing**

Antimicrobial testing was done for NPs containing bone cement (Cemex with 7:3, 8:2 and 9:1 NPs) listed in Table 23, using the protocol described in section 2.2.5. Different stains were tested including catalogue and clinical strains. The catalogue strains are Gram-positive bacteria methicillin-resistant *Staphylococcus aureus* (NCTC 12493), *Streptococcus pyogenes* (ATCC 19615), and *Staphylococcus epidermidis* (ATCC 12228) along with Gram-negative bacterium *Acinetobacter baumannii* (NCIMB 9214), *Pseudomonas aeruginosa* (NCIMB 10548), *Escherichia coli* (NCTC 10418). The clinical strains tested (12 clinical strains) were obtained from Bristol hospital patients with PJI in the period 2013-2015 and species were confirmed by polymerase chain reaction. The patients were anonymised by giving a code for each selected strain. These clinical strains are: *E. coli* 59293, *Enterococcus faecalis* 58181, MRSA 23140, MRSA 38924, MRSA 59275, *A. baumannii* 44646, *A. baumannii* 44640, *A. baumannii* 44643, *S. epidermidis* 59272, *S. epidermidis* 53222, *S. epidermidis* 59199.

### **7.2.8 Mechanical testing**

Mechanical testing was performed as described in section 2.2.6 for different bone cements (Cemex with 7:3, 8:2 and 9:1 NPs). Compressive strength testing was performed at 0 and 3 months' time. Also, bending and fracture toughness testing were performed.

### **7.2.9 Water uptake testing**

Bone cement nanocomposites (Cemex with 7:3, 8:2 and 9:1 NPs) were incubated in 3 ml PBS at 37°C for 3 months; for the first 2 weeks, the samples were weighed daily; after that the samples were weighed every 3 days (Perni et al., 2015), as described in section 2.2.7 and 2.2.7. Water uptake was calculated by dividing the increase in sample weight at different time points by the initial sample weight at time zero, and plotted as a percentage. Water uptake studies give an insight about the cement behaviour after being wetted in solution to simulate the *in-vivo* conditions inside the joint with the synovial fluid.

### **7.2.10 Nanoparticles distribution in bone cement**

The distribution of nanoparticles in cement nanocomposites (Cemex with 7:3, 8:2 and 9:1 NPs) was studied by fluorescence imaging using fluorescent nanoparticles as described in section 2.2.9.

### **7.2.11 Cytotoxicity testing**

#### **7.2.11.1 MTT**

MTT test was done for (Cemex with 7:3, 8:2 and 9:1 NPs) bone cements for days 1,2,4 and 7 using the protocol described in 2.2.8.1.

#### **7.2.11.2 LDH**

LDH assay test was done for (Cemex with 7:3, 8:2 and 9:1 NPs) bone cements for days 1,2,4 and 7 using the same protocol described in section 2.2.8.2.

#### **7.2.11.3 Calcium production assay-Alizarin red**

Alizarin red test was done for (Cemex with 7:3, 8:2 and 9:1 NPs) bone cements after 21 days with the same protocol described in section 2.2.8.3.

#### **7.2.11.4 NO**

The concentration of NO released by cells into the media was determined for Cemex with 7:3, 8:2 and 9:1 NPs for days 1,2,4 and 7 using the protocol detailed in section 2.2.8.3 and 2.2.8.4.

#### **7.2.11.5 Fluorescence images**

Fluorescence images (actin staining and live/dead) were done for (Cemex with 7:3, 8:2 and 9:1 NPs) bone cement for using the same protocol described in section 2.2.8.5.

#### **7.2.12 Statistical analysis**

All data were expressed as means  $\pm$  standard deviation (SD) from at least three independent values. To assess the statistical significance of results between groups, one-way analysis of variance (ANOVA) was performed. Experimental results were considered statistically significant at 95 % confidence level ( $p < 0.05$ ). All analyses were run using the SPSS ® software.

## 7.3 Results

### 7.3.1 Nanoparticles surface and material characterization.

TGA was performed for assessing the organic content after LbL coating for different NPs combinations (7:3, 8:2 and 9:1). TGA thermograms of silica NPs and the same NPs with different number of quadruple layers are shown in Figure 74. An initial weight loss around (5%) was observed at about 100 °C, which is normally attributed to the evaporation of adsorbed water from the samples (Wang et al., 2014). The organic content in each sample (Table 24) was calculated based on the weight loss beyond 100 °C, which truly corresponds to the combustion of organic matter (Du *et al.*, 2015). The build of organic matter with increasing number of quadruple layers is shown in Figure 75.

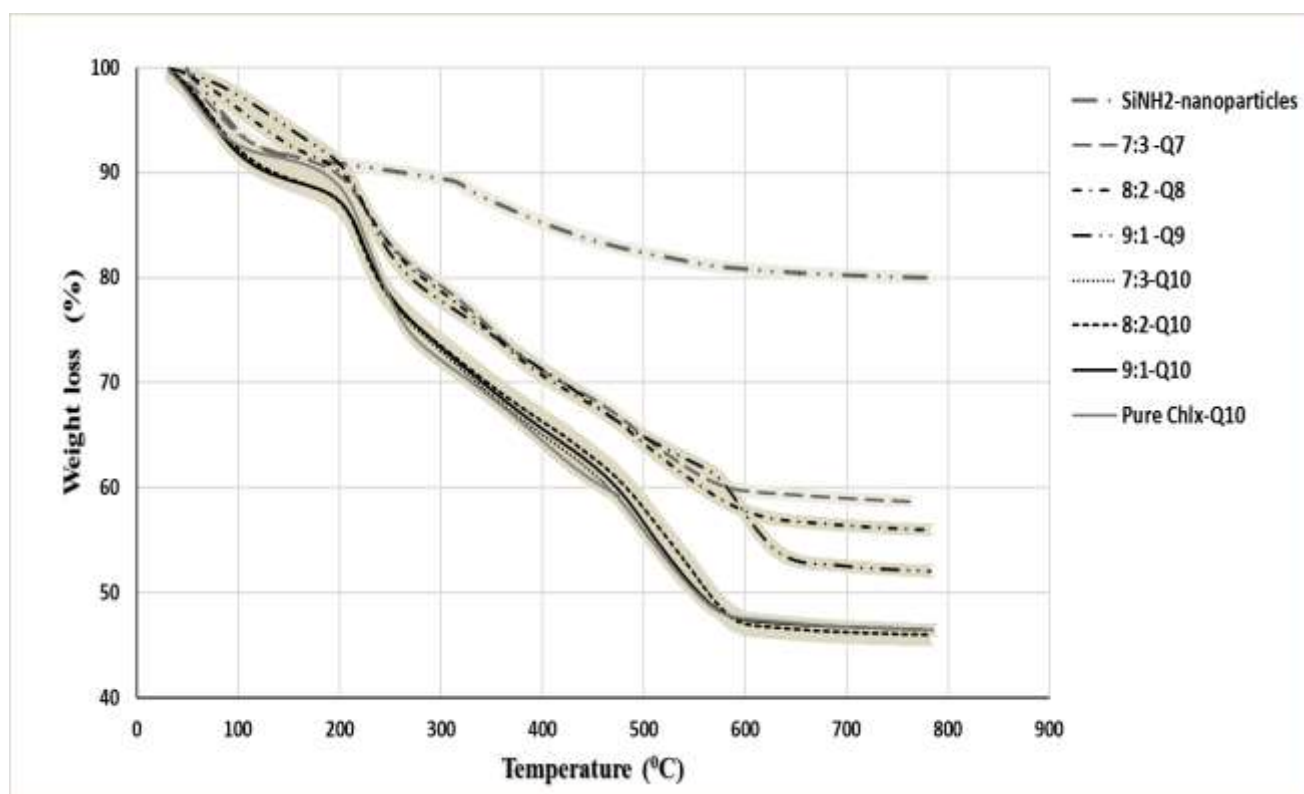


Figure 74: TGA for Silica nanoparticles, **7:3-Q7**: 7 quadruple layers of 7:3 NPs combination, **8:2-Q8**: 8 quadruple layers of 8:2 combination, **9:1-Q9**: 9 quadruple layers of 9:1 combination, **7:3-Q10**: 10 quadruple layers of 7:3 NPs combination, **8:2-Q10**: 10 quadruple layers of 8:2 combination, **9:1-Q10**: 10 quadruple layers of 9:1 combination, **Pure chlx-Q10**: 10 quadruple layers containing chlorhexidine ( $n = 3 \pm SD$ ).

Samples	Organic content (%)
SiNH <sub>2</sub> -Nanoparticles	14.95 ± 1.0
<b>7:3-Q7</b>	46.19 ± 1.46
<b>8:2-Q8</b>	48.71 ± 1.23
<b>9:1-Q9</b>	52.72 ± 1.90
<b>7:3-Q10</b>	58.49 ± 1.51
<b>8:2-Q10</b>	58.22 ± 1.77
<b>9:1-Q10</b>	58.77 ± 1.68
<b>Pure chlx-Q10</b>	58.34 ± 1.59

Table 24: Percentage of organic matter in different layers of chlorhexidine NPs and chlorhexidine gentamicin combination NPs calculated from Figure 74 ( $n = 3 \pm SD$ ).

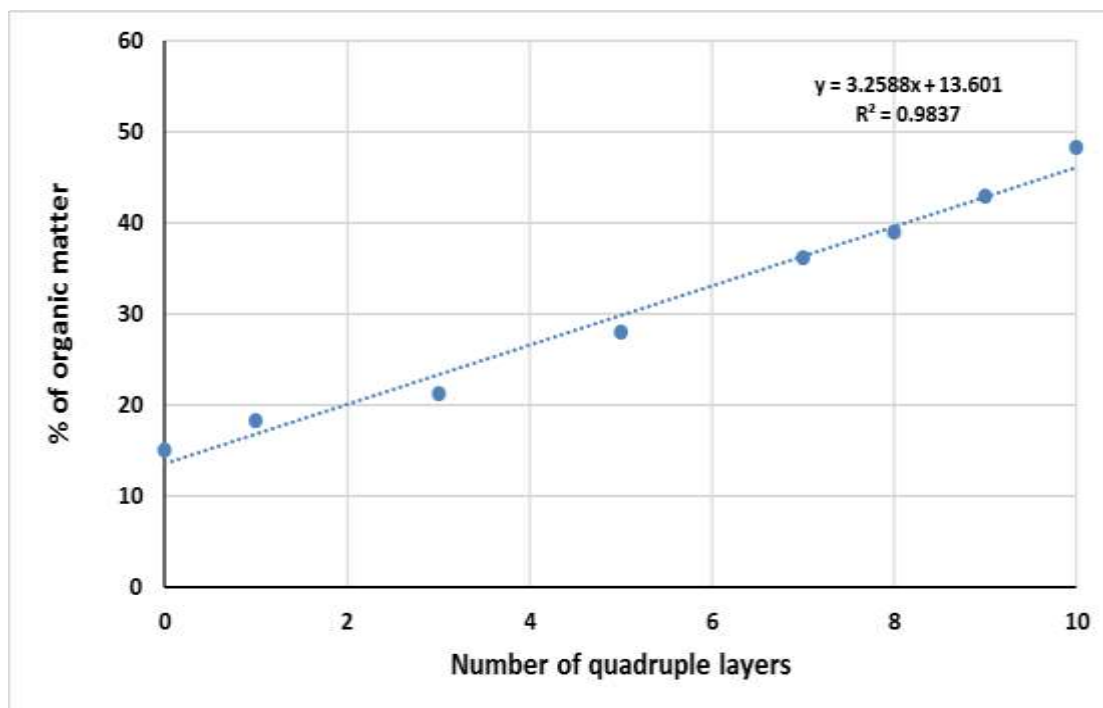


Figure 75: The build-up of organic matter with increasing number of quadruple layers.

The organic content for the amino functionalised silica NPs is 14.95%. After adding 7 quadruple layers, the organic content increased to 46.19%. Then, adding

one quadruple layer (Q8) of chlorhexidine increased the organic content to 48.71%, which makes a 2.5% increase in organic matter. Adding the ninth quadruple layer increased the organic content by 4% to reach 52.72%. Layering 10 quadruple layers on the surface of amino-functionalised silica NPs yielded similar organic content of around 58% irrespective whether the layers containing chlorhexidine or gentamicin or chlorhexidine alone (p-value >0.05). This is also confirmed by linear relationship ( $R^2=0.9837$ ) between the number of quadruple layers and the build-up of organic matter on the surface of the NPs as seen in Figure 75.

### **7.3.2 Bone cement settling time**

The possible effects of the chlorhexidine and gentamicin LbL coated nanoparticles on the kinetics of Cemex bone cement settling time was investigated (before and after adding 9:1 NPs), through the evaluation of the rheological properties of bone cement dough after mixing (Figure 76 and Figure 77). Storage modulus ( $G'$ ) was nearly the same as loss modulus ( $G''$ ) in Cemex alone cement and Cemex-9:1 NPs nanocomposite; there was an increase at fast rate at the beginning which slowed down later reaching a plateau. The presence of nanoparticles required the same settling time of 6-7 minutes (defined as the time needed for the dough to reach constant rheological properties) compared to Cemex alone cement settling time. The stored energy representing the elastic portion of the cement is measured by the storage modulus. While, the energy dissipated as heat representing the viscous portion is measured by loss modulus.

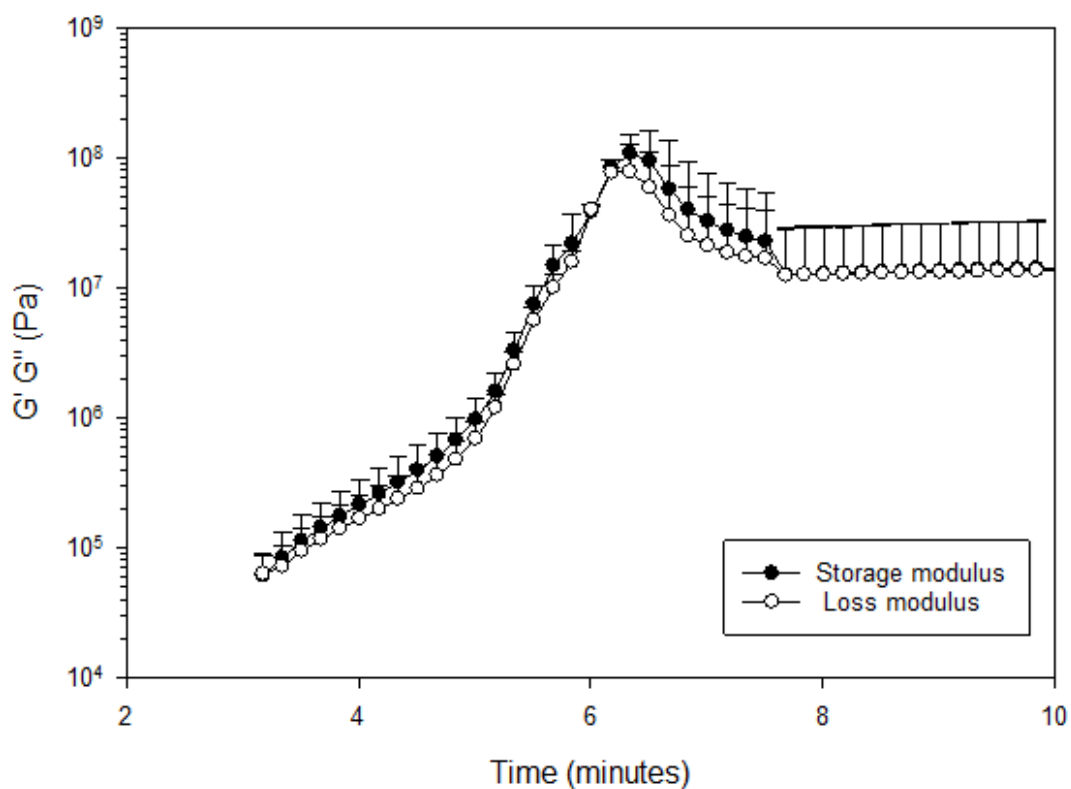


Figure 76: Storage ( $G'$ ) and loss ( $G''$ ) modulus for Cemex alone bone cement.

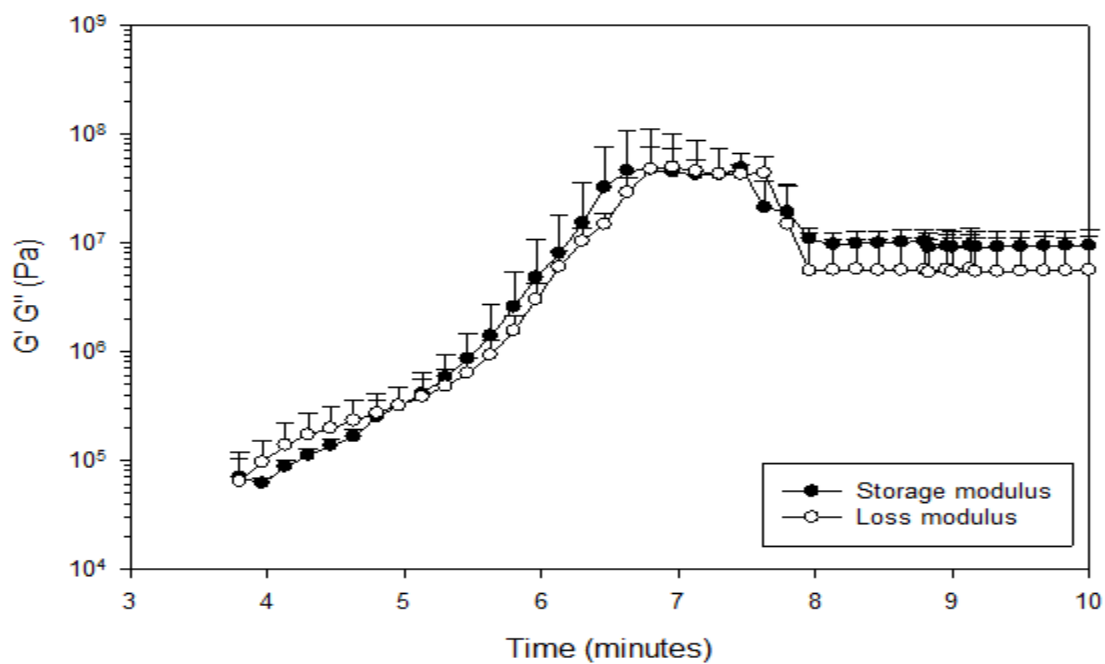


Figure 77: Storage ( $G'$ ) and loss ( $G''$ ) modulus for Cemex-9:1 NP.

### 7.3.3 Bone cement drug release profile

Chlorhexidine and gentamicin release were studied in PBS (pH 7.3), which is the pH value in healthy joints (Ribeiro et al., 2012). Gentamicin was quantified by fluorescence spectroscopy after conjugation with o-phthalaldehyde, while chlorhexidine was quantified by HPLC with UV-detection at 239 nm from the same sample, each data point is an average of three independent sample measurements. Figure 78 shows the cumulative release from Cemex bone cement containing different types of NPs (7:3, 8:2 and 9:1). Also, Figure 79 shows chlorhexidine cumulative release from Cemex bone cement containing different types of NPs (7:3, 8:2 and 9:1).

All bone cements stopped releasing chlorhexidine and gentamicin after 30 days. Regarding gentamicin release, the total cumulative concentration released was 1180  $\mu\text{g/ml}$  from Cemex-7:3, 1000  $\mu\text{g/ml}$  from Cemex-8:2, and 870  $\mu\text{g/ml}$  from Cemex-9:1. There was a proportional increase in the cumulative release for gentamicin with increasing the number of gentamicin layers, however the increase was not significantly different between release profiles ( $p\text{-value} > 0.05$ ). Regarding chlorhexidine release, the total cumulative concentration released was 1130  $\mu\text{g/ml}$  from Cemex-7:3, 1500  $\mu\text{g/ml}$  from Cemex-8:2, and 1900  $\mu\text{g/ml}$  from Cemex-9:1. The release was also proportional to the number of chlorhexidine layers; however, it was not significantly different between the release profile of different nanocomposites ( $p\text{-value} > 0.05$ ).

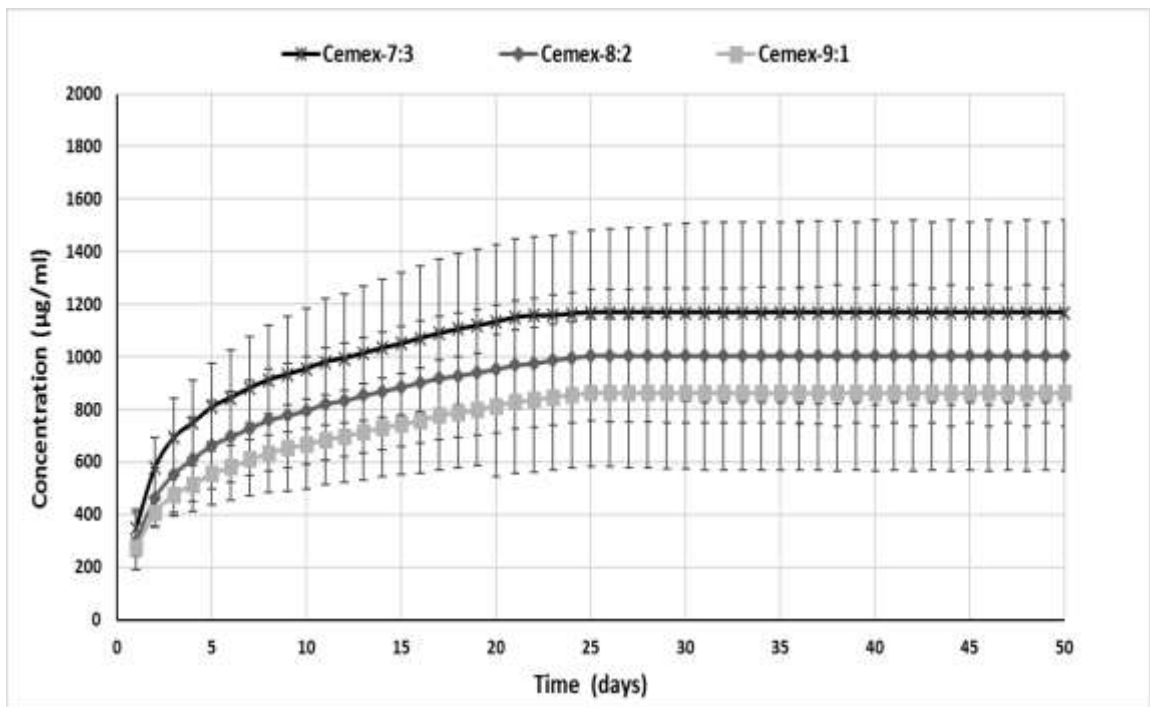


Figure 78: Gentamicin cumulative release from Cemex bone cement containing different types of NPs (7:3, 8:2 and 9:1) ( $n = 3 \pm SD$ ).

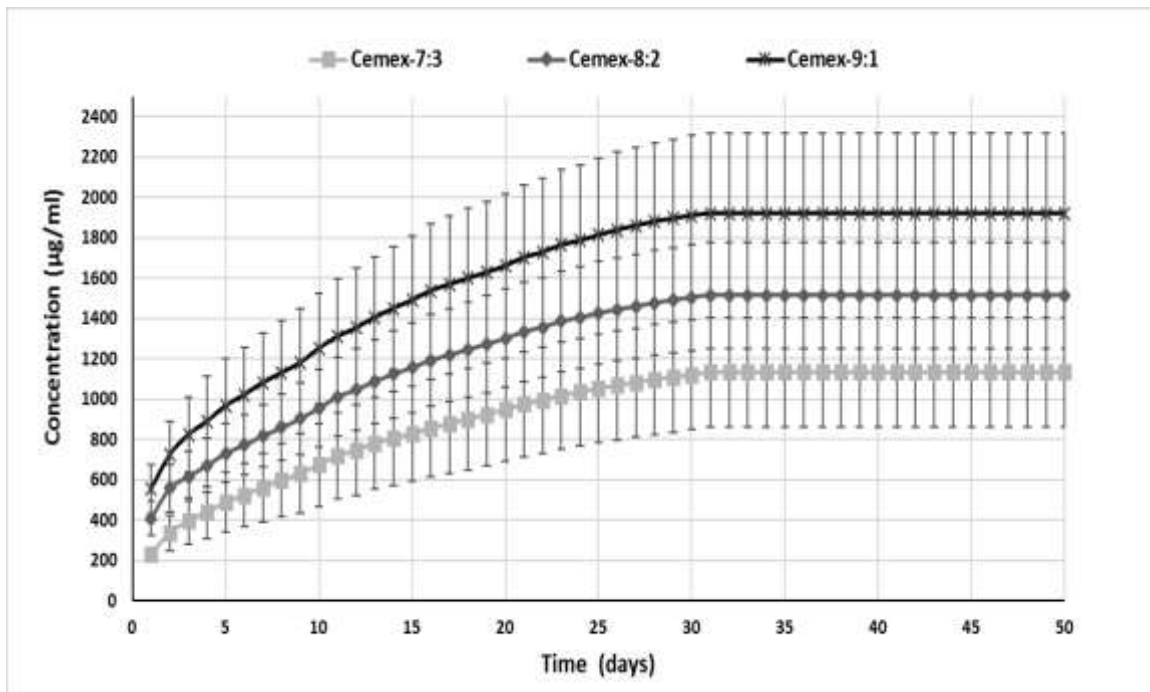


Figure 79: Chlorhexidine cumulative release from Cemex bone cement containing different types of NPs (7:3, 8:2 and 9:1) ( $n = 3 \pm SD$ ).

#### 7.3.4 Antimicrobial analysis

Antimicrobial testing was performed against different types of bacteria that are encountered in PJI for Cemex bone cement containing different types of NPs (7:3, 8:2 and 9:1). First, the antimicrobial analysis was performed using catalogue strains (Figure 80), the bacteria tested methicillin-resistant *Staphylococcus aureus* (NCTC 12493), *Streptococcus pyogenes* (ATCC 19615), *Staphylococcus epidermidis* (ATCC 12228), *Acinetobacter baumannii* (NCIMB 9214), *Pseudomonas aeruginosa* (NCIMB 10548), *Escherichia coli* (NCTC 10418). Then, antimicrobial analysis was performed using clinical patients stains resistant to gentamicin (Figure 81), These clinical strains are: *E. coli* 59293, *Enterococcus faecalis* 58181, MRSA 23140, MRSA 38924, MRSA 59275, *A. baumannii* 44646, *A. baumannii* 44640, *A. baumannii* 44643, *S. epidermidis* 59272, *S. epidermidis* 53222, *S. epidermidis* 59199.

Catalogue strains inhibition duration was similar between different types of nanocomposites (p-value>0.9) against different types of strains. The antimicrobial activity continued for up to 48 days as seen in *Streptococcus pyogenes* and *Staphylococcus epidermidis*. The antimicrobial activity lasted for 38 days for all types of nanocomposites against *Escherichia coli*, *Pseudomonas aeruginosa* and MRSA. The least antimicrobial activity was observed against *Acinetobacter baumannii* for nearly 30 days. Clinical stains resistant to gentamicin inhibition was similar between different types of nanocomposites (p-value> 0.7). The least inhibition duration was observed in *Acinetobacter baumannii* clinical strains which only lasted for less than 7 days. The antimicrobial activity against *Staphylococcus epidermidis* continued for up to 28 days. While, the antimicrobial activity continued for up to 25 days against *Escherichia coli* and MRSA, and 20 days against *Enterococcus faecalis*.

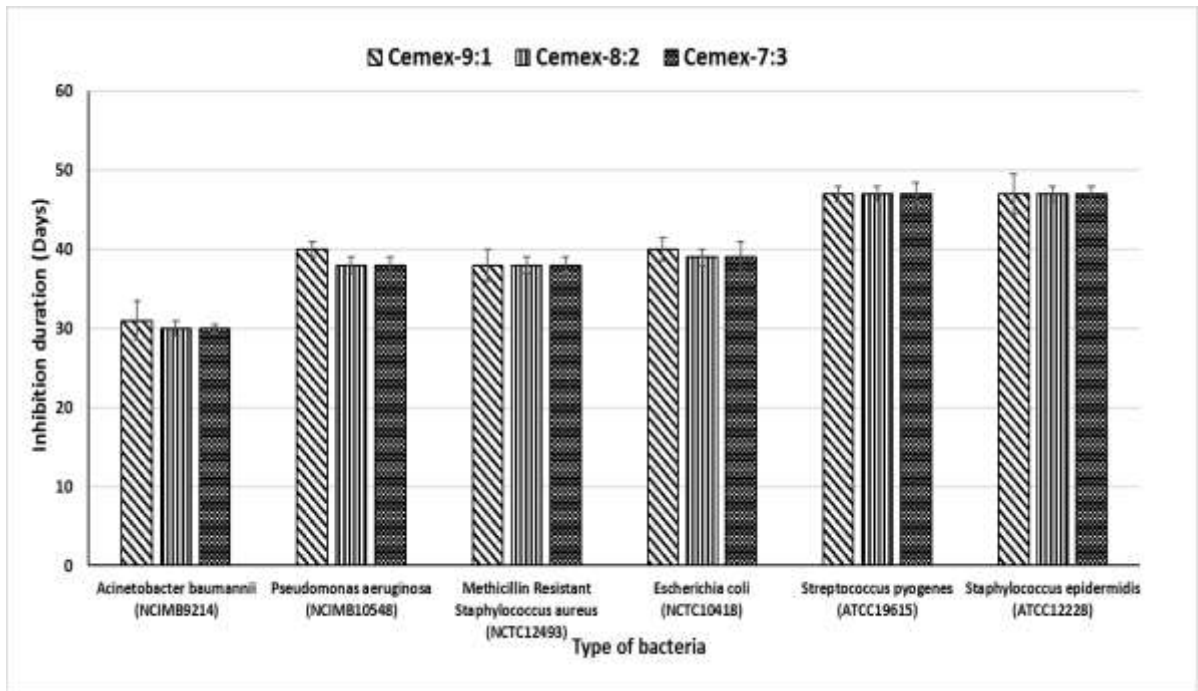


Figure 80: Antimicrobial testing of Cemex cement containing different types of NPs (7:3, 8:2 and 9:1) ( $n = 3 \pm SD$ ).

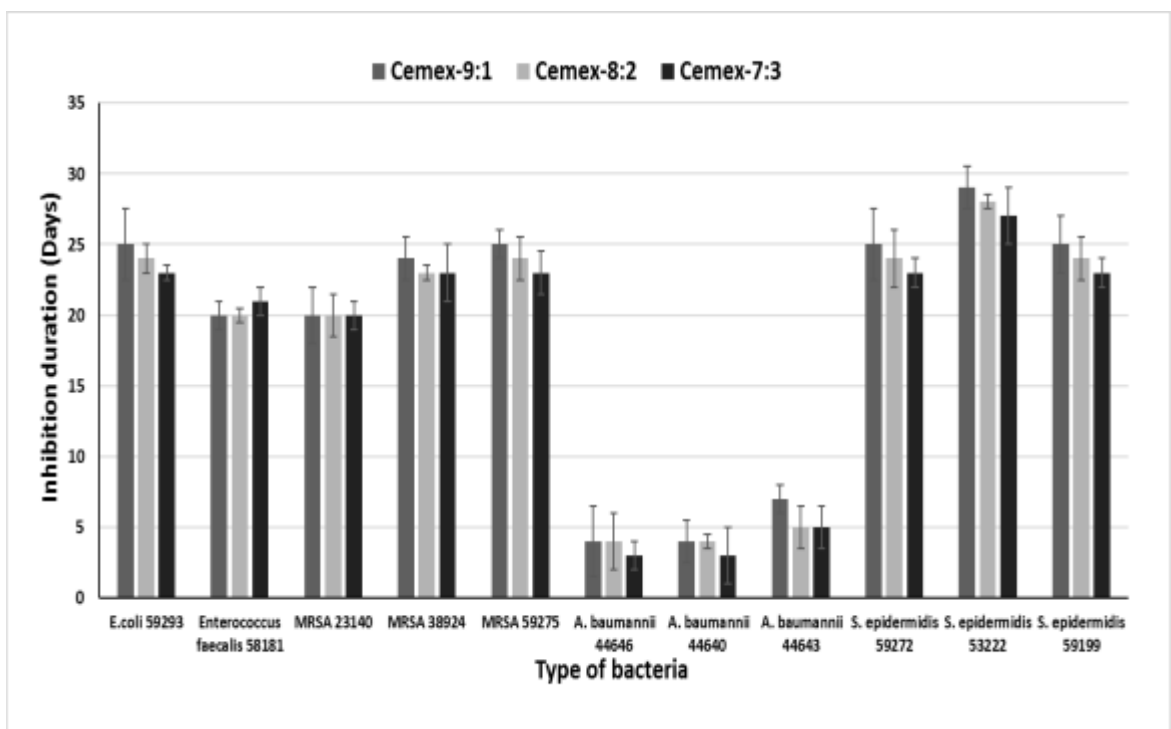


Figure 81: Antimicrobial testing against gentamicin resistant clinical strains for Cemex cement containing different types of NPs (7:3, 8:2 and 9:1) ( $n = 3 \pm SD$ ).

### 7.3.5 Mechanical testing

The compressive strength was tested for different types of nanocomposites (Cemex-7:3, 8:2 and 9:1) after 24 hours in air, and after 3 months of incubation in release media PBS, pH 7.3 at 37 °C (Figure 82) according to ISO standard 5833:2002. Cemex-9:1 had similar compressive strength at 0 and 3 months' time compared to Cemex alone cement (p-value > 0.2) which was > 80 MPa at zero time and >70 MPa after 3 months of incubation. However, Cemex-7:3 and Cemex-8:2 had significantly lower compressive strength compared to Cemex (p-value < 0.05) which was > 70 MPa for Cemex-8:2. The bending and fracture toughness test were performed for Cemex-9:1 nanocomposite and Cemex alone as a reference. There was no significant difference in bending and fracture toughness between Cemex-9:1 nanocomposite and Cemex alone (p-value > 0.25). The compressive and bending properties of the Cemex-9:1 nanocomposite meets the criteria for in the ISO standard 5833:2002 (>70 MPa compressive strength, >50MPa for bending strength).

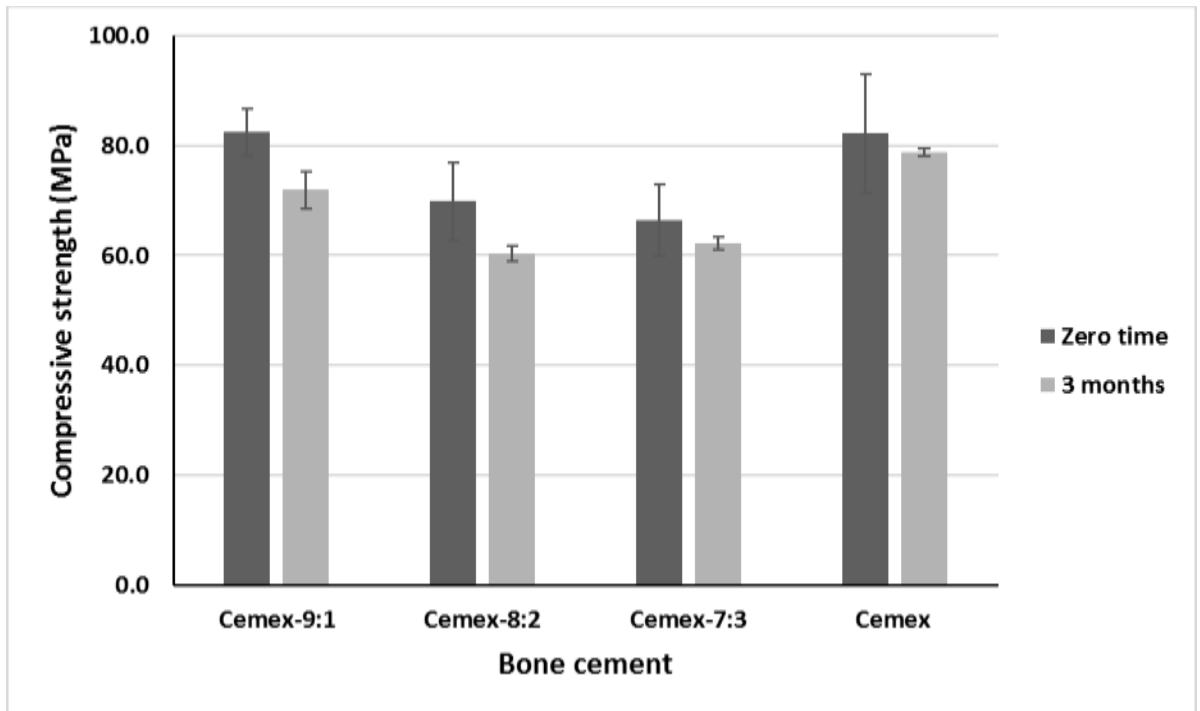


Figure 82: Compressive strength testing for Cemex alone and with different types of NPs (7:3, 8:2 and 9:1) at zero time and after 3 months of incubation on PBS at 37°C. ((n = 3 ±SD).

	Bending strength (MPa)	Bending modulus (MPa)	Fracture toughness (MPam <sup>1/2</sup> )
Cemex	54.3 ± 2.0	2901 ± 62	2.4 ± 0.5
Cemex-9:1	52.6 ± 2.0	2980 ± 150	2.5 ± 0.5

Table 25: Bending strength and modulus, and fracture toughness for Cemex and Cemex containing 9:1 NPs.

### 7.3.6 Water uptake testing

The weight of different types of nanocomposites (Cemex-7:3, 8:2 and 9:1) and Cemex was recorded after incubation in PBS buffer media pH 7.3, to study the water uptake behaviour for up to 30 days (Figure 83). The bone cement samples increased in weight during the first 7 days because of water uptake, and after that, the amount of water in the samples remained stable.

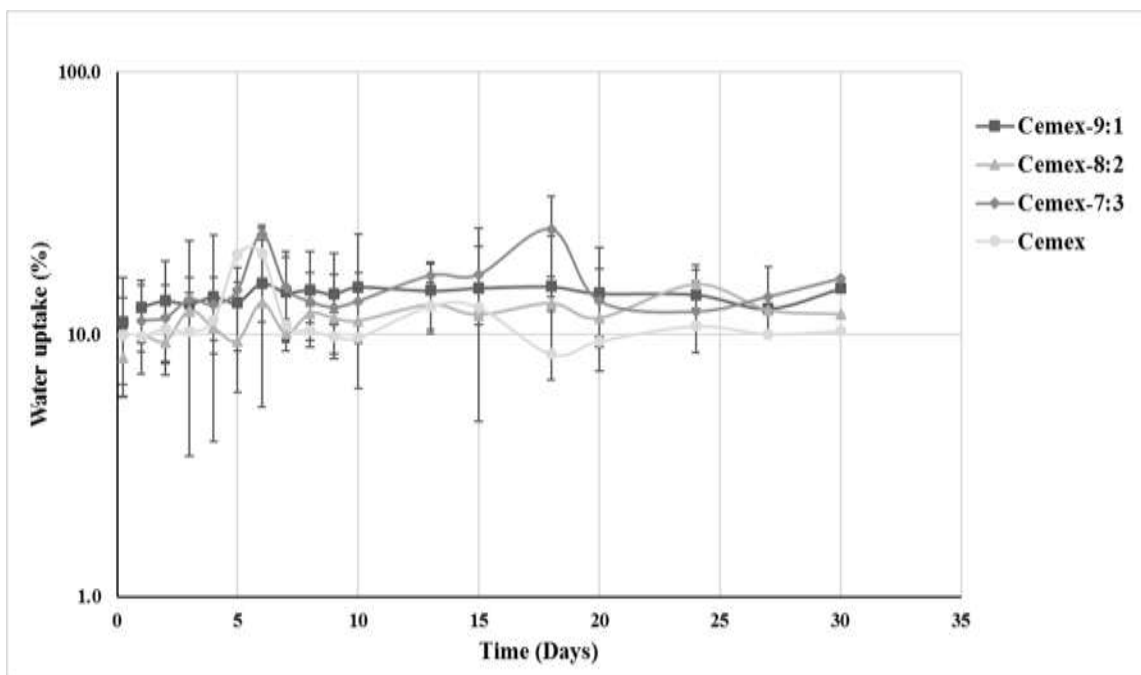
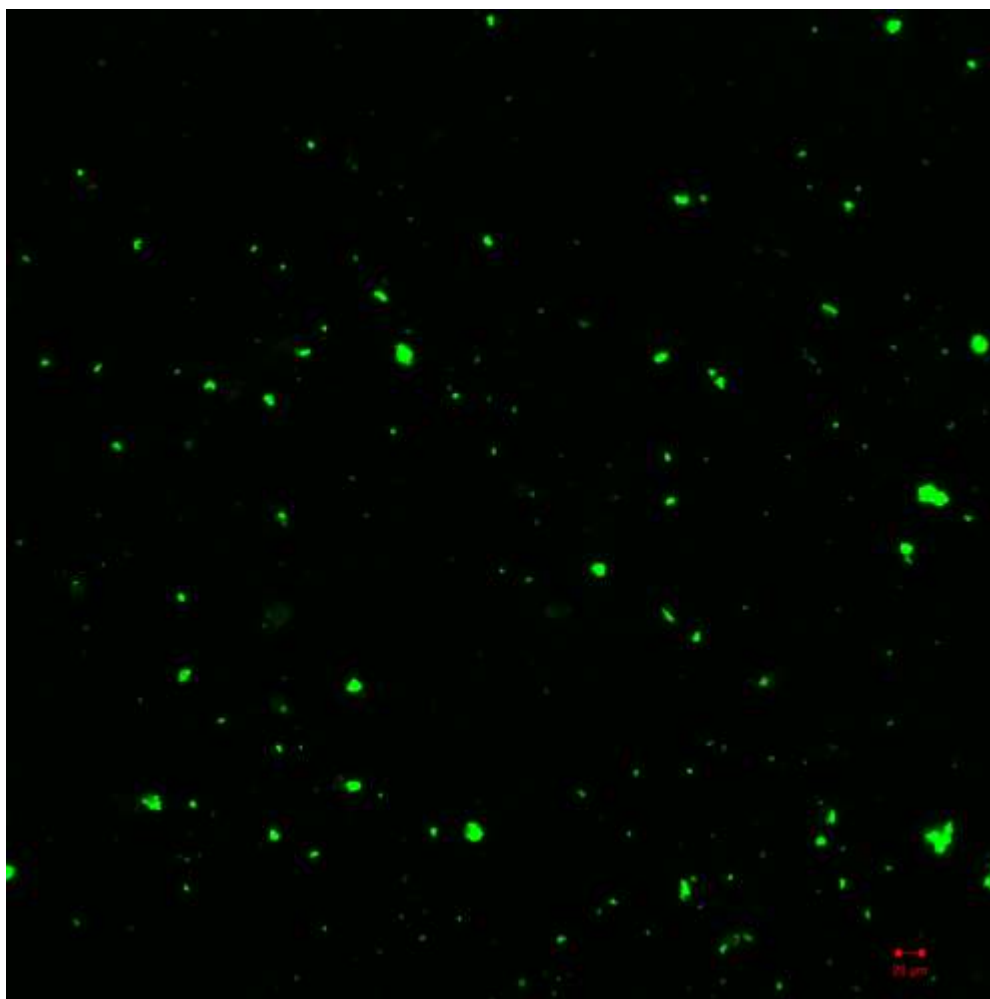


Figure 83: Water uptake study for Cemex and Cemex nanocomposite containing different types of NPs (7:3, 8:2 and 9:1) after incubation in PBS buffer, pH 7.3 ( $n=3+SD$ ).

### 7.3.7 Nanoparticles distribution in bone cement

The distribution of nanoparticles inside the bone cement was studied by fluorescence imaging of fluorescence-labelled nanoparticles incorporated into the cement. Figure 84 shows nanoparticle distribution in Cemex-9:1 nanocomposite ((9% NPs w/w). The nanoparticles appear to be homogenously distributed throughout the cement matrix with minimal agglomeration



*Figure 84: Nanoparticle distribution of Cemex-9:1 nanocomposite (9% w/w) (bar=20 $\mu$ m).*

### 7.3.8 Cytotoxicity analysis

#### 7.3.8.1 MTT

Relative to osteoblast exposed to Cemex® commercial cement (no added antibiotic), all nanocomposite cements (Cemex 9:1, 8:2 and 7:3 NP) showed similar cell viability at day 1 (p-value >0.115) (Figure 85). At day 2, the viability of cells exposed to Cemex-8:2 and 7:3 was significantly lower than Cemex alone (p-value <0.05), but Cemex-9:1 showed similar viability to Cemex commercial cement (p-value 0.683). At day 4 and 7, all nanocomposites showed similar viability to Cemex alone (p-value >0.8), which reflects cells recovering with time after initial exposure to different nanocomposites.

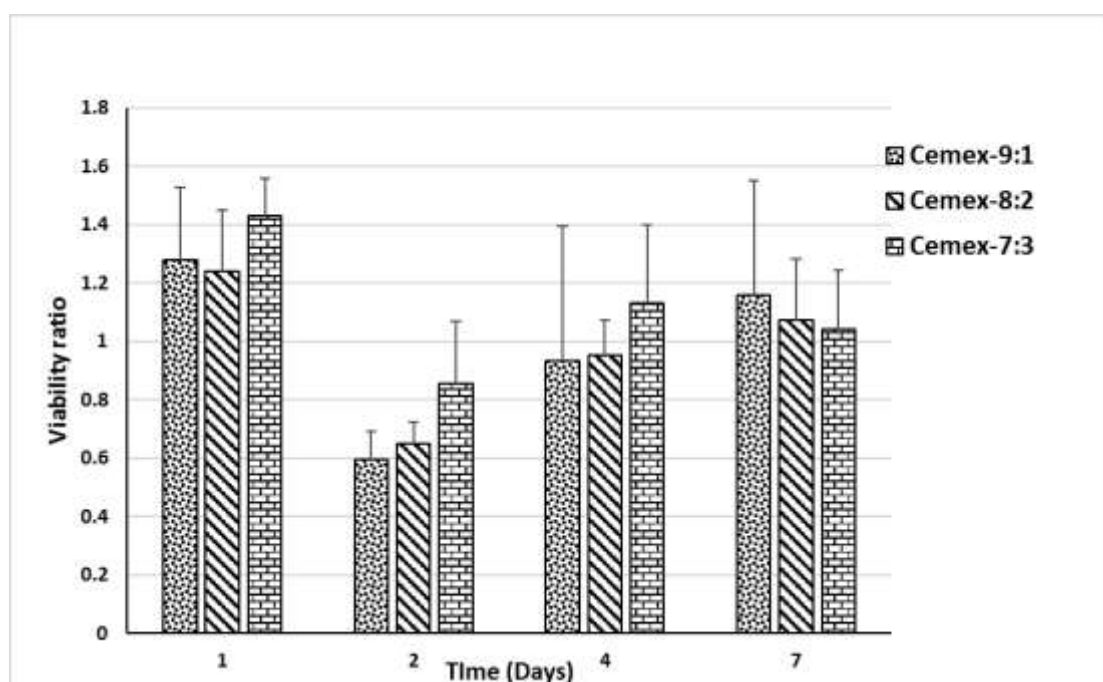


Figure 85: Viability of osteoblasts exposed to different types of bone cements: Cells control, Cemex, Cemex nanocomposite containing different NPs (7:3, 8:2 and 9:1), assessed through **MTT test** at Optical density of 570 nm presented as viability ratio (nanocomposite/Cemex) ( $n=6+SD$ ).

### **7.3.8.2 LDH**

Relative to the viability of osteoblasts exposed to Cemex® (commercial cement), the viability ratio at day 1 for all nanocomposites was around 1 which means it is similar to the Cemex alone (p-value >0.9). At day 2, cells viability for Cemex-8:2 nanocomposite (viability ratio is 0.8) was significantly lower than Cemex 9:1 and Cemex 7:3 (p-value <0.05). At day 4 and 7, all nanocomposites showed similar cell viability (p-value >0.8), which was more 0.8 viability ratio similar to Cemex commercial cement until they recovered total at day 7 reaching viability ratio around 1.

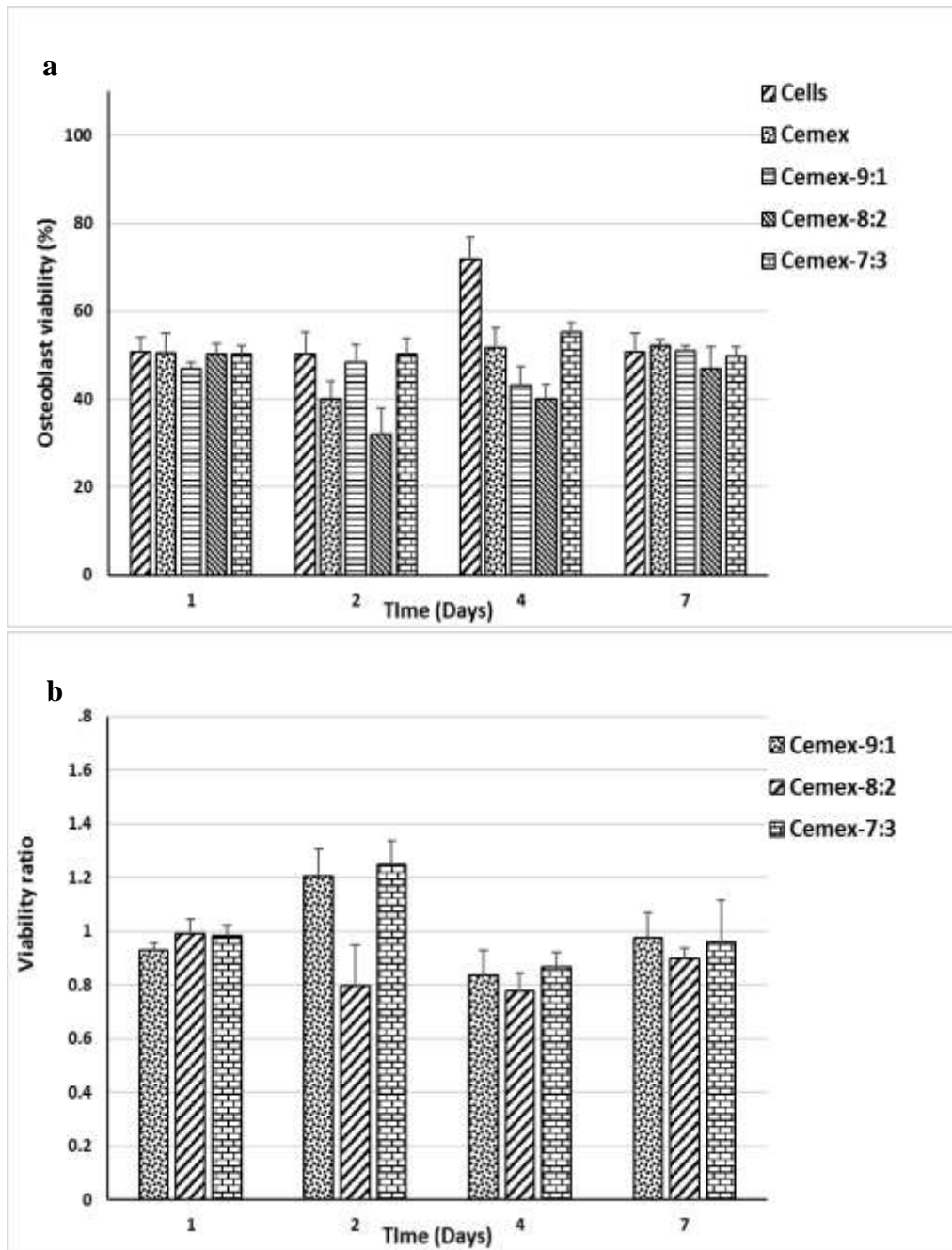


Figure 86: Viability of osteoblasts exposed to different types of bone cements: Cells control, Cemex, Cemex nanocomposite containing different NPs (7:3, 8:2 and 9:1), assessed through **LDH test**: (a) percentage viability, (b) viability ratio (nanocomposite/Cemex) ( $n=6+SD$ ).

### 7.3.8.3 NO production

In general, Cemex nanocomposites (Cemex-9:1, 8:2 and 7:3) showed higher nitrite production at different days tested, when compared to Cemex® or cells control (Figure 87) (p-value <0.05).

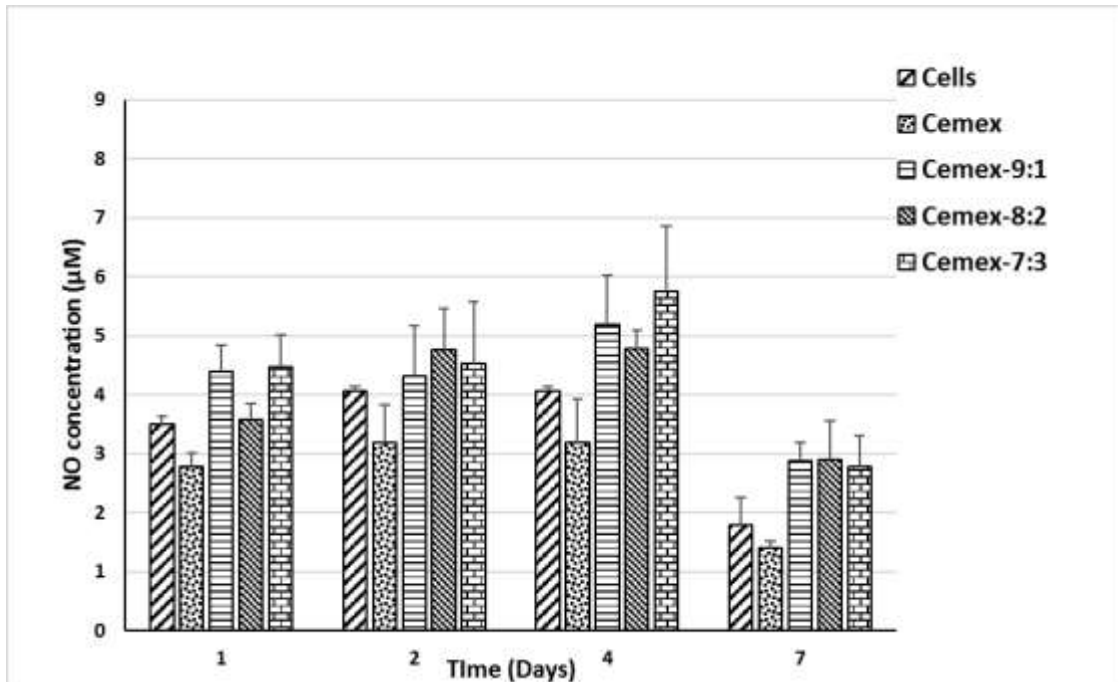


Figure 87: Nitrite production for osteoblasts exposed to different types of bone cements: Cells control, Cemex, Cemex nanocomposite containing different NPs (7:3, 8:2 and 9:1) (n=6+SD).

#### 7.3.8.4 Calcium production assay-Alizarin red

The calcium production data are shown in Figure 88, Where different Cemex nanocomposites had similar results compared to Cemex® (p-value <0.05).

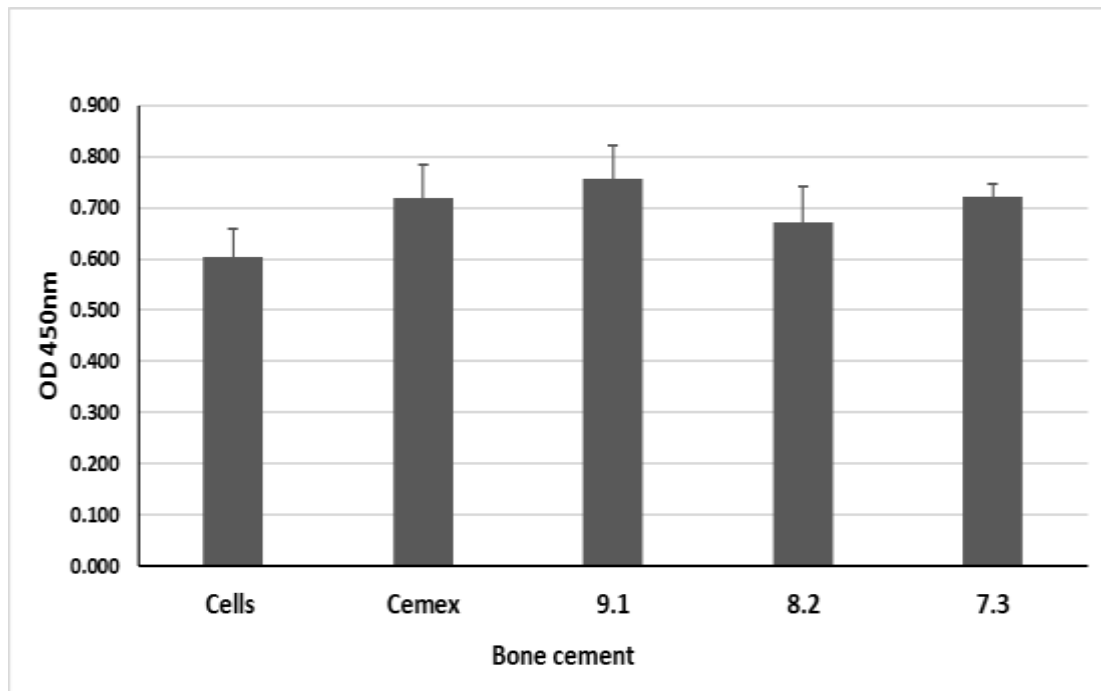
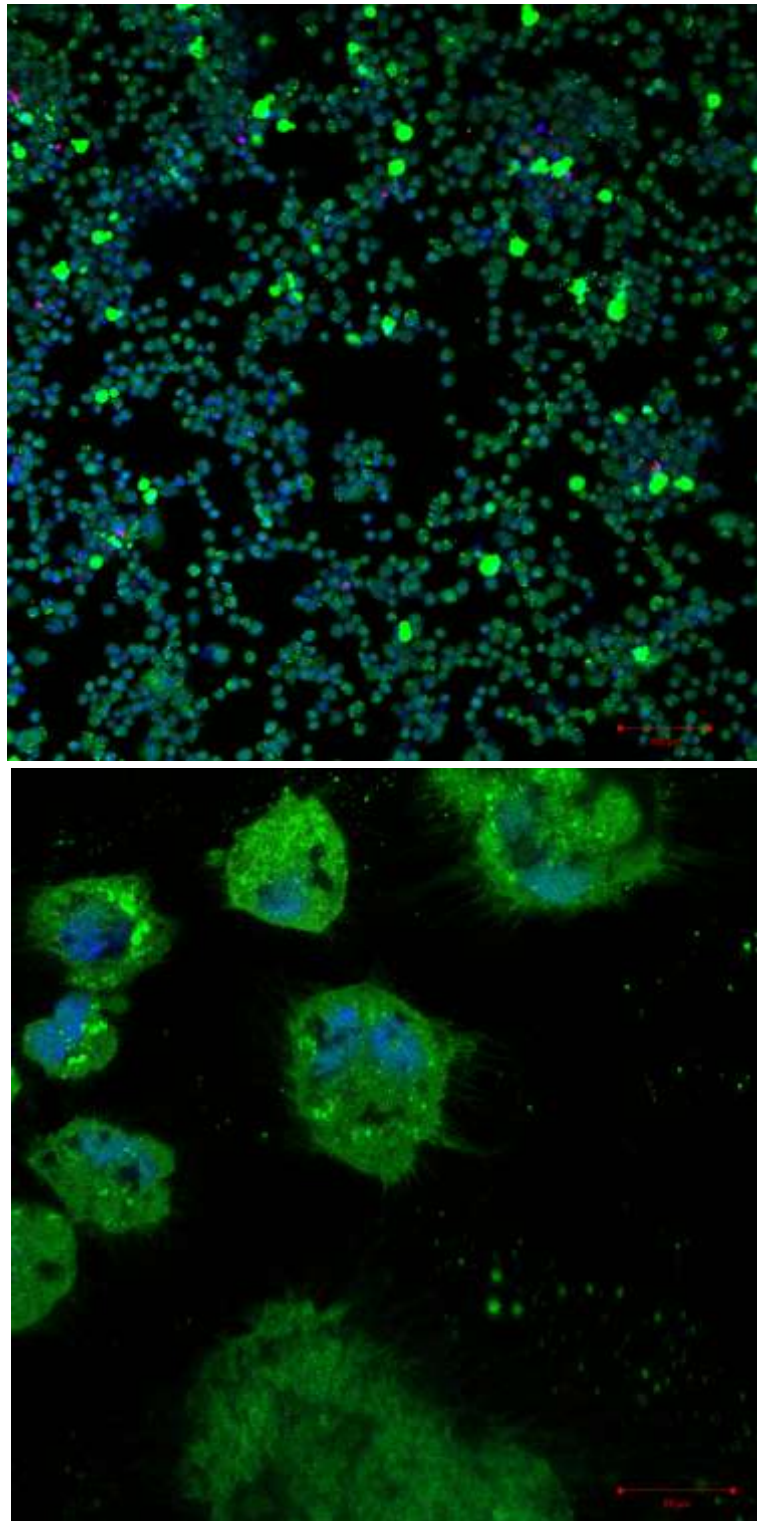


Figure 88: Alizarin red assay for osteoblasts after 21 days grown on different types of bone cements: Cells control, Cemex, Cemex nanocomposite containing different NPs (7:3, 8:2 and 9:1) (n=6+SD).

#### **7.3.8.5 Fluorescence images**

Live and dead fluorescent images for Cemex-7:3 (Figure 89), Cemex-8:2 (Figure 90) and Cemex-9:1 (Figure 91) nanocomposites show the live cells (green colour), dead cells (red colour) and cells nuclei (blue colour). Also, actin/dapi fluorescent images for Cemex-7:3 (Figure 92), Cemex-8:2 (Figure 93) and Cemex-9:1 (Figure 94) show actin filaments (red colour) and cell nuclei (blue colour). Live/dead images showed minimum dead cells (red colour) which was masked by the most abundant live cells (green colour) for all nanocomposites. Actin/dapi cell images showed cells filament spreading and developed for cells cytoskeleton which is similar to Cemex images in previous chapter (Figure 71).



*Figure 89: Live/dead images for Cemex-7:3 nanocomposite with two different scales. (Top: 100  $\mu\text{m}$  bar, bottom: 20  $\mu\text{m}$  bar).*

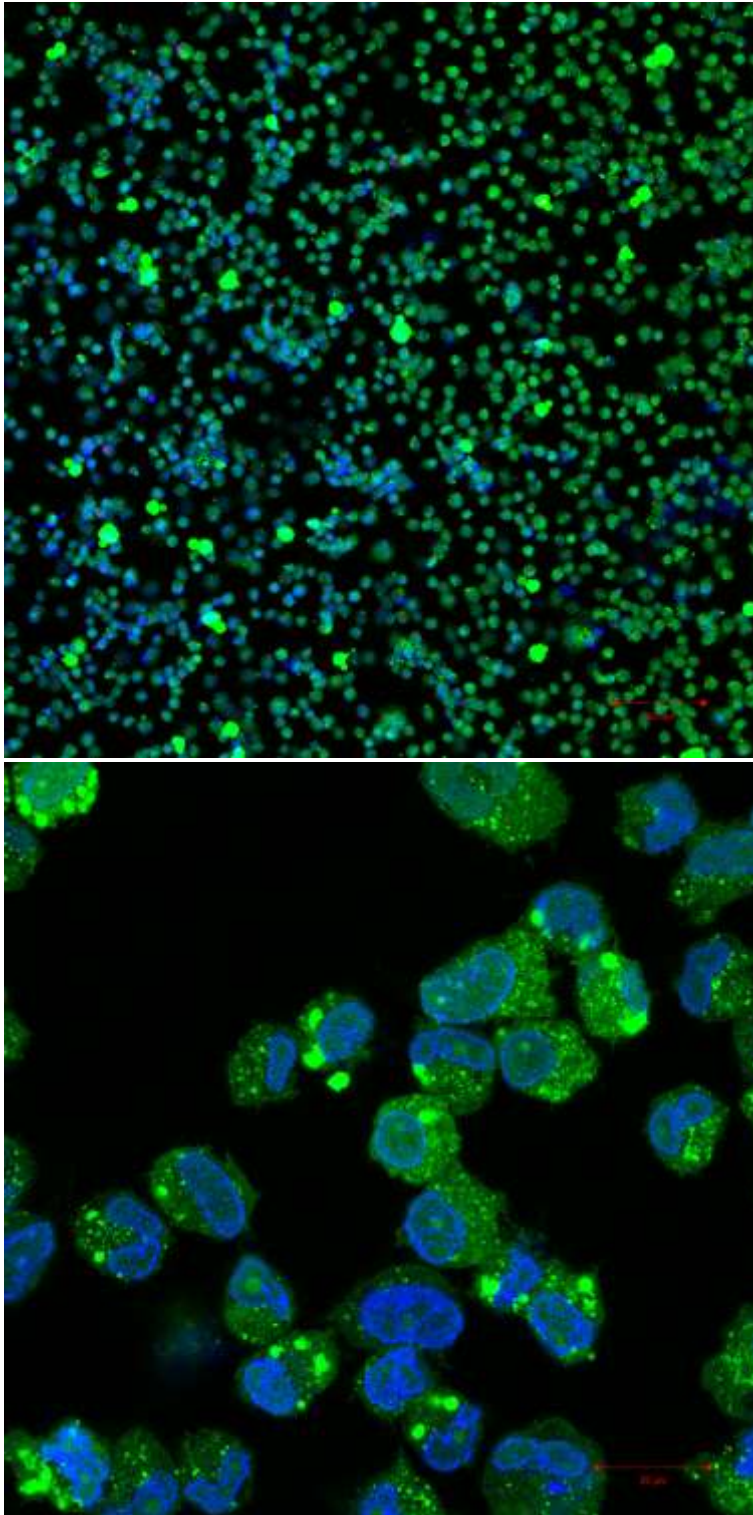


*Figure 90: Live/dead images for Cemex-8:2 nanocomposite with two different scales. (Top: 100  $\mu\text{m}$  bar, bottom: 20  $\mu\text{m}$  bar).*

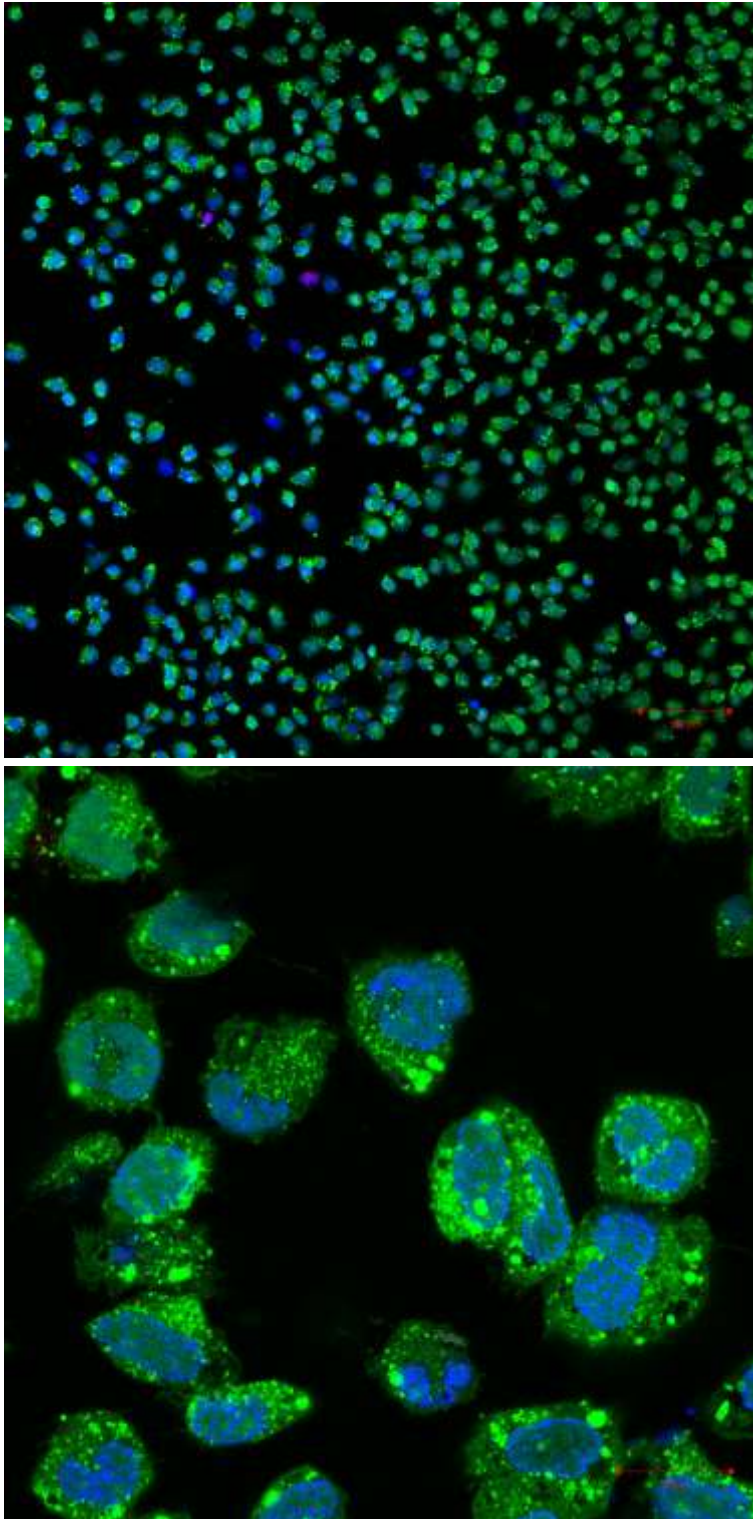


*Figure 91: Live/dead images for Cemex-9:1 nanocomposite with two different scales. (Top: 100  $\mu\text{m}$  bar, bottom: 20  $\mu\text{m}$  bar).*

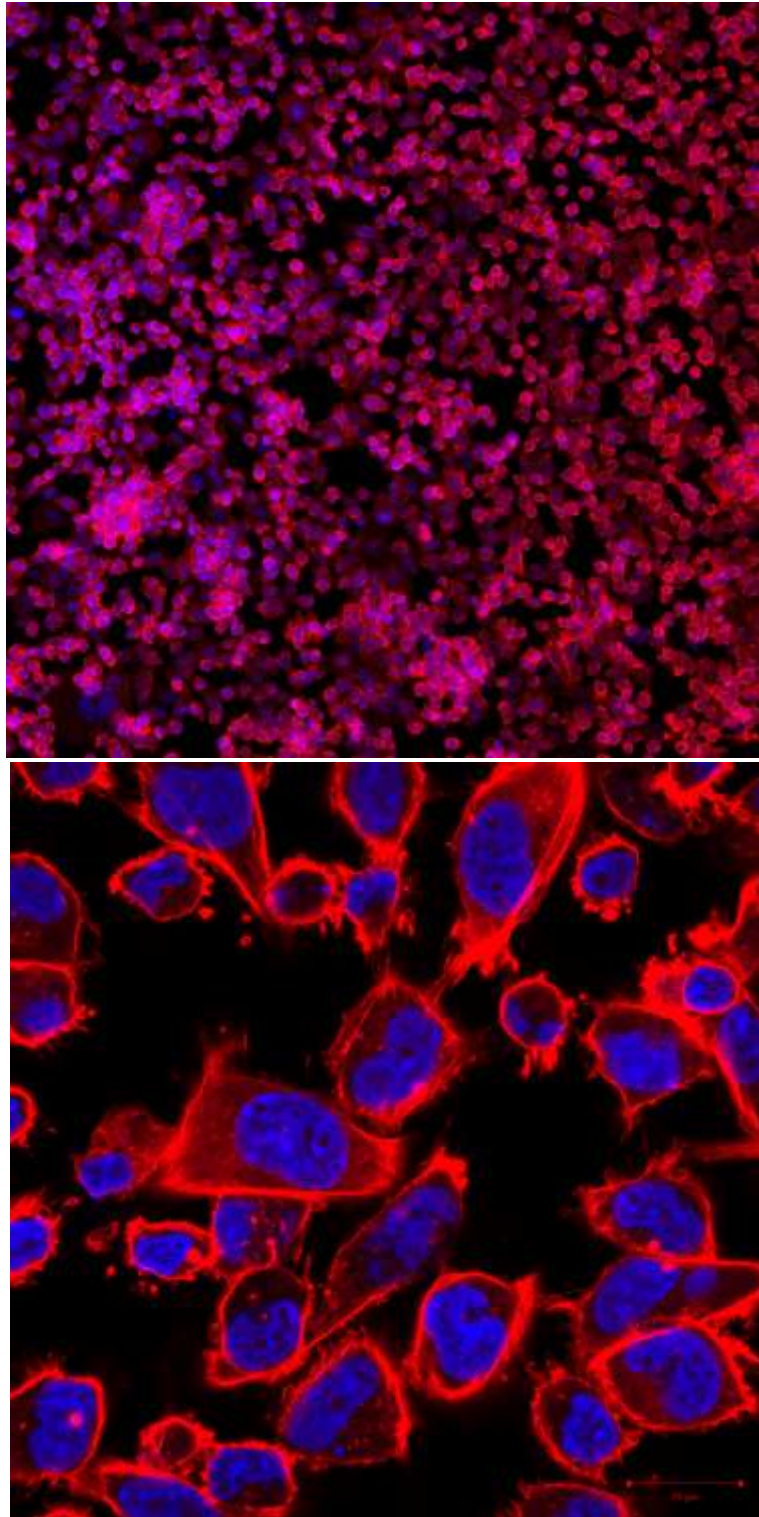


*Figure 92: Actin/dapi images for Cemex-7:3 nanocomposite with two different scales. (Top: 100  $\mu\text{m}$  bar, bottom: 20  $\mu\text{m}$  bar).*

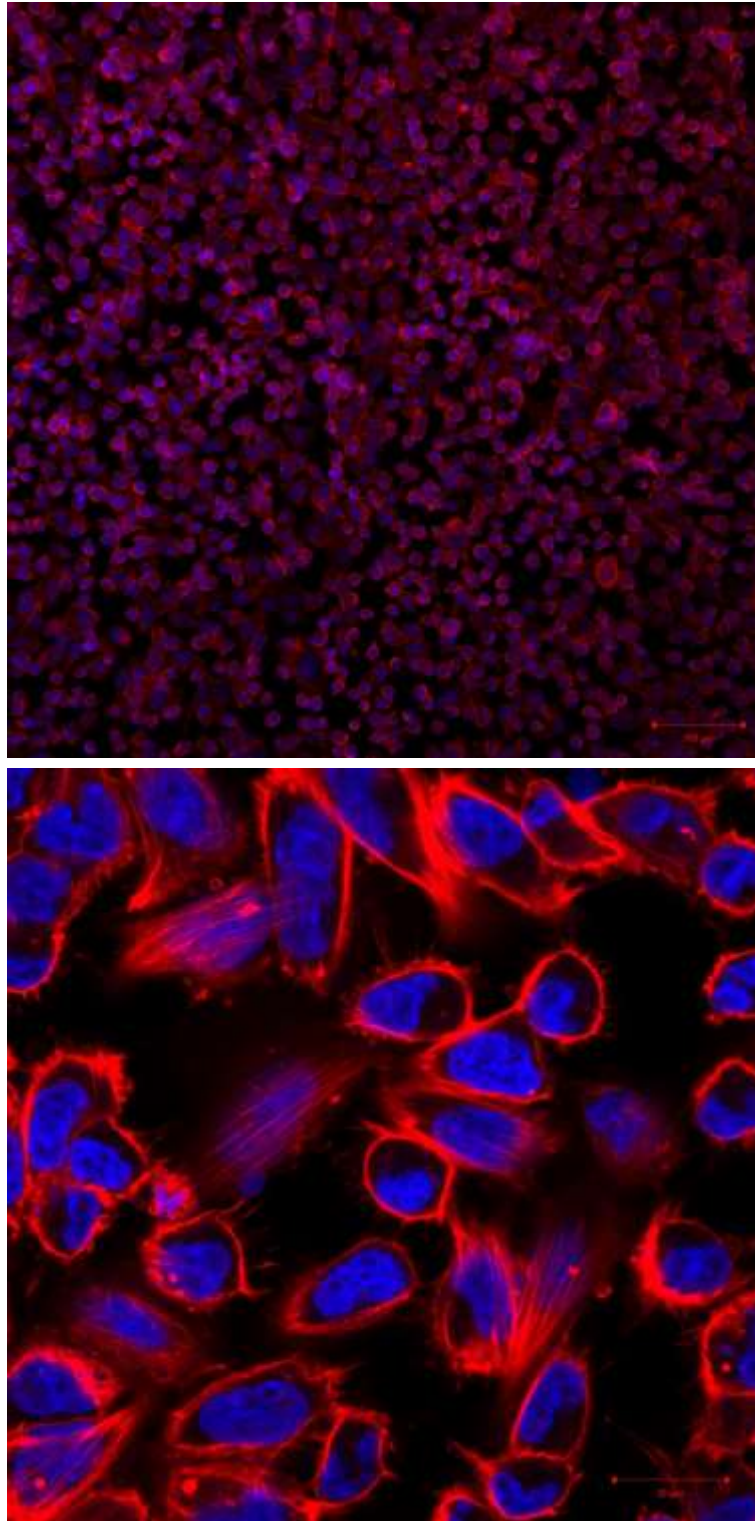


*Figure 93: Actin/dapi images for Cemex-8:2 nanocomposite with two different scales. (Top: 100  $\mu$ m bar, bottom: 20  $\mu$ m bar).*

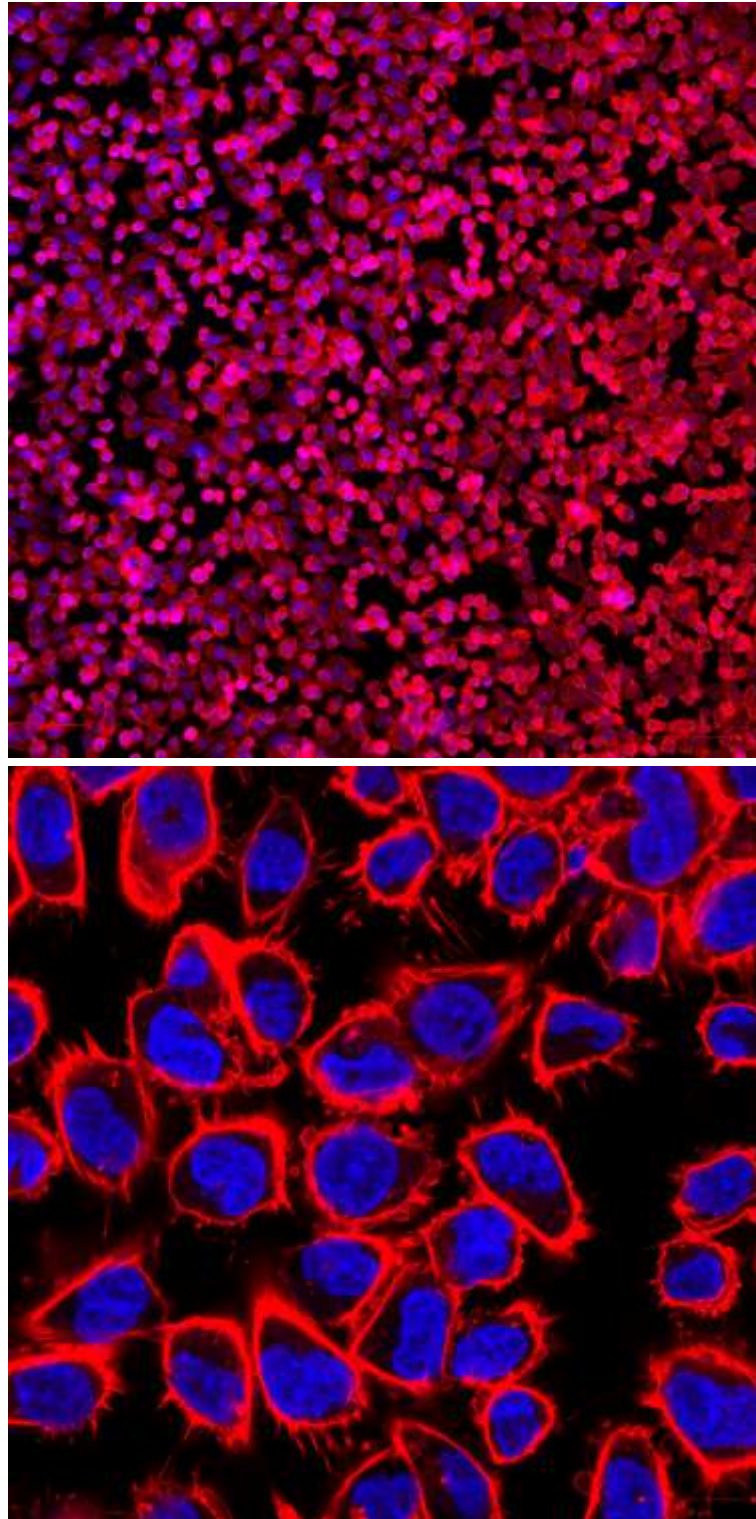


*Figure 94: Actin/dapi images for Cemex-9:1 nanocomposite with two different scales. (Top: 100  $\mu\text{m}$  bar, bottom: 20  $\mu\text{m}$  bar).*

## **7.4 Discussion**

### **7.4.1 Nanoparticle surface and material characterization**

TGA is a commonly used type of analysis to assess the presence of organic matter on the surface of nanoparticles, based on the observation of mass loss (Mai et al. 2013). Furthermore, TGA is used to evaluate surface functionalization on the surface of nanoparticles (Zhong et al. 2015). Therefore, during LbL assembly, the deposition of polyelectrolytes on the surface of nanoparticles was evaluated quantitatively using TGA analysis (Wu et al. 2015).

The thermogram for the amino functionalised silica nanoparticles (Figure 74) was similar to the one obtained by (Branda et al. 2010). Moreover, the calculated organic matter percentage for the amino functionalised silica nanoparticles (Table 24) was in agreement with the one reported by (Liu et al. 2015). A consistent increase in the organic content was observed for amino functionalised silica nanoparticles and different quadruple layer with increasing the number of layers on the surface of the amino functionalised silica nanoparticles. This consistent increase in the organic content confirmed the deposition of the layered polyelectrolytes and drug on the surface of the amino functionalised silica nanoparticles.

### **7.4.2 Drug release profile**

The use of ALBCs has become a well-established practice to prevent infections after TJR (Engesaeter et al., 2006; Parvizi et al., 2008). However, large amounts of antibiotics need to be added to achieve therapeutic levels (up to 1g per 40g of cement) (Letchmanan et al. 2017). There are several problems related to the release profile of antibiotics from ALBCs. The burst release for in the first few hours after surgery, followed by low release below inhibitory levels which doesn't provide prophylaxis for a long period of time. Also, the sub-inhibitory concentrations released adds to the problem of emerging antibiotic resistant bacterial strains (Dunne et al., 2008; Gasparini et al., 2014). In addition, more than 90% of the

loaded antibiotics remain entrapped inside the cement matrix (Dunne et al., 2007; Van et al., 2000).

Many studies studied the *in-vivo* and *in-vitro* combination antibiotics released from PMMA cements (Anagnostakos et al., 2009; Duey et al., 2012). The antibiotics are released from the cement at different rates according to their physicochemical properties, and sometimes improving release kinetics especially when combining two water-soluble antibiotics in the cement. The elution of vancomycin and amikacin were nearly the same when used in combination or when used individually (Kuechle et al., 1991). The combination of tobramycin and vancomycin *in vitro* can increase tobramycin and vancomycin release by 68% and 103%, respectively, compared to adding each one alone (Penner et al., 1996). Also, *in-vivo* studies of vancomycin and tobramycin improved the release of both antibiotics (Masri et al., 1998). In another study, the addition of vancomycin improved the release of gentamicin (Anagnostakos et al., 2009). Other combinations of antibiotics are possible and considered off-label use for the drugs, however, antibiotic impregnated PMMA cements are commercially available (e.g. Vancogenx®, Merete GmbH, Berlin, Germany). Despite of the common practice of combining two antibiotics in bone cement, the data is limited about their release *in-vivo* from prosthetic devices after implantation.

The release from different nanocomposites (Cemex-9:1, 8:2 and 7:3) showed less burst release effect, and continued for up to 30 days for both gentamicin and chlorhexidine. The nanoparticles were homogeneously distributed inside the cement (Figure 84). These findings confirm the reproducibility of the developed LbL coated nanoparticles when comparing the release profiles for chlorhexidine and gentamicin nanocomposites tested in previous chapters. The enhancement of release could be attributed to the increased surface area available for drug release from nanoparticles, because of the formation of nano-channel networks that facilitate the diffusion of drugs (Shen *et al.* 2016). Silica nanoparticles are biocompatible as drug delivery system with high loading capacity and ease of synthesis. Mesoporous silica nanoparticles loaded with gentamicin have been incorporated into bone cement, and achieved long sustained release >30 days Shen *et al.* (2016). Also, gentamicin has been loaded in liposomal formulation and

incorporated into as liquid in the bone cement, and achieved sustained release for nearly 30 days (Ayre et al. 2015).

Chlorhexidine has been incorporated in cementous dental and orthopaedic composites/implants either in the form of powder, or loaded into nanoparticles (Riool et al., 2017; Yan et al., 2017). Chlorhexidine was incorporated into glass-ionomer cement, after encapsulation in mesoporous silica nanoparticles at loading efficiency of 44.62% w/w. The loading continued of up to 30 days, for cement loaded with different concentrations (1%, 5%, and 10% (w/w)). however, chlorhexidine incorporation as powder in brushite calcium phosphate bone cement resulted in 60 % of the drug released after 24 hours, and 95% after 2 weeks, where the cement was loaded with different concentration (3, 6, 9, 12 % w/w) (Young et al., 2008).

Clinical studies looked at the concentration of combination antibiotics in PMMA spacers used after TJRs (Isiklar et al., 1999; Anagnostakos et al., 2009). The intraarticular antibiotic concentrations were measured in the first few days after inserting vancomycin-tobramycin-loaded spacers. Highest concentrations measured at day 1 were 19 µg/ml for vancomycin and 107 µg/ml for tobramycin. The concentrations determined from the wound drainage fluids were 10-30 times higher than MICs for infecting organisms (Masri et al., 1998). In another work, the concentration of vancomycin was 57 µg/mL on day 1 from vancomycin-impregnated spacers in the treatment of orthopaedic implant related *S. epidermidis* infections, also determined from the drainage fluids (Isiklar et al., 1999). (Anagnostakos et al., 2009) studied the release of gentamicin and vancomycin from beads and spacers in the drainage fluid using a two-stage protocol in the treatment of infected hip arthroplasties. Peak mean concentrations from PMMA beads and spacers were reached for gentamicin (115.70 µg/ml and 21.15 µg/ml, respectively) and vancomycin (80.40 µg/ml and 37.0 µg/ml, respectively) on day 1. The last measured concentrations for the beads group was 3.70 µg/ml for gentamicin and 23.00 µg/ml for vancomycin after 13 days, and 1.85 µg/ml for gentamicin and 6.60 µg/ml for vancomycin after 7 days in the spacer group.

### 7.4.3 Antimicrobial efficacy

Antimicrobial testing was done against common bacteria involved in PJIs, both in early and delayed infections (early infection starts during first 24hrs-1 week, and late infections after 1 month according to orthopaedic surgeons.) (Wendling et al. 2016; Wu et al. 2016). In this chapter, the combination of chlorhexidine and gentamicin in the same LbL coated construct nanoparticles achieved a longer duration of antimicrobial inhibition (*Figure 80*) compared with each antimicrobial cement alone in previous chapters (*Figure 57* and *Figure 41*) when tested against catalogue stains. All drug combination nanocomposites (Cemex-9:1, 8:2 and 7:3) achieved an antimicrobial inhibition up to 48 days, compared to less than 30 days for chlorhexidine and gentamicin nanocomposite alone. This enhanced antimicrobial inhibition suggests the presence of either synergistic or additive effect between chlorhexidine and gentamicin, where synergism is when the effect of two antimicrobial agents produces a combined effect greater than the sum of each antimicrobial alone (Bollenbach, 2015). The antimicrobial properties of the combination nanocomposites were tested against clinical strains resistant to gentamicin, and different combinations inhibited bacterial growth for up to 25 days (*Figure 81*).

Many causative organisms in prosthetic infections have been reported to be resistant to certain antibiotics, e.g. nearly 50% of *Staphylococci* involved PJIs are now resistant to gentamicin (Staats et al., 2017). *Staphylococcus aureus* have been implicated in up to 55% of PJIs, but other stains can also be found e.g. *Propionibacterium* species. Polymicrobial infections have been increasingly detected with complex microbiological treatment and poor clinical outcome (Helbig et al., 2018). Therefore, this emerging resistance increased interest in using PMMA bone cements with combination antimicrobial agents, such as gentamicin, vancomycin and cefuroxime. It was reported that 41% and 66% of *Staphylococci* isolates, taken from patients with prosthetic joint infections, were resistant to gentamicin and tobramycin respectively, resistance is also reported with *Staphylococcus aureus* (Anguita-Alonso et al., 2005; Helbig et al., 2018). Also, the resistance is significantly higher in patients with previous use of ALBC, which indicates the selection of aminoglycoside resistant strains after using ALBC (Corona et al., 2014; Staats et al., 2017). Consequently, the development of non-

antibiotic based therapies is becoming extremely urgent for the treatment and prevention of infections in general, and particularly in PJIs.

Chlorhexidine resistance is rarely encountered in *Escherichia coli*, *Salmonella* spp., *Staphylococcus aureus* or coagulase negative staphylococci. However, some resistant isolates can be found in *Enterobacter* spp., *Pseudomonas* spp., *Proteus* spp., *Providencia* spp. and *Enterococcus* spp. (Kampf, 2016). Chlorhexidine is commonly used at different concentrations (0.5%–4%) of the water-soluble gluconate form. Chlorhexidine acts by binding strongly, through the biguanide groups, to exposed anionic groups on the cell membrane and cell wall, which causes the disruption of osmotic equilibrium of the cell (Horner et al., 2012). Chlorhexidine has many medical applications, it has been widely examined in dental cements (Fan et al., 2016; Seneviratne et al., 2014; Takahashi et al., 2006), although it has not been investigated widely in acrylic bone cements (Rodriguez et al., 2015). It has many applications as a disinfectant and antiseptic for skin infections, cleaning wounds (O'Malley, 2008; Peel et al., 2014), sterilization of surgical instruments (Knox et al., 2015; Magalini et al., 2013), and many dental applications including treatment of dental plaque, gingivitis and endodontic disease (Lucchese et al., 2012; Supranoto et al., 2015).

One of the approaches for the treatment of antibiotic resistant strains is the use drug combinations to effectively eradicate the multi drug resistant phenotypes (Markley et al., 2015), to either directly target resistant mechanisms or to provide more than mode of action by targeting different sites in bacterial cell (Tamma et al., 2012). Combination antibiotic therapy provide many advantages as compared to monotherapy such as a broader antibacterial spectrum, synergistic effects and minimizes the risk for emerging resistance during therapy (Markley et al., 2015). Also, combinations are increasingly used to improve the efficacy of available drugs against multidrug resistant strains (Dolgin, 2010). The guanidium groups in chlorhexidine's structure is responsible for the antimicrobial activity by binding to bacterial cell membrane causing cell function disruption (Denyer, 1995). On the other hand, the bactericidal activity of gentamicin is concentration dependant which inhibit protein synthesis in bacteria (Tam et al., 2006). It has the ability to bind prokaryotic ribosomes which cause inhibition of protein synthesis and in consequence bacterial death (Ince et al., 2007).

The combination of gentamicin and penicillin is recommended for the treatment of infective endocarditis and prosthetic joint infections in adults (Anagnostakos and Kelm, 2009; Polin, 2012). A study confirmed the presence of synergism of penicillin and gentamicin against clinical group B *Streptococcus* isolates, where synergism was defined as a  $\geq 100$ -fold ( $\geq 2$  log) increase in killing at 24 h (as measured by colony counts [CFU/mL]) with the combination therapy in comparison with the most active single drug (Ruppen et al., 2016). In addition, the synergetic effect of vancomycin and gentamicin combination was documented against *MRSA*. Time-kill curves were determined for vancomycin at 10 mg/ml and gentamicin at 1 mg/ml. Six *MRSA* strains showed low-level gentamicin resistance (MIC 0.5 to  $>128$  mg/ml.), where vancomycin-gentamicin demonstrated synergism against these gentamicin resistant strains (Mulazimoglu et al., 1996). On the other hand, recent studies demonstrated that chlorhexidine has a synergistic antimicrobial activity when combined with silver ions and loaded into mesoporous silica NPs (MSN), resulting in improved efficacy in the treatment of resistant *Candida*-associated denture stomatitis (Lu et al., 2017). The synergistic action was ascribed to the wide pores of MSNs offered chemical functionalization and permitted simultaneous hosting chlorhexidine and nano-silvers, which allowed the simultaneous release of silver ions and chlorhexidine under acidic conditions. Also, compared to larger silver NPs, the silica matrix could prevent nano-silvers' aggregation and facilitate the dissolution of silver ions (Lu et al., 2017). In another study, chlorhexidine and metallic silver showed synergistic bactericidal action against action toward the gram-negative *Pseudomonas aeruginosa* and the gram-positive *Staphylococcus epidermidis* (Ben-Knaz et al., 2013).

#### **7.4.4 Surface and material properties of bone cement**

##### **7.4.4.1 Bone cement settling time**

The rheological properties of PMMA bone cement is crucial for the handling properties during curing phase. The settling time is an important factor in developing the final mechanical properties of the cement, the degree of penetration and strength of the prosthesis/cement interface (Rodrigues et al., 2009). It is preferred that the incorporation of nanoparticles doesn't have significant effect on

the settling time, which is defined as the time when the temperature of the cement reaches halfway between ambient and the peak exothermic temperatures (“ISO 5833:2002,” 2002). However, using the viscoelastic parameters such as  $G'$  and  $G''$  provide a better description for the behaviour of the cement and a better measure of handling and setting characteristics (Farrar and Rose, 2001).

The introduction of nanoparticle in the bone cement didn't change the settling time and rheological behaviour compared to the commercial cement, which is consistent with nanocomposite behaviour in previous chapters. The viscoelastic behaviour of the cement changed from being mainly liquid-like at the beginning of mixing into solid-like after setting. where  $G'$  (storage modulus) corresponds to the elastic behaviour of the material and  $G''$  (loss modulus) corresponds to the viscous behaviour (Khaled et al., 2011). This change in rheological properties is critical, because implant insertion by surgeon should be delayed until the cement has a sufficient degree of viscosity, but before complete hardening of the cement (Vaishya et al., 2013).

#### **7.4.4.2 Mechanical properties**

The incorporation of a second antibiotic in bone cement adds to the problem of loading antibiotics into PMMA cements, hence only less than 3% of total powdered antibiotics can be added without compromising the cement mechanical properties. The use of gentamicin powder at concentration higher than 3% caused a significant decrease in the compressive and elastic modulus of bone cement, while lower concentrations kept these parameters at acceptable ranges (He et al., 2002). The acceptable ranges for the mechanical properties of a set bone cement are  $> 70$  MPa compressive strength,  $> 1800$  MPa bending modulus and  $> 50$  MPa bending strength (Lee, 2005). The compressive strength for different types of bone cements was determined according to the ISO standard 5833:2002. The incorporation of chlorhexidine powder in cements is commonly reported to decrease the compressive strength (Holt et al., 2007; Rodriguez et al., 2015).

In this work, the addition of nanoparticles didn't compromise the mechanical properties of the nanocomposite, compared to the commercial cement as seen in Cemex-9:1 (Figure 82 and Table 25). The mechanical properties meet the criteria set by ISO standard 5833:2002. The nanocomposite loaded with 9% of NPs had

compressive strength of >80 MPa, which is in accordance with Shen *et al.* (2016) work which reported a compressive strength of 85 MPa for %10 mesoporous silica NP loaded bone cement. The presence of nanoparticles seems to provide better mixing and less agglomeration inside the cement mantle, which can preserve the mechanical properties of the cement, as seen in the NP distribution images (Figure 84). The agglomeration of powdered antibiotics forms clusters which act as crack propagation points that weakens the mechanical strength of the cement. Also, the presence of chlorhexidine powder can interfere with PMMA polymerization reaction because of its free radical quenching effect (Rodriguez et al., 2015). The bending strength and modulus for the nanocomposite also comply with cement mechanical requirements set in ISO 5833:2002 (bending strength > 50 MPa and bending modulus > 1800 MPa). Even though the joint is mainly stressed by compression, testing other forms of stress (bending, fracture) is important to account for other forms of stresses.

#### **7.4.4.3 Water uptake testing**

Water uptake of the bone cement in physiologic conditions changes the mechanical properties of the cement, because water decreases the attraction between polymer chains and increase their flexibility (Arnold and Venditti, 2001). Water uptake not only affects the mechanical properties of the bone cement, but also found to change structure and surface properties of the cement by decreasing the molecular weight of PMMA over time (Hughes et al., 2003). Therefore, studying the water uptake behaviour is important to estimate any initial changes in the physicochemical properties of the cement.

In this work, the presence of NPs did not affect the water uptake behaviour compared the commercial cement, and no water was absorbed after 30 days (Figure 83). The weight of bone cement samples stopped increasing after 4-5 days, which explains the similarity in the compressive strength after 3 months. The presence of NPs didn't affect the water uptake behaviour nor the compressive strength compared to commercial cement (Cemex®). However, long term exposure of cement to physiological fluids play an important role in cement overall performance (Bettencourt et al., 2004).

#### 7.4.5 Cytocompatibility

The present study shows that the combination nanocomposite (Cemex-9:1) showed similar viability to control (Cemex®) as tested by MTT, LDH and fluorescence images. However, other nanocomposite combinations (Cemex-8:2 and 7:3) showed transient reduction in cell viability, where the osteoblast viability proliferation returned to normal at day 7 for all types of combinations. In our study, the cumulative release for the combination of nanocomposite is < 700 µg/ml gentamicin, and < 800 µg/ml chlorhexidine in the first 7 days. Nitrite production was similar in all different bone cement samples, compared to osteoblasts cell control sample which are documented to produce nitrite at normal in-vitro growth conditions (Sosroseno et al., 2009). Calcium production was nearly the same for different nanocomposites with insignificantly higher averages, that could be attributed to electrochemical reaction between alizarin and silica nanoparticles in the bone cement (Liu et al., 2015).

Aminoglycoside antibiotics (e.g. gentamicin and tobramycin) are commonly used in ALBCs because they satisfy the properties required for antibiotics to be incorporated into bone cements, such as thermo-stability at high temperature, availability in powder form etc. In addition, their evidence of effectiveness and safety after frequent use in TJR has been studied by the meta-analysis done by Parvizi et al (2008). Gentamicin at concentrations up to 750 µg/ml was not toxic for human fetal osteoblasts, and the number of growing cells was not affected by gentamicin concentration up to 1000 µg/ml with slight changes in cellular structure (Belcarz et al., 2009). In another study, gentamicin resulted in significant cell toxicity at 800 µg/ml (Rathbone et al., 2011). In another work, gentamicin at concentration of 1700 µg/ml induced a reduction of 15-20 % in osteoblast proliferation in the first 48 hours, which returned to control values after 72 hours. Also, it did not have any significant effect on osteoblast mineralization and bone nodule formation (Philp et al. 2017).

Chlorhexidine is a well-tolerated and widely used antiseptic available in different formulations, including wipes, cloths, solutions at different concentrations (0.5%-4%) (Conroy et al., 1999; Edmiston et al., 2008). Chlorhexidine has many applications in TJR as pre-operative skin cleansing, surgical site preparation,

surgent team hand antisepsis and intra-articular irrigation of infected joints (Azzam et al., 2010; Garibaldi, 1988; Widmer, 2013). However, Chlorhexidine can be cytotoxic to human fibroblasts at low concentrations as 0.02% (van Meurs et al., 2014). Extensive chondrolysis was reported in accidental irrigation of 1% chlorhexidine solution during knee arthroscopy in a case series of five patients (Douw et al., 1998). Chlorhexidine solution is shown to be cytotoxic to human osteoblasts, fibroblasts and lymphocytes in dose and time dependent manner (Faria et al., 2009; Giannelli et al., 2008; Mariotti and Rumpf, 1999). Chlorhexidine at a concentration of 0.2 % was cytotoxic to Saos-2 cell and human gingival fibroblasts (John et al., 2014).

Although using combination antimicrobial agents can increase cell toxicity, combination antibiotic therapy provides many advantages as compared to monotherapy such as a broader antibacterial spectrum, synergistic effects and minimizes the risk for emerging resistance during therapy (Markley et al., 2015). Also, combinations are increasingly used to improve the efficacy of available drugs against multidrug resistant strains (Dolgin, 2010). The use of combination antimicrobial therapy is associated with increased risk of side effects i.e. ototoxicity and nephrotoxicity, especially when taken systemically (Prayle et al., 2010). Therefore, it is been recommended to use a the most selective single agent as soon as the antibiotic susceptibility profile of the causative agent is known, or using a local delivery whenever possible to reduce drugs concentration in the systemic circulation and their consequent side effects (Jackson et al., 2011). However, combination antibiotic therapy provides many advantages as compared to monotherapy such as a broader antibacterial spectrum, synergistic effects and minimizes the risk for emerging resistance during therapy (Markley et al., 2015). Also, combinations are increasingly used to improve the efficacy of available drugs against multidrug resistant strains (Dolgin, 2010).

## **7.5 Conclusion**

The chlorhexidine and gentamicin combination LbL construct has been successfully coated on silica nanoparticle. Then, these nanoparticles, with different combination ratios, were incorporated into bone cement commercial formulation Cemex®, without adversely affecting the mechanical performance. The novel LbL coated silica NPs provided a controlled, gradual and prolonged release of

chlorhexidine for up to 30 days. The NP containing bone cement showed superior antimicrobial activity against different bacterial catalogue stains. In addition, the nanocomposites showed antimicrobial activity against gentamicin resistant clinical strains. The nanocomposites showed cytocompatibility and were nontoxic to osteoblast without adversely affecting calcium production. In conclusion, the application of LbL nano-delivery systems may play a vital role in improving the release of antibiotics and other therapeutic agents from the bone cement, which is needed to provide prophylaxis from PJIs infection after TJRs.

## 8 Conclusion

PMMA bone cements use is considered a gold standard in hip and knee replacements. The use of ALBCs is considered a standard practice in the prevention and treatment of PJIs after TJRs, where the loaded cement delivers powdered antibiotics locally. Although antibiotics are widely incorporated in PMMA bone cements, there are many concerns about the release kinetics of added antibiotics. In reality, antibiotics release from the bone cement is a burst for the first few hours after surgery, followed by slow release below inhibitory levels within few days. This release profile does not provide long term prophylaxis from early and delayed stage infections (early infection starts during first 24hrs-1 week, and late infections after 1 months according to orthopaedic surgeons). In addition, the continuing emergence of resistant microbial strains limits the success of conventional antibiotic-based therapies in the prevention and treatment of PJIs. There is a continuing need to improve the release kinetics of antibiotics from PMMA cements, and to improve its antimicrobial performance by exploring new alternatives for conventional antibiotics currently used.

The main purpose of this research programme was to develop a novel nano-composite antimicrobial PMMA bone cement containing antibiotic or non-antibiotic antimicrobial agents or a combination of both, for the prevention of PIs after TJR which is one of the major causes for revision surgery. In order to achieve this, a new drug delivery LbL nano system where developed for loading different antimicrobial agents in the same carrier. Also, it was necessary to gain an understanding of the properties and characteristics of PMMA bone cement, such as release profile, setting properties, mechanical properties and cytocompatibility. A decent understanding of the different test methods used to determine the properties of PMMA was also required and knowledge of the principles behind the test methods allowed for a critical assessment of the results.

Previous studies showed that novel nanotechnology drug delivery systems offer many advantages to overcome the current challenges with antimicrobial therapy. However, the use of LbL coating technique at nano-scale level has not been researched for application in PMMA cements. In this study, antimicrobial thin films were constructed through LbL deposition technique using different types of

tetralayers. The films were deposited by alternating depositions between alginate and hydrolytically degradable polymer (B1); gentamicin and chlorhexidine was directly incorporated without the need for pre-modification. LbL was effective in controlling release of each single and combination antimicrobial agents from silica nanoparticles for at least 4 weeks without initial burst release, giving a promising profile for the application in infection prevention and treatment, either by using the LbL as a coating for biomedical implants and devices, or by incorporation of the coated nanoparticles into bone cements.

In chapter 3, this study has highlighted that the mechanism of gentamicin or chlorhexidine release is governed by electrostatic interaction between different polyelectrolytes when PBAE were employed, confuting the establish assumption that hydrolysis is the key factor when these polymers are used. Our results also provide guidance in the polyelectrolyte properties required to achieve a desired release profile; i.e. to increase the release kinetic a polyelectrolyte with lower charge is required instead of more easily hydrolysed one; as it would be the case if hydrolysis was the governing mechanism in drug release from LbL coatings.

In chapter 5, the gentamicin LbL coated silica nanoparticles have been successfully incorporated into bone cement commercial formulations Cemex and Palacos, without adversely affecting the mechanical performance. The novel LbL coated silica NPs provided a more controlled, gradual and prolonged release for up to 30 days of antimicrobial used compared to commercial formulations containing powdered antibiotics. The NP containing bone cement showed superior antimicrobial activity against different bacterial stains. The nanocomposites showed cytocompatibility towards human osteoblasts without adversely affecting calcium production.

In chapter 6, the chlorhexidine loaded LbL coated silica nanoparticles have been successfully incorporated into bone cement commercial formulation Cemex®, without adversely affecting the mechanical performance. The novel LbL coated silica NPs provided a controlled, gradual and prolonged release of chlorhexidine for up to 30 days. The NP containing bone cement showed superior antimicrobial activity against different bacterial stains. Cytocompatibility testing showed an

expected decrease in cell viability for the nanocomposite with osteoblasts. In conclusion, the application of LbL nano-delivery systems may play a vital role in improving the release of antibiotics and other therapeutic agents from the bone cement, which is needed to reduce infection rates after TJRs. Also, it offers an alternative approach for loading non-antibiotic based antimicrobial into bone cement without compromising other properties needed for performance.

In chapter 7, the chlorhexidine and gentamicin combination LbL construct has been successfully coated on silica nanoparticle. Then, these nanoparticles, with different combination ratios, were incorporated into bone cement commercial formulation Cemex®, without adversely affecting the mechanical performance. The novel LbL coated silica NPs provided a controlled, gradual and prolonged release of chlorhexidine for up to 30 days. The NP containing bone cement showed superior antimicrobial activity against different bacterial catalogue stains for up to 50 days (Cemex-9:1). In addition, the nanocomposites showed antimicrobial activity against gentamicin resistant clinical strains. The nanocomposites showed cytocompatibility towards human osteoblasts without adversely affecting calcium production.

In conclusion, this study helps to explore single antimicrobial agents or in combination. combination antibiotic therapy provides many advantages as compared to monotherapy such as a broader antibacterial spectrum, synergistic effects and minimizes the risk for emerging resistance during therapy. Also, combinations are increasingly used to improve the efficacy of available drugs against multidrug resistant strains. The application of LbL nano-delivery systems may play a vital role in improving the release of antibiotics and other therapeutic agents from bone cement. Also, LbL nano-delivery systems makes it possible for having combination antimicrobial agents in the same carrier, which is needed to provide prophylaxis from PJIs infection after TJRs.

## 9 Future work

The work carried out in this study has contributed to the existing body of knowledge and as a result, a series of further questions have emerged from this. The following experiments have been deemed outside the scope and time frame of this study, but they may form the basis for potential future research.

Although nanocomposites loaded with different types of nanoparticles (gentamicin, chlorhexidine and combination LbL coated nanoparticles) were assessed for cytocompatibility using cell line Saos-2, the biocompatibility of these nanocomposites should be questioned in more detail. A series of *in vitro* experiments investigating the toxicity of the nanocomposites on tissues and cells is needed, to clarify their clinical applicability. If the outcome of such experiments is favourable, animal trials may then be justifiable to assess the extent of their biocompatibility.

The development of the LbL nano-coated silica particles has created exciting possibilities for the delivery of therapeutic agents from bone cement. The therapeutic agents that can be loaded into the bone cement is not restricted to gentamicin and chlorhexidine, but can include other antimicrobial agents (alone or in combination), anti-inflammatory agents and osteogenic agents needed after TJRs. Any therapeutic molecule with sufficient charge and size suitable for LbL coating can be replaced by the used model drugs (gentamicin and chlorhexidine). In addition, other polyelectrolytes can be used instead of alginate and B1 to construct the LbL system, to ensure optimum drug loading and to tailor the release. The use of other polyelectrolytes with different molecular weight, hydrolysis kinetics, charge, chemical structure can be researched for optimizing the performance of LbL system. Also, using different substrates for LbL coating may change the performance of the delivery system and its effect on the mechanical and cytocompatibility of the bone cement.

Successful implementation of the LbL nano-delivery system would require industrial scale production methods. Batch production methods to obtain large quantities of materials may alter the properties of the final product and therefore careful consideration and investigation of the processes are required.

The final experimental work that is of great interest is the wider applicability of the LbL nano-based delivery system in various biomaterials. Having enhanced the properties of PMMA bone cement, the use of such a technology may be advantageous to other biomaterials, such as restorative dental materials or catheters. Although this is merely speculative, it is worthwhile investigating and may create further opportunities for future research and collaborations.

## 10 References

1. Abdelghany, S.M., Quinn, D.J., Ingram, R.J., Gilmore, B.F., Donnelly, R.F., Taggart, C.C., Scott, C.J., 2012. Gentamicin-loaded nanoparticles show improved antimicrobial effects towards *Pseudomonas aeruginosa* infection. *International Journal of Nanomedicine* 7, 4053–4063.
2. Abid, Jain, S., Jackeray, R., Chattopadhyay, S., Singh, H., 2017. Formulation and characterization of antimicrobial quaternary ammonium dendrimer in poly (methyl methacrylate) bone cement. *J Biomed Mater Res B Appl Biomater*;105(3), 521-530.
3. Allahverdiyev, A.M., Kon, K.V., Abamor, E.S., Bagirova, M., Rafailovich, M., 2011. Coping with antibiotic resistance: combining nanoparticles with antibiotics and other antimicrobial agents. *Expert Rev Anti Infect Ther* 9, 1035–1052.
4. Almazin, S.M., Dziak, R., Andreana, S., Ciancio, S.G., 2009. The effect of doxycycline hyclate, chlorhexidine gluconate, and minocycline hydrochloride on osteoblastic proliferation and differentiation in vitro. *J. Periodontol.* 80, 999–1005.
5. Al-Niimi, A., Rice, L.W., Shitanshu, U., Garvens, B., Fitzgerald, M., Zerbel, S., Safdar, N., 2016. Safety and tolerability of chlorhexidine gluconate (2%) as a vaginal operative preparation in patients undergoing gynecologic surgery. *American Journal of Infection Control* 44, 996–998.
6. Alvarez, M.B., Childress, P., Philip, B.K., Gerard-O’Riley, R., Hanlon, M., Herbert, B.-S., Robling, A.G., Pavalko, F.M., Bidwell, J.P., 2012. Immortalization and characterization of osteoblast cell lines generated from wild-type and *Nmp4*-null mouse bone marrow stromal cells using murine telomerase reverse transcriptase (mTERT). *J Cell Physiol* 227, 1873–1882.
7. Ambard, A.J., Mueninghoff, L., 2006. Calcium phosphate cement: Review of mechanical and biological properties. *Journal of Prosthodontics* 15, 321–328.
8. Anagnostakos, K., 2017. Therapeutic Use of Antibiotic-loaded Bone Cement in the Treatment of Hip and Knee Joint Infections. *J Bone Jt Infect* 2, 29–37.
9. Anagnostakos, K., Fürst, O., Kelm, J., 2006. Antibiotic-impregnated PMMA hip spacers: Current status. *Acta Orthopaedica* 77, 628–637.
10. Anagnostakos, K., Kelm, J., 2009. Enhancement of antibiotic elution from acrylic bone cement. *Journal of Biomedical Materials Research - Part B Applied Biomaterials*, 90 B (1), 467–475.
11. Anagnostakos, K., Wilmes, P., Schmitt, E., Kelm, J., 2009. Elution of gentamicin and vancomycin from polymethylmethacrylate beads and hip spacers in vivo. *Acta Orthopaedica* 80, 193–197.

12. Andersen, F.A., 1999. Note regarding the safety assessment of Chlorhexidine, Chlorhexidine Diacetate, Chlorhexidine Digluconate, and Chlorhexidine Dihydrochloride. *International Journal of Toxicology* 18 (12), 69-88.
13. Anguita-Alonso, P., Hanssen, A.D., Osmon, D.R., Trampuz, A., Steckelberg, J.M., Patel, R., 2005. High rate of aminoglycoside resistance among staphylococci causing prosthetic joint infection. *Clin. Orthop. Relat. Res.* 439, 43-47.
14. Arce, V.B., Gargarello, R.M., Ortega, F., Romañano, V., Mizrahi, M., Ramallo-López, J.M., Cobos, C.J., Airoldi, C., Bernardelli, C., Donati, E.R., Mártire, D.O., 2015. EXAFS and DFT study of the cadmium and lead adsorption on modified silica nanoparticles. *Spectrochimica Acta - Part A: Molecular and Biomolecular Spectroscopy* 151, 153-163.
15. Archer, S., 1993. Measurement of nitric oxide in biological models. *FASEB J.* 7 (2), 349-360.
16. Ariga, K., Lvov, Y.M., Kawakami, K., Ji, Q., Hill, J.P., 2011. Layer-by-layer self-assembled shells for drug delivery. *Advanced Drug Delivery Reviews, Layer-by-Layer Self-Assembled Nanoshells for Drug Delivery* 63, 762-771.
17. Arnold, J.C., Venditti, N.P., 2001. Effects of environment on the creep properties of a poly(ethylmethacrylate) based bone cement. *J Mater Sci Mater Med* 12, 707-717.
18. Aslam, S., Darouiche, R.O., 2012. Prosthetic joint infections. *Current Infectious Disease Reports* 14, 551-557.
19. Ayre, Wayne Nishio, Birchall, J.C., Evans, S.L., Denyer, S.P., 2016. A novel liposomal drug delivery system for PMMA bone cements. *J Biomed Mater Res B Appl Biomater*, 104(8), 1510-1524.
20. Azzam, K.A., Seeley, M., Ghanem, E., Austin, M.S., Purtill, J.J., Parvizi, J., 2010. Irrigation and debridement in the management of prosthetic joint infection: traditional indications revisited. *J Arthroplasty* 25, 1022-1027.
21. Balouiri, M., Sadiki, M., Ibnsouda, S.K., 2016. Methods for in vitro evaluating antimicrobial activity: A review. *Journal of Pharmaceutical Analysis* 6, 71-79.
22. Barrack, R.L., Nakamura, S.J., Hopkins, S.G., Rosenzweig, S., 2004. Winner of the 2003 James A. Rand Young Investigator's Award. Early failure of cementless mobile-bearing total knee arthroplasty. *J Arthroplasty* 19, 101-106.
23. Belcarz, A., Ginalska, G., Zalewska, J., Rzeski, W., Ślósarczyk, A., Kowalczyk, D., Godlewski, P., Niedźwiadek, J., 2009. Covalent coating of hydroxyapatite by keratin stabilizes gentamicin release. *J. Biomed. Mater. Res.* 89B, 102-113.
24. Bellis, C.A., Nobbs, A.H., O'Sullivan, D.J., Holder, J.A., Barbour, M.E., 2016. Glass ionomer cements functionalised with a concentrated paste of chlorhexidine hexametaphosphate provides dose-dependent chlorhexidine release over at least 14 months. *Journal of Dentistry* 45, 53-58.
25. Ben-Knaz, R., Pedahzur, R., Avnir, D., 2013. Bioactive doped metals: high synergism in the bactericidal activity of chlorhexidine@silver towards wound pathogenic bacteria. *RSC Adv.* 3, 8009-8015.

26. Béraud, R., Huneault, L., 2005. Prevention and treatment of bone infections. Local antibiotic controlled release formulations. *Point Veterinaire* 36, 12–13.
27. Berry, D.J., Harmsen, W.S., Cabanela, M.E., Morrey, B.F., 2002. Twenty-five-year survivorship of two thousand consecutive primary Charnley total hip replacements: factors affecting survivorship of acetabular and femoral components. *J Bone Joint Surg Am* 84-A, 171–177.
28. Bertazzoni, M., Benini, A., Magnan, B., Bartolozzi, P., 2004. Release of gentamicin and vancomycin from temporary human hip spacers in two-stage revision of infected arthroplasty. *Journal of Antimicrobial Chemotherapy* 53, 329–334.
29. Bertazzoni Minelli, E., Benini, A., Samaila, E., Bondi, M., Magnan, B., 2015. Antimicrobial activity of gentamicin and vancomycin combination in joint fluids after antibiotic-loaded cement spacer implantation in two-stage revision surgery. *J Chemother* 27, 17–24.
30. Bettencourt, A., Calado, A., Amaral, J., Alfaia, A., Vale, F.M., Monteiro, J., Montemor, M.F., Ferreira, M.G.S., Castro, M., 2004. Surface studies on acrylic bone cement. *International Journal of Pharmaceutics* 278, 181–186.
31. Beyth, N., Hourri-Haddad, Y., Domb, A., Khan, W., Hazan, R., 2015. Alternative Antimicrobial Approach: Nano-Antimicrobial Materials. *Evid Based Complement Alternat Med* 2015.
32. Bhandari, M., Smith, J., Miller, L.E., Block, J.E., 2012. Clinical and economic burden of revision knee arthroplasty. *Clin Med Insights Arthritis Musculoskelet Disord* 5, 89–94.
33. Bidolegui, F., Arce, G., Lugones, A., Pereira, S., Vindver, G., 2014. Tranexamic Acid Reduces Blood Loss and Transfusion in Patients Undergoing Total Knee Arthroplasty without Tourniquet: A Prospective Randomized Controlled Trial. *Open Orthop J* 8, 250–254.
34. Bollenbach, T., 2015. Antimicrobial interactions: mechanisms and implications for drug discovery and resistance evolution. *Current Opinion in Microbiology, Antimicrobials • Microbial systems biology* 27, 1–9.
35. Boner, V., Kuhn, P., Mendel, T., Gisep, A., 2009. Temperature evaluation during PMMA screw augmentation in osteoporotic bone-an in vitro study about the risk of thermal necrosis in human femoral heads. *Journal of Biomedical Materials Research - Part B Applied Biomaterials* 90 B, 842–848.
36. Boyd, D., Clarkin, O.M., Wren, A.W., Towler, M.R., 2008. Zinc-based glass polyalkenoate cements with improved setting times and mechanical properties. *Acta Biomaterialia* 4, 425–431.
37. Branda, F., Silvestri, B., Luciani, G., Costantini, A., Tescione, F., 2010. Synthesis structure and stability of amino functionalized PEGylated silica nanoparticles. *Colloids and Surfaces A: Physicochemical and Engineering Aspects* 367, 12–16.
38. Brinmo, O., Ramanathan, D., Schiltz, N.K., Pillai, A.L.P.C., Klika, A.K., Barsoum, W.K., 2016. Irrigation and Debridement Before a 2-Stage Revision Total Knee Arthroplasty Does Not Increase Risk of Failure. *The Journal of Arthroplasty* 31, 461–464.

39. Buller, L.T., Sabry, F.Y., Easton, R.W., Klika, A.K., Barsoum, W.K., 2012. The Preoperative Prediction of Success Following Irrigation and Debridement With Polyethylene Exchange for Hip and Knee Prosthetic Joint Infections. *The Journal of Arthroplasty* 27, 857-864.e4.
40. Bumpass, D.B., Nunley, R.M., 2012. Assessing the value of a total joint replacement. *Current Reviews in Musculoskeletal Medicine* 5, 274–282.
41. Buttaro, M.A., Gimenez, M.I., Greco, G., Barcan, L., Piccaluga, F., 2005. High active local levels of vancomycin without nephrotoxicity released from impacted bone allografts in 20 revision hip arthroplasties. *Acta Orthopaedica* 76, 336–340.
42. Campoccia, D., Montanaro, L., Speziale, P., Arciola, C.R., 2010. Antibiotic-loaded biomaterials and the risks for the spread of antibiotic resistance following their prophylactic and therapeutic clinical use. *Biomaterials* 31, 6363–6377.
43. Cannillo, V., Colmenares-Angulo, J., Lusvarghi, L., Pierli, F., Sampath, S., 2009. In vitro characterisation of plasma-sprayed apatite/wollastonite glass-ceramic biocoatings on titanium alloys. *Journal of the European Ceramic Society* 29, 1665–1677.
44. Chandrika, N.T., Garneau-Tsodikova, S., 2016. A review of patents (2011–2015) towards combating resistance to and toxicity of aminoglycosides. *Med. Chem. Commun.* 7, 50–68.
45. Chaudhary, H., Kohli, K., Kumar, V., 2014. A novel nano-carrier transdermal gel against inflammation. *International Journal of Pharmaceutics* 465, 175–186.
46. Chen, D.W.-C., Liu, S.-J., 2015. Nanofibers used for delivery of antimicrobial agents. *Nanomedicine* 10, 1959–1971.
47. Chen, S.-Y., Ou, S.-F., Teng, N.-C., Kung, C.-M., Tsai, H.-L., Chu, K.-T., Ou, K.-L., 2013. Phase transformation on bone cement: Monocalcium phosphate monohydrate into calcium-deficient hydroxyapatite during setting. *Ceramics International* 39, 2451–2455.
48. Chiang, C.-C., Chiu, F.-Y., 2012. Cefuroxime-impregnated cement and systemic cefazolin for 1 week in primary total knee arthroplasty: An evaluation of 2700 knees. *Journal of the Chinese Medical Association* 75, 167–170.
49. Chiu, F.Y., Lin, C.F., Chen, C.M., Lo, W.H., Chung, T.Y., 2001. Cefuroxime-impregnated cement at primary total knee arthroplasty in diabetes mellitus. A prospective, randomised study. *J Bone Joint Surg Br* 83, 691–695.
50. Chlebicki, M.P., Safdar, N., O'Horo, J.C., Maki, D.G., 2013. Preoperative chlorhexidine shower or bath for prevention of surgical site infection: a meta-analysis. *Am J Infect Control* 41, 167–173.
51. Choy, W.-S., Yang, D.-S., Lee, K.-W., Lee, S.-K., Kim, K.-J., Chang, S.-H., 2014. Cemented versus cementless fixation of a tibial component in Lchitosan mobile-bearing total knee arthroplasty performed by a single surgeon. *Journal of Arthroplasty* 29, 2397–2401.

52. Chuang, H.F., Smith, R.C., Hammond, P.T., 2008. Polyelectrolyte Multilayers for Tunable Release of Antibiotics. *Biomacromolecules* 9, 1660–1668.
53. Cobo, J., Del, P., 2011. Prosthetic joint infection: Diagnosis and management. *Expert Review of Anti-Infective Therapy* 9, 787–802.
54. Conaghan, P.G., Porcheret, M., Kingsbury, S.R., Gammon, A., Soni, A., Hurley, M., Rayman, M.P., Barlow, J., Hull, R.G., Cumming, J., Llewelyn, K., Moscogiuri, F., Lyons, J., Birrell, F., 2015. Impact and therapy of osteoarthritis: the Arthritis Care OA Nation 2012 survey. *Clinical Rheumatology* 34, 1581–1588.
55. Conroy, B.P., Anglen, J.O., Simpson, W.A., Christensen, G., Phaup, G., Yeager, R., Gainor, B.J., 1999. Comparison of castile soap, benzalkonium chloride, and bacitracin as irrigation solutions for complex contaminated orthopaedic wounds. *J Orthop Trauma* 13, 332–337.
56. Cook, W.D., Forrest, M., Goodwin, A.A., 1999. A simple method for the measurement of polymerization shrinkage in dental composites. *Dental Materials* 15, 447–449.
57. Cooper, H.J., Valle, C.J.D., 2013. The two-stage standard in revision total hip replacement. *Bone Joint J* 95-B, 84–87.
58. Corona, P.S., Espinal, L., Rodríguez-Pardo, D., Pigrau, C., Larrosa, N., Flores, X., 2014. Antibiotic susceptibility in gram-positive chronic joint arthroplasty infections: increased aminoglycoside resistance rate in patients with prior aminoglycoside-impregnated cement spacer use. *J Arthroplasty* 29, 1617–1621.
59. Cram, P., Lu, X., Kates, S.L., Singh, J.A., Li, Y., Wolf, B.R., 2012. Total knee arthroplasty volume, utilization, and outcomes among medicare beneficiaries, 1991-2010. *JAMA - Journal of the American Medical Association* 308, 1227–1236.
60. Crowder, A.R., Duffy, G.P., Trousdale, R.T., 2005. Long-term results of total knee arthroplasty in young patients with rheumatoid arthritis. *J Arthroplasty* 20, 12–16.
61. Czekanska, E.M., Stoddart, M.J., Ralphs, J.R., Richards, R.G., Hayes, J.S., 2014. A phenotypic comparison of osteoblast cell lines versus human primary osteoblasts for biomaterials testing. *J Biomed Mater Res A* 102, 2636–2643.
62. Danziger, R.S., Zuckerbraun, B.S., Pensler, J.M., 1997. Role of nitric oxide in the regulation of osteoblast metabolism. *Plast. Reconstr. Surg.* 100, 670–673.
63. Decker, T., Lohmann-Matthes, M.L., 1988. A quick and simple method for the quantitation of lactate dehydrogenase release in measurements of cellular cytotoxicity and tumor necrosis factor (TNF) activity. *J. Immunol. Methods* 115, 61–69.
64. Demey, G., Servien, E., Lustig, S., Si, S., Neyret, P., 2011. Cemented versus uncemented femoral components in total knee arthroplasty. *Knee Surgery, Sports Traumatology, Arthroscopy* 19, 1053–1059.
65. Denyer, S.P., 1995. Mechanisms of action of antibacterial biocides. *International Biodeterioration & Biodegradation* 36, 227–245.

66. Deshmukh, P.K., Ramani, K.P., Singh, S.S., Tekade, A.R., Chatap, V.K., Patil, G.B., Bari, S.B., 2013. Stimuli-sensitive layer-by-layer (LbL) self-assembly systems: Targeting and biosensory applications. *Journal of Controlled Release* 166, 294–306.
67. Devalapally, H., Shenoy, D., Little, S., Langer, R., Amiji, M., 2007. Poly(ethylene oxide)-modified poly(beta-amino ester) nanoparticles as a pH-sensitive system for tumor-targeted delivery of hydrophobic drugs: part 3. Therapeutic efficacy and safety studies in ovarian cancer xenograft model. *Cancer Chemother. Pharmacol.* 59, 477–484.
68. Dickey, B.T., Kehoe, S., Boyd, D., 2013. Novel adaptations to zinc–silicate glass polyalkenoate cements: The unexpected influences of germanium based glasses on handling characteristics and mechanical properties. *Journal of the Mechanical Behavior of Biomedical Materials* 23, 8–21.
69. Dolgin, E., 2010. Sequencing of superbugs seen as key to combating their spread. *NATURE MEDICINE* 16, 1054–1054.
70. Donlan, R.M., 2001. Biofilms and device-associated infections. *Emerging Infect. Dis.* 7, 277–281.
71. Douw, C.M., Bulstra, S.K., Vandenbroucke, J., Geesink, R.G., Vermeulen, A., 1998. Clinical and pathological changes in the knee after accidental chlorhexidine irrigation during arthroscopy. Case reports and review of the literature. *J Bone Joint Surg Br* 80, 437–440.
72. Drago, L., Boot, W., Dimas, K., Malizos, K., Hänsch, G.M., Stuyck, J., Gawlitta, D., Romanò, C.L., 2014. Does Implant Coating With Antibacterial-Loaded Hydrogel Reduce Bacterial Colonization and Biofilm Formation in Vitro? *Clinical Orthopaedics and Related Research* 472, 3311–3323.
73. Du, P., Zhao, X., Zeng, J., Guo, J., Liu, P., 2015. Layer-by-layer engineering fluorescent polyelectrolyte coated mesoporous silica nanoparticles as pH-sensitive nanocarriers for controlled release. *Applied Surface Science* 345, 90–98.
74. Duey, R.E., Chong, A.C., McQueen, D.A., Womack, J.L., Song, Z., Steinberger, T.A., Wooley, P.H., 2012. Mechanical properties and elution characteristics of polymethylmethacrylate bone cement impregnated with antibiotics for various surface area and volume constructs. *The Iowa orthopaedic journal* 32, 104–115.
75. Dunbar, M.J., 2009. Antibiotic bone cements: their use in routine primary total joint arthroplasty is justified. *Orthopedics* 32.
76. Dunne, N., Hill, J., McAfee, P., Todd, K., Kirkpatrick, R., Tunney, M., Patrick, S., 2007. In vitro study of the efficacy of acrylic bone cement loaded with supplementary amounts of gentamicin: Effect on mechanical properties, antibiotic release, and biofilm formation. *Acta Orthopaedica* 78, 774–785.
77. Dunne, N.J., Hill, J., McAfee, P., Kirkpatrick, R., Patrick, S., Tunney, M., 2008. Incorporation of large amounts of gentamicin sulphate into acrylic bone cement: effect on handling and mechanical properties, antibiotic release, and biofilm formation. *Proc Inst Mech Eng H* 222, 355–365.

78. Dunne, N.J., Orr, J.F., 2001. Influence of mixing techniques on the physical properties of acrylic bone cement. *Biomaterials* 22, 1819–1826.
79. Edmiston, C.E., Krepel, C.J., Seabrook, G.R., Lewis, B.D., Brown, K.R., Towne, J.B., 2008. Preoperative shower revisited: can high topical antiseptic levels be achieved on the skin surface before surgical admission? *J. Am. Coll. Surg.* 207, 233–239.
80. Emerson, R.H., Head, W.C., Emerson, C.B., Rosenfeldt, W., Higgins, L.L., 2002. A comparison of cemented and cementless titanium femoral components used for primary total hip arthroplasty: a radiographic and survivorship study. *J Arthroplasty* 17, 584–591.
81. Engesaeter, L.B., Espehaug, B., Lie, S.A., Furnes, O., Havelin, L.I., 2006. Does cement increase the risk of infection in primary total hip arthroplasty? Revision rates in 56,275 cemented and uncemented primary THAs followed for 0-16 years in the Norwegian Arthroplasty Register. *Acta Orthop* 77, 351–358.
82. Espehaug, B., Furnes, O., Havelin, L.I., Engesaeter, L.B., Vollset, S.E., 2002. The type of cement and failure of total hip replacements. *J Bone Joint Surg Br* 84, 832–838.
83. Evans, R.P., 2004. Successful treatment of total hip and knee infection with articulating antibiotic components: a modified treatment method. *Clin. Orthop. Relat. Res.* 37–46.
84. Fan, W., Li, Y., Sun, Q., Ma, T., Fan, B., 2016. Calcium-silicate mesoporous nanoparticles loaded with chlorhexidine for both anti- *Enterococcus faecalis* and mineralization properties. *Journal of Nanobiotechnology* 14, 72.
85. Faria, G., Cardoso, C.R.B., Larson, R.E., Silva, J.S., Rossi, M.A., 2009. Chlorhexidine-induced apoptosis or necrosis in L929 fibroblasts: A role for endoplasmic reticulum stress. *Toxicol. Appl. Pharmacol.* 234, 256–265.
86. Farrar, D.F., Rose, J., 2001. Rheological properties of PMMA bone cements during curing. *Biomaterials* 22, 3005–3013.
87. Feng, W., Nie, W., He, C., Zhou, X., Chen, L., Qiu, K., Wang, W., Yin, Z., 2014. Effect of pH-responsive alginate/chitosan multilayers coating on delivery efficiency, cellular uptake and biodistribution of mesoporous silica nanoparticles based nanocarriers. *Achitosan Applied Materials and Interfaces* 6, 8447–8460.
88. Firme, C.P., Bandaru, P.R., 2010. Toxicity issues in the application of carbon nanotubes to biological systems. *Nanomedicine* 6, 245–256.
89. Font-Rodriguez, D.E., Scuderi, G.R., Insall, J.N., 1997. Survivorship of cemented total knee arthroplasty. *Clin. Orthop. Relat. Res.* 79–86.
90. Freemont, A., 2012. The pathology of joint replacement and tissue engineering. *Diagnostic Histopathology* 18, 169–176.
91. Fsadni, C., Fsadni, P., 2013. Prosthetic joint infections. *Malta Medical Journal* 25, 15–20.

92. Fulkerson, E., Valle, C.J.D., Wise, B., Walsh, M., Preston, C., Di Cesare, P.E., 2006. Antibiotic susceptibility of bacteria infecting total joint arthroplasty sites. *J Bone Joint Surg Am* 88, 1231–1237.
93. Gálvez-López, R., Peña-Monje, A., Antelo-Lorenzo, R., Guardia-Olmedo, J., Moliz, J., Hernández-Quero, J., Parra-Ruiz, J., 2014. Elution kinetics, antimicrobial activity, and mechanical properties of 11 different antibiotic loaded acrylic bone cement. *Diagnostic Microbiology and Infectious Disease* 78, 70–74.
94. Garibaldi, R.A., 1988. Prevention of intraoperative wound contamination with chlorhexidine shower and scrub. *J. Hosp. Infect.* 11 Suppl B, 5–9.
95. Gasparini, G., De, G., Calonego, G., Bora, T.D., Caroleo, B., Galasso, O., 2014. Drug elution from high-dose antibiotic-loaded acrylic cement: A comparative, in vitro study. *Orthopedics* 37, e999–e1005.
96. Ge, L., Li, Q., Wang, M., Ouyang, J., Li, X., Xing, M.M., 2014. Nanosilver particles in medical applications: synthesis, performance, and toxicity. *Int J Nanomedicine* 9, 2399–2407.
97. Gentile, P., Carmagnola, I., Nardo, T., Chiono, V., 2015. Layer-by-layer assembly for biomedical applications in the last decade. *Nanotechnology* 26, 422001.
98. Giannelli, M., Chellini, F., Margheri, M., Tonelli, P., Tani, A., 2008. Effect of chlorhexidine digluconate on different cell types: a molecular and ultrastructural investigation. *Toxicol In Vitro* 22, 308–317.
99. Gill, G.S., Chan, K.C., Mills, D.M., 1997. 5- to 18-year follow-up study of cemented total knee arthroplasty for patients 55 years old or younger. *J Arthroplasty* 12, 49–54.
100. Gimeno, M., Pinczowski, P., Pérez, M., Giorello, A., Martínez, M.Á., Santamaría, J., Arruebo, M., Luján, L., 2015. A controlled antibiotic release system to prevent orthopedic-implant associated infections: An in vitro study. *European Journal of Pharmaceutics and Biopharmaceutics* 96, 264–271.
101. Ginebra, M.-P., Canal, C., Espanol, M., Pastorino, D., Montufar, E.B., 2012. Calcium phosphate cements as drug delivery materials. *Advanced Drug Delivery Reviews* 64, 1090–1110.
102. Grech, J.M.R., Mano, J.F., Reis, R.L., 2008. Chitosan beads as templates for layer-by-layer assembly and their application in the sustained release of bioactive agents. *Journal of Bioactive and Compatible Polymers* 23, 367–380.
103. Greidanus, N.V., Peterson, R.C., Masri, B.A., Garbuz, D.S., 2011. Quality of Life Outcomes in Revision Versus Primary Total Knee Arthroplasty. *The Journal of Arthroplasty* 26, 615–620.
104. Ha, C.-W., 2006. A technique for intraoperative construction of antibiotic spacers. *Clin. Orthop. Relat. Res.* 445, 204–209.
105. Habraken, W.J.E.M., Wolke, J.G.C., Jansen, J.A., 2007. Ceramic composites as matrices and scaffolds for drug delivery in tissue engineering. *Advanced Drug Delivery Reviews* 59, 234–248.

106. Haddad, F.S., Masri, B.A., Campbell, D., McGraw, R.W., Beauchamp, C.P., Duncan, C.P., 2000. The PROSTALAC functional spacer in two-stage revision for infected knee replacements. *Journal of Bone and Joint Surgery - Series B* 82, 807–812.
107. Han, U., Seo, Y., Hong, J., 2016. Effect of pH on the structure and drug release profiles of layer-by-layer assembled films containing polyelectrolyte, micelles, and graphene oxide. *Scientific Reports* 6.
108. He, W., Mosselhy, D.A., Zheng, Y., Feng, Q., Li, X., Yang, X., Yue, L., Hannula, S.-P., 2018. Effects of silica-gentamicin nanohybrids on osteogenic differentiation of human osteoblast-like SaOS-2 cells. *Int J Nanomedicine* 13, 877–893.
109. He, Y., Trotignon, J.P., Loty, B., Tcharkhtchi, A., Verdu, J., 2002. Effect of antibiotics on the properties of poly(methylmethacrylate)-based bone cement. *J. Biomed. Mater. Res.* 63, 800–806.
110. Helbig, L., Bechberger, M., Aldeeri, R., Ivanova, A., Haubruck, P., Miska, M., Schmidmaier, G., Omlor, G.W., 2018. Initial peri- and postoperative antibiotic treatment of infected nonunions: results from 212 consecutive patients after mean follow-up of 34 months. *Ther Clin Risk Manag* 14, 59–67.
111. Hibbard, J.S., 2005. Analyses comparing the antimicrobial activity and safety of current antiseptic agents: a review. *J Infus Nurs* 28, 194–207.
112. Hidalgo, E., Dominguez, C., 2001. Mechanisms underlying chlorhexidine-induced cytotoxicity. *Toxicology in Vitro* 15, 271–276.
113. Higgs, W.A.J., Lucksanasombool, P., Higgs, R.J.E.D., Swain, M.V., 2001. Comparison of the material properties of PMMA and glass-ionomer based cements for use in orthopaedic surgery. *Journal of Materials Science: Materials in Medicine* 12, 453–460.
114. Holt, D.M., Watts, J.D., Beeson, T.J., Kirkpatrick, T.C., Rutledge, R.E., 2007. The Anti-microbial Effect Against *Enterococcus faecalis* and the Compressive Strength of Two Types of Mineral Trioxide Aggregate Mixed With Sterile Water or 2% Chlorhexidine Liquid. *Journal of Endodontics* 33, 844–847.
115. Horner, C., Mawer, D., Wilcox, M., 2012. Reduced susceptibility to chlorhexidine in staphylococci: is it increasing and does it matter? *J. Antimicrob. Chemother.* 67, 2547–2559.
116. Hsieh, P.-H., Chen, L.-H., Chen, C.-H., Lee, M.S., Yang, W.-E., Shih, C.-H., 2004. Two-stage revision hip arthroplasty for infection with a custom-made, antibiotic-loaded, cement prosthesis as an interim spacer. *J Trauma* 56, 1247–1252.
117. Hsieh, P.-H., Huang, K.-C., Tai, C.-L., 2009. Liquid Gentamicin in Bone Cement Spacers: In Vivo Antibiotic Release and Systemic Safety in Two-Stage Revision of Infected Hip Arthroplasty: *The Journal of Trauma: Injury, Infection, and Critical Care* 66, 804–808.
118. Hughes, K.F., Ries, M.D., Pruitt, L.A., 2003. Structural degradation of acrylic bone cements due to in vivo and simulated aging. *J. Biomed. Mater. Res.* 65A, 126–135.

119. Huh, A.J., Kwon, Y.J., 2011. "Nanoantibiotics": a new paradigm for treating infectious diseases using nanomaterials in the antibiotics resistant era. *J Control Release* 156, 128–145.
120. C. Schoonover, G. M. Brauer, and W. T. Sweeney, 1952. Effect of water on the induction period of the polymerization of methyl methacrylate : *NIST Journal of Research*.
121. Ignarro, L.J., Buga, G.M., Wood, K.S., Byrns, R.E., Chaudhuri, G., 1987. Endothelium-derived relaxing factor produced and released from artery and vein is nitric oxide. *Proc. Natl. Acad. Sci. U.S.A.* 84, 9265–9269.
122. Ince, A., Schütze, N., Karl, N., Löhr, J.F., Eulert, J., 2007. Gentamicin negatively influenced osteogenic function in vitro. *Int Orthop* 31, 223–228.
123. Isiklar, Z.U., Demirörs, H., Akpınar, S., Tandogan, R.N., Alparslan, M., 1999. Two-stage treatment of chronic staphylococcal orthopaedic implant-related infections using vancomycin impregnated PMMA spacer and rifampin containing antibiotic protocol. *Bull Hosp Jt Dis* 58, 79–85.
124. ISO 5833:2002 [WWW Document], 2002. URL <https://www.iso.org/standard/30980.html> (accessed 3.18.17).
125. Izquierdo-Barba, I., Colilla, M., Vallet-Regí, M., 2008. Nanostructured Mesoporous Silicas for Bone Tissue Regeneration [WWW Document]. *Journal of Nanomaterials*. URL <https://www.hindawi.com/journals/jnm/2008/106970/> (accessed 1.23.18).
126. Jackson, J., Leung, F., Duncan, C., Mugabe, C., Burt, H., 2011. The use of bone cement for the localized, controlled release of the antibiotics vancomycin, linezolid, or fusidic acid: Effect of additives on drug release rates and mechanical strength. *Drug Delivery and Translational Research* 1, 121–131.
127. Jaekel, D.J., Day, J.S., Klein, G.R., Levine, H., Parvizi, J., Kurtz, S.M., 2012. Do dynamic cement-on-cement knee spacers provide better function and activity during two-stage exchange? *Clin. Orthop. Relat. Res.* 470, 2599–2604.
128. James, P., Worthington, H.V., Parnell, C., Harding, M., Lamont, T., Cheung, A., Whelton, H., Riley, P., 2017. Chlorhexidine mouthrinse as an adjunctive treatment for gingival health. *Cochrane Database Syst Rev* 3, CD008676.
129. John, G., Becker, J., Schwarz, F., 2014. Effects of taurolidine and chlorhexidine on SaOS-2 cells and human gingival fibroblasts grown on implant surfaces. *Int J Oral Maxillofac Implants* 29, 728–734.
130. Johnson, V.L., Hunter, D.J., 2014. The epidemiology of osteoarthritis. *Best Practice & Research Clinical Rheumatology, Osteoarthritis: Moving from Evidence to Practice* 28, 5–15.
131. Kalhapure, R.S., Suleman, N., Mocktar, C., Seedat, N., Govender, T., 2015. Nanoengineered Drug Delivery Systems for Enhancing Antibiotic Therapy. *J. Pharm. Sci.* 104, 872–905.
132. Kallala, R., Anderson, P., Morris, S., Haddad, F.S., 2013. The cost analysis of cemented versus cementless total hip replacement operations on the NHS. *Bone Joint J* 95-B, 874–876.

133. Kallala, R.F., Vanhegan, I.S., Ibrahim, M.S., Sarmah, S., Haddad, F.S., 2015. Financial analysis of revision knee surgery based on NHS tariffs and hospital costs. *Bone Joint J* 97-B, 197–201.
134. Kampf, G., 2016. Acquired resistance to chlorhexidine – is it time to establish an ‘antiseptic stewardship’ initiative? *Journal of Hospital Infection* 94, 213–227.
135. Karpiński, T.M., Szkaradkiewicz, A.K., 2015. Chlorhexidine--pharmacobiological activity and application. *Eur Rev Med Pharmacol Sci* 19, 1321–1326.
136. Kendrick, B.J.L., Kaptein, B.L., Valstar, E.R., Gill, H.S., Jackson, W.F.M., Dodd, C. a. F., Price, A.J., Murray, D.W., 2015. Cemented versus cementless Oxford unicompartmental knee arthroplasty using radiostereometric analysis: a randomised controlled trial. *Bone Joint J* 97-B, 185–191.
137. Kenny, S.M., Buggy, M., 2003. Bone cements and fillers: A review. *Journal of Materials Science: Materials in Medicine* 14, 923–938.
138. Khaled, S.M.Z., Charpentier, P.A., Rizkalla, A.S., 2011. Physical and mechanical properties of PMMA bone cement reinforced with nano-sized titania fibers. *J Biomater Appl* 25, 515–537.
139. Kim, L., Montejano, L.B., Cao, Z., Zhao, Y., Ang, D., 2012. Health care costs in US patients with and without a diagnosis of osteoarthritis. *Journal of Pain Research* 5, 23–30.
140. Kinnari, T.J., Esteban, J., Martin-de-Hijas, N.Z., Sánchez-Muñoz, O., Sánchez-Salcedo, S., Colilla, M., Vallet-Regí, M., Gomez-Barrena, E., 2009. Influence of surface porosity and pH on bacterial adherence to hydroxyapatite and biphasic calcium phosphate bioceramics. *Journal of Medical Microbiology* 58, 132–137.
141. Knox, R.W., Demons, S.T., Cunningham, C.W., 2015. A novel method to decontaminate surgical instruments for operational and austere environments. *Wilderness and Environmental Medicine* 26, 509–513.
142. Kokubo, T., Kim, H.-M., Kawashita, M., 2003. Novel bioactive materials with different mechanical properties. *Biomaterials, Focus on Biomaterials Science in Asia* 24, 2161–2175.
143. Krause, W.R., Hofmann, A., 1989. Antibiotic Impregnated Acrylic Bone Cements: A Comparative Study of the Mechanical Properties. *Journal of Bioactive and Compatible Polymers* 4, 345–361.
144. Krüger, R., Groll, J., 2012. Fiber reinforced calcium phosphate cements - On the way to degradable load bearing bone substitutes? *Biomaterials* 33, 5887–5900.
145. Kuechle, D.K., Landon, G.C., Musher, D.M., Noble, P.C., 1991. Elution of vancomycin, daptomycin, and amikacin from acrylic bone cement. *Clin. Orthop. Relat. Res.*, 264, 302–308.
146. Kurd, M.F., Ghanem, E., Steinbrecher, J., Parvizi, J., 2010. Two-stage Exchange Knee Arthroplasty: Does Resistance of the Infecting Organism Influence the Outcome? *Clin Orthop Relat Res* 468, 2060–2066.

147. Kurtjak, M., Vukomanović, M., Kramer, L., Suvorov, D., 2016. Biocompatible nano-gallium/hydroxyapatite nanocomposite with antimicrobial activity. *J Mater Sci: Mater Med* 27 (11), 170.
148. Kurtz, S., Mowat, F., Ong, K., Chan, N., Lau, E., Halpern, M., 2005. Prevalence of primary and revision total hip and knee arthroplasty in the United States from 1990 through 2002. *Journal of Bone and Joint Surgery - Series A* 87, 1487–1497.
149. Kurtz, S.M., Lau, E., Ong, K., Zhao, K., Kelly, M., Bozic, K.J., 2009. Future young patient demand for primary and revision joint replacement: National projections from 2010 to 2030. *Clinical Orthopaedics and Related Research* 467, 2606–2612.
150. Kurtz, S.M., Lau, E., Watson, H., Schmier, J.K., Parvizi, J., 2012. Economic burden of periprosthetic joint infection in the united states. *Journal of Arthroplasty* 27, 61-65.
151. Labek, G., Thaler, M., Janda, W., Agreiter, M., Stöckl, B., 2011. Revision rates after total joint replacement. *J Bone Joint Surg Br* 93-B (3), 293–297.
152. Lamagni, T., 2014. Epidemiology and burden of prosthetic joint infections. *Journal of Antimicrobial Chemotherapy* 69 (Suppl 1), i5–i10.
153. Lecoeur, H., 2002. Nuclear Apoptosis Detection by Flow Cytometry: Influence of Endogenous Endonucleases. *Experimental Cell Research* 277, 1–14.
154. Lee, C., 2005. The Mechanical Properties of PMMA Bone Cement. In: *The Well-Cemented Total Hip Arthroplasty*. Springer Berlin Heidelberg, pp. 60–66.
155. Lee, T.-H., Hu, C.-C., Lee, S.-S., Chou, M.-Y., Chang, Y.-C., 2010. Cytotoxicity of chlorhexidine on human osteoblastic cells is related to intracellular glutathione levels. *Int Endod J* 43(5), 430–435.
156. Lefort, A., Arthur, M., Garry, L., Carbon, C., Courvalin, P., Fantin, B., 2000. Bactericidal Activity of Gentamicin against *Enterococcus faecalis* In Vitro and In Vivo. *Antimicrob. Agents Chemother.* 44, 2077–2080.
157. Legrand, C., Bour, J.M., Jacob, C., Capiaumont, J., Martial, A., Marc, A., Wudtke, M., Kretzmer, G., Demangel, C., Duval, D., 1992. Lactate dehydrogenase (LDH) activity of the cultured eukaryotic cells as marker of the number of dead cells in the medium [corrected]. *J. Biotechnol.* 25(3), 231–243.
158. Letchmanan, K., Shen, S.-C., Ng, W.K., Kingshuk, P., Shi, Z., Wang, W., Tan, R.B.H., 2017. Mechanical properties and antibiotic release characteristics of poly (methyl methacrylate)-based bone cement formulated with mesoporous silica nanoparticles. *Journal of the Mechanical Behavior of Biomedical Materials* 72, 163–170.
159. Lewis, G., 1997. Properties of acrylic bone cement: State of the art review. *J. Biomed. Mater. Res.* 38, 155–182.
160. Lewis, G., 2009. Properties of antibiotic-loaded acrylic bone cements for use in cemented arthroplasties: A state-of-the-art review. *Journal of Biomedical Materials Research - Part B Applied Biomaterials* 89, 558–574.

161. Lewis, G., Janna, S., 2006. Estimation of the optimum loading of an antibiotic powder in an acrylic bone cement: Gentamicin sulfate in SmartSet HV. *Acta Orthopaedica* 77, 622–627.
162. Li, L.-L., Wang, L.-M., Xu, Y., Lv, L.-X., 2012. Preparation of gentamicin-loaded electrospun coating on titanium implants and a study of their properties in vitro. *Archives of Orthopaedic and Trauma Surgery* 132, 897–903.
163. Li, S., Li, W., Khashab, N.M., 2012. Stimuli responsive nanomaterials for controlled release applications. *Nanotechnology Reviews* 1, 493–513.
164. Liddle, A.D., Judge, A., Pandit, H., Murray, D.W., 2014. Adverse outcomes after total and unicompartmental knee replacement in 101330 matched patients: A study of data from the National Joint Registry for England and Wales. *The Lancet* 384, 1437–1445.
165. Lim, S.M., Song, D.K., Oh, S.H., Lee-Yoon, D.S., Bae, E.H., Lee, J.H., 2008. In vitro and in vivo degradation behavior of acetylated chitosan porous beads. *Journal of Biomaterials Science, Polymer Edition* 19, 453–466.
166. Litwic, A., Edwards, M.H., Dennison, E.M., Cooper, C., 2013. Epidemiology and burden of osteoarthritis. *British Medical Bulletin* 105, 185–199.
167. Liu, S., Wei, M., Zheng, X., Xu, S., Xia, F., Zhou, C., 2015. Alizarin red S functionalized mesoporous silica modified glassy carbon electrode for electrochemical determination of anthracene. *Electrochimica Acta* 160, 108–113.
168. Liu, X.-W., Zi, Y., Xiang, L.-B., Wang, Y., 2015. Total hip arthroplasty: a review of advances, advantages and limitations. *Int J Clin Exp Med* 8, 27–36.
169. Liu, Y., Peterson, D.A., Kimura, H., Schubert, D., 1997. Mechanism of cellular 3-(4,5-dimethylthiazol-2-yl)-2,5-diphenyltetrazolium bromide (MTT) reduction. *J. Neurochem.* 69, 581–593.
170. Liu, Y., Wang, X., Song, W., Wang, G., 2015. Synthesis and characterization of silica nanoparticles functionalized with multiple TEMPO groups and investigation on their oxidation activity. *Polymer Chemistry* 6, 7514–7523.
171. Lu, H.-T., 2013. Synthesis and characterization of amino-functionalized silica nanoparticles. *Colloid J* 75, 311–318.
172. Lu, M., Wang, Q., Chang, Z., Wang, Z., Zheng, X., Shao, D., Dong, W., Zhou, Y., 2017. Synergistic bactericidal activity of chlorhexidine-loaded, silver-decorated mesoporous silica nanoparticles. *Int J Nanomedicine* 12, 3577–3589.
173. Lucchese, A., Storti, E., Roncati, M., Danesi, M.V., Hehsani, S., Sberna, M.T., 2012. Effectiveness of chlorhexidine on dental plaque: a new technique. *Minerva Stomatol* 61, 449–456.
174. Luo, D., Shahid, S., Wilson, R.M., Cattell, M.J., Sukhorukov, G.B., 2016. Novel Formulation of Chlorhexidine Spheres and Sustained Release with Multilayered Encapsulation. *Achitosan Appl. Mater. Interfaces* 8, 12652–12660.

175. Lynn, D.M., Langer, R., 2000. Degradable Poly( $\beta$ -amino esters): Synthesis, Characterization, and Self-Assembly with Plasmid DNA. *J. Am. Chem. Soc.* 122, 10761–10768.
176. Magalini, S., Pepe, G., Panunzi, S., De Gaetano, A., Abatini, C., Di Giorgio, A., Foco, M., Gui, D., 2013. Observational study on preoperative surgical field disinfection: povidone-iodine and chlorhexidine-alcohol. *Eur Rev Med Pharmacol Sci* 17, 3367–3375.
177. Magnan, B., Bondi, M., Maluta, T., Samaila, E., Schirru, L., Dall'Oca, C., 2013. Acrylic bone cement: Current concept review. *Musculoskeletal Surgery* 97, 93–100.
178. Mai, T.B., Tran, T.N., Islam, M.R., Park, J.M., Lim, K.T., 2013. Covalent functionalization of silica nanoparticles with poly(N-isopropylacrylamide) employing thiol-ene chemistry and activator regenerated by electron transfer ATRP protocol. *J Mater Sci* 49, 1519–1526.
179. Malik, M.H.A., Chougale, A., Pradhan, N., Gambhir, A.K., Porter, M.L., 2005. Primary total knee replacement: a comparison of a nationally agreed guide to best practice and current surgical technique as determined by the North West Regional Arthroplasty Register. *Ann R Coll Surg Engl* 87, 117–122.
180. Mangram, A.J., Horan, T.C., Pearson, M.L., Silver, L.C., Jarvis, W.R., 1999. Guideline for Prevention of Surgical Site Infection, 1999. Centers for Disease Control and Prevention (CDC) Hospital Infection Control Practices Advisory Committee. *Am J Infect Control* 27, 97–132; quiz 133–134; discussion 96.
181. Mansour, H.M., Rhee, Y.-S., Wu, X., 2009. Nanomedicine in pulmonary delivery. *Int J Nanomedicine* 4, 299–319.
182. Maradit, K., Larson, D.R., Crowson, C.S., Kremers, W.K., Washington, R.E., Steiner, C.A., Jiranek, W.A., Berry, D.J., 2015. Prevalence of Total Hip and Knee Replacement in the United States. *The Journal of bone and joint surgery. American volume* 97, 1386–1397.
183. Maradit, K., Visscher, S.L., Moriarty, J.P., Reinalda, M.S., Kremers, W.K., Naessens, J.M., Lewallen, D.G., 2013. Determinants of direct medical costs in primary and revision total knee arthroplasty knee. *Clinical Orthopaedics and Related Research* 471, 206–214.
184. Mariotti, A.J., Rumpf, D.A., 1999. Chlorhexidine-induced changes to human gingival fibroblast collagen and non-collagen protein production. *J. Periodontol.* 70, 1443–1448.
185. Markley, J.D., Bernard, S., Delacruz, O., 2015. Combination Antibiotic Therapy for the Definitive Management of Select Multidrug-Resistant Gram-Negative Rod Infections. *Curr Treat Options Infect Dis* 7, 273–290.
186. Martínez-Moreno Javier, Merino Virginia, Nácher Amparo, Rodrigo José Luis, Climente Mónica, Merino-Sanjuán Matilde, 2017. Antibiotic-loaded Bone Cement as Prophylaxis in Total Joint Replacement. *Orthopaedic Surgery* 9, 331–341.

187. Masri, B.A., Duncan, C.P., Beauchamp, C.P., 1998. Long-term elution of antibiotics from bone-cement: An in vivo study using the prosthesis of antibiotic-loaded acrylic cement (PROSTALAC) system. *Journal of Arthroplasty* 13, 331–338.
188. Masri, B. A., Duncan, C.P., Beauchamp, C.P., 1998. Long-term elution of antibiotics from bone-cement: an in vivo study using the prosthesis of antibiotic-loaded acrylic cement (PROSTALAC) system. *J Arthroplasty* 13, 331–338.
189. Masters, J.P.M., Smith, N.A., Foguet, P., Reed, M., Parsons, H., Sprowson, A.P., 2013. A systematic review of the evidence for single stage and two stage revision of infected knee replacement. *BMC Musculoskeletal Disorders* 14, 222.
190. McLendon, J.M., Joshi, S.R., Sparks, J., Matar, M., Fewell, J.G., Abe, K., Oka, M., McMurtry, I.F., Gerthoffer, W.T., 2015. Lipid nanoparticle delivery of a microRNA-145 inhibitor improves experimental pulmonary hypertension. *Journal of Controlled Release* 210, 67–75.
191. McNeil, S.E. (Ed.), 2011. *Characterization of Nanoparticles Intended for Drug Delivery*, *Methods in Molecular Biology*. Humana Press, Totowa, NJ., 79(3), 701.
192. Medernach, R.L., Logan, L.K., 2018. The Growing Threat of Antibiotic Resistance in Children. *Infect. Dis. Clin. North Am.* 32, 1–17.
193. Meer, J.W.M.V.D., Fears, R., Meulen, V.T., 2016. Can we Tackle the Antibiotic Threat? *European Review* 24, 49–62.
194. Meyer, J., Piller, G., Spiegel, C.A., Hetzel, S., Squire, M., 2011. Vacuum-mixing significantly changes antibiotic elution characteristics of commercially available antibiotic-impregnated bone cements. *Journal of Bone and Joint Surgery - Series A* 93, 2049–2056.
195. Miller, R.B., McLaren, A.C., Leon, C.M., Vernon, B.L., McLemore, R., 2011. Surfactant-stabilized emulsion increases gentamicin elution from bone cement. *Clin. Orthop. Relat. Res.* 469, 2995–3001.
196. Milstone, A.M., Passaretti, C.L., Perl, T.M., 2008. Chlorhexidine: expanding the armamentarium for infection control and prevention. *Clin. Infect. Dis.* 46, 274–281.
197. Min, J., Braatz, R.D., Hammond, P.T., 2014. Tunable staged release of therapeutics from layer-by-layer coatings with clay interlayer barrier. *Biomaterials* 35, 2507–2517.
198. Mocharla, R., Mocharla, H., Hodes, M.E., 1987. A novel, sensitive fluorometric staining technique for the detection of DNA in RNA preparations. *Nucleic Acids Res.*, 15(24), 10589.
199. Moojen, D.J.F., Hentenaar, B., Charles Vogely, H., Verbout, A.J., Castelein, R.M., Dhert, W.J.A., 2008. In Vitro Release of Antibiotics from Commercial PMMA Beads and Articulating Hip Spacers. *The Journal of Arthroplasty* 23, 1152–1156.

200. Moskowitz, J.S., Blaisse, M.R., Samuel, R.E., Hsu, H.-P., Harris, M.B., Martin, S.D., Lee, J.C., Spector, M., Hammond, P.T., 2010. The effectiveness of the controlled release of gentamicin from polyelectrolyte multilayers in the treatment of *Staphylococcus aureus* infection in a rabbit bone model. *Biomaterials* 31, 6019–6030.
201. Mu, H., Tang, J., Liu, Q., Sun, C., Wang, T., Duan, J., 2016. Potent Antibacterial Nanoparticles against Biofilm and Intracellular Bacteria. *Scientific Reports* 6, 18877.
202. Mulazimoglu, L., Drenning, S.D., Muder, R.R., 1996. Vancomycin-gentamicin synergism revisited: effect of gentamicin susceptibility of methicillin-resistant *Staphylococcus aureus*. *Antimicrob. Agents Chemother.* 40, 1534–1535.
203. Münker, T.J.A.G., van de Vijfeijken, S.E.C.M., Mulder, C.S., Vespasiano, V., Becking, A.G., Kleverlaan, C.J., Becking, A.G., Dubois, L., Karssemakers, L.H.E., Milstein, D.M.J., van de Vijfeijken, S.E.C.M., Depauw, P.R.A.M., Hoefnagels, F.W.A., Vandertop, W.P., Kleverlaan, C.J., Münker, T.J.A.G., Maal, T.J.J., Nout, E., Riool, M., Zaat, S.A.J., 2018. Effects of sterilization on the mechanical properties of poly(methyl methacrylate) based personalized medical devices. *Journal of the Mechanical Behavior of Biomedical Materials* 81, 168–172.
204. Nandi, S.K., Mukherjee, P., Roy, S., Kundu, B., De, D.K., Basu, D., 2009. Local antibiotic delivery systems for the treatment of osteomyelitis – A review. *Materials Science and Engineering: C* 29, 2478–2485.
205. NAR, 2010. The Norwegian Arthroplasty Register. URL <http://nrlweb.ihelse.net/eng/default.htm> [accessed 8<sup>th</sup> march 2016]
206. Neo, M., Kotani, S., Nakamura, T., Yamamuro, T., Ohtsuki, C., Kokubo, T., Bando, Y., 1992. A comparative study of ultrastructures of the interfaces between four kinds of surface-active ceramic and bone. *J. Biomed. Mater. Res.* 26, 1419–1432.
207. N.H.S. choices, 2014. Hip replacement - How it is done - NHS Choices [Online] Available at: <http://www.nhs.uk/Conditions/Hip-replacement/Pages/How-it-is-performed.aspx> [Accessed: 7 March 2016].
208. Ni, G.X., Choy, Y.S., Lu, W.W., Ngan, A.H.W., Chiu, K.Y., Li, Z.Y., Tang, B., Luk, K.D.K., 2006. Nano-mechanics of bone and bioactive bone cement interfaces in a load-bearing model. *Biomaterials* 27, 1963–1970.
209. Nien, Y.-H., Chen, J., 2006. Studies of the mechanical and thermal properties of cross-linked poly (methylmethacrylate-acrylic acid-allylmethacrylate)-modified bone cement. *Journal of Applied Polymer Science* 100, 3727–3732.
210. Niu, Y., Chan, W.-I., Yu, N., Gan, J., Dong, L., Wang, C., 2015. APTES-modified nanosilica - But neither APTES nor nanosilica - Inhibits endothelial cell growth via arrest of cell cycle at G1 phase. *Journal of Biomaterials Applications* 30, 608–617.
211. NJR, 2015. National joint registry 12th annual report. URL <http://www.njrcentre.org.uk/njrcentre/Portals/0/Documents/England/Reports/>

212. Nourmohammadi, J., Sadrnezhad, S.K., Behnam, G., 2008. Bone-like apatite layer formation on the new resin-modified glass-ionomer cement. *Journal of Materials Science: Materials in Medicine* 19, 3507–3514.
213. O'Brien, D., Boyd, D., Madigan, S., Murphy, S., 2010. Evaluation of a novel radiopacifying agent on the physical properties of surgical spineplex®. *Journal of Materials Science: Materials in Medicine* 21, 53–58.
214. Odum, S.M., Fehring, T.K., Lombardi, A.V., Zmistowski, B.M., Brown, N.M., Luna, J.T., Fehring, K.A., Hansen, E.N., Periprosthetic Infection Consortium, 2011. Irrigation and debridement for periprosthetic infections: does the organism matter? *J Arthroplasty* 26, 114–118.
215. Oei, J.D., Zhao, W.W., Chu, L., DeSilva, M.N., Ghimire, A., Rawls, H.R., Whang, K., 2012. Antimicrobial acrylic materials with in situ generated silver nanoparticles. *J. Biomed. Mater. Res.* 100B, 409–415.
216. Olivares-Navarrete, R., Raines, A.L., Hyzy, S.L., Park, J.H., Hutton, D.L., Cochran, D.L., Boyan, B.D., Schwartz, Z., 2012. Osteoblast maturation and new bone formation in response to titanium implant surface features are reduced with age. *J. Bone Miner. Res.* 27, 1773–1783.
217. O'Malley, P., 2008. Chlorhexidine wipes: The new weapon against surgical site infections? *Clinical Nurse Specialist* 22, 61–62.
218. Ong, K.L., Lau, E., Suggs, J., Kurtz, S.M., Manley, M.T., 2010. Risk of subsequent revision after primary and revision total joint arthroplasty. *Clinical Orthopaedics and Related Research* 468, 3070–3076.
219. Oonishi, H., 2012. A long term histological analysis of effect of interposed hydroxyapatite between bone and bone cement in THA and TKA. *Journal of Long-Term Effects of Medical Implants* 22, 165–176.
220. Oosterwaal, P.J., Mikx, F.H., van den Brink, M.E., Renggli, H.H., 1989. Bactericidal concentrations of chlorhexidine-digluconate, amine fluoride gel and stannous fluoride gel for subgingival bacteria tested in serum at short contact times. *J. Periodont. Res.* 24, 155–160.
221. Owens, B.D., White, D.W., Wenke, J.C., 2009. Comparison of irrigation solutions and devices in a contaminated musculoskeletal wound survival model. *J Bone Joint Surg Am* 91, 92–98.
222. Pabinger, C., Berghold, A., Boehler, N., Labek, G., 2013. Revision rates after knee replacement. Cumulative results from worldwide clinical studies versus joint registers. *Osteoarthritis and Cartilage* 21, 263–268.
223. Park, S.-J., Song, E.-K., Seon, J.-K., Yoon, T.-R., Park, G.-H., 2010. Comparison of static and mobile antibiotic-impregnated cement spacers for the treatment of infected total knee arthroplasty. *Int Orthop* 34, 1181–1186.
224. Parvizi, J., Saleh, K.J., Ragland, P.S., Pour, A.E., Mont, M.A., 2008. Efficacy of antibiotic-impregnated cement in total hip replacement. *Acta Orthop* 79, 335–341.

225. Patel, A., Pavlou, G., Mújica-Mota, R.E., Toms, A.D., 2015. The epidemiology of revision total knee and hip arthroplasty in England and Wales: A comparative analysis with projections for the United States. a study using the national joint registry dataset. *Bone and Joint Journal* 97-B, 1076–1081.
226. Patel, P.D., Klika, A.K., Murray, T.G., Elsharkawy, K.A., Krebs, V.E., Barsoum, W.K., 2010. Influence of technique with distally fixed modular stems in revision total hip arthroplasty. *J Arthroplasty* 25, 926–931.
227. Paz, E., Sanz-Ruiz, P., Abenojar, J., Vaquero-Martín, J., Forriol, F., Del Real, J.C., 2015. Evaluation of Elution and Mechanical Properties of High-Dose Antibiotic-Loaded Bone Cement: Comparative “In Vitro” Study of the Influence of Vancomycin and Cefazolin. *The Journal of Arthroplasty* 30, 1423–1429.
228. Peel, T.N., Cheng, A.C., Busing, K.L., Dowsey, M.M., Choong, P.F.M., 2014. Alcoholic Chlorhexidine or Alcoholic Iodine Skin Antisepsis (ACAISA): protocol for cluster randomised controlled trial of surgical skin preparation for the prevention of superficial wound complications in prosthetic hip and knee replacement surgery. *BMJ Open* 4(5).
229. Penner, M.J., Duncan, C.P., Masri, B.A., 1999. The in vitro elution characteristics of antibiotic-loaded CMW and Palacos-R bone cements. *Journal of Arthroplasty* 14, 209–214.
230. Penner, M.J., Masri, B.A., Duncan, C.P., 1996. Elution characteristics of vancomycin and tobramycin combined in acrylic bone-cement. *J Arthroplasty* 11, 939–944.
231. Perni, S., Prokopovich, P., 2014. Continuous release of gentamicin from gold nanocarriers. *RSC Advances* 4, 51904–51910.
232. Perni, S., Prokopovich, P., 2017. Poly-beta-amino-esters nano-vehicles based drug delivery system for cartilage. *Nanomedicine* 13, 539–548.
233. Perni, S., Thenault, V., Abdo, P., Margulis, K., Magdassi, S., Prokopovich, P., 2015. Antimicrobial activity of bone cements embedded with organic nanoparticles. *International Journal Of Nanomedicine* 10, 6317–6329.
234. Persson, C., Baleani, M., Guandalini, L., Tigani, D., Viceconti, M., 2006. Mechanical effects of the use of vancomycin and meropenem in acrylic bone cement. *Acta Orthopaedica* 77, 617–621.
235. Polin, R.A., 2012. Management of neonates with suspected or proven early-onset bacterial sepsis. *Pediatrics* 129, 1006–1015.
236. Prasad, M., Patthi, B., Singla, A., Gupta, R., Jankiram, C., Kumar, J.K., Vashishtha, V., Malhi, R., 2016. The Clinical Effectiveness of Post-Brushing Rinsing in Reducing Plaque and Gingivitis: A Systematic Review. *J Clin Diagn Res* 10, ZE01-07.
237. Prayle, A., Watson, A., Fortnum, H., Smyth, A., 2010. Side effects of aminoglycosides on the kidney, ear and balance in cystic fibrosis. *Thorax* 65, 654–658.
238. Prokopovich, P., Köbrick, M., Brousseau, E., Perni, S., 2015. Potent antimicrobial activity of bone cement encapsulating silver nanoparticles

- capped with oleic acid. *Journal of Biomedical Materials Research - Part B Applied Biomaterials* 103, 273–281.
239. Prokopovich, P., Leech, R., Carmalt, C.J., Parkin, I.P., Perni, S., 2013. A novel bone cement impregnated with silver-tiopronin nanoparticles: Its antimicrobial, cytotoxic, and mechanical properties. *International Journal of Nanomedicine* 8, 2227–2237.
  240. Rand, J.A., Trousdale, R.T., Ilstrup, D.M., Harmsen, W.S., 2003. Factors affecting the durability of primary total knee prostheses. *J Bone Joint Surg Am* 85-A, 259–265.
  241. Rathbone, C.R., Cross, J.D., Brown, K.V., Murray, C.K., Wenke, J.C., 2011. Effect of various concentrations of antibiotics on osteogenic cell viability and activity. *J. Orthop. Res.* 29, 1070–1074.
  242. Ravichandran, R., Gandhi, S., Sundaramurthi, D., Sethuraman, S., Krishnan, U.M., 2013. Hierarchical mesoporous silica nanofibers as multifunctional scaffolds for bone tissue regeneration. *J. Biomater. Sci.-Polym. Ed.* 24, 1988–2005.
  243. Reich, A., Bae, A.S., Barnes, A.M., Cabral, W.A., Hinek, A., Stimec, J., Hill, S.C., Chitayat, D., Marini, J.C., 2015. Type V OI primary osteoblasts display increased mineralization despite decreased COL1A1 expression. *J. Clin. Endocrinol. Metab.* 100, E325–332.
  244. Ribeiro, M., Monteiro, F.J., Ferraz, M.P., 2012. Infection of orthopedic implants with emphasis on bacterial adhesion process and techniques used in studying bacterial-material interactions. *Biomater* 2, 176–194.
  245. Riool, M., Dirks, A.J., Jaspers, V., de Boer, L., Loontjens, T.J., van der Loos, C.M., Florquin, S., Apachitei, I., Rijk, L.N., Keul, H.A., Zaat, S.A., 2017. A chlorhexidine-releasing epoxy-based coating on titanium implants prevents *Staphylococcus aureus* experimental biomaterial-associated infection. *Eur Cell Mater* 33, 143–157.
  246. Ritter, M.A., Farris, A., 2010. Outcome of infected total joint replacement. *Orthopedics* 33(3).
  247. Ritter, M.A., Lutgring, J.D., Davis, K.E., Faris, P.M., Berend, M.E., 2007. Total knee arthroplasty effectiveness in patients 55 years old and younger: osteoarthritis vs. rheumatoid arthritis. *Knee* 14, 9–11.
  248. Robertsson, O., Knutson, K., Lewold, S., Lidgren, L., 2001. The Swedish Knee Arthroplasty Register 1975–1997: an update with special emphasis on 41,223 knees operated on in 1988–1997. *Acta Orthop Scand* 72, 503–513.
  249. Rodrigues, D.C., Gilbert, J.L., Hasenwinkel, J.M., 2009. Pseudoplasticity and setting properties of two-solution bone cement containing poly (methyl methacrylate) microspheres and nanospheres for kyphoplasty and vertebroplasty. *J. Biomed. Mater. Res.* 91B, 248–256.
  250. Rodriguez, L.C., Palmer, K., Montagner, F., Rodrigues, D.C., 2015. A novel chlorhexidine-releasing composite bone cement: Characterization of antimicrobial effectiveness and cement strength. *Journal of Bioactive and Compatible Polymers* 30, 34–47.

251. Romanò, C.L., Gala, L., Logoluso, N., Romanò, D., Drago, L., 2012. Two-stage revision of septic knee prosthesis with articulating knee spacers yields better infection eradication rate than one-stage or two-stage revision with static spacers. *Knee Surg Sports Traumatol Arthrosc* 20, 2445–2453.
252. Rorabeck, C.H., 1999. Total knee replacement: Should it be cemented or hybrid? *Can J Surg* 42, 21–26.
253. Ruppen, C., Lupo, A., Decosterd, L., Sendi, P., 2016. Is Penicillin Plus Gentamicin Synergistic against Clinical Group B Streptococcus isolates? An In vitro Study. *Front Microbiol* 7, 1680.
254. Saldaña, L., Bensiamar, F., Boré, A., Vilaboa, N., 2011. In search of representative models of human bone-forming cells for cytocompatibility studies. *Acta Biomaterialia* 7, 4210–4221.
255. Sandegren, L., 2014. Selection of antibiotic resistance at very low antibiotic concentrations. *Ups J Med Sci* 119, 103–107.
256. Schmidmaier, G., Lucke, M., Wildemann, B., Haas, N.P., Raschke, M., 2006. Prophylaxis and treatment of implant-related infections by antibiotic-coated implants: a review. *Injury* 37, S105–S112.
257. Schmidt, H.H.H.W., Walter, U., 1994. NO at work. *Cell* 78, 919–925.
258. Schwarz, M.L.R., Kowarsch, M., Rose, S., Becker, K., Lenz, T., Jani, L., 2009. Effect of surface roughness, porosity, and a resorbable calcium phosphate coating on osseointegration of titanium in a minipig model. *Journal of Biomedical Materials Research - Part A* 89, 667–678.
259. Scott, C.P., Higham, P.A., 2003. Antibiotic Bone Cement for the Treatment of *Pseudomonas Aeruginosa* in Joint Arthroplasty: Comparison of Tobramycin and Gentamicin-Loaded Cements. *Journal of Biomedical Materials Research - Part B Applied Biomaterials* 64, 94–98.
260. Seneviratne, C.J., Leung, K.C.-F., Wong, C.-H., Lee, S.-F., Li, X., Leung, P.C., Lau, C.B.S., Wat, E., Jin, L., 2014. Nanoparticle-Encapsulated Chlorhexidine against Oral Bacterial Biofilms. *PLoS One* 9(8), e103234.
261. SHA, 2013. Swedish Hip Arthroplasty. Register [online]. URL <http://www.shpr.se/en/> (accessed 7.3.16).
262. Sharma, A., Arya, D.K., Dua, M., Chhatwal, G.S., Johri, A.K., 2012. Nanotechnology for targeted drug delivery to combat antibiotic resistance. *Expert Opinion on Drug Delivery* 9, 1325–1332.
263. Shen, S.-C., Ng, W.K., Dong, Y.-C., Ng, J., Tan, R.B.H., 2016. Nanostructured material formulated acrylic bone cements with enhanced drug release. *Materials Science and Engineering C* 58, 233–241.
264. Shen, S.-C., Ng, W.K., Shi, Z., Chia, L., Neoh, K.G., Tan, R.B.H., 2011. Mesoporous silica nanoparticle-functionalized poly(methyl methacrylate)-based bone cement for effective antibiotics delivery. *Journal of Materials Science: Materials in Medicine* 22, 2283–2292.
265. Shi, Z., Neoh, K.G., Kang, E.T., Wang, W., 2006. Antibacterial and mechanical properties of bone cement impregnated with chitosan nanoparticles. *Biomaterials* 27, 2440–2449.

266. Sikora, A., Bartczak, D., Geißler, D., Kestens, V., Roebben, G., Ramaye, Y., Varga, Z., Palmai, M., Shard, A.G., Goenaga-Infante, H., Minelli, C., 2015. A systematic comparison of different techniques to determine the zeta potential of silica nanoparticles in biological medium. *Analytical Methods* 7, 9835–9843.
267. Singh, J.A., Dohm, M., Sprowson, A.P., Wall, P.D., Richards, B.L., Gossec, L., Hawker, G.A., Riddle, D.L., Buchbinder, R., 2015. Outcome domains and measures in total joint replacement clinical trials: Can we harmonize them? An OMERACT collaborative initiative. *Journal of Rheumatology* 42, 2496–2502.
268. Sistla, S.C., Prabhu, G., Sistla, S., Sadasivan, J., 2010. Minimizing wound contamination in a “clean” surgery: comparison of chlorhexidine-ethanol and povidone-iodine. *Chemotherapy* 56, 261–267.
269. Skyttä, E.T., Jarkko, L., Antti, E., Huhtala, H., Ville, R., 2011. Increasing incidence of hip arthroplasty for primary osteoarthritis in 30- to 59-year-old patients. *Acta Orthop* 82, 1–5.
270. Small, J.V., Zobeley, S., Rinnerthaler, G., Faulstich, H., 1988. Coumarin-phalloidin: a new actin probe permitting triple immunofluorescence microscopy of the cytoskeleton. *J. Cell. Sci.* 89 (Pt 1), 21–24.
271. Smith, D.C., Maiman, R., Schwechter, E.M., Kim, S.J., Hirsh, D.M., 2015. Optimal Irrigation and Debridement of Infected Total Joint Implants with Chlorhexidine Gluconate. *J Arthroplasty* 30, 1820–1822.
272. Smith, R.C., Riollano, M., Leung, A., Hammond, P.T., 2009. Layer-by-Layer Platform Technology for Small-Molecule Delivery. *Angewandte Chemie International Edition* 48, 8974–8977.
273. Snyder, S.H., 1992. Nitric oxide: first in a new class of neurotransmitters. *Science* 257, 494–496.
274. Sochart, D.H., Porter, M.L., 1997. The long-term results of Charnley low-friction arthroplasty in young patients who have congenital dislocation, degenerative osteoarthrosis, or rheumatoid arthritis. *J Bone Joint Surg Am* 79, 1599–1617.
275. Sosroseno, W., Bird, P.S., Seymour, G.J., 2009. Nitric oxide production by a human osteoblast cell line stimulated with *Aggregatibacter actinomycetemcomitans* lipopolysaccharide. *Oral Microbiol. Immunol.* 24, 50–55.
276. Soto-Cantu, E., Cueto, R., Koch, J., Russo, P.S., 2012. Synthesis and Rapid Characterization of Amine-Functionalized Silica. *Langmuir* 28, 5562–5569.
277. Squire, M.W., Ludwig, B.J., Thompson, J.R., Jagodzinski, J., Hall, D., Andes, D., 2008. Premixed Antibiotic Bone Cement: An In Vitro Comparison of Antimicrobial Efficacy. *The Journal of Arthroplasty, American Association of Hip and Knee Surgeons (AAHKS) Supplement* 23, 110–114.
278. Srivastav, A.K., Nadkarni, B., Srivastav, S., Mittal, V., Agarwal, S., 2009. Prophylactic use of antibiotic-loaded bone cement in primary total knee arthroplasty: Justified or not? *Indian J Orthop* 43, 259–263.

279. Staats, K., Sevelde, F., Kaider, A., Böhler, C., Sigmund, I.K., Puchner, S.E., Windhager, R., Holinka, J., 2017. The influence of antibiotic-loaded cement spacers on the risk of reinfection after septic two-stage hip revision surgery. *Infection* 45, 885–891.
280. Stammers, J., Kahane, S., Ranawat, V., Miles, J., Pollock, R., Carrington, R.W.J., Briggs, T., Skinner, J.A., 2015. Outcomes of infected revision knee arthroplasty managed by two-stage revision in a tertiary referral centre. *The Knee* 22, 56–62.
281. Stöber, W., Fink, A., Bohn, E., 1968. Controlled growth of monodisperse silica spheres in the micron size range. *Journal of Colloid and Interface Science* 26, 62–69.
282. Strange, S., Whitehouse, M.R., Beswick, A.D., Board, T., Burston, A., Burston, B., Carroll, F.E., Dieppe, P., Garfield, K., Gooberman-Hill, R., Jones, S., Kunutsor, S., Lane, A., Lenguerrand, E., MacGowan, A., Moore, A., Noble, S., Simon, J., Stockley, I., Taylor, A.H., Toms, A., Webb, J., Whittaker, J.-P., Wilson, M., Wylde, V., Blom, A.W., 2016. One-stage or two-stage revision surgery for prosthetic hip joint infection - the INFORM trial: A study protocol for a randomised controlled trial. *Trials* 17.
283. Supranoto, S.C., Slot, D.E., Addy, M., Van der Weijden, G.A., 2015. The effect of chlorhexidine dentifrice or gel versus chlorhexidine mouthwash on plaque, gingivitis, bleeding and tooth discoloration: a systematic review. *Int J Dent Hyg* 13, 83–92.
284. Swearingen, M.C., Granger, J.F., Sullivan, A., Stoodley, P., 2016. Elution of antibiotics from poly(methyl methacrylate) bone cement after extended implantation does not necessarily clear the infection despite susceptibility of the clinical isolates. *Pathog Dis* 74.
285. Takahashi, Y., Imazato, S., Kaneshiro, A.V., Ebisu, S., Frencken, J.E., Tay, F.R., 2006. Antibacterial effects and physical properties of glass-ionomer cements containing chlorhexidine for the ART approach. *Dental Materials* 22, 647–652.
286. Taladriz-Blanco, P., Pérez-Juste, J., Kandoth, N., Hervés, P., Sortino, S., 2013. Layer-by-layer assembled gold nanoparticles with a tunable payload of a nitric oxide photocage. *Journal of Colloid and Interface Science* 407, 524–528.
287. Tam, V.H., Kabbara, S., Vo, G., Schilling, A.N., Coyle, E.A., 2006. Comparative pharmacodynamics of gentamicin against *Staphylococcus aureus* and *Pseudomonas aeruginosa*. *Antimicrobial Agents and Chemotherapy* 50, 2626–2631.
288. Tamanna, T., Bulitta, J.B., Yu, A., 2015. Controlling antibiotic release from mesoporous silica nano drug carriers via self-assembled polyelectrolyte coating. *Journal of Materials Science: Materials in Medicine* 26, 1–7.
289. Tamma, P.D., Cosgrove, S.E., Maragakis, L.L., 2012. Combination Therapy for Treatment of Infections with Gram-Negative Bacteria. *Clin Microbiol Rev* 25, 450–470.

290. Tan, H., Ao, H., Ma, R., Lin, W., Tang, T., 2014. In Vivo Effect of Quaternized Chitosan-Loaded Polymethylmethacrylate Bone Cement on Methicillin-Resistant *Staphylococcus epidermidis* Infection of the Tibial Metaphysis in a Rabbit Model. *Antimicrob. Agents Chemother.* 58, 6016–6023.
291. Tan, H., Guo, S., Yang, S., Xu, X., Tang, T., 2012. Physical characterization and osteogenic activity of the quaternized chitosan-loaded PMMA bone cement. *Acta Biomaterialia* 8, 2166–2174.
292. Tan, Honglue, Peng, Z., Li, Q., Xu, X., Guo, S., Tang, T., 2012. The use of quaternised chitosan-loaded PMMA to inhibit biofilm formation and downregulate the virulence-associated gene expression of antibiotic-resistant *staphylococcus*. *Biomaterials* 33, 365–377.
293. Tan, H.L., Lin, W.T., Tang, T.T., 2012. The use of antimicrobial-impregnated PMMA to manage periprosthetic infections: controversial issues and the latest developments. *The International Journal Of Artificial Organs* 35, 832–839.
294. Tashiro, K., Inamura, M., Kawabata, K., Sakurai, F., Yamanishi, K., Hayakawa, T., Mizuguchi, H., 2009. Efficient Adipocyte and Osteoblast Differentiation from Mouse Induced Pluripotent Stem Cells by Adenoviral Transduction. *STEM CELLS* 27, 1802–1811.
295. Tejwani, N.C., Immerman, I., 2008. Myths and legends in orthopaedic practice: are we all guilty? *Clin. Orthop. Relat. Res.* 466, 2861–2872.
296. Tiwari, M., 2012. Nano cancer therapy strategies. *Journal of Cancer Research and Therapeutics* 8, 19–22.
297. Tommasi, G., Perni, S., Prokopovich, P., 2016. An Injectable Hydrogel as Bone Graft Material with Added Antimicrobial Properties. *Tissue Eng Part A* 22, 862–872.
298. Tracey, W.R., Linden, J., Peach, M.J., Johns, R.A., 1990. Comparison of spectrophotometric and biological assays for nitric oxide (NO) and endothelium-derived relaxing factor (EDRF): nonspecificity of the diazotization reaction for NO and failure to detect EDRF. *J. Pharmacol. Exp. Ther.* 252, 922–928.
299. Trampuz, A., Widmer, A.F., 2006. Infections associated with orthopedic implants. *Current Opinion in Infectious Diseases* 19, 349–356.
300. Trampuz, A., Zimmerli, W., 2005. Prosthetic joint infections: Update in diagnosis and treatment. *Swiss Medical Weekly* 135, 243–251.
301. Tsukada, S., Wakui, M., 2016. A Case Series of Total Hip Arthroplasty Using Cementless Hip Stem Customized for Patients of a Specific Race: 10- to 15-Year Results. *J Arthroplasty* 31, 190–193.
302. Vaishya, R., Chauhan, M., Vaish, A., 2013. Bone cement. *Journal of Clinical Orthopaedics and Trauma* 4, 157–163.
303. Vallet-Regí, M., Balas, F., 2008. Silica Materials for Medical Applications. *Open Biomed Eng J* 2, 1–9.

304. Van, de B., Neut, D., Schenk, W., Van, H., Van, der M., Busscher, H.J., 2000. Gentamicin release from polymethylmethacrylate bone cements and *Staphylococcus aureus* biofilm formation. *Acta Orthopaedica Scandinavica* 71, 625–629.
305. van de Belt, H., Neut, D., Schenk, W., van Horn, J.R., van Der Mei, H.C., Busscher, H.J., 2001. *Staphylococcus aureus* biofilm formation on different gentamicin-loaded polymethylmethacrylate bone cements. *Biomaterials* 22, 1607–1611.
306. van Meurs, S.J., Gawlitta, D., Heemstra, K.A., Poolman, R.W., Vogely, H.C., Kruyt, M.C., 2014. Selection of an optimal antiseptic solution for intraoperative irrigation: an in vitro study. *J Bone Joint Surg Am* 96, 285–291.
307. Vanhegan, I.S., Morgan-Jones, R., Barrett, D.S., Haddad, F.S., 2012. Developing a strategy to treat established infection in total knee replacement. *J Bone Joint Surg Br* 94-B, 875–881.
308. van'T Hof, R.J., Ralston, S.H., 2001. Nitric oxide and bone. *Immunology* 103, 255–261.
309. Varoni, E., Tarce, M., Lodi, G., Carrassi, A., 2012. Chlorhexidine (CHX) in dentistry: state of the art. *Minerva Stomatol* 61, 399–419.
310. Vergaro, V., Abdullayev, E., Lvov, Y.M., Zeitoun, A., Cingolani, R., Rinaldi, R., Leporatti, S., 2010. Cytocompatibility and uptake of halloysite clay nanotubes. *Biomacromolecules* 11, 820–826.
311. Vergaro, V., Scarlino, F., Bellomo, C., Rinaldi, R., Vergara, D., Maffia, M., Baldassarre, F., Giannelli, G., Zhang, X., Lvov, Y.M., Leporatti, S., 2011. Drug-loaded polyelectrolyte microcapsules for sustained targeting of cancer cells. *Advanced Drug Delivery Reviews, Layer-by-Layer Self-Assembled Nanoshells for Drug Delivery* 63, 847–864.
312. Vessely, M.B., Whaley, A.L., Harmsen, W.S., Schleck, C.D., Berry, D.J., 2006. The Chitranjan Ranawat Award: Long-term survivorship and failure modes of 1000 cemented condylar total knee arthroplasties. *Clin. Orthop. Relat. Res.* 452, 28–34.
313. Vielgut, I., Sadoghi, P., Wolf, M., Holzer, L., Leithner, A., Schwantzer, G., Poolman, R., Frankl, B., Glehr, M., 2015. Two-stage revision of prosthetic hip joint infections using antibiotic-loaded cement spacers: When is the best time to perform the second stage? *International Orthopaedics (SICOT)* 39, 1731–1736.
314. Waggoner, A., DeBiasio, R., Conrad, P., Bright, G.R., Ernst, L., Ryan, K., Nederlof, M., Taylor, D., 1989. Multiple spectral parameter imaging. *METH.CELL BIOL., METH.CELL.BIOL., Methods in cell biology* 30, 449–478.
315. Walker, L.C., Baker, P., Holleyman, R., Deehan, D., 2017. Microbial resistance related to antibiotic-loaded bone cement: a historical review. *Knee Surg Sports Traumatol Arthrosc* 25, 3808–3817.
316. Walsh, C., 2000. Molecular mechanisms that confer antibacterial drug resistance. *Nature* 406, 775–781.

317. Wang, B., Jin, T., Xu, Q., Liu, H., Ye, Z., Chen, H., 2016. Direct Loading and Tunable Release of Antibiotics from Polyelectrolyte Multilayers To Reduce Bacterial Adhesion and Biofilm Formation. *Bioconjug. Chem.* 27, 1305–1313.
318. Wang, C., Hou, H., Nan, K., Sailor, M.J., Freeman, W.R., Cheng, L., 2014. Intravitreal controlled release of dexamethasone from engineered microparticles of porous silicon dioxide. *Exp. Eye Res.* 129, 74–82.
319. Wang, K., Street, A., Dowrick, A., Liew, S., 2012. Clinical outcomes and patient satisfaction following total joint replacement in haemophilia - 23-year experience in knees, hips and elbows. *Haemophilia* 18, 86–93.
320. Wei, Wenbo, Abdullayev, E., Hollister, A., Mills, D., Lvov, Y.M., 2012. Clay Nanotube/Poly(methyl methacrylate) Bone Cement Composites with Sustained Antibiotic Release. *Macromol. Mater. Eng.* 297, 645–653.
321. Wei, W., Abdullayev, E., Hollister, A., Mills, D., Lvov, Y.M., 2012. Clay nanotube/poly(methyl methacrylate) bone cement composites with sustained antibiotic release. *Macromolecular Materials and Engineering* 297, 645–653.
322. Wendling, A., Mar, D., Wischmeier, N., Anderson, D., McIff, T., 2016. Combination of modified mixing technique and low frequency ultrasound to control the elution profile of vancomycin-loaded acrylic bone cement. *Bone Joint Res* 5, 26–32.
323. Whittaker, J.P., Warren, R.E., Jones, R.S., Gregson, P.A., 2009. Is prolonged systemic antibiotic treatment essential in two-stage revision hip replacement for chronic Gram-positive infection? *J Bone Joint Surg Br* 91, 44–51.
324. Widmer, A.F., 2013. Surgical hand hygiene: scrub or rub? *J. Hosp. Infect.* 83 Suppl 1, S35-39.
325. Wiegand, I., Hilpert, K., Hancock, R.E.W., 2008. Agar and broth dilution methods to determine the minimal inhibitory concentration (MIC) of antimicrobial substances. *Nat. Protocols* 3, 163–175.
326. Wong, S.Y., Moskowitz, J.S., Veselinovic, J., Rosario, R.A., Timachova, K., Blaisse, M.R., Fuller, R.C., Klibanov, A.M., Hammond, P.T., 2010. Dual functional polyelectrolyte multilayer coatings for implants: Permanent microbicidal base with controlled release of therapeutic agents. *Journal of the American Chemical Society* 132, 17840–17848.
327. Wood, K.C., Chuang, H.F., Batten, R.D., Lynn, D.M., Hammond, P.T., 2006. Controlling interlayer diffusion to achieve sustained, multiagent delivery from layer-by-layer thin films. *Proc. Natl. Acad. Sci. U.S.A.* 103, 10207–10212.
328. Wu, K., Chen, Y.-C., Hsu, Y.-M., Chang, C.-H., 2016. Enhancing Drug Release From Antibiotic-loaded Bone Cement Using Porogens. *J Am Acad Orthop Surg* 24, 188–195.
329. Wu, Y., Long, Y., Li, Q.-L., Han, S., Ma, J., Yang, Y.-W., Gao, H., 2015. Layer-by-Layer (LBL) Self-Assembled Biohybrid Nanomaterials for Efficient Antibacterial Applications. *Achitosan Appl. Mater. Interfaces* 7, 17255–17263.

330. Wyatt, M., Hooper, G., Frampton, C., Rothwell, A., 2014. Survival outcomes of cemented compared to uncemented stems in primary total hip replacement. *World J Orthop* 5, 591–596.
331. Xu, H.H.K., Quinn, J.B., Takagi, S., Chow, L.C., Eichmiller, F.C., 2001. Strong and macroporous calcium phosphate cement: Effects of porosity and fiber reinforcement on mechanical properties. *Journal of Biomedical Materials Research* 57, 457–466.
332. Yan, H., Yang, H., Li, K., Yu, J., Huang, C., 2017. Effects of Chlorhexidine-Encapsulated Mesoporous Silica Nanoparticles on the Anti-Biofilm and Mechanical Properties of Glass Ionomer Cement. *Molecules* 22, 1225.
333. Young, A.M., Ng, P.Y.J., Gbureck, U., Nazhat, S.N., Barralet, J.E., Hofmann, M.P., 2008. Characterization of chlorhexidine-releasing, fast-setting, brushite bone cements. *Acta Biomaterialia* 4, 1081–1088.
334. Yu, T., Ye, J., Gao, C., Yu, L., Wang, Y., 2010. Effect of biomedical organic compounds on the setting reaction of calcium phosphates. *Colloids and Surfaces B: Biointerfaces* 75, 363–369.
335. Zahar, A., Webb, J., Gehrke, T., Kendoff, D., 2015. One-stage exchange for prosthetic joint infection of the hip. *HIP International* 25, 301–307.
336. Zhang, J., Liu, W., Schnitzler, V., Tancret, F., Bouler, J.-M., 2014. Calcium phosphate cements for bone substitution: Chemistry, handling and mechanical properties. *Acta Biomaterialia* 10, 1035–1049.
337. Zhang, J.T., Tancret, F., Bouler, J.M., 2011. Fabrication and mechanical properties of calcium phosphate cements (CPC) for bone substitution. *Materials Science and Engineering: C, Sixth Symposium on Biological Materials Science, 139th Annual Meeting & Exhibition of The Minerals, Metals & Materials Society* 31, 740–747.
338. Zhang, L., Ge, S., Liu, H., Wang, Q., Wang, L., Xian, C.J., 2015. Contact damage failure analyses of fretting wear behavior of the metal stem titanium alloy–bone cement interface. *Journal of the Mechanical Behavior of Biomedical Materials* 51, 132–146.
339. Zhang, L., Pornpattananangku, D., Hu, C.-M.J., Huang, C.-M., 2010. Development of nanoparticles for antimicrobial drug delivery. *Curr. Med. Chem.* 17, 585–594.
340. Zhao, X., Olsen, I., Pratten, J., Knowles, J.C., Young, A.M., 2011. Reactive calcium-phosphate-containing poly(ester-co-ether) methacrylate bone adhesives: setting, degradation and drug release considerations. *J Mater Sci: Mater Med* 22, 1993–2004.
341. Zhong, G., Guo, W., Liu, Y., Wei, Y., Meng, X., Hu, Z., Liu, F., 2015. Preparation of tetrasulfide-functionalized silica particles by hydrothermal assisted grafting method for removal of lead (II) via dynamic solid phase extraction. *Colloids and Surfaces A: Physicochemical and Engineering Aspects* 485, 63–72.
342. Zimmerli, W., Ochsner, P.E., 2003. Management of infection associated with prosthetic joints. *Infection* 31, 99–108.

343. Zimmerli, W., Trampuz, A., Ochsner, P.E., 2004. Current concepts: Prosthetic-joint infections. *New England Journal of Medicine* 351, 1645–1654.